PB-232 445

NATURAL PRECIPITATION WASHOUT OF SULFUR COMPOUNDS FROM PLUMES

BATTELLE-PACIFIC NORTHWEST LABORATORIES

PREPARED FOR
ENVIRONMENTAL PROTECTION AGENCY

JUNE 1973

DISTRIBUTED BY:

NTIS
National Technical Information Service
U. S. DEPARTMENT OF COMMERCE

BIBLIOGRAPHIC DATA SHEET	1. Report No. EPA-R3-73-047	2.	PB 232 445

4. Title and Subtitle
Natural Precipitation Washout of Sulfur Compounds from Plumes

5. Report Date
June 1973 .

6.

7. Author(s)
M. Terry Dana, J. M. Hales, W.G.N. Slinn, M.A. Wolf

8. Performing Organization Rept. No.

9. Performing Organization Name and Address
Battelle, Pacific Northwest Laboratories
Atmospheric Sciences Department
Battelle Boulevard
Richland, Washington 99352

10. Project/Task/Work Unit No.
BNW 389 / B46621

11. Contract/Grant No.
EPA-IAG-0104 (D)

12. Sponsoring Organization Name and Address
EPA Division of Meteorology
Research Triangle Park
North Carolina 27709

13. Type of Report & Period Covered
Final Report

14.

15. Supplementary Notes

16. Abstracts

This report describes field measurement and modeling of the washout of SO_2 and sulfate from plumes. Field measurements of precipitation washout were conducted in conjunction with both controlled test sources and actual power plant plumes. A primary achievement of this work has been the formulation of an SO_2 washout model, which predicts rain-borne SO_2 concentrations that agree favorably with those observed. An approximate theoretical analysis of sulfate washout in conjunction with field observations indicates that sulfate formation and scavenging exhibit a strong inverse dependence on acidity levels in the background rain.

17. Key Words and Document Analysis. 17a. Descriptors

Washout
SO_2
Sulfate
Plumes
Power Plants

17b. Identifiers/Open-Ended Terms

Reproduced by
NATIONAL TECHNICAL
INFORMATION SERVICE
U S Department of Commerce
Springfield VA 22151

17c. COSATI Field/Group

18. Availability Statement	19. Security Class (This Report) UNCLASSIFIED	21. No. of Pages 215
	20. Security Class (This Page UNCLASSIFIED	22. Price $5.75

FORM NTIS-35 (REV. 3-72)

USCOMM-DC 14952-P72

EPA-R3-73-047

NATURAL PRECIPITATION WASHOUT OF SULFUR COMPOUNDS FROM PLUMES

by

M. Terry Dana, J. M. Hales,
W. G. N. Slinn, and M. A. Wolf

Atmospheric Sciences Department
Battelle, Pacific Northwest Laboratories
P. O. Box 999, Richland, Washington 99352

Interagency Agreement No. IAG-025 (D)
Program Element No. 1A1009

EPA Project Officer: Herbert Viebrock

Meteorology Laboratory
National Environmental Research Center
Research Triangle Park, North Carolina 27711

Prepared for

OFFICE OF RESEARCH AND DEVELOPMENT
U.S.ENVIRONMENTAL PROTECTION AGENCY
WASHINGTON, D.C. 20460

June 1973

ia

This report has been reviewed by the Environmental Protection Agency and approved for publication. Approval does not signify that the contents necessarily reflect the views and policies of the Agency, nor does mention of trade names or commercial products constitute endorsement or recommendation for use.

CONTENTS

Page
ABSTRACT iv
LIST OF FIGURES v
LIST OF TABLES ix
ACKNOWLEDGMENTS xi

SECTIONS

I. CONCLUSIONS 1
II. RECOMMENDATIONS 3
III. INTRODUCTION 5
IV. PROGRESS IN WASHOUT MODELING 17
V. SECOND-SERIES QUILLAYUTE EXPERIMENTS 24
VI. CENTRALIA EXPERIMENTS 63
VII. FURTHER ANALYSES OF KEYSTONE RESULTS 121
VIII. RECOMMENDED APPLICATIONS OF THE EPAEC MODEL FOR ENVIRONMENTAL IMPACT ANALYSES 126
IX. REFERENCES 131
X. NOMENCLATURE 134
XI. APPENDICES 139

ABSTRACT

A model has been developed for prediction of the reversible washout of SO_2 *emitted from power-plant plumes and other sources. Predictions of this computer-code model compare favorably with washout measurements made during fifteen controlled-source experiments and four power plant experiments. An application of the model to previous experimental conditions of high background rain acidity shows that "negative washout" can and has occurred as a result of desorption of* SO_2 *from the rain below the* SO_2 *plume. The resulting washdown effect was analyzed mathematically, and shown to be not a significant pollution problem on the distance scale of current interest, but could be important for gases that are more strongly dissolved than* SO_2. *The effect of dry deposition upon the experimental results of the study appears to be unimportant for rainfall rates over about one mm* hr^{-1}.

Sulfate washout measurements were made during the power plant study, and an approximate reaction-washout analysis indicates that a rapid initial oxidation occurs, which slows at increasing downwind distance. The sulfate washout coefficient appears to be about 0.05 hr^{-1} *for background* pH $\gtrsim 5.2$, *but could be much smaller for more acid rains.*

This report was submitted in fulfillment of work specified in proposal No. 300A00585 (BNW-389), *Amendment 2, by Battelle, Pacific Northwest Laboratories under the sponsorship of the Environmental Protection Agency. Work was completed as of July, 1972.*

FIGURES

Page

1. Chronological Summary of Major Segments of the EPA-Sponsored Washout Program 6
2. Schematic of Keystone Rain Sampling Network 7
3. SO_2 Washout Concentrations at Keystone - Run 9, February 10, 1970 9
4. SO_2 Washout Concentrations at Keystone - Run 18, April 24, 1970 10
5. SO_2 Washout Concentrations at Keystone - Run 4, November 2, 1969 11
6. Quillayute Sampling Network - First Series 14
7. Predicted and Measured SO_2 Concentrations at Quillayute, First Series - Typical Run, Dashed and Solid Curves Show Model Predictions 16
8. The Redistribution of an SO_2 Plume Caused by Washout 23
9. Quillayute Sampling Network - Second Series 26
10. 30.5 m SO_2 Release Tower - Quillayute Second Series 28
11. Portion of the West Sampling Arcs - Quillayute Second Series 29
12. Measured and Calculated SO_2 Concentration in Rain - Run 11 36
13. Measured and Calculated SO_2 Concentrations in Rain - Run 12 W 37
14. Measured and Calculated SO_2 Concentration in Rain - Run 12 E 38
15. Measured and Calculated SO_2 Concentration in Rain - Run 14 W 39
16. Measured and Calculated SO_2 Concentration in Rain - Run 14 E 40
17. Measured and Calculated SO_2 Concentration in Rain - Run 15 W 41

Page

18. Measured and Calculated SO_2 Concentration in Rain - Run 15 E . . . 42

19. Measured and Calculated SO_2 Concentration in Rain - Run 16 W . . . 43

20. Measured and Calculated SO_2 Concentration in Rain - Run 16 E . . . 44

21. Measured and Calculated SO_2 Concentration in Rain - Run 17 . . . 45

22. Measured and Calculated SO_2 Concentration in Rain - Run 18 . . . 46

23. Measured and Calculated SO_2 Concentration in Rain - Run 19 . . . 47

24. Measured and Calculated SO_2 Concentration in Rain - Run 20 . . . 48

25. Measured *versus* Predicted SO_2 Washout Rates - Quillayute Second Series . . . 50

26. Error in Washout Concentration Measurements, as a Result of Dry Deposition . . . 61

27. Map of Centralia Steam Plant Area . . . 64

28. Centralia Sampling Network . . . 66

29. Centralia Steamplant with Rawinsonde Antenna at Control Center in Foreground . . . 68

30. Centralia Sampling Location: $SO_4^=$ and SO_2 Samplers, Left; pH and SO_2 Bubbler Box, Right . . . 69

31. Measured SO_2 Concentrations in Air - Run C-1 . . . 73

32. Rawinsonde Data - Run C-2 . . . 74

33. Measured SO_2 Concentrations in Rain - Run C-2 . . . 75

34. Predicted SO_2 Concentrations in Rain - Run C-2 EPAEC Model Calculations Based on Gas-Phase Limited Transport and an SO_2 Reaction Decoy Half-Life of 15 Minutes . . . 76

35. Measured SO_2 Concentrations in Air - Run C-2 . . . 77

Page

36. Measured Sulfate Concentrations in Rain - Run C-2 (Background Corrected) 78

37. Measured Free Hydrogen-Ion Concentrations - Run C-2 (From pH Measurements, Background Corrected) 79

38. Rawinsonde Data - Run C-3 80

39. Measured SO_2 Concentrations in Rain - Run C-3 81

40. Predicted SO_2 Concentrations in Rain - Run C-3 EPAEC Model Calculations Based on Gas-Phase Limited Transport and an SO_2 Reaction Decay Half-Life of 15 Minutes 82

41. Measured SO_2 Concentrations in Air - Run C-3 83

42. Measured Free Hydrogen-Ion Concentrations - Run C-3 (From pH Measurements, Background Corrected) 84

43. Measured SO_2 Concentrations in Rain - Run C-4 85

44. Predicted SO_2 Concentrations in Rain - Run C-4 EPAEC Model Calculations Based on Gas-Phase Limited Transport and an SO_2 Reaction Decay Half-Life of 15 Minutes 86

45. Measured SO_2 Concentrations in Air - Run C-4 87

46. Measured Sulfate Concentrations in Rain - Run C-4 (Background Corrected) 88

47. Measured Free Hydrogen-Ion Concentrations - Run C-4 (From pH Measurements, Background Corrected) 89

48. Measured SO_2 Concentrations in Rain - Run C-5 90

49. Predicted SO_2 Concentrations in Rain - Run C-5 EPAEC Model Calculations Based on Gas-Phase Limited Transport and an SO_2 Reaction Decay Half-Life of 15 Minutes 91

50. Measured SO_2 Concentrations in Air - Run C-5 92

51. Measured Sulfate Concentrations in Rain - Run C-5 (Background Corrected) 93

Page

52. Measured Free Hydrogen-Ion Concentrations - Run C-5 (From pH Measurements, Background Corrected) 94

53. Schematic of Idealized Plumes Employed by EPAEC Model for Centralia Calculations 101

54. Rain-borne SO_2 Concentrations at Ground Level as Function of Raindrop Size 105

55. Schematic of Features of Reaction/Washout Process 110

56. Washout Coefficient as a Function of Particle Size 112

57. Solutions to Equation (28) For Run C-2 116

58. EPAEC Model Calculation for Keystone Run 4, Arc A, Using Data of Table 23 122

59. Representation of Simplified Film Theory 173

60. Superficial Flow Diagram of EPAEC Model 177

61. Sub-Routine Hierarchy in EPAEC Model 177

62. Pictorial Bases for EPAEC Model 179

TABLES

Page

1. Basic Data Used for Washdown Calculation 21

2. Release and Sampling Parameters - Quillayute, Second Series . . 25

3. Times, Temperatures and Rainfall Rates - Quillayute, Second Series 31

4. Raindrop Size Frequency Distributions - Quillayute Second Series 32

5. Wind Parameters Calculated from Anemometer Data - Quillayute Second Series 33

6. Measured Washout Rates - Quillayute Second Series 35

7. Summary of Dry Deposition Results 57

8. Transport Parameters for Dry Deposition Tests 59

9. Calculated Incident Rain Concentrations for Dry Deposition Runs D1 and D3 60

10. Centralia Steam-Electric Plant Statistics (February-March, 1972) 65

11. Run Data - Centralia 71

12. Raindrop Size Frequency Distributions - Centralia 72

13. Summary of Washout Measurements - Centralia 72

14. Trace Metals Analysis - Centralia Run C-4 97

15. Average Wind Data from Anemometers - Centralia 98

16. First-Order Rate Constants for SO_2 Decay Used in Centralia Model Calculations 100

17. Effective Stack Heights and Loft Velocities Used in Applying the EPAEC Model to the Centralia Results (After Briggs[13]) . . . 102

18. EPAEC Calculations of SO_2 Washout Concentrations - Centralia, Run C-5 103

19. Extreme Limits of Sulfate Washout Coefficients and Reaction Rate Constants 113

Page

20. Revised Extrema of Sulfate Washout Coefficients and Reaction-Rate Constants 114

21. Solutions to Equation (28) for Applicable Centralia Sampling Line Pairs 117

22. Comparison of Sulfate Washout Rates: Observed *versus* Those Calculated Using Equations (28) and (29) 120

23. Keystone Run 4 Base Data 125

24. Results of Application of Sulfate Washout Model to Keystone, Run 4, Arc A Data 125

25. Summary of Required Input Data for the EPAEC Code, and Recommended Values for Initial Use 127

26. Example Input Data Format for EPAEC Code 130

27-35. Measured SO_2 Concentrations - Quillayute Second Series 141

36-49. Measured SO_2 Concentrations - Centralia 149

50-58. Measured $SO_4^=$ and H^+ Concentrations - Centralia 161

59. Computer Nomenclature 185

ACKNOWLEDGMENTS

This research was conducted by scientific and technical personnel of the Atmospheric Sciences Department of Battelle, Pacific Northwest Laboratories under related services agreement BNW-389 with the Richland Operations Office, U. S. Atomic Energy Commission for the Environmental Protection Agency.

The principal investigators were. M. Terry Dana, Jeremy M. Hales, W. G. N. Slinn, and M. A. Wolf. Special appreciation is due D. W. Glover, who directed and performed much of the design and development of special field equipment. Other Battelle, Pacific Northwest Laboratories personnel who contributed significantly were:

R. E. Kerns
R. N. Lee
M. C. Miller
J. Mishima
J. W. Sloot
W. A. Stone

We are expecially grateful for the contributions of the following persons and organizations, whose assistance was valuable in the success of the field effort:

The management of the Centralia Steam Plant, particularly:

Pacific Power and Light Company
Washington Irrigation and Development Company.

Washington State Aeronautics Commission, Seattle, Washington

Mr. Clarence Davis, Manager, Quillayute State Landing Field

Mr. Donald Carte, Meteorologist-In-Charge, National Weather Service, Forks, Washington

Professor Donald Adams, Washington State University.

SECTION I.

CONCLUSIONS

A method of calculating SO_2 washout from plumes has been developed. This method is based upon reversible gas absorption phenomena, and is applicable to circumstances involving power-plant plumes emitted from tall stacks, as well as for less complicated situations. It can be employed for predicting washout of pollutant gases other than SO_2 upon substitution of the appropriate physical properties.

The washout calculation procedure is accomplished in terms of a model given in FORTRAN IV computer code, which is listed and documented in an appendix to this report. The basic precepts of the model--reversible behavior and negligible plume distortion by washout--were checked theoretically and experimentally and found to be valid under the conditions of present interest.

Field experiments conducted during this program showed that SO_2 concentrations in rain often can be calculated to within a factor of two of observed values, although the predictive capability is reduced for near-source conditions, and complicated by the occurrence of chemical reaction. The accuracy of the present model, moreover, is improved, compared to that of previous calculation procedures; the latter predict results high by several orders of magnitude under circumstances involving tall stacks. Additionally, the washout model predicts behavior consistent with earlier measurements near the Keystone plant, which appeared anomalous at the time. These model-verified observations include:

1. Washout of SO_2 from a concentrated, high-elevation plume can be obscured by the presence of low-elevation, low-concentration background levels.
2. The acidity of rain strongly influences its SO_2-scavenging potential.

3. "Negative" washout of SO_2 occurs under appropriate circumstances--that is, rain that has passed through a power plant plume often contains less SO_2 than that which has not.

Sulfate washout from power plant plumes was measured during this study; the results indicate that the rate of sulfur removal *via* sulfate washout is from one to five times more rapid than that *via* SO_2 washout. A definitive model of sulfate washout was not developed during this study; however, the field results applied to an approximate analysis lead to a conclusion that the reaction process occurs rapidly near the source, and decreases with distance downwind. The overall reaction-rate constant--for all sampling distances--derived from this analysis is in the neighborhood of 5 hr^{-1}, with corresponding sulfate washout coefficients ranging below about 0.07 hr^{-1}.

SECTION II.

RECOMMENDATIONS

The computer model developed by this project is recommended for use in environmental impact analyses of fossil-fuel power plants, as well as for assessments of washout of gases from plumes of other types. Selected local wind, rain, and pollutant-source characteristics, plus physical properties. background levels, and topography can be applied to the model to calculate concentrations of pollutant in rain as a function of distance from the source.

The simplified plume description, assuming a bivariate-normal distribution with spread parameters given by the equations of Smith and Singer, and loft given by the equations of Briggs. is recommended for use with the washout model for impact-analysis purposes. More specialized calculations may require other models of plume behavior; these can be easily incorporated within the overall washout model at the user's option.

The washout model developed during this study is focused primarily on removal of SO_2. Sulfate washout is an additional important aspect of the overall sulfur-removal process in power-plant plumes; accordingly, an extension of the present model to provide for sulfate washout calculations is desirable. Such an extension is complicated by a lack of knowledge of the microphysics of sulfate formation and removal. Through a modest effort, however, the present washout model can be extended to provide a macroscopic calculation procedure. This would provide a computational framework which would accept (in subroutine form) any given microphysical model of sulfate formation within plumes and proceed to perform corresponding washout computations. This extension is useful for testing of microphysical models under practical conditions; it is also desirable because it will yield an improved environmental impact analysis tool once the appropriate microphysical models have been established. For these reasons the development of an extended washout model is recommended as a limited addition to the present work.

With the exception of the microphysics of sulfate formation and washout, a majority of the processes leading to sulfur removal from plumes are now fairly well understood. Improvements in our ability to estimate washout rates, therefore, can be expected to stem directly from future improvements in our ability to describe the features required for model input. Such features are categorized below, in order of expected importance in improving our existing ability to compute sulfur compound washout from power plant plumes.

1. Sulfate formation and washout-rate phenomena.
2. Plume description ("diffusion" model considerations).
3. Dry deposition processes and their effect on plume description.
4. SO_2 absorption microphysics.

If future research is sponsored by the Environmental Protection Agency on washout of sulfur from power plant plumes, we recommend that specific areas be given priority in the order listed above.

SECTION III.

INTRODUCTION

In October, 1969, Battelle-Northwest began field studies of precipitation washout of sulfur compounds from coal-fired power plant plumes under sponsorship of the Division of Meteorology, Environmental Protection Agency (then the National Air Pollution Control Administration). At that time, we conducted an initial series of field experiments in the vicinity of the Keystone Generating Station in western Pennsylvania. Subsequent years' investigations included controlled-release SO_2 washout experiments at Quillayute airfield, Washington, and a return to power plant effluent washout experiments at the Centralia, Washington Steam Plant. (Figure 1 summarizes the locations and times of the field efforts under this program.)

Results of the Keystone and early Quillayute experiments have been documented previously (Hales, Thorp, and Wolf:[1] Dana, Hales, and Wolf[2]). These references will be cited often in the present report, and we shall refer to them hereafter as "HTW" and "DHW" for convenience. The purpose of this report is to describe results from additional Quillayute experiments and from Centralia, and to focus subsequent conclusions of these into the context of the total EPA washout program. The remainder of this introduction provides an overall perspective on the program by summarizing briefly the design and findings of the Keystone and early Quillayute work, and by outlining the bases of the investigations to be reported in later chapters.

KEYSTONE

The precipitation washout study at Keystone consisted basically of obtaining chemical analyses of precipitation samples collected at various locations beneath the power plant plume. Although SO_2 was the compound of primary interest, we also measured the concentrations of other species--NO_3^-, NO_2^-, H^+, $SO_4^=$--in specific samples. Figure 2 is a layout of sampling locations with respect to the Keystone power plant.

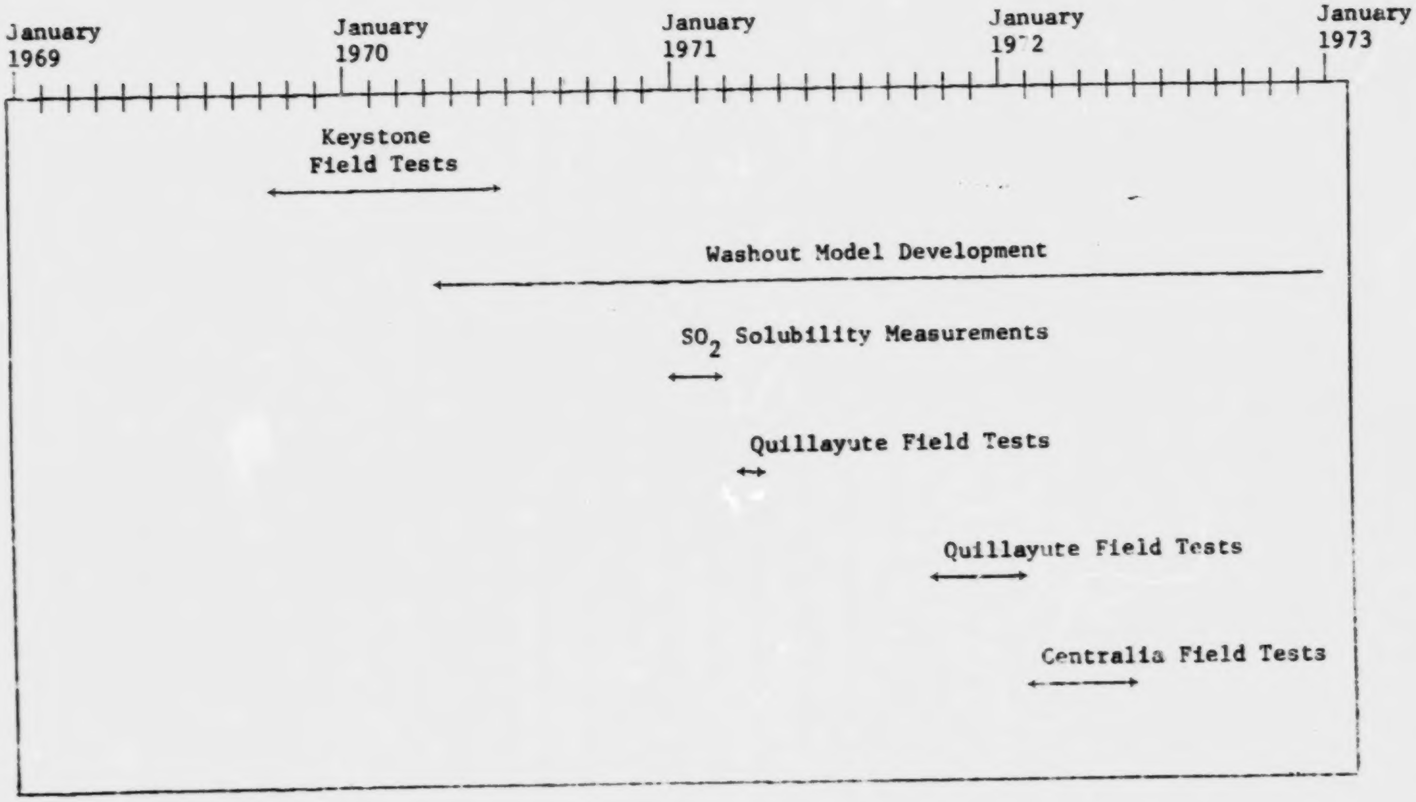

FIGURE 1. CHRONOLOGICAL SUMMARY OF MAJOR SEGMENTS OF THE EPA-SPONSORED WASHOUT PROGRAM.

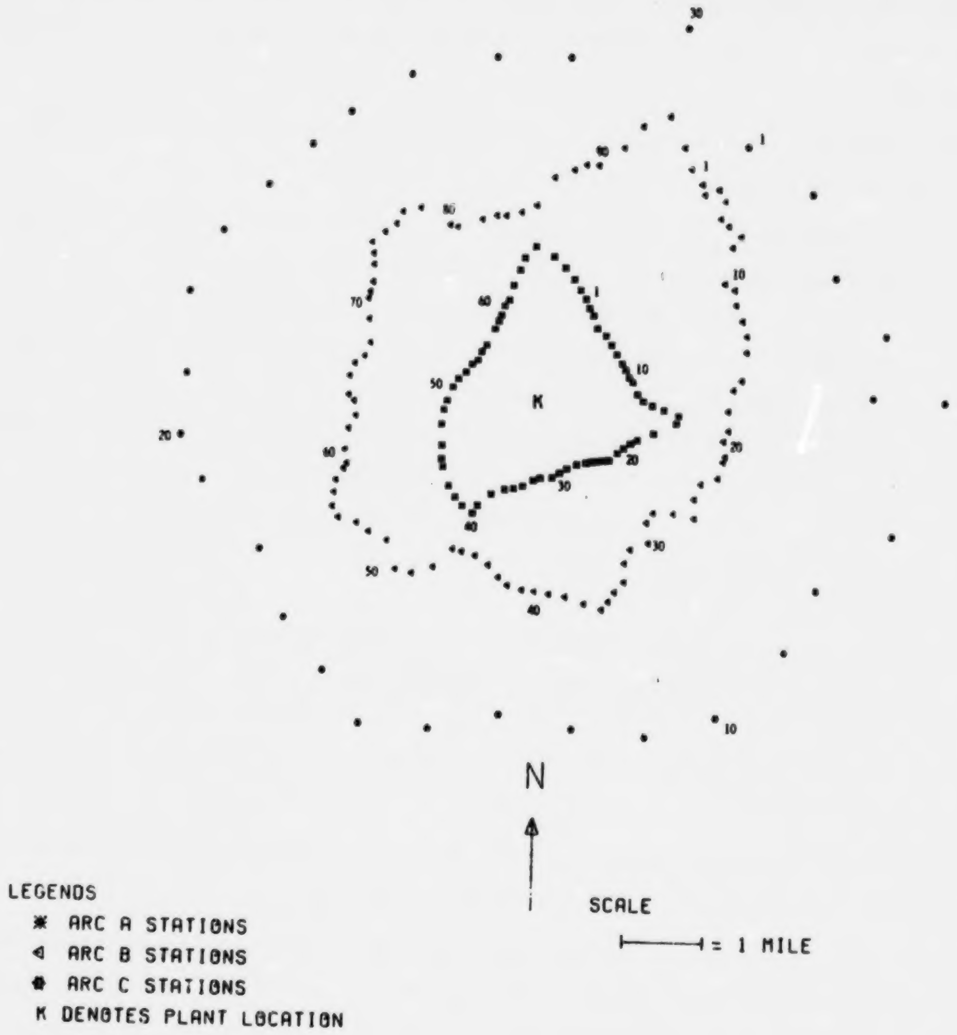

30
1
1
80
80
10
70
60
1
10
50
K
20
20
60
20
30
40
30
50
40
10
N
SCALE
= 1 MILE
LEGENDS
✱ ARC A STATIONS
◁ ARC B STATIONS
● ARC C STATIONS
K DENOTES PLANT LOCATION

FIGURE 2. SCHEMATIC OF KEYSTONE RAIN SAMPLING NETWORK.

Measured SO_2 levels in the collected rain did not follow behavior predicted at the time; in fact, it was exceedingly difficult to determine the influence of the plume on the SO_2 content of the precipitation. At times the spatial distribution of SO_2 concentration levels in the rain showed a relatively high SO_2 content but indicated no relationship to plume location whatsoever (cf. Fig. 3); other distributions, such as that shown in Figure 4, showed little SO_2 in precipitation collected at any location. Still other experiments, such as that shown in Figure 5, indicated an inverse relationship between SO_2 content and plume position--a paradoxical "negative washout" effect.

These results, in combination with additional findings described in HTW, led to the following conclusions:

C-1. Washout of SO_2 from high-elevation plumes is an inefficient process, at least at distances within a few miles from the source. Washout rates are less than those predicted from classical washout theory, and never amount to more than a fraction of one percent of the source per mile at the Keystone plant.

C-2. Washout of background SO_2 from low elevations is usually sufficient to obscure contributions from the Keystone plume.

C-3. Free hydrogen-ion concentrations (obtained from pH measurements) correlate somewhat with plume location, at least when background levels are low.

C-4. Measured sulfate content of the rain correlates somewhat with plume location, although background levels tend to obscure this relationship.

C-5. SO_2 content of the rain shows a strong inverse correlation with rain acidity.

In addition to these conclusions the following speculations were made as proposed explanations of the observed behavior:

S-1. SO_2 absorption by the falling raindrops must be a reversible process, with significant amounts of captured SO_2 desorbing during the rain drops' fall beneath the more concentrated regions of the plume.

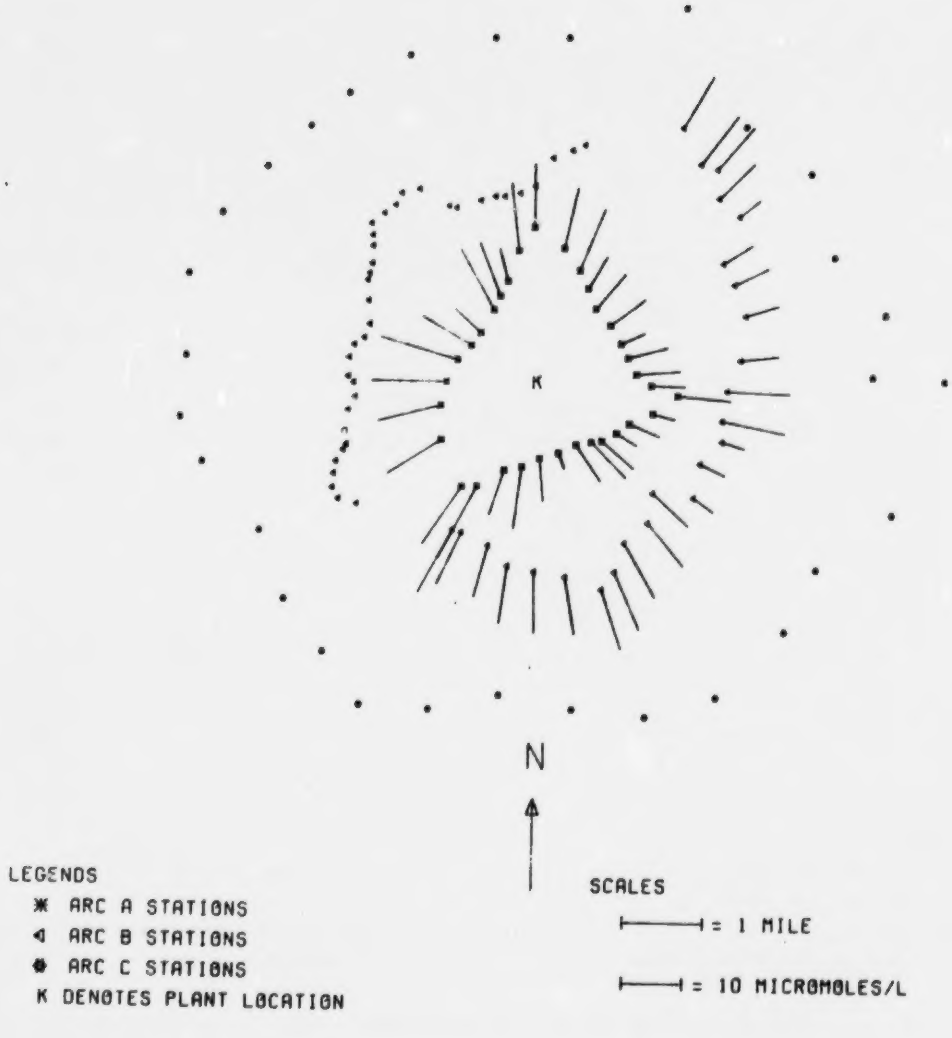
K
N
LEGENDS
✱ ARC A STATIONS
◂ ARC B STATIONS
● ARC C STATIONS
K DENOTES PLANT LOCATION
SCALES
= 1 MILE
= 10 MICROMOLES/L

FIGURE 3. SO_2 WASHOUT CONCENTRATIONS AT KEYSTONE - RUN 9, FEBRUARY 10, 1970.

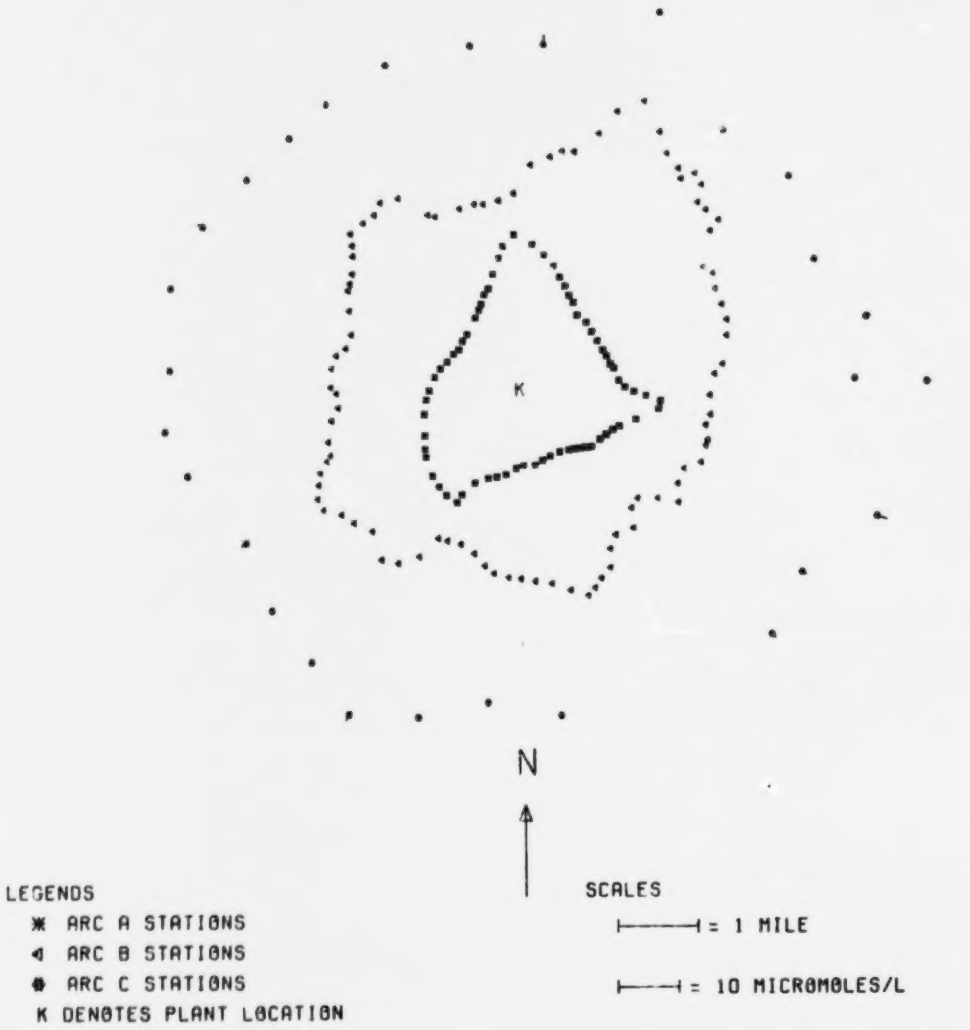
K
N
LEGENDS
✱ ARC A STATIONS
◀ ARC B STATIONS
● ARC C STATIONS
K DENOTES PLANT LOCATION
SCALES
├───┤ = 1 MILE
├──┤ = 10 MICROMOLES/L

FIGURE 4. SO_2 WASHOUT CONCENTRATIONS AT KEYSTONE - RUN 18, APRIL 24, 1970.

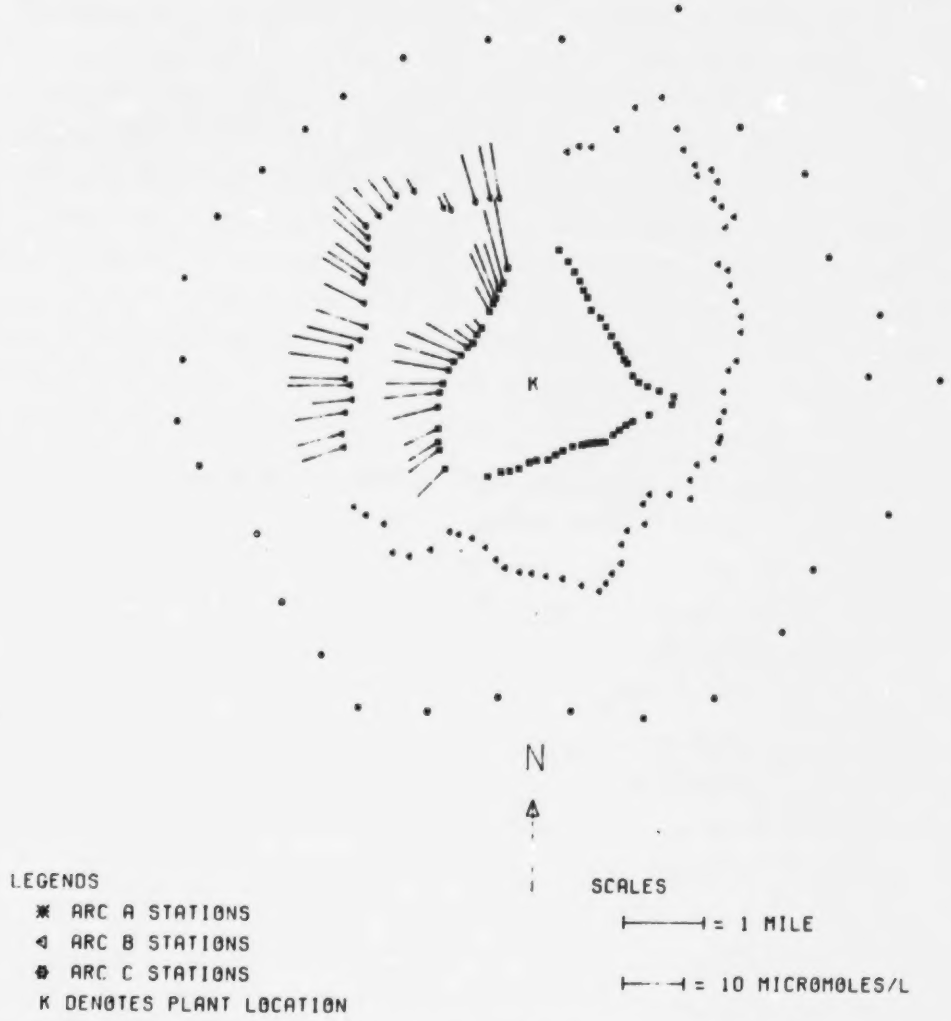

FIGURE 5. SO_2 WASHOUT CONCENTRATIONS AT KEYSTONE - RUN 4, NOVEMBER 2, 1969.

S-2. SO_2 solubility is strongly dependent on rain acidity, with this dependency forming the basis for the strong correlation between pH and washout. The negative washout effect shown in Figure 5 is a consequence of the rain increasing its acidity by scavenging nonvolatile acid-forming materials from the plume, causing SO_2 to desorb to concentration levels below those reflecting background concentrations in rain collected at surrounding locations.

S-3. If the desorption effect (S-1) is valid, then a redistribution of the SO_2 plume takes place as a result of the descent of the rain, lowering the altitude of the plume with increasing distance from the source. This effect will be referred to as "washdown" in the succeeding text.

S-4. The validity of S-1 also requires that an exact description of the plume be used to calculate washout rates. This is in contrast to a consideration of particulate plumes, where only a total mass term is required. Also, if nonlinearities exist in the microphysical relationships dictating washout of SO_2, then fluctuations of the plume with time may become an important consideration.

S-5. There is a rapid initial oxidation of SO_2 to $SO_4^=$ in the plume near the source; this reaction proceeds at a much slower rate at greater distances.

Speculation S-5 is based on measurements of sulfate in rain collected at various downwind distances from the plant. It is questionable for two reasons, these being the inherent noise in the measurements (turbidimetric), and the fact that washout measurements provide a rather indirect means of assessing in-plume behavior. This speculation is in accord, however, with many of the more direct attempts to study in-plume oxidation processes.

The speculations pertaining to reversibility and the influence of acid-forming impurity provided a basis for performing more valid calculations of SO_2 washout. Subsequently, this approach has been generalized to apply to all gases, and has been described in a separate publication.[3]

Additional field research was necessary to test the validity of the above postulates. We felt that a relocation of sites of field studies to areas low in pollution background would be advantageous, owing to the noted interference effects. Moreover, we believed that controlled field experiments--employing releases of pure SO_2--would be valuable for direct testing of the desorption mechanism. Information obtained from these tests plus results of another power plant study could then be employed in a final analysis of washout from power plant plumes.

INITIAL QUILLAYUTE STUDY

The site chosen for the controlled release experiments was the Quillayute airfield, located on the Olympic Peninsula in western Washington State. This location is characterized by near-zero SO_2 background concentrations, and ample rainfall. SO_2 was released simultaneously from two towers (adjustable heights from 0 to 30 m) and was analyzed in rain collected on surrounding arcs, as shown in Figure 6. Comparison of washout concentrations resulting from different release heights enabled us to observe the desorption effect. In addition to the field experiments, laboratory studies were conducted to evaluate quantitatively the relationship between SO_2 solubility, concentration, and rain acidity. Also, an attempt was made to model SO_2 washout based upon the postulated reversible behavior.

The SO_2 solubility measurements were successful in extending quantitative knowledge of SO_2-H_2O interactions down to ambient concentrations of the order of parts per billion. They demonstrated conclusively the strong influence of rain acidity on solubility under these conditions, verifying partially the above speculation S-2 (cf. DHW, pg. 29).

Two models of reversible gas washout were developed; one was a computer model, and the other a simplified linear version amenable to hand calculation. The first of these is described in detail in Appendix C of this report. The second has been documented in former reports (DHW; Hales[4]), and in the open literature.[5] The basis for these models is summarized in Appendix B. As expected, the Quillayute SO_2 washout results did not exhibit the anomalous behavior observed at Keystone. The absence of background impurities and non-volatile acid-forming plume constituents allowed the crosswind concentration distributions to assume even, well-defined patterns, reflecting the quasi-Gaussian form of the plume. In addition, we observed the

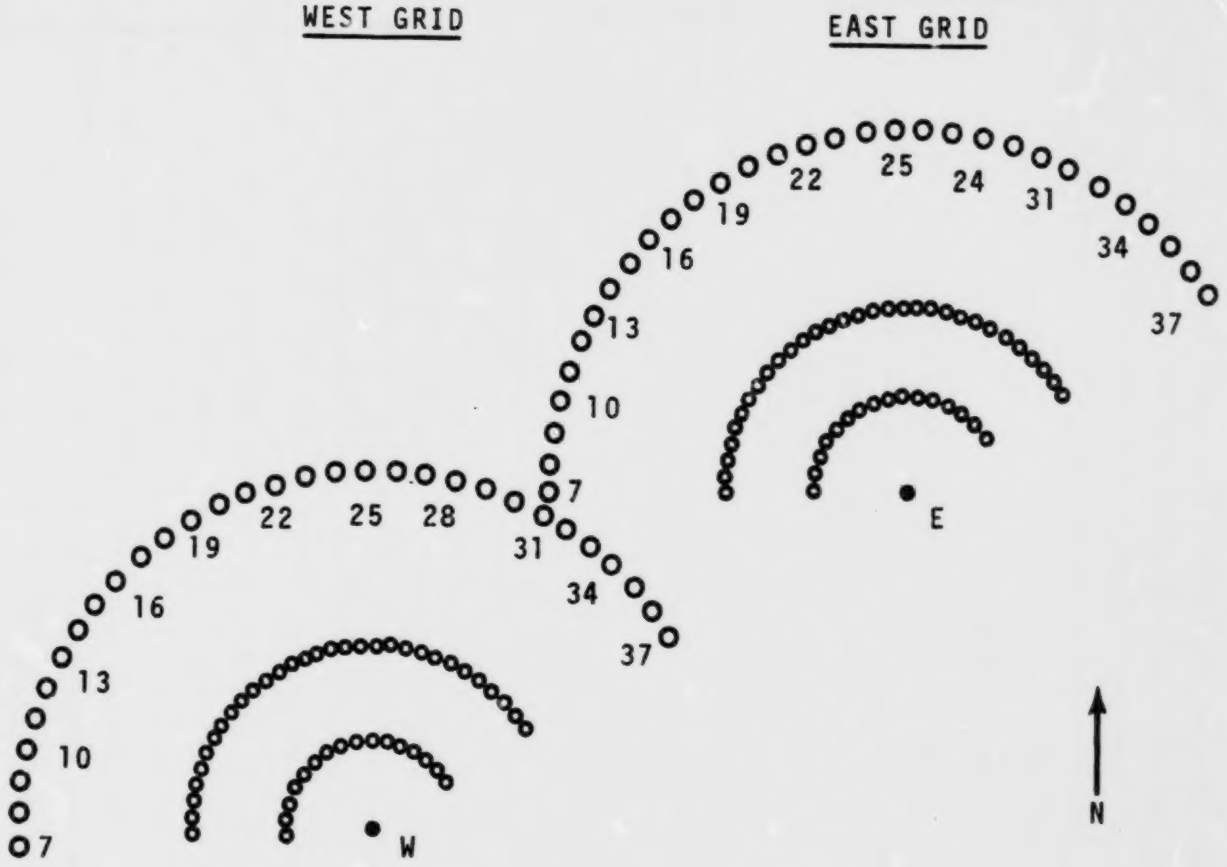
WEST GRID
EAST GRID
7
10
13
16
19
22
25
28
31
34
37
W
7
10
13
16
19
22
25
24
31
34
37
E
N

FIGURE 6. QUILLAYUTE SAMPLING NETWORK - FIRST SERIES.

measured concentrations to compare reasonably well with predictions of the newly-derived models. Figure 7 is an example of such a comparison.

Conclusions of the initial Quillayute series can be itemized as follows:

C-6. SO_2 washout is indeed a reversible phenomenon and desorption can and will occur under appropriate circumstances, which readily exist in the natural atmosphere.

C-7. Solubility of SO_2 in rain depends strongly on rain acidity, and can be accounted for quantitatively.

C-8. The reversible-absorption-based models of washout provide a fairly accurate means of SO_2 washout prediction--at least under the ideal conditions exemplified by the Quillayute studies.

Other aspects of the problem, such as the influence upon washout of time-fluctuations of the plume, were not elucidated adequately by these experiments. In addition, the relative effect of dry deposition was brought into question, and not resolved. To further examine these complications, we felt that an additional series of experiments at Quillayute would be beneficial to the program. These were conducted immediately prior to the power plant runs, which were held at Centralia, Washington, early in 1972. The remaining sections of this report provide a detailed description of these studies.

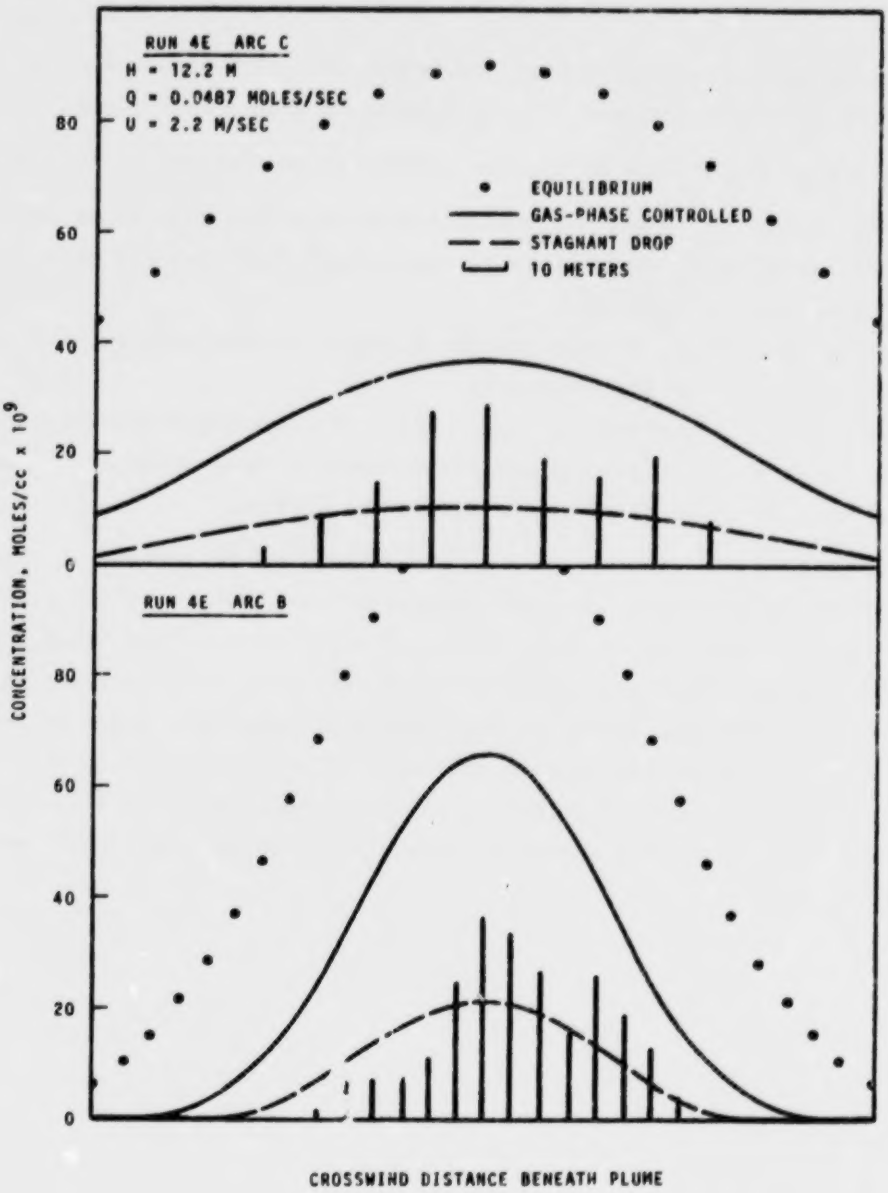

FIGURE 7. PREDICTED AND MEASURED SO_2 CONCENTRATIONS AT QUILLAYUTE - FIRST SERIES. TYPICAL RUN - DASHED AND SOLID CURVES SHOW MODEL PREDICTIONS.

SECTION IV.

PROGRESS IN WASHOUT MODELING

INTRODUCTION

The washout modeling activities of this program, as indicated in Figure 1, have been in progress since the latter stages of the Keystone field series. We have described modeling during earlier phases of this project (DHW); accordingly, this section will concern only modifications of these earlier models, and related progress since the time of the previous report.

MODEL MODIFICATIONS

The nonlinear washout model utilized by the previous study to calculate SO_2 scavenging rates at Quillayute has been modified substantially to increase its versatility, applicability, and numerical accuracy. Additional changes have been made to gain greater simplicity by eliminating features which, at this stage of development, do not appear necessary for the provision of reliable results. A complete description of the nonlinear model is given in Appendix B, and the final version of the computer code (EPAEC) is provided in Appendix C. Modifications of the previous model to formulate this final version are itemized as follows:

1. The Euler algorithm for solution of the basic differential equation for concentration response of a falling drop was replaced by a fourth-order Runge-Kutta technique, resulting in a substantial increase in computational accuracy.
2. The code has been rewritten in terms of a master subroutine (MASTER) enabling an overall program to be written rapidly for a particular plant, topographical situation, and computational requirement. One simply writes a calling program that reads the required data, computes results by the command "CALL MASTER," and prints the results as desired. Alternatively, one can employ the general calling program (EPAEC) listed in Appendix C, and supply appropriate data in the formats required.

3. Equilibrium washout was investigated using the previously-derived criteria (DHW, pg. 20). In terms of a Gaussian plume superimposed on a constant background level, this may be expressed by the form

$$\frac{-6\pi K_y H'\bar{u}\sigma_y\sigma_z^2 y_{Ab}\big|_{\text{ground level}}}{v_t a Q \exp(-\frac{1}{2} - \frac{1}{2} y^2/\sigma_y^2)} > \text{constant}. \qquad (1)$$

Here,
a = drop radius,
H' = modified Henry's law constant,
h = release height,
K_y = overall mass transfer coefficient,
σ_z and σ_y = plume dispersion parameters in the z- and y-directions.

A more complete definition of these terms is provided in Appendix B and in the table of nomenclature, Section X.

By observation of computed values, it was found that scavenged gas concentrations in raindrops will be within one percent of the equilibrium values whenever (1) is satisfied with the constant being set equal to 15. This condition was incorporated with the computer code, allowing bypass of the normal computation scheme under such conditions. This feature results in a considerable savings in computer time when washout at large downwind distances is calculated.

4. The provision for a general wind profile has been eliminated. This was done primarily because of our finding that the amount of effort required to account for wind shear is not justified by sufficiently increased accuracy in prediction. This feature can be written back into the code at a later date, if desired

5. A feature to incorporate plume loft into the model was added. This is performed simply by including as data a "loft velocity" which recalculates the effective stack height for each downwind distance. This results essentially in a linearly lofting plume model, which is useful for calculations for points near the source.

6. Chemical-reaction decay of SO_2 is incorporated into the model by assuming a quasi-first-order gas-phase reaction. Various reaction rates can be accommodated by adjustment of the rate constant, which is read as input data.

7. Background SO_2 influences are accounted for. The background SO_2 concentration is supplied as input data.

As indicated by the documentation and flow chart given in Appendix C, this model retains the advantages of modular construction, so that various components may be replaced easily, if desired. The Pasquill-Gifford plume model[6] used here, for example, can be replaced by a more sophisticated counterpart, simply by replacing the subroutine YAB. Similarly, the wash out of gases other than SO_2 may be calculated with this model upon supplying the appropriate input data after replacing the solubility subroutine HPRIME, which applies specifically to the system SO_2-H_2O. Additional aspects of the washout computer code are discussed in detail in Appendix C.

RAINDROP MICROPHYSICS

Previous calculations of mass transfer to stagnant drops performed during this project have been based upon a linearization of the liquid-phase mass transfer coefficient,[3]

$$k_x = \frac{5D_{Ax}c_x}{a} \quad , \qquad (2)$$

where D_{Ax} is the diffusivity of SO_2 in water, and c_x is the total liquid phase concentration (nominally 1/18 moles/cm^3 for water). Equation (2) is based upon the concentration response of a stagnant drop experiencing a linear increase of gaseous pollutant concentration in time. Since raindrops do not generally experience linear increases, however, Equation (2) is only an approximation to actual stagnant-drop behavior. A rigorous solution for these circumstances was presented in HTW on page 40; use of this result in the washout model however, requires knowledge of an interfacial concentration and necessitates time-consuming iterative calculations.

The above problems can be avoided by deriving a rigorous drop-response equation that is based on the bulk gas concentration rather than that existing at the drop surface. This was accomplished in the present study by combining the equation for mass transport through the gas phase

$$N_{Ao} = -k_y(y_{Ab} - Hx_{Ao}) \quad , \tag{3}$$

with the equation expressed in HTW, page 40, subject to step-function concentration forcing, and applying Duhamel's theorem.[7] The result is

$$x_{Ab} = \frac{6\beta}{H} \int_o^{\hat{t}} \{[y_{Ab}(\hat{t} - \tau) - Hx_{Ai}] \sum_{n=1}^{\infty} \exp(-\alpha_n^2\tau)[\frac{\alpha_n^2 + (\beta - 1)^2}{\alpha_n^2 + \beta(\beta - 1)}]$$

$$\sin \alpha_n[\frac{1}{\alpha_n^2} \sin \alpha_n - \frac{1}{\alpha_n} \cos \alpha_n]\}d\tau + x_{Ai} \quad , \tag{4}$$

where H = Henry's law constant, (see Nomenclature)

N_{Ao} = flux of SO_2 from the drop surfaces,

k_y = gas-phase mass transfer coefficient,

x_{Ab} = bulk mole fraction of A in liquid,

x_{Ai} = initial mole fraction of A in liquid,

x_{Ao} = interfacial mole fraction of A in liquid,

y_{Ab} = bulk mole fraction of A in gas,

$\hat{t} = D_{Ax} \cdot \text{time}/a^2$

α_n = roots of $a\alpha \text{Cot} a\alpha + a\beta - 1 = 0$,[8]

$\beta = Hak_y/c_x D_{Ax}$.

The assumption of constant H has entered into the derivation of (4). This constraint can be eliminated in numerical applications, however, simply by recalculating a "constant" H as numerical computation proceeds.

PLUME WASHDOWN

Lowering of altitude of a gaseous plume by virtue of the uptake-release action of falling rain has been examined to determine the importance of this effect insofar as practical scavenging calculations are concerned. Assessment of this effect requires solution of the coupled conservation equations for pollutant in the rain and in the gas phase;[3] it presents a more complex approach than that taken in previous modeling, which was based essentially upon the assumption that the rain had no effect on the position of the plume.

A number of alternative mathematical approaches to this problem were considered. We finally found, however, that the most fruitful approach was to combine the coupled, linearized conservation equations, apply repeated Fourier and Laplace transformations to remove all differential forms, and then invert to obtain the solutions.

Inversion of the transformed equations was performed to give, for the gaseous plume,

$$y_{Ab}(t,y.z) = \frac{Q}{\sqrt{2\pi}\ \bar{u}\sigma_y} \frac{\exp\{\frac{-y^2}{2\sigma_y^2}\}\ \exp\{\frac{-[z-(h-wt)]^2}{2\sigma_z^2+4w\delta t}\}}{(2\pi\sigma_z^2+4\pi w\delta t)^{\frac{1}{2}}} , \qquad (5)$$

which posesses a characteristic "washdown velocity" given by $w = JH(c_y/c_x)$, J being the rainfall rate and c_y and c_x being the total molar concentrations of matter in the gas and liquid phases, respectively. δ is a characteristic length parameter defined in Appendix D.

A detailed description of the derivation of (5) is given in Appendix D, and it will suffice here to provide an example to indicate the predictions of this analysis insofar as practical modeling aspects are concerned. For this example we have chosen a rain-plume situation characterized by the parameters given in Table 1, which are representative of actual rains and SO_2 characteristics. For reasons of simplicity, we have chosen a "plume"

TABLE 1. BASIC DATA USED FOR WASHDOWN CALCULATION.

Rain Rate, J	10^{-4} cm/sec
Raindrop Diameter, a	.03 cm
Terminal Velocity, v_t	-300 cm/sec
Mass-transfer Coefficient, K_y	8.2 moles/cm^2 sec
Effective Henry's Law Constant, $(H \frac{c_y}{c_x})$	3.3×10^3

with zero diffusion for this example, which is sufficiently realistic for illustrative purposes.

Solutions of Equation (5) for the above conditions are shown in Figure 8, where the concentration of the gaseous SO_2 plume is plotted versus height for a number of discreet transit times ($t = x/\bar{u}$). In this plot the initial plume (an impulse function at $t = 0$) is seen to spread out in a downward direction as it is washed down by the rain.

The primary result of this analysis is the indication that, although the gaseous plume is indeed "washed down," this effect is not a highly significant one for SO_2 plumes over the time and distance scales of interest to this project. The "nonfeedback" aspect of the EPAEC model (i.e., the assumption that the rain does not affect the plume's shape), is therefore justifiable under these circumstances.

A word of caution, however, is in order about the application of these results to other gases. The source of concern is in the use of handbook values for H obtained at high concentrations of the gases. In some cases, e.g., N_2O, CH_4, tritium compounds, krypton, etc., for which simple solutions of the gases are formed, this is probably acceptable and the results predict that such plumes would fall orders of magnitude more slowly than an SO_2 plume. For other gases which are strongly dissolved, the washdown effect can be appreciable. Ammonia gas, for example, is about ten times as soluble in water as SO_2, resulting in an order-of-magnitude increase in the washdown effect. This could indeed be a significant factor for the assessment of the environmental impact of an NH_3 plume.

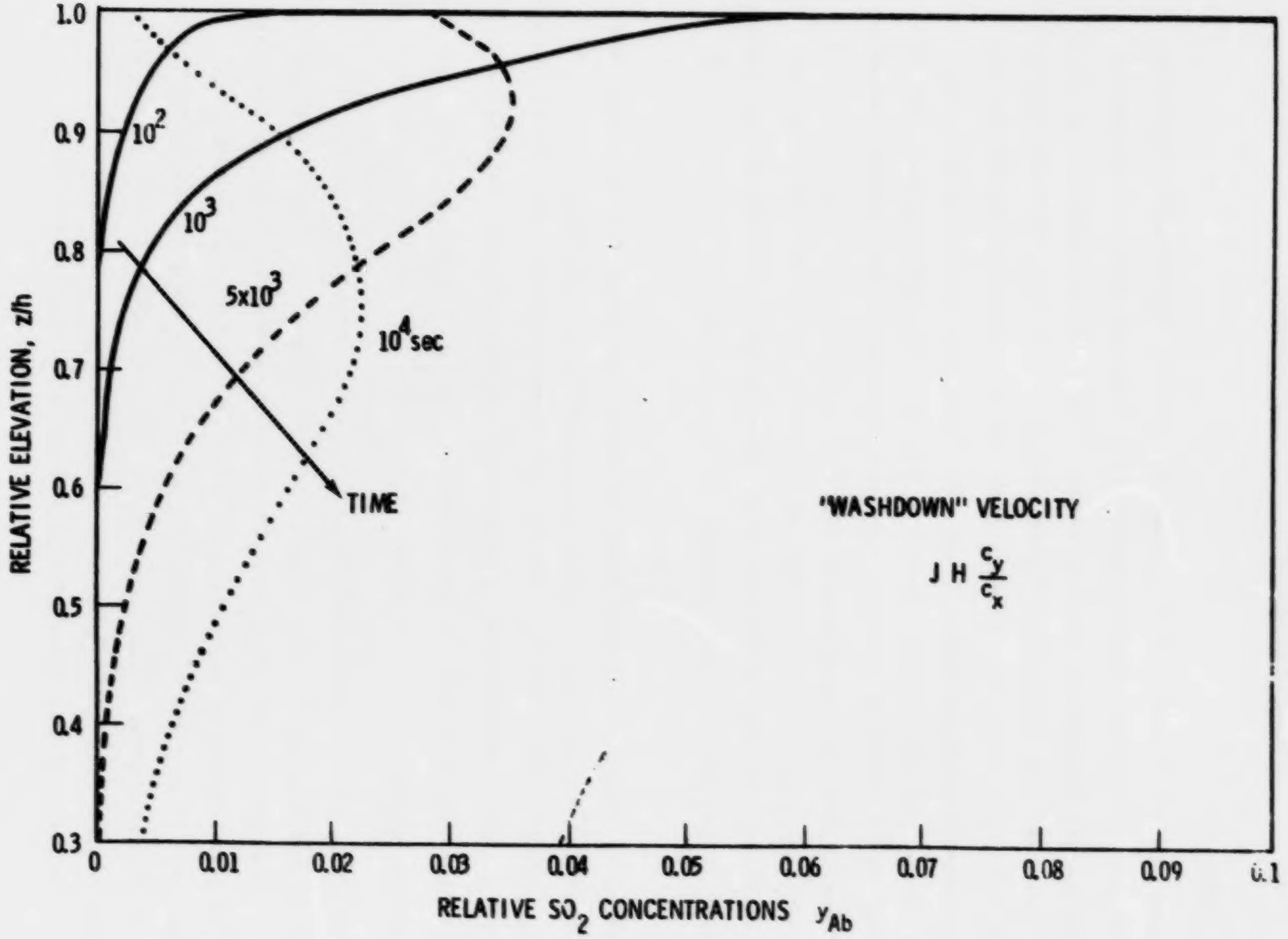

FIGURE 8. THE REDISTRIBUTION OF AN SO_2 PLUME CAUSED BY WASHOUT.

SECTION V.

SECOND-SERIES QUILLAYUTE EXPERIMENTS

INTRODUCTION

The second series of controlled-release SO_2 washout experiments conducted at Quillayute during November-December, 1971, was designed to supplement knowledge gained during the initial series. This design involved an expansion of the sampling array to overcome some physical difficulties experienced earlier, and thus provide more cases of well-defined desorption behavior (higher release heights in contrast with low-level releases) for further testing of the washout models. More distant sampling was also desired, in anticipation of a closer approach to equilibrium washout behavior. Special measurement techniques were added to evaluate the contribution of dry deposition to SO_2 concentrations measured in collected rain. We expected also that an additional series of experiments would expand the range of natural conditions--as they pertain to washout--against which to test the models.

Realization of these objectives required additional sampling equipment and a slightly modified procedure; these changes will be described below. In general, however, the basic methods are the same as those reported in detail previously, (DHW); accordingly, a repetition of the complete collection and analysis procedure will not be given here.

EXPERIMENTAL METHOD

Sulfur dioxide was released from two independent regulated systems, utilizing polyethylene tubes for its transfer to the tops of portable telescoping towers. In general, the tower releases were at different heights, and were conducted simultaneously to ensure identical meteorological conditions. The flow rate of SO_2 was controllable, but previous results indicated that use of different release rates for the two sources added little to the significance of the results. Therefore, for all washout experiments in the series, a convenient SO_2 flow rate of 0.04 gram-moles/sec was used.

During the previous Quillayute series, the full release height of 30.5 m was not generally usable because the wind speeds encountered (usually above 5 m/sec) caused the raindrops to fall at such an angle that those which entered the collectors would have undercut the plume. Thus, for this series, we modified the earlier grid (shown in Figure 6) to include a sampling line at a greater distance from the source on the east grid. The west grid was left as before. The new sampling arrangement is shown in Figure 9. The more distant line (Line D), whose samplers averaged 290 m from the source, was placed such that the maximum release height of 30.5 m could be used with nearly all observed wind speeds. Line D was situated, for convenience, along the existing warming apron and taxistrip configuration of the airport.

The behavior of plumes originating lower than 30.5 m was investigated earlier; the experience led us to choose a convenient west grid release height which would be sufficiently different from that of the east grid to reflect the influence of reversibility. The choice was 16.8 m. Table 2 lists sampling geometry and release parameters which apply to all the washout runs of the current series.

TABLE 2. RELEASE AND SAMPLING PARAMETERS-QUILLAYUTE SECOND SERIES.

Grid	Tower Height, m	Operative Arcs[a]	SO_2 Release Rate Q, mole/sec
East	30.5	C, D	0.04
West	16.8	A, B, C	0.04

[a] A arc - 30.5 m
B arc - 61.0 m
C arc - 122 m
D line - 290 m (average)

The rain samplers--the locations of which are shown as points in Figure 9--consisted of waste basket-mounted funnels attached to 250 ml plastic bottles. The bottles were precharged with a small amount of tetrachloromercurate (TCM) solution for fixing of the SO_2 in the rain water. Air concentration measurements with simple bubblers were deleted from the procedure for the regular

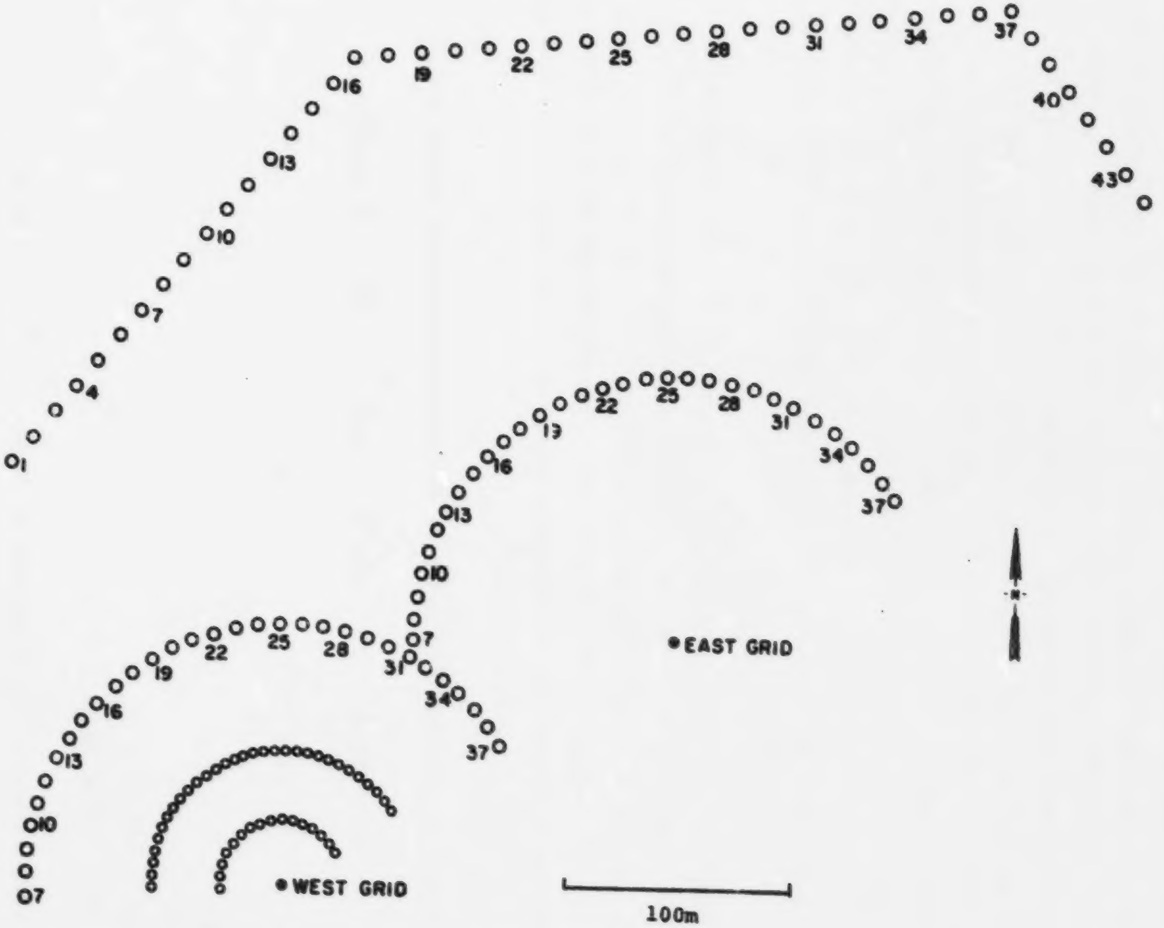
1
4
7
10
13
16
19
22
25
28
31
34
37
40
43
1
7
10
13
16
19
22
25
28
31
34
37
7
10
13
16
19
22
25
28
31
34
37
EAST GRID
WEST GRID
100m

FIGURE 9. QUILLAYUTE SAMPLING NETWORK - SECOND SERIES.

sampling arcs because past experience has shown these measurements to be nearly in agreement with concentrations calculated from a bivariate-normal diffusion model. Bubblers were used on Line D, however, since such measurements had not been made at that distance before. Sulfur dioxide concentrations in the sampled rain and the bubbler fluid were analyzed as before using Technicon Autoanalyzers in the mobile laboratory at the site.

Wind data were collected by Gill three-component anemometers, mounted at the SO_2 release points. A third such anemometer, located atop a small tower midway between the release towers, was added to the current study. The height of the third Gill was 8 m; thus, for all the dual SO_2 release experiments, complete wind data were collected at heights of 8, 16.8 and 30.5 m.

Additional supporting equipment included a raindrop size spectrometer (raindrops sized by image sizing of spots from water sensitive paper) and a fast-response rain gauge. These, plus the translators and magnetic recorder for the Gills, were located at the control trailer, midway between the release towers. Figures 10 and 11 are photographs showing the experimental layout and equipment.

A typical dual-release experiment proceeded as follows: the source towers were raised to their appropriate heights, and the mean wind speed and direction were determined. If the direction was suitable for sampling on both grids (wind approximately normal to the tower baseline) and the rain was sufficiently steady, the sampling funnels were deployed and the SO_2 generators made ready. Upon signal from the field director, the bottles and bubblers were set out, with SO_2 releases following immediately. During the releases, the Gill recorder was operated and monitored by the field director. The usual release time was ten or twenty minutes, shortened at the discretion of the field director, as dictated by wind and rain conditions. At the conclusion of the release, the bubblers and rain samples were returned to the laboratory, where analysis generally commenced immediately. On all occasions, the chemical analyses were completed within 24 hours of the experiment.

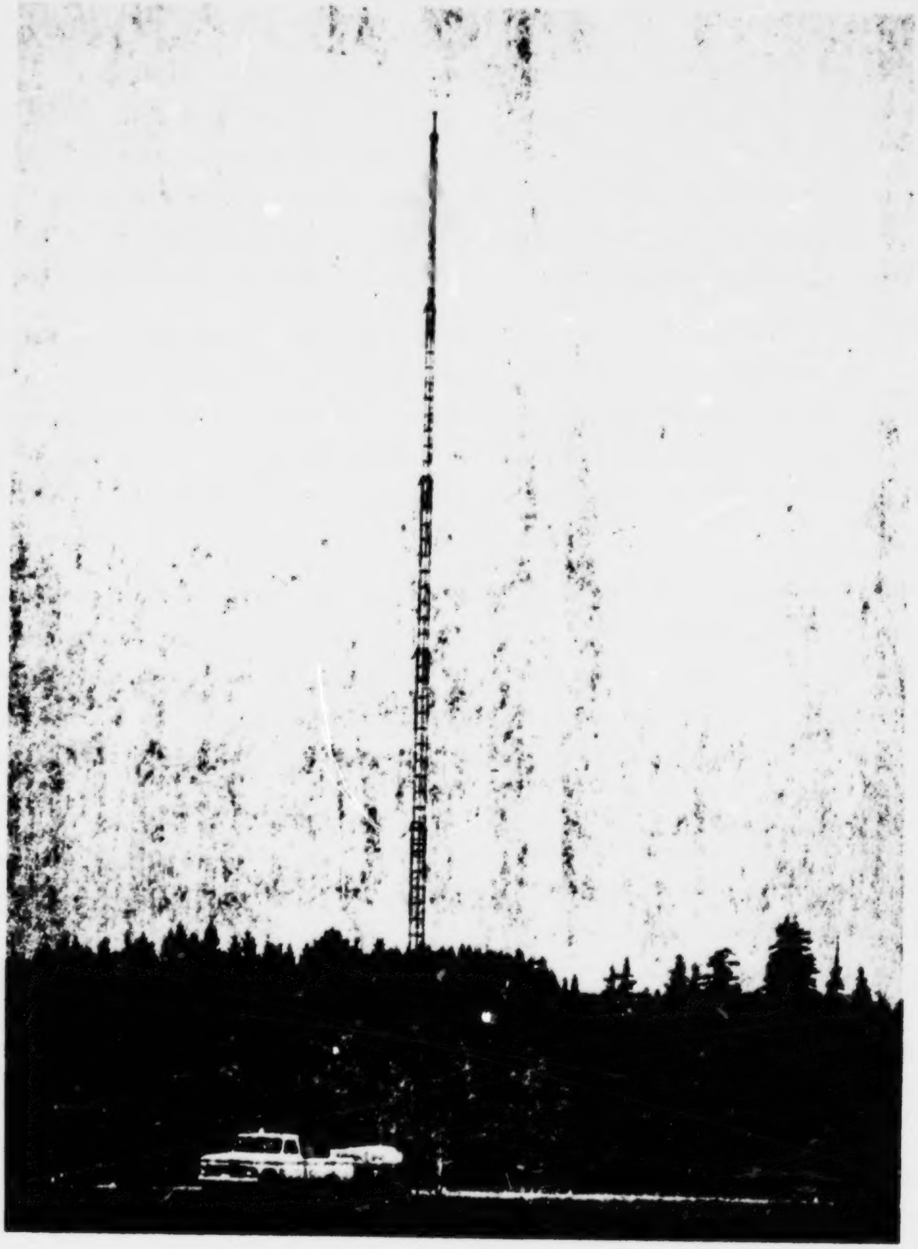

FIGURE 10. 30.5 m SO_2 RELEASE TOWER - QUILLAYUTE SECOND SERIES.

Reproduced from
best available copy.

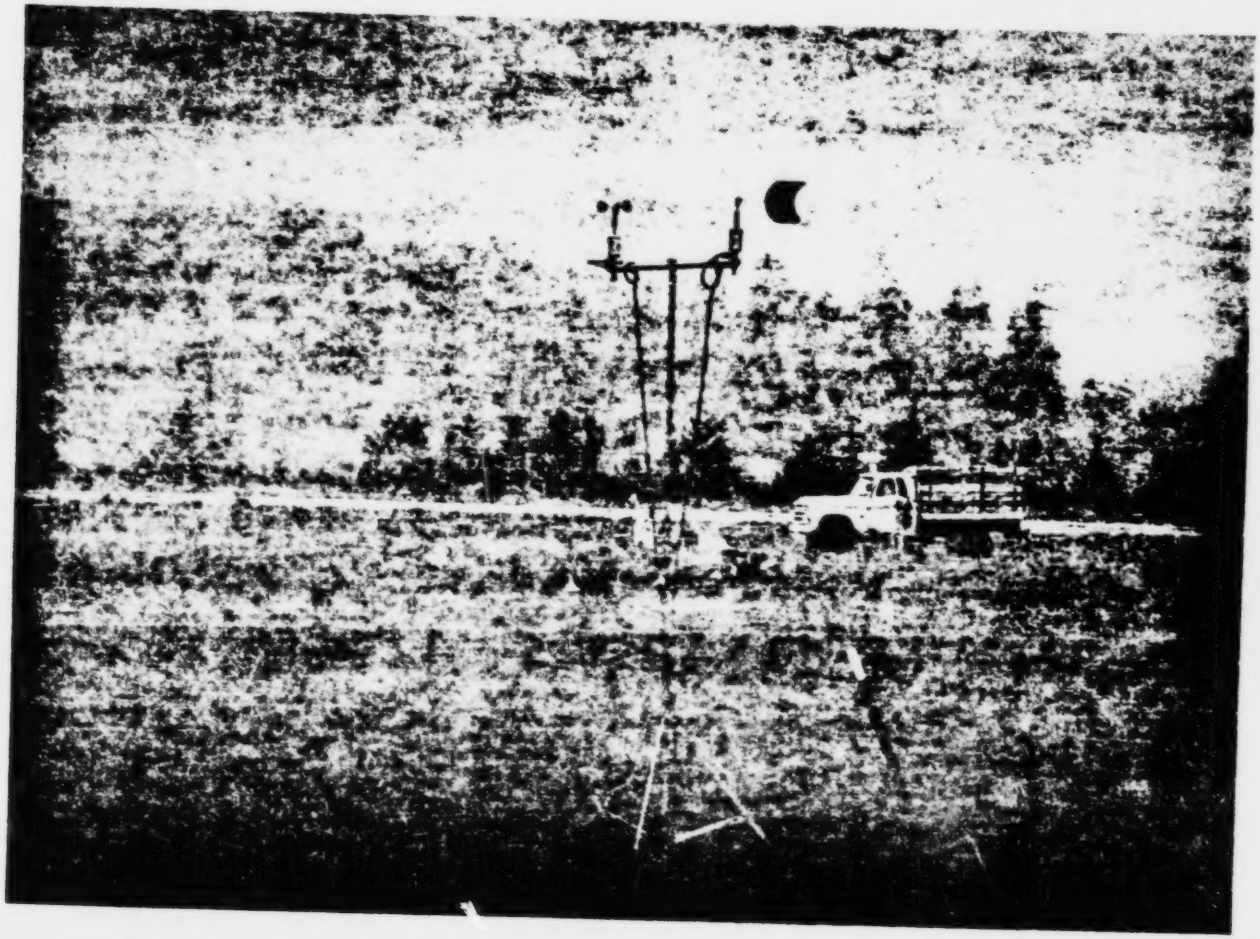

FIGURE 11. PORTION OF THE WEST SAMPLING ARCS - QUILLAYUTE SECOND SERIES.

EXPERIMENTAL RESULTS--WASHOUT MEASUREMENTS

During the field period November 29-December 17, 1971, fifteen SO_2 releases were made for the purpose of washout measurement. These consisted of five dual-releases and five single releases. The latter were the result of several different situations. The first run, Run 11 (Runs 1-10 are the experiments of the initial Quillayute series in March-April, 1971), was conducted on the east grid only because of a temporary shortage of SO_2 cylinders. Run 17 was conducted on the west grid only so that concurrent dry deposition measurements could be made, using personnel normally assigned to the east grid. Runs 18-20, all on the same day, were also west grid only because the wind direction was not favorable for using both grids. This opportunity, however, was utilized to make dry deposition measurements on the west grid during these runs. Table 3 lists pertinent run conditions. The dry deposition experiments, which will be described later in this chapter, are included in this table for chronological placement.

The rainfall encountered during the experimental period was mainly of the continuous pre- or near-frontal passage type, which is characteristic of the site during the winter months. With few exceptions--namely Runs 13 and 20, which were probably convective showers and occured near the end of storms--the rain was continuous and of remarkable constancy in rainfall rate. A number of raindrop size spectra were collected and one or two from each run were sized using a Zeiss particle counter. Table 4 is a listing of the raindrop spectra selected from these data, which were deemed typical of the runs. The spectra are consistent in character with pre-frontal continuous rain spectra observed in the past at Quillayute. The exceptions, the spectra for Runs 13 and 20, were typical convective shower spectra, consisting mainly of relatively small raindrops.

Data obtained from the Gill anemometers were processed by translating the Metrodata tapes to IBM-compatible tapes using a special-purpose computer. These new tapes were then processed on a UNIVAC 1108 system to produce mean and short-term wind speeds and directions, and standard deviations (σ_φ and σ_θ) for a variety of sampling and averaging times. The computer program employed for this purpose utilized the following equations:

TABLE 3. TIMES, TEMPERATURES, AND RAINFALL RATES-QUILLAYUTE SECOND SERIES.

Run No.	Date	Time, PST	Rainfall Rate, mm/hr	Temperature, °C
11 E	12-4-71	1355-1407	1.5	4.4
12 E	12-8-71	1039-1058	2.7	5.0
12 W	12-8-71	1039-1058	2.7	5.0
13 E	12-8-71	1438-1445	1.7	9.4
13 W	12-8-71	1438-1445	1.7	9.4
D1[a]	12-9-71	1155-1215	1.3	
D2[a]	12-11-71	1122-1133		
D3[a]	12-11-71	1154-1205		
14 E	12-11-71	1329-1349	1.8	2.2
14 W	12-11-71	1329-1349	1.8	2.2
15 E	12-11-71	1502-1521	1.1	2.2
15 W	12-11-71	1502-1517	0.88	2.2
16 E	12-13-71	1321-1337	2.2	2.2
16 W	12-13-71	1321-1337	2.2	2.2
17 W[b]	12-13-71	1513-1523	2.5	2.2
18 W[c]	12-16-71	0940-0950	3.1	8.3
19 W	12-16-71	1108-1118	3.2	8.3
20 W	12-16-71	1512-1522	1.1	8.3

[a] Dry deposition run

[b] Includes dry deposition run D4

[c] Includes dry deposition run D5

TABLE 4. RAINDROP SIZE FREQUENCY[a] DISTRIBUTIONS-QUILLAYUTE SECOND SERIES.

	Diameter, cm									
Run No.	.024	.030	.038	.046	.060	.074	.094	.118	.148	.190
11	.22	.14	.105	.085	.105	.095	.095	.075	.045	.035
12	.135	.16	.275	.11	.095	.080	.065	.045	.03	.005
13	.22	.13	.07	.07	.11	.12	.08	.13	.07	
14	.27	.167	.157	.107	.093	.07	.05	.043	.027	.016
15	.16	.155	.215	.12	.11	.09	.065	.055	.025	.005
16	.17	.19	.17	.11	.13	.09	.06	.06	.02	
17	.25	.23	.21	.20	.04	.06	.01			
18	.272	.32	.241	.106	.018	.017	.017	.009		
19	.11	.19	.29	.24	.06	.03	.02	.05	.01	
20	.60	.15	.12	.05	.02	.02	.04			

[a] Tabulated values are the proportion of raindrops contained in the interval between the diameter of that entry and the preceding diameter.

$$\bar{u} = \frac{((\Sigma u)^2 + (\Sigma v)^2)^{\frac{1}{2}}}{N} , \qquad (6)$$

$$\bar{\theta} = 180° - 57.3 \frac{\Sigma(\tan^{-1} \frac{u}{v})}{N} , \qquad (7)$$

$$\sigma_\theta = \{\frac{\Sigma([\tan^{-1} \frac{u}{v}]^2)}{N} - [\frac{\Sigma(\tan^{-1} \frac{u}{v})}{N}]^2\}^{\frac{1}{2}} , \qquad (8)$$

$$\sigma_w = \{\frac{\Sigma w^2}{N} - [\frac{\Sigma w}{N}]^2\}^{\frac{1}{2}} , \qquad (9)$$

$$\sigma_\varphi = \frac{\sigma_w}{\bar{u}} , \qquad (10)$$

where N is the number of discrete data points sampled and the remaining terminology, as defined in Section X, takes its usual significance.

Average values of the wind parameters obtained from the anemometer data in the above manner are given in Table 5; the values of σ_φ and σ_θ given

TABLE 5. WIND PARAMETERS CALCULATED FROM ANEMOMETER DATA-QUILLAYUTE SECOND SERIES

Run	h	$\bar{\theta}$, deg.[b]	$\bar{u}$, cm/sec	Arc A[a]		Arc B[a]		Arc C[a]		Line D[a]		VERT[c] cm/sec	Run Time, sec
				σ_θ	σ_θ	σ_ϕ	σ_θ	σ_θ	σ_ϕ	σ_θ	σ_ϕ		
11	8	156	495	.270	.231	.256	.206	.236	.173	.210	.125	+24	
	16.8	152	477	.266	.384	.251	.352	.226	.302	.183	.239	+29	
	30.5	154	585	.237	.335	.224	.310	.212	.274	.177	.222	+23	710
12	8	149	492	.237	.267	.216	.236	.183	.201	.156	.152	+29	1090
	16.8	153	543	.243	.344	.227	.312	.200	.263	.159	.190	-0.3	1091
	30.5	156	619	.182	.270	.173	.246	.158	.210	.131	.159	+50	1088
13	8	199	404	.213	.213	.200	.174	.191	.146	.171	.117	+28.5	378
	16.8	202	494	.199	.279	.187	.253	.167	.217	.145	.171	+57	376
	30.5	202	516	.182	.333	.170	.317	.154	.287	.129	.247	-25	378
14	8	155	389	.221	.278	.209	.246	.195	.209	.168	.158	+6.1	1088
	16.8	152	327	.244	.364	.220	.323	.186	.275	.134	.206	+14	1090
	30.5	158	454	.222	.331	.206	.309	.184	.273	.157	.210	+31	1088
15	8	145	410	.283	.279	.266	.250	.244	.196	.198	.160	+17	1092
	16.8	146	367	.310	.426	.282	.387	.250	.336	.199	.264	+29	1085
	30.5	153	524	.208	.313	.196	.284	.178	.240	.156	.193	+20	1089
16	8	181	328	.177	.241	.168	.220	.151	.173	.127	.121	+10	922
	16.8	185	297	.204	.346	.193	.312	.176	.270	.152	.226	+18	923
	30.5	186	441	.184	.269	.177	.256	.163	.227	.138	.205	+17	921
17	8	164	402	.255	.309	.232	.284	.203	.238	.166	.176	+27.5	546
	16.8	161	454	.268	.383	.252	.351	.239	.314	.201	.256	+23.5	544
	30.5	161	584	.227	.258	.216	.235	.197	.213	.167	.161	+3.59	545
18	8	191	188	.139	.163	.130	.140	.124	.102	.084	.082	+5.4	538
	16.8	203	179	.218	.436	.206	.390	.192	.326	.167	.243	+22	545
19	8	227	347	.194	.194	.182	.169	.165	.125	.141	.084	-1.3	546
	16.8	228	325	.242	.279	.234	.253	.222	.217	.206	.163	+1.7	545
20	8	213	287	.200	.224	.183	.203	.167	.177	.108	.113	+20.7	584
	16.8	217	245	.213	.314	.202	.268	.182	.237	.157	.158	-6.5	585

[a] Standard deviations in radians

[b] Degrees deviation from true north

[c] Average vertical velocity

here are based on sampling and averaging times equal to the SO_2 release times and one-fourth the transit times, respectively; values actually used for EPAEC computations are underlined. Standard deviations calculated for additional combinations of sampling and averaging times were utilized for various exploratory analyses of the washout data; these will be described later in this section.

Results of the SO_2 analyses of collected rainwater are shown in Figures 12 through 24, which are distribution plots of rainfall concentration *versus* wind direction. The solid bars represent the observed concentrations; the lines show the results of EPAEC model calculations, which will be discussed in the analysis section. The lower figure in each case is the deposition for the inner sampling arc and the upper figure is the more distant arc (line). The distributions are essentially complete, indicating containment of the plume by the deployed collectors. Run 13 is not included in these figures, because of an early termination of the shower. Very little rain fell during the actual release time, which led to severe dilution of the SO_2 content by the previous heavier rain; thus, little detectable SO_2 was present. Inactive sampler regions are indicated by cross-hatching. In most of the dual-release runs, some SO_2 from the west source was deposited on Line D, which was outfitted with collectors to receive east-grid SO_2. Thus, the distributions for the west source on Line D are not complete, and concentrations are indicated there only for Runs 12 and 16, where suitable sampling and separation occurred. Complete rain concentration data are tabulated in Appendix A.

The total deposition of SO_2 for each arc was determined, and washout rates (the amount of SO_2 deposited per unit distance downwind per unit time) calculated using the approximation

$$M \cong \frac{\Sigma m_i \Delta y}{AT} \quad , \tag{11}$$

where Σm_i is the total amount of SO_2 collected on the arc, Δy is the distance between collectors on the arc, A is the area of one precipitation collector (1000 cm^2), and T is the time of the release. These washout rates are listed in Table 6, in terms of both absolute values and percentages of the emission rate.

TABLE 6. MEASURED WASHOUT RATES
QUILLAYUTE SECOND SERIES

Run	Arc	M, (moles/sec cm) × 10^{10}	M/Q, (percent /cm) × 10^5
11 E	C	25.9	0.65
	D	56.0	1.40
12 W	B	41.4	1.04
	C	99.5	2.49
E	C	8.22	0.21
13[a] E	B	0	0
	C	2.54	0.06
W	C	0.71	0.02
	D	0.94	0.02
14 W	B	66.5	1.67
	C	143	3.58
E	C	30.5	0.76
	D	60.6	1.52
15 W	A	10.3	0.26
	C	85.4	2.14
E	C	18.6	0.46
	D	58.4	1.46
16 W	A	29.0	0.73
	C	146	3.65
	D	119	2.98
E	C	41.0	1.03
	D	b	b
17 W	A	9.86	0.25
	C	189	4.72
18 W	B	103	2.58
	C	214	5.35
19 W	B	31.0	0.78
	C	127	3.18
20 W	B	14.6	0.37
	C	53.9	1.35

[a] Due to early stop of generation, concentrations measured marginal. Non-zero values of M represent measurable rain concentration in only one sampler.

[b] Overlap plumes from two sources occured.

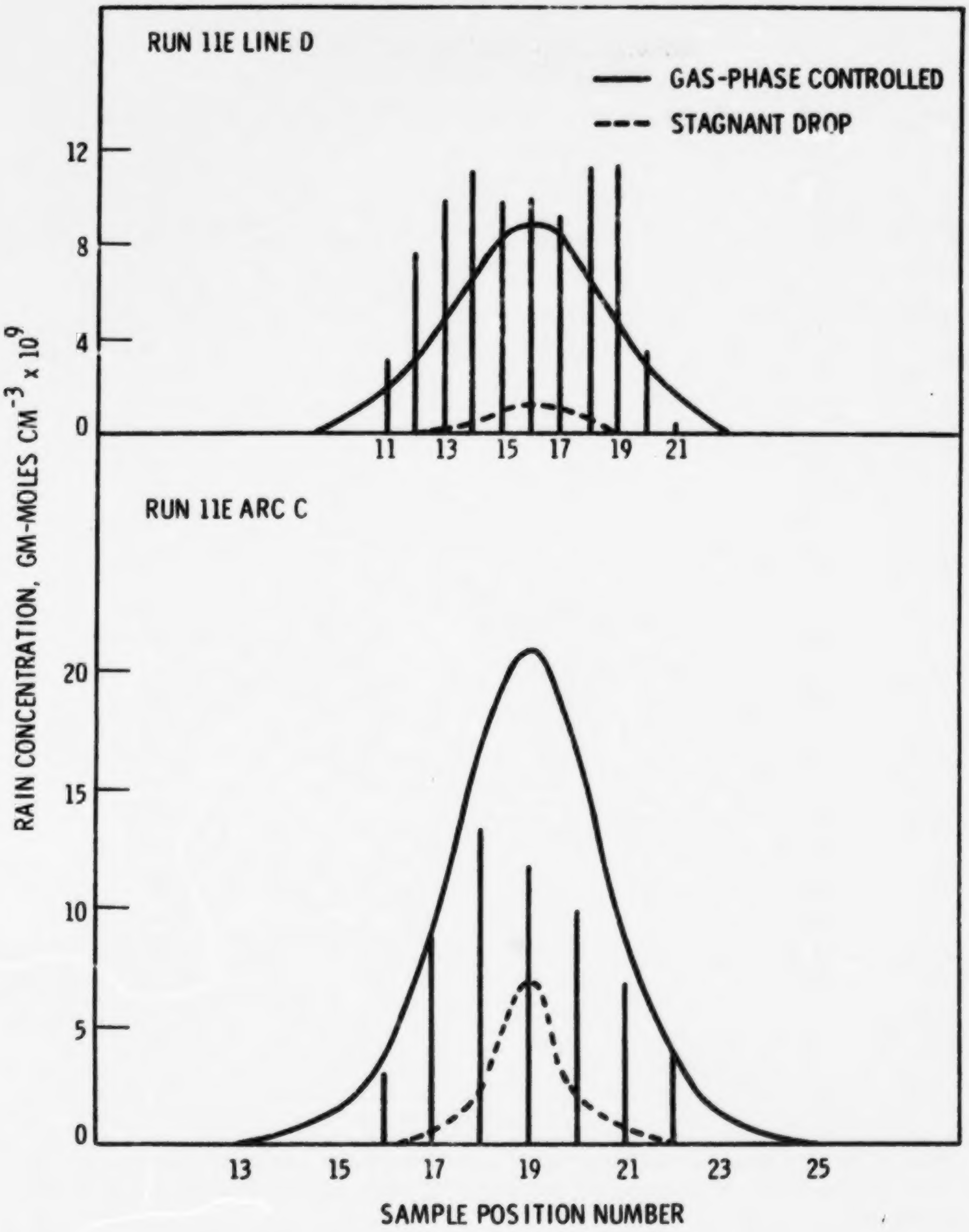

FIGURE 12. MEASURED AND CALCULATED SO_2 CONCENTRATION IN RAIN - RUN 11.

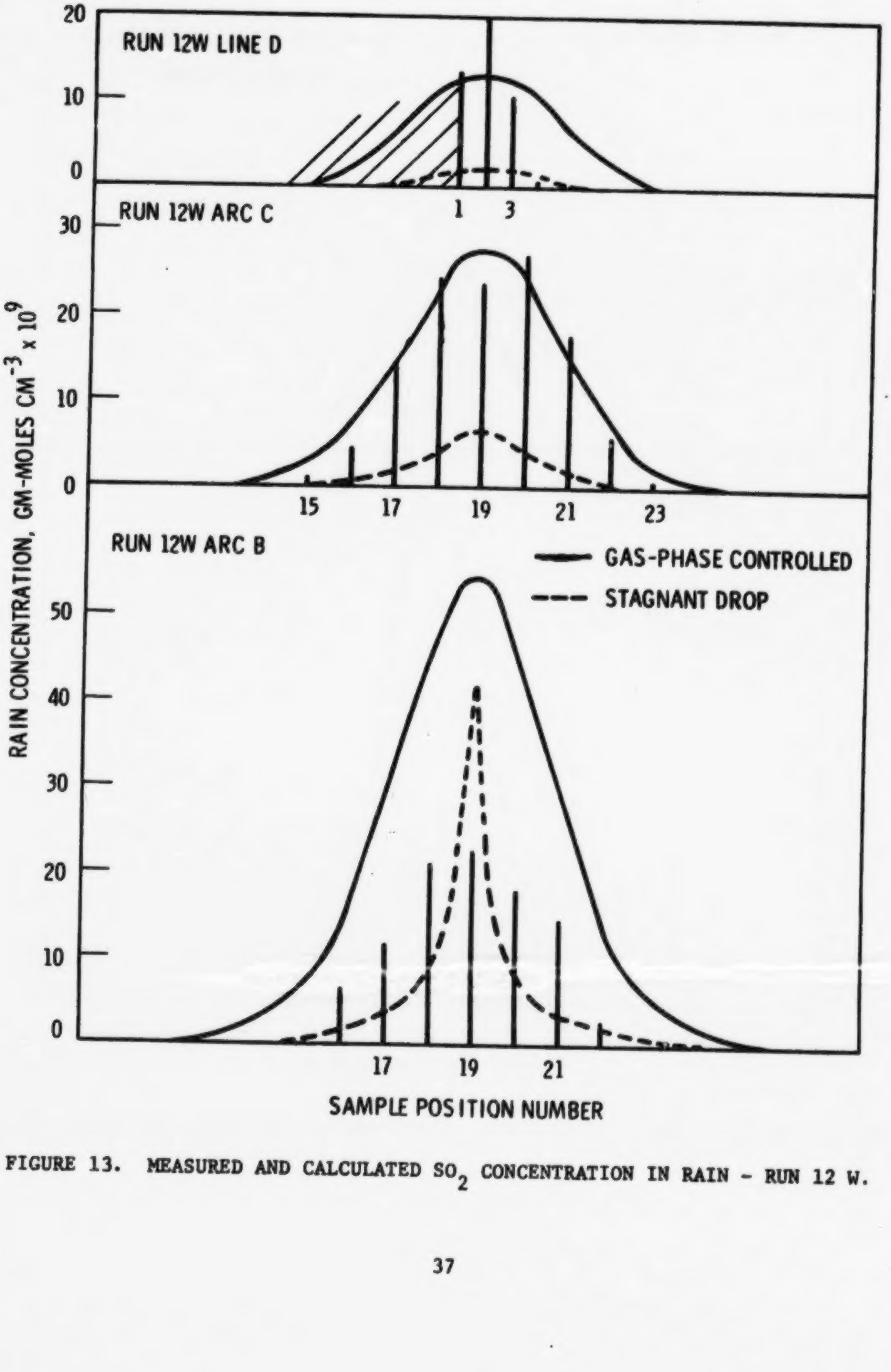

FIGURE 13. MEASURED AND CALCULATED SO_2 CONCENTRATION IN RAIN - RUN 12 W.

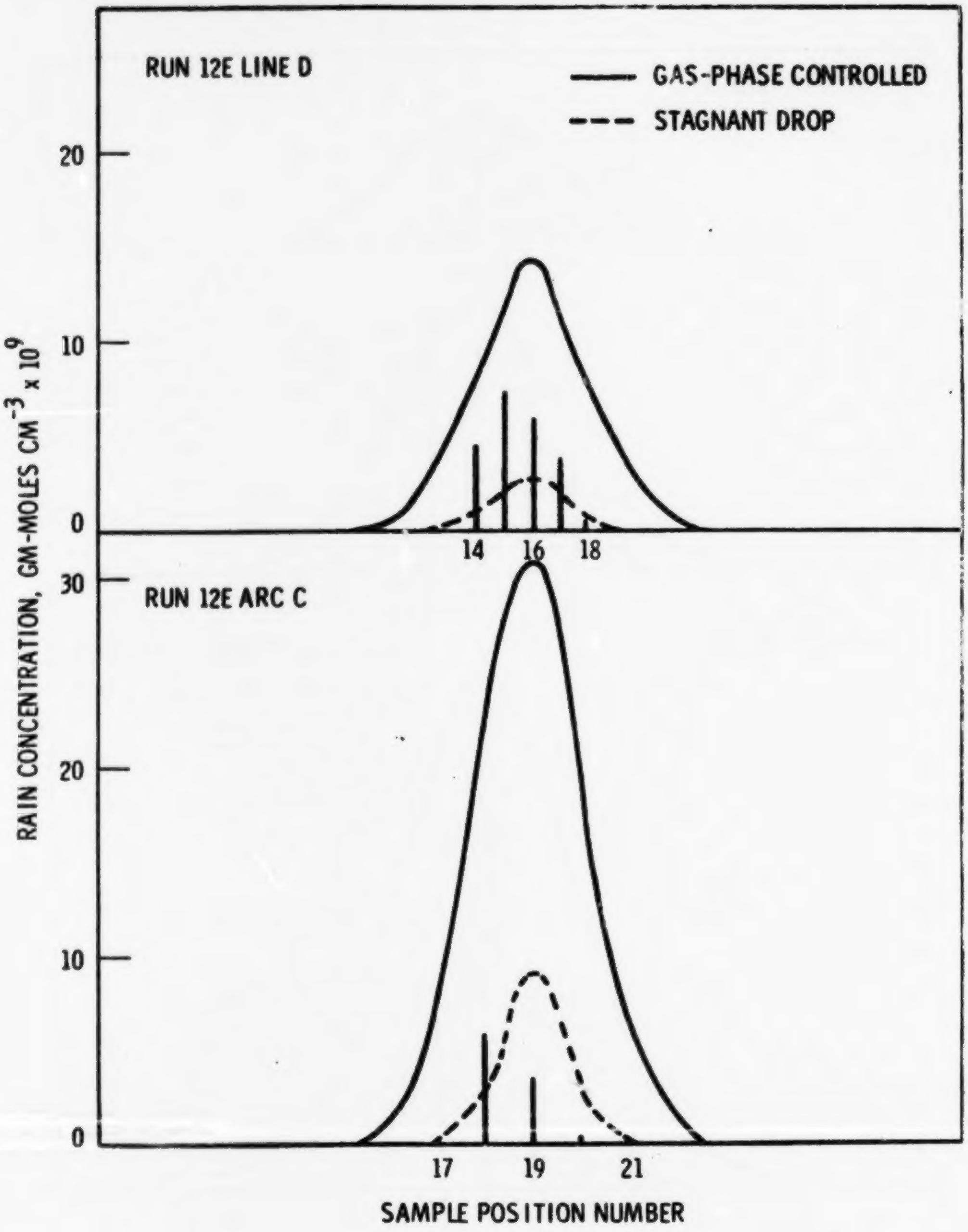

FIGURE 14. MEASURED AND CALCULATED SO_2 CONCENTRATION IN RAIN - RUN 12 E.

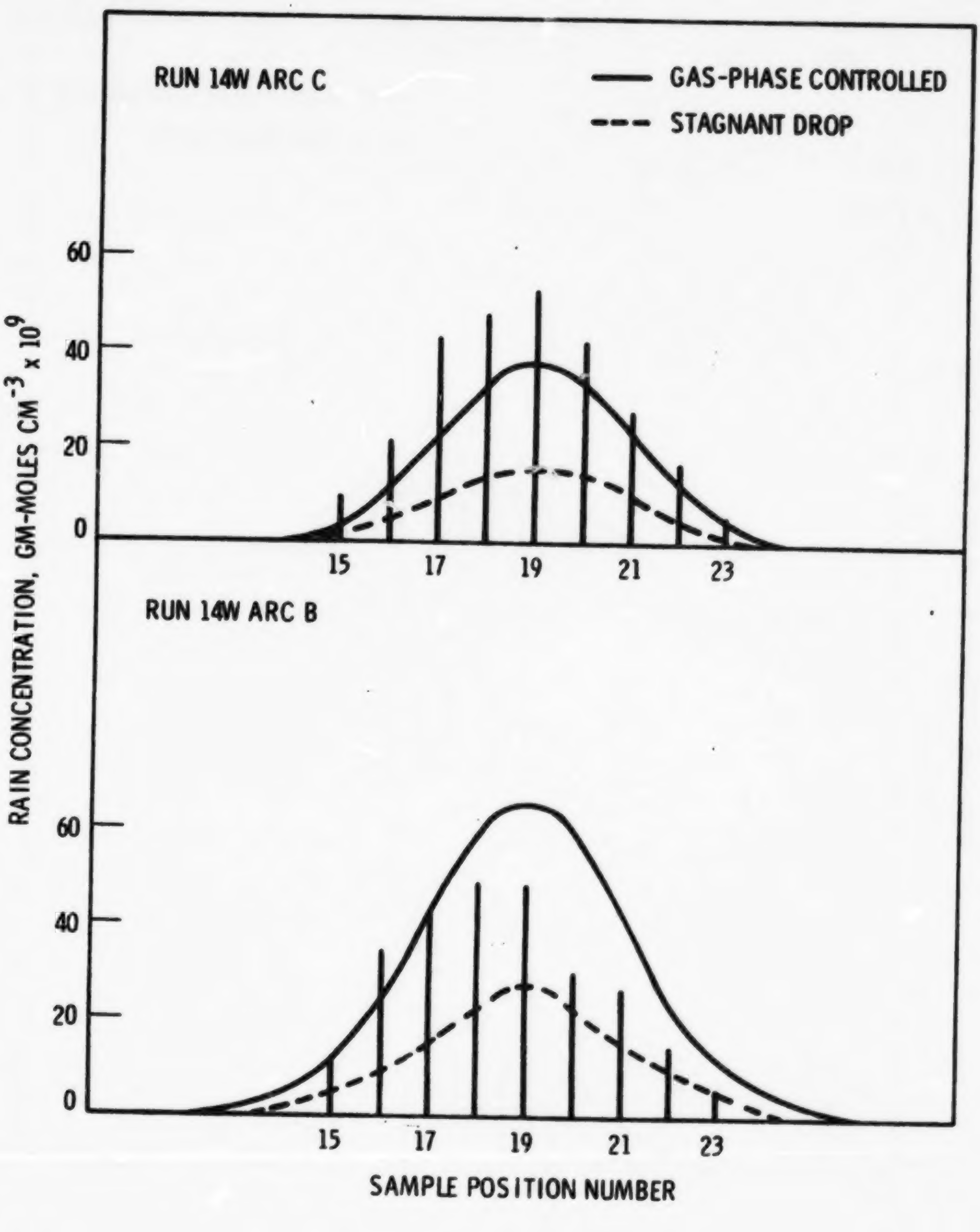

FIGURE 15. MEASURED AND CALCULATED SO_2 CONCENTRATION IN RAIN - RUN 14 W.

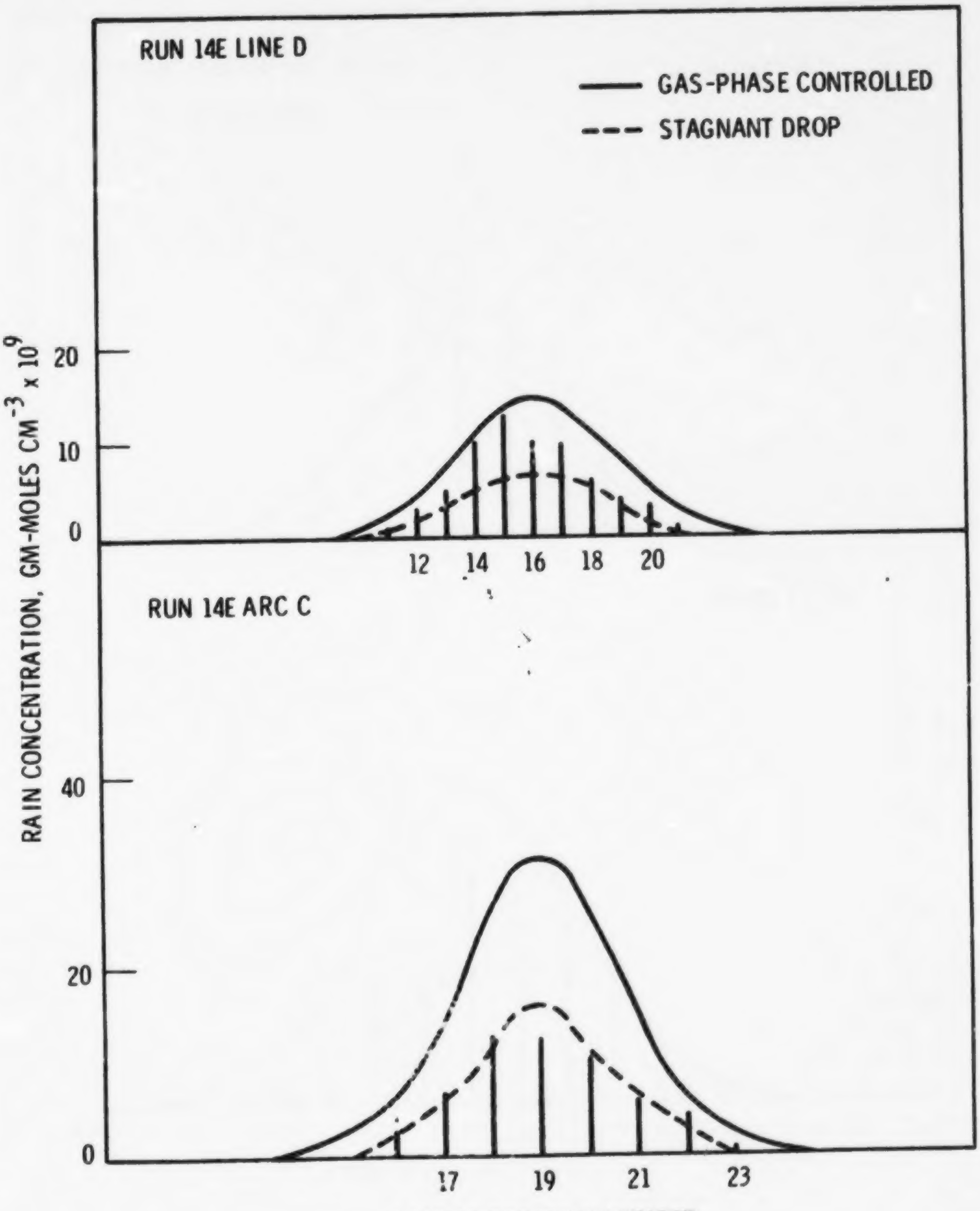

FIGURE 16. MEASURED AND CALCULATED SO_2 CONCENTRATION IN RAIN - RUN 14 E.

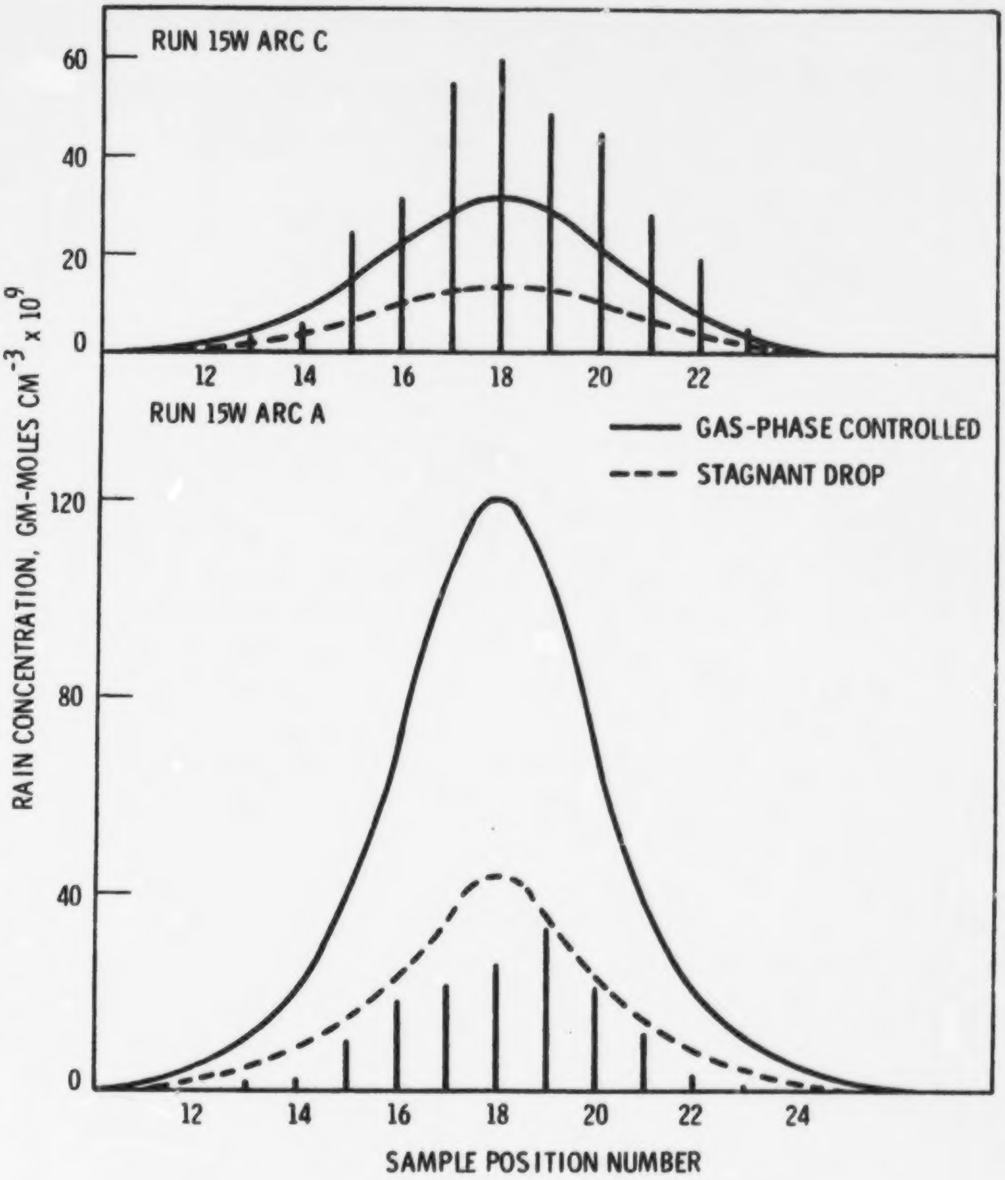

FIGURE 17. MEASURED AND CALCULATED SO_2 CONCENTRATION IN RAIN - RUN 15 W.

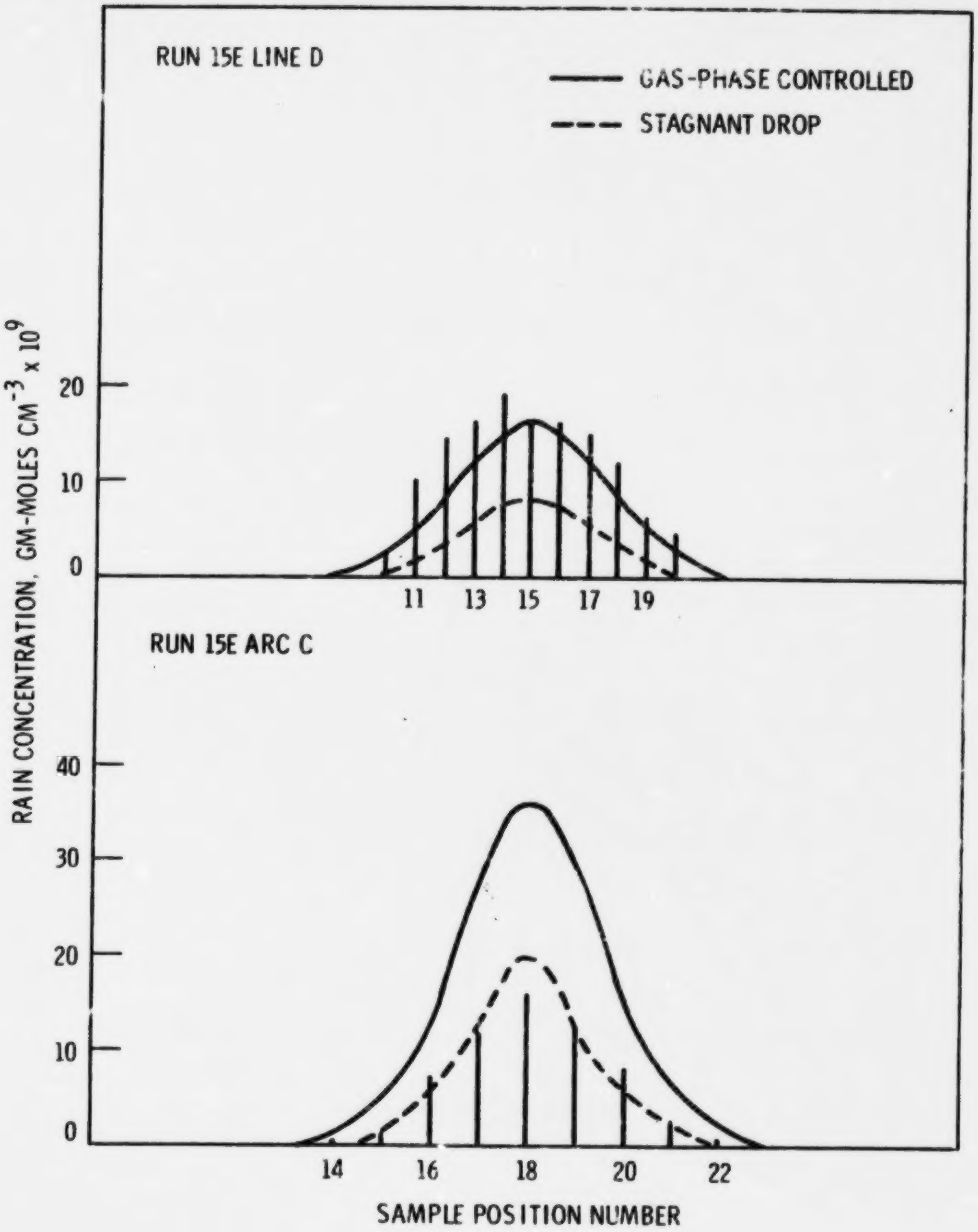

FIGURE 18. MEASURED AND CALCULATED SO_2 CONCENTRATION IN RAIN - RUN 15 E.

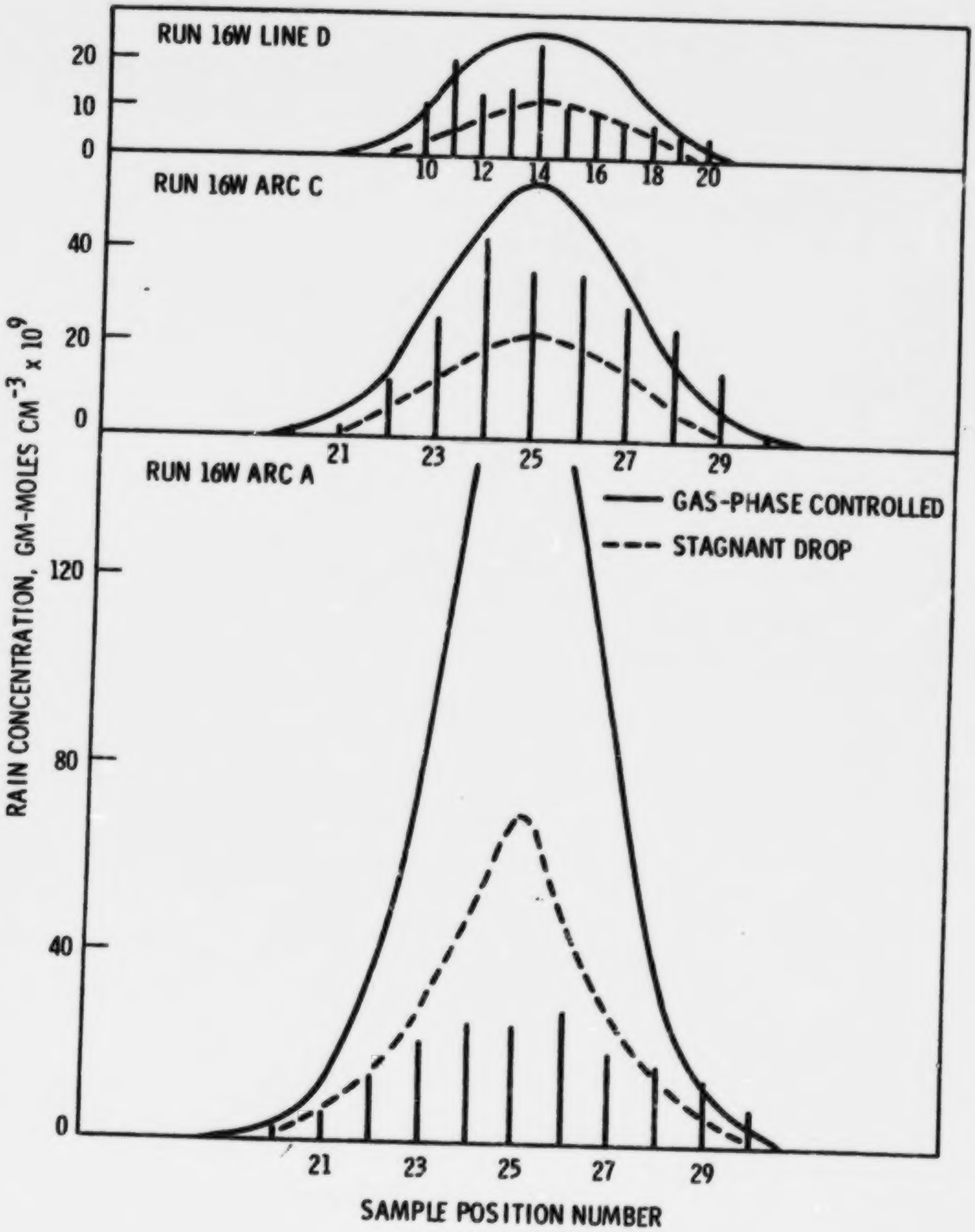

FIGURE 19. MEASURED AND CALCULATED SO_2 CONCENTRATION IN RAIN - RUN 16 W.

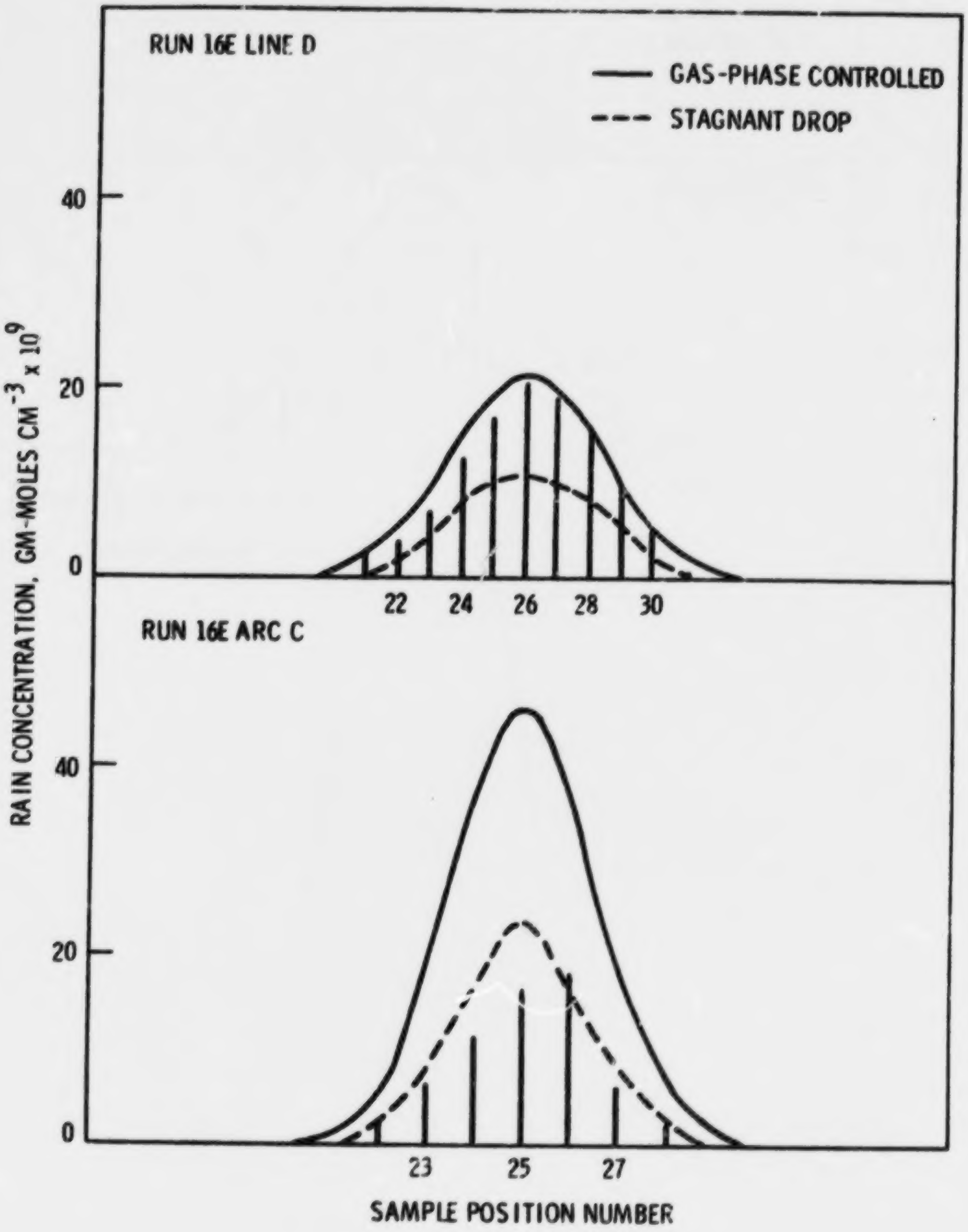

FIGURE 20. MEASURED AND CALCULATED SO_2 CONCENTRATION IN RAIN - RUN 16 E.

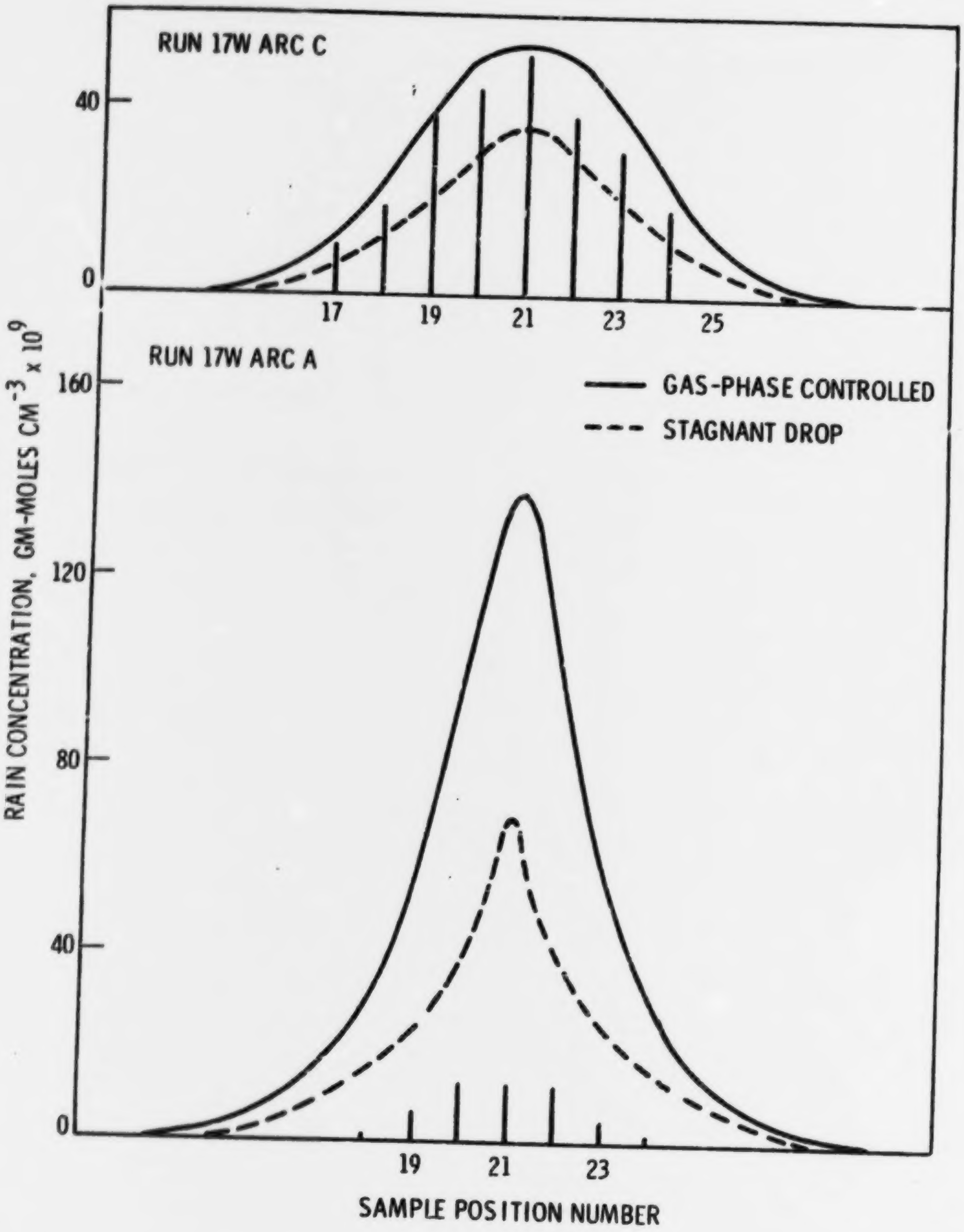

FIGURE 21. MEASURED AND CALCULATED SO_2 CONCENTRATION IN RAIN - RUN 17.

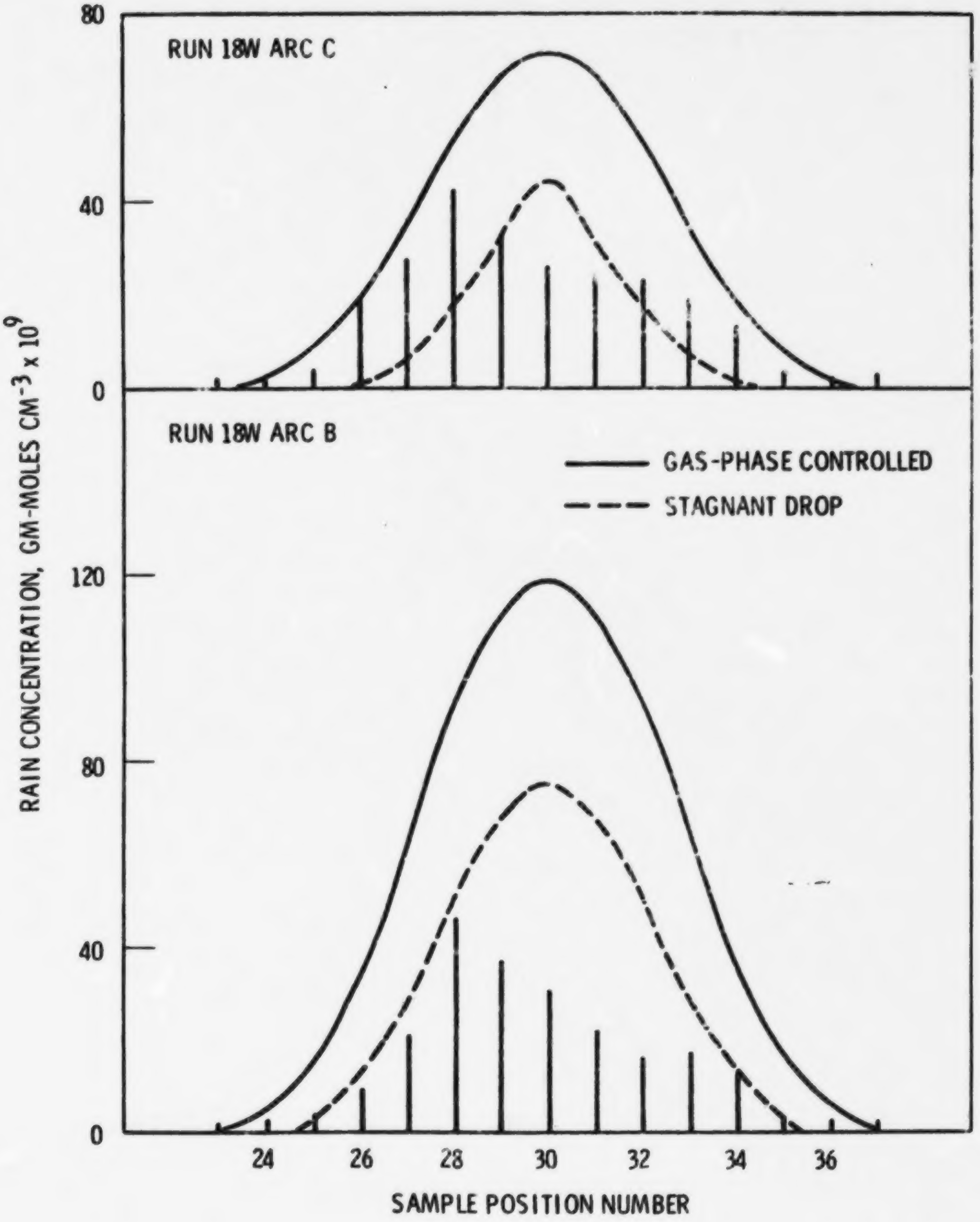

FIGURE 22. MEASURED AND CALCULATED SO_2 CONCENTRATION IN RAIN - RUN 18.

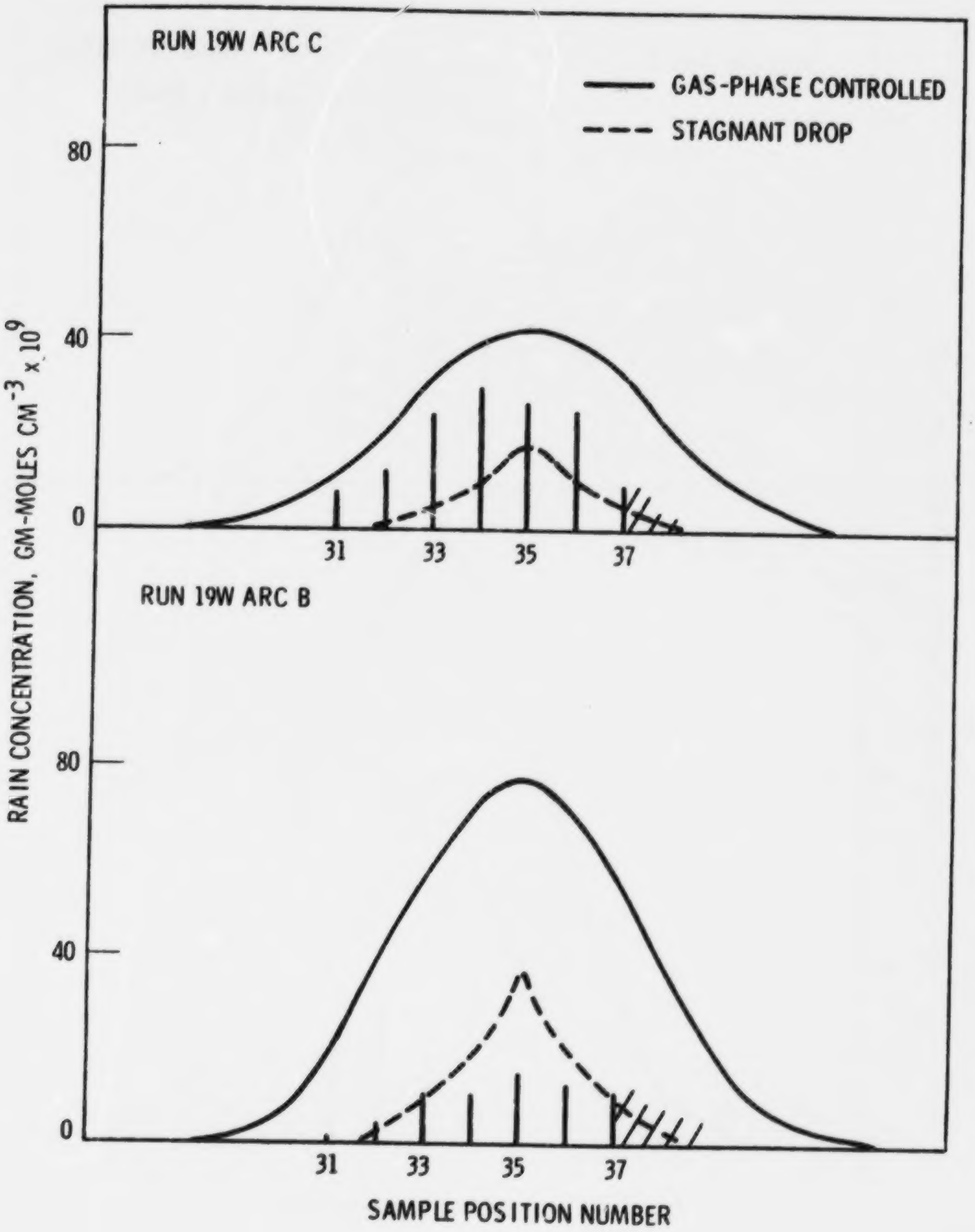

FIGURE 23. MEASURED AND CALCULATED SO_2 CONCENTRATION IN RAIN - RUN 19.

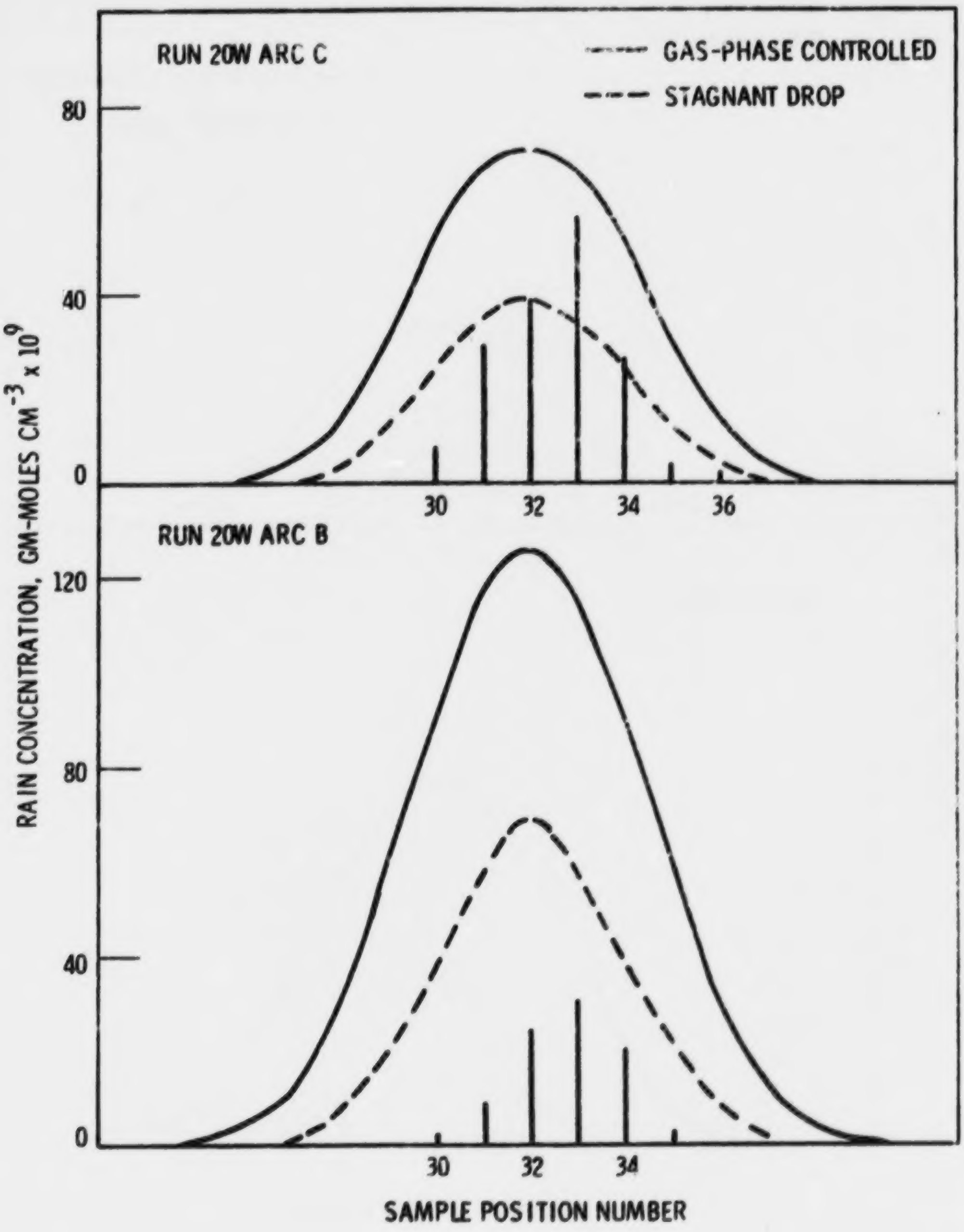

FIGURE 24. MEASURED AND CALCULATED SO_2 CONCENTRATION IN RAIN - RUN 20.

ANALYSIS OF WASHOUT RESULTS

The experimental results presented in the previous sections were analyzed by comparison with predictions of the EPAEC model, based on the input data given in Tables 2 through 5. As noted previously, these calculations were performed using plume-spread parameters based on sampling and averaging times of the SO_2-release time and one-fourth the source-receptor travel time, respectively, indicating the tacit assumption of mean-plume behavior. These calculations were based on assumptions identical to those of the analysis of previous Quillayute data (DHW); aside from the improvements in the numerical algorithms of the EPAEC code, therefore, the calculations are similar and are directly comparable. As seen from the comparisons of results given in Figures 12 through 24, the computed values generally tend to be close to those observed, although the agreement does not seem to have improved from that found in the previous study. Values tend to fall between the well-mixed drop--stagnant drop limits, and worse agreement between the computed and observed values is found, generally, for near-source sampling Arcs A and B. These characteristics also can be observed from Figure 25, which is a plot of observed washout rates (M from Table 6) *versus* those computed from the EPAEC model. In Figure 25, the limits of the tie lines pertain to gas-phase limited and stagnant drop behavior.

The experimental results, similar to those observed previously, reflect the presence of reversible washout. This effect is shown much more clearly and dramatically by the Centralia results in the following section, however, and discussion of this effect will be limited here. The observations at the new, more distant sampling line (Line D) conform with model predictions in an acceptable manner, giving further evidence of applicability of the washout model and its basic precepts.

The relatively poor agreement between observed and calculated washout rates at close downwind distances is thought to be primarily a consequence of plume "undercutting" by the rain, combined with poor definition of the plume near the source resulting from the point-source approximation. The EPAEC model provides for the possibility of plume undercutting by the raindrops; however, the resulting trajectories are strongly dependent on raindrop size and any

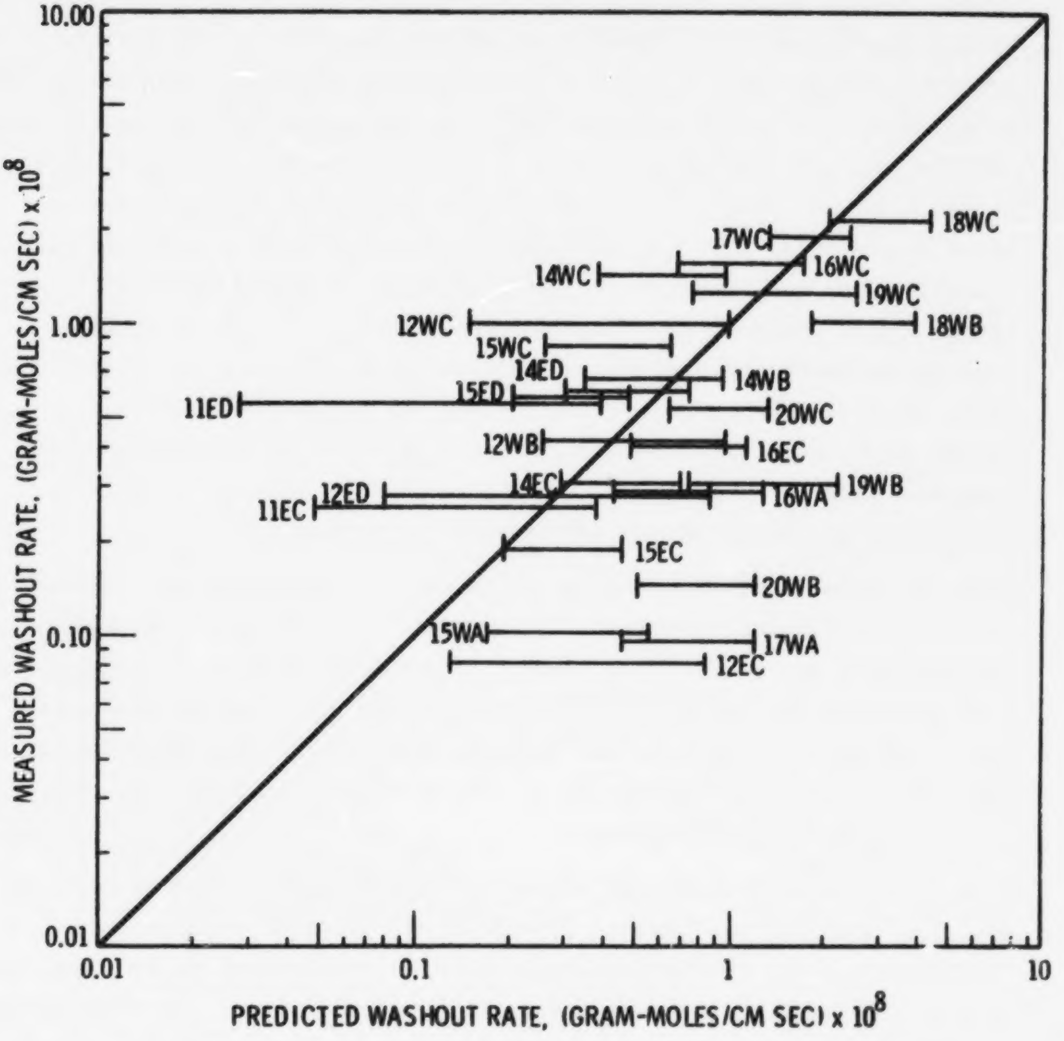

FIGURE 25. MEASURED *versus* PREDICTED SO_2 WASHOUT RATES - QUILLAYUTE SECOND SERIES.

degree of non-representation of true conditions by the measured spectra will seriously affect the resulting calculations. This is particularly true for showery rain conditions (Runs 13 and 20), where the rain spectra are characterized by smaller raindrops, and are quite variable over short time periods. Additionally, the extremely high concentrations predicted by the plume model at distances near the source (∞ at (0,0,h)) are unrealistic and cause inaccuracies in the numerical computations. If an incoming drop, as envisioned by the model, just clears the release point and encounters the "plume," a few centimeters, say, downwind from the source, it will experience an extremely high concentration for a short time period. The computer code will recover itself from the resulting perturbation--at the expense of numerical accuracy, however. These aspects lead to the conclusion that although the EPAEC code leaves much to be desired insofar as near-source calculations are concerned, the noted lack of agreement does not at all challenge the validity of its basic precepts, particularly with regard to reversibility. An additional noteworthy point in this regard is the possibility of SO_2 desorption from rain during its time of residence on the funnel surfaces of the samplers. The fact that the washout model consistently overestimates observed concentrations on the inner arcs suggests that such an effect may indeed have been present; the discrepancy between observed and predicted results may have arisen more from an inability to measure washout precisely under these conditions than from any shortcomings of the model. This possibility will be reviewed in greater detail in a later section where the dry deposition measurements of this project are discussed.

During this program we applied a number of variations of the basic EPAEC model in attempts to improve agreement with the experimental results. Each of these variations falls into one of the following two classifications:

1. Attempts to improve the raindrop-microphysics component of the EPAEC model;
2. Attempts to improve the spatial and temporal definition of the plume-model component of the EPAEC model.

After rather extensive investigation we concluded that such elaborations did not improve washout predictions sufficiently to warrant their incorporation into the basic computer code. For this reason we will not provide the detailed results of these investigations here; rather, we will only itemize and summarize them in the following paragraphs.

Stagnant Drop Response

As discussed in Section IV, the stagnant-drop option of the EPAEC code--as it exists presently--is based on the quasi-steady-state, linearized mass-transfer coefficient

$$k_x = \frac{5D_{Ay}c_x}{a} \quad , \tag{2}$$

the more rigorous relationship being given by Equation (4). Equation (4) can be incorporated into the EPAEC code at the expense of additional computer time and complexity, an interpolation or search routine for the roots α_n being required. Test solutions employing Equation (4) however, were found to approach those corresponding to Equation (2) closely under practical conditions. In view of this finding, and in view also of the magnitudes of deviations caused by other features of the model, we have concluded that incorporation of this more rigorous equation is not desirable under present circumstances. As a consequence, the stagnant-drop option of the computer listing in Appendix C is presented in terms of the less exact approach.

Equilibrium Washout

On the basis of the previously developed washout theory, equilibrium washout (SO_2 concentration in rain in equilibrium with that in air at ground level) should occur under conditions satisfying the criterion of Equation (1). The Quillayute test conditions do not, in general, satisfy this criterion. In the previous report (DHW), however, we observed that in many cases experimental washout concentrations were near those calculated assuming equilibrium conditions in conjunction with a fluctuating (peak-to-mean) plume description. At that time it was apparent that this behavior occurred primarily because of a coincidental overlap of predictions based on equilibrium behavior and that assumed by the EPAEC model. This behavior also suggested two possible additional explanations, however. The first of these was that dry deposition and desorption of SO_2 from rain on the sampler surfaces is extremely rapid, and tends to mask the effects of washout.

Further dry deposition tests and the experimental results from Centralia, both to be described later in this report, provided evidence contrary to the two alternative explanations given above. In view of these findings we terminated further application of equilibrium-based theory to the Quillayute results.

Lofting-Plume Modification

Anemometer data from the Quillayute tests indicated a vertical component of average wind velocity that ranged between -.25 and +.57 meters per second with positive values predominant. The exact cause of this non-zero component is unknown, although it probably resulted from upwind orographic complexities. If this trend continued for long distances downwind, it could effectively loft the SO_2 plumes and consequently affect washout behavior. This possibility was tested by supplying appropriate loft velocities (VERT in the computer code) to the EPAEC model. The results of these tests showed washout rates to be rather insensitive to loft in the ranges possible at Quillayute, hence further analysis of this effect was abandoned. The loft provision of EPAEC, however, was utilized extensively for near-source calculations at Centralia. Further discussion of this feature will be presented in Section VI.

Fluctuating-Plume Modifications

The disadvantages of applying mean-plume models for calculating gas washout from actual, fluctuating plumes have been discussed previously (HTW, p. 207; DHW, p. 61; Hales[3]). It is sufficient here to note that the generally nonlinear equilibrium relationship between gas-phase and liquid-phase concentrations of a species requires that the time-fluctuating concentrations encountered by the raindrop as it falls through the plume be represented accurately. The importance of this requirement to the washout calculation depends on the solubility and mass-transfer relationships of the particular species. We suggest, therefore, that the performance of the EPAEC model in its application to SO_2 washout might be improved by replacing the original mean-plume submodel with one accounting for time fluctuations of concentration in a more realistic manner.

The peak-to-mean analysis, used previously for equilibrium washout calculations (DHW), is unsuitable to the EPAEC model which requires knowledge of a complete distribution of pollutant concentration along the raindrop trajectory. A means for defining concentration distributions in instantaneous plumes which is compatible with the EPAEC model was suggested by Pasquill[9] and is based on the method of Smith and Hay[10] for defining the concentration of a puff. This method, which applies basically to homogeneous, isotropic turbulence, was extended empirically to actual atmospheric conditions. Pasquill indicates that the standard deviations of the vertical and lateral dimensions of the instantaneous plume (σ_z and σ_y, respectively) should be related to their respective components of the total intensity of turbulence, i_φ and i_θ, by the following relationships:

$$\sigma_z = 3i_\varphi^2 x \quad , \tag{12}$$

$$\sigma_y = 3i_\theta^2 x \quad . \tag{13}$$

The Quillayute results were analyzed using this approach. This analysis was performed by computing turbulence intensities (i_φ and i_θ) from the anemometer data, which were employed in conjunction with Equations (12) and (13) to obtain the instantaneous spread parameters σ_y and σ_z. The spread parameters thus obtained were utilized with the washout model to provide estimates of the "instantaneous" washout patterns, which were superimposed over the observed distribution of wind directions to arrive at estimates of time-average washout behavior.

The instantaneous-plume approach was found to produce results that were in somewhat better agreement with the observations than those based on time-averaged plume behavior. This improvement, however, was not sufficient to justify the additional complexity and computer time necessary for these calculations. For this reason, we did not proceed with further examination of this aspect of the investigation. It should be noted, however, that although the instantaneous plume approach did not appear practical in this series of experiments, it may prove worthwhile for the washout of gases having different transfer rates and solubilities or if the (low frequency) wind-direction variability is of greater amplitude. In view of the associated theoretical complexities, however, additional investigation is necessary to develop a sound technique for applying the instantaneous plume approach.

EXPERIMENTAL RESULTS AND ANALYSIS - DRY DEPOSITION

All previous experimental analyses of washout under this program have been based on the tacit assumption that dry deposition of SO_2 on collected rain is an unimportant source of error in washout measurements. This assumption is undoubtedly valid insofar as deposition on rain in sample-collection bottles is concerned; the narrow constriction of the bottle neck essentially eliminates any gas-phase transport of SO_2. Deposition to (or desorption from) rain during its residence on funnel surfaces, however, is less well understood. During the Keystone experiments we performed tests wherein SO_2-containing water drops were allowed to fall from a syringe through clean air onto a rain collector. Analysis of SO_2 contents of the collected drops and the original solution showed perturbations caused by the drop-funnel interaction to be insignificant. These tests were conducted in confined atmospheres, however, and some questions remain with respect to behavior under field sampling conditions where increased ventilation of the sampler surfaces may occur. Because of this uncertainty and because of the expected importance of dry deposition to natural surfaces as a sink of SO_2, we conducted several tests of this effect during the Quillayute series.

The Quillayute dry deposition tests involved the use of special dry deposition samplers. These consisted of normal washout collectors which were shielded to prevent natural rainwater from entering, but open to the ambient air concentration of SO_2. The "rain" provided to the funnels consisted of drops of either distilled water or a dilute TCM solution, issued by hypodermic needles. The needles were mounted on rotating arms so that the entire areas of the funnels could be covered by the water enroute to the bottle. The rate of dripping from the needles (rainfall rate) could be varied to approximate that of the ambient rain. In a given dry deposition experiment, two of these samplers were placed side-by-side. These were identical except that one employed distilled water and the other used TCM solution as the dripped liquid. Also nearby was a normal washout sampler. In terms of fluxes of SO_2 through the top openings of the funnels, these three samplers allowed the following measurements:

Flux 1. Due to rain, containing washed-out SO_2, impacting the funnel naturally and draining into the bottle where the SO_2 is fixed (normal collector);

Flux 2. Due to distilled water, impacting the funnel, absorbing SO_2 while residing there, and draining into the bottle where the SO_2 is fixed (artificial rain dripper and shielded funnel);

Flux 3. Due to TCM solution, impacting the funnel, absorbing SO_2 while residing there, and draining into the bottle (artificial TCM rain dripper and shielded funnel).

Seven experiments were performed during which these three samplers were used. In most cases, a bubbler air sampler was also included for concentration measurement at the approximate level of the funnel surface. Three of the experiments were conducted independently from washout experiments (identified as D1, D2, and D3--cf. Table 3), and four were conducted along with washout Runs 17-20. Of the latter, two (19 and 20) led to null results as the collectors were not properly located with respect to wind direction.

Table 7 presents experimental details and results of the five successful dry deposition experiments. Incompleteness due to technical difficulty and meteorological phenomena are noted. Gas-phase concentrations are presented here, for convenience, as corresponding equilibrium values in the liquid phase. Deposition fluxes may be determined from the concentrations listed in this table by multiplying by the rain rate J.

Interpretation of dry-deposition behavior from the Quillayute results is complicated by a number of factors. An approximate analysis can be performed, however, by applying an extension of the reversible mass-transfer theory employed for scavenging calculations. It should be noted in this regard that the deposition velocity concept, which is based on the assumption of irreversible behavior, is not applicable for these purposes.

TABLE 7. SUMMARY OF DRY DEPOSITION RESULTS

Run	H_2O Drip Sampler	Normal Rain Sampler	TCM Drip Sampler	Equilibrium With Ambient Air	H_2O/Natural/TCM "Rain" Rates, (cm/sec) × 10^5	Source Height m	Sampling Distance m
D1	52	38	72	214	2.5/3.6/11.1	3	30.5
D2	29	No Rain	76	159	7.0/ 0 /27.8	8.5	61
D3	24	43	50	140	8.3/7.9/7.9	8.5	61
D4[a]	1	3.2	0	No Measure	4.2/6.9/1.7	16.8	30.5
D5[b]	0	4.2	.04	59	4.2/8.7/7.0	16.8	61

[a] Concurrent with Run 17

[b] Concurrent with Run 18

It is convenient to begin by considering the inner surface of a funnel being used as a rain collector. The rain impinging on this surface will be exposed to the ambient air for a short time before running into the collection bottle. Because of this, a certain area a^* of water will be exposed to the ambient air in the form of drops, rivulets, or films, providing a surface for interphase transfer of SO_2. a^* is expected to depend in a complex way on a number of factors, including the surface properties of the collector; it should increase with rain rate, (roughly) approaching the collector surface area A^* as the rate becomes large.

The rate of SO_2 transport to the surface water on a collector depends upon both a^* and the concentration driving force. This relationship can be expressed in a semi-empirical manner as follows:

$$F_d = \frac{w_d}{A} = \frac{K_x a^*}{c_x A}(c_{eq} - c_{avg}) \quad , \tag{14}$$

where F_d is the flux, w_d (moles/sec) is the rate of SO_2 transport to the surface water by the dry deposition mechanism, c_{eq} is the concentration of SO_2 in the deposited water that would exist at ambient air concentrations under equilibrium conditions, and c_x is the total liquid-phase concentration (nominally 1/18 moles/cm^3, preserved in the equation to provide a definition of the mass-transfer coefficient K_x consistent with the treatment throughout this report). A denotes the area of the funnel mouth and c_{avg} is some representative average concentration of SO_2 in the surface water. We will estimate c_{avg} in the present treatment by assuming that

$$c_{avg} = \frac{1}{2}(c_r + c_f) \quad , \tag{15}$$

where c_r is the concentration of SO_2 in the rain impinging on the surface and c_f is that of the water collected in the sampler bottle.

K_x is similar in concept to the mass-transfer coefficient used for washout calculations except that it is based, for convenience, on the liquid-phase driving force. K_x will vary in a complex manner with air ventilation of the sampler, surface water configuration, and rain rate. Neither K nor a* can be predicted *a priori*. One can proceed, however, using the well-known chemical-engineering technique of lumping these variables together and proceeding on a semi-empirical basis.

If one assumes that the Quillayute data arising from the covered, distilled-water drip sampler characterizes behavior from incoming rain at zero concentration, then $c_{avg} = 1/2\ c_r$ and $K_x a^*/c_x A$ can be calculated. As indicated by the results shown in Table 8, the relationships between $K_x a^*/c_x A$ and rain rate or wind speed is not totally clear. The zero value for D5 is expected to have arisen primarily from low concentration measurement error, and probably can be excluded for present purposes; the other values are centered reasonably closely around 10^{-5} cm^3/sec, suggesting that this value of $K_x a^*/c_x A$ might be utilized for order of magnitude estimates of dry deposition behavior. In proceeding, one should note that data from the rotating syringe apparatus provides only approximate values of $K_x a^*$, since both the mass-transfer coefficient and the surface area might be expected to vary for natural rain, which encounters the surface with a variety of drop sizes and impact velocities. The present values are expected to be reasonable first estimates of natural behavior, however, and will be employed in the subsequent analysis of deposition phenomena.

Equation (14) can be extended to allow prediction of dry deposition conditions by defining fluxes for separate mechanisms. Thus if a total flux F_t

TABLE 8. TRANSPORT PARAMETERS FOR DRY DEPOSITION TESTS

Run	"Rain" Rate, $(\mathrm{cm/sec}) \times 10^5$	$\bar{u}$, cm/sec	$K_x a^*/c_x A$, $(\mathrm{cm/sec}) \times 10^5$
D1	2.5	149	.69
D2	5.5	253	1.41
D3	6.3	230	1.55
D5	4.2	188	0

is defined as the net rate of SO_2 (washout + dry deposition) passing through the top end of the collection funnel divided by the area of the opening, then

$$F_t = F_r + F_d = c_f J \quad , \tag{16}$$

where $F_r = c_r J$ and $F_d = (c_f - c_r)J$ are the fluxes for washout and dry deposition to the funnel surface. Incorporating Equations (14) and (15) one obtains

$$(c_f - c_r) = \frac{K_x a^*}{J c_x A}\left(c_{eq} - \tfrac{1}{2}(c_f + c_r)\right) \quad , \tag{17}$$

which can be utilized to estimate concentrations in incident rain from washout sampler data.

Employing values of c_f, J, and $K_x a^*/c_x A$ from the available sampler data from the two complete deposition tests (runs D1 and D3), (17) yields the results shown in Table 9. These results indicate a high rate of dry deposition relative to that by washout under the circumstances of runs D1 and D3. This should be expected for these conditions of low emission heights and relatively close distances from the source, since the rain had little time to pick up SO_2 from the plumes before it encountered the samplers. This effect is amplified under the more severe conditions of run D1; quite obviously washout cannot be measured accurately in this manner under these circumstances.

TABLE 9. CALCULATED INCIDENT RAIN CONCENTRATIONS FOR DRY DEPOSITION RUNS D1 AND D3.

Run	Concentrations of SO_2 In Liquid, (moles/cm^3) × 10^9 Measured From Rain Sampler (c_f)	Concentrations of SO_2 In Liquid, (moles/cm^3) × 10^9 Calculated Incident (c_r)
D1	38	0.72
D3	43	17.7

Equation (14) can be used to apply the results of the dry deposition tests to estimate errors in the washout measurements arising from dry deposition. Provided the group $K_x a^*/c_x A$ is known, this equation can be applied to determine the ratio of the incident-to-measured concentrations, c_r/c_f, for any set of values of the rain rate and the ratio c_{eq}/c_f. Choosing $K_x a^*/c_x A = 10^{-5}$ cm/sec (as suggested by the above dry deposition results), one obtains error curves such as those shown in Figure 26 where the concentration ratio is expressed as a function of the rain rate for parametric values of c_{eq}/c_t.

The curves in Figure 26 illustrate several important aspects of dry deposition errors and of the limits of this analysis. Rain impinging on the collectors in a state subsaturated with respect to its surroundings ($c_{eq}/c_f < 1$) will result in measured concentrations below those of the incident rain because of desorption; conversely, situations involving $c_{eq}/c_f > 1$ will exhibit positive deviations. Whenever c_{eq}/c_t is close to 1, of course, there will be little deviation owing to the absence of any driving potential for mass transfer.

It is evident that the Quillayute-type samplers provide an extremely poor measure of washout whenever rain rates are low. This measurement capability improves with increasing rain rate, approaching an ideal situation ($c_r = c_f$) as the rain rate becomes large. Fortunately, the Quillayute experiments involved rain rates greater than 2×10^{-5} cm/sec (0.9 mm/hr), and values of c_{eq}/c_t ranging between zero and approximately two. Corresponding estimates of sampling errors, then, range from zero to on the order of thirty percent. Such sampling errors are not considered to be serious in view of the noted deviations between experiment and the washout model. Applying the indicated

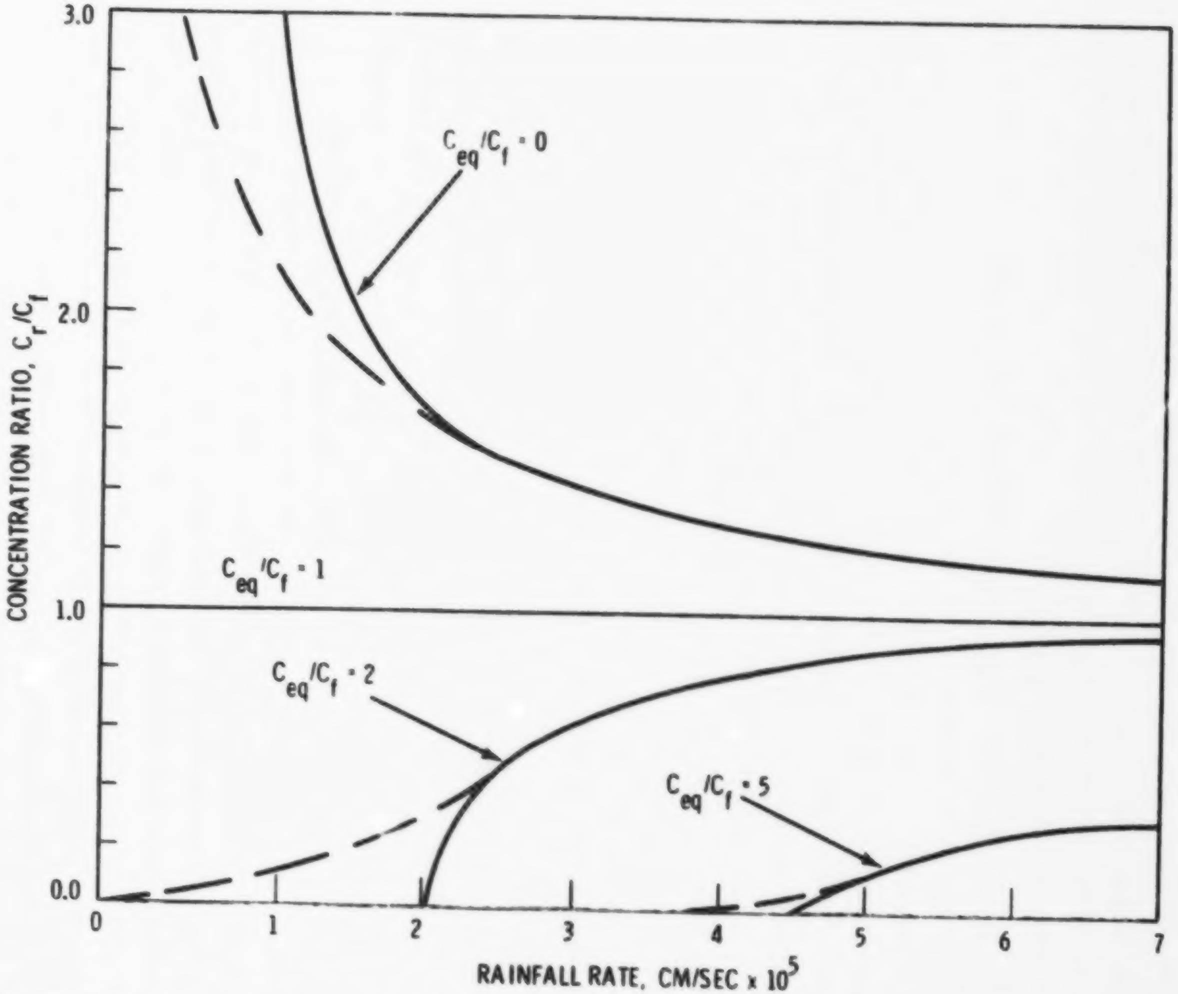

FIGURE 26. ERROR IN WASHOUT CONCENTRATION MEASUREMENTS, AS A RESULT OF DRY DEPOSITION.

corrections does improve the agreement between predicted and experimental results, especially for the near-source arcs where high estimates from the washout model have been noted. The magnitude of this correction, however, is often insufficient to bring the experimental values to within the predicted range. It is also evident that the previously mentioned problems with undercutting and near-source plume modeling play a prominent role in distortion of the predicted results.

The rather odd behavior of the Figure 26 curves at low rain rates should be noted. This is an outcome of the assumption of a constant value of $K_x a^*/c_x A$, which becomes more invalid as the rain rate decreases, until mass conservation is violated and prediction of negative concentrations results. Since a^* must tend toward zero for very small rain rates, actual behavior should follow approximately that indicated by the dashed lines in this region. Such behavior is immaterial to the present situation, which involves rain rates in the region where deposition measurements were made (that is, always above the dotted-line region). It is still important to note, however, the strong qualitative evidence that the Quillayute type of sampler provides an extremely poor measurement method whenever rain rates are very low.

Finally, the results from the dry deposition samplers utilizing TCM solution in their rotating needles should be noted. Since this solution was expected to act as a total sink for SO_2 immediately after it contacted the liquid phase, these samplers provided a measure of gas-phase resistance to mass transfer in the dry deposition process. Corresponding calculations of $K_x a^*/c_x A$ for these experiments showed this group to be about twice as large as that obtained for the pure water experiments, indicating an approximately equal importance of gas-phase and liquid-phase influence on the dry deposition process. Such behavior, in addition to providing an explanation for the previously mentioned finding of low desorption rates from non-ventilated samplers, further illustrates the complexities of this problem. In view of these factors, any application of the deposition results of this section for sampling conditions outside the observed range of wind speeds and rain rates should be performed with caution.

SECTION VI.

CENTRALIA EXPERIMENTS

INTRODUCTION

The recent construction of the first major coal-fired power plant in the Pacific Northwest at Centralia, Washington, provided a convenient site for further study of the washout of power plant effluents. In addition to the economic attractiveness of the site--it is located essentially midway between Hanford and Quillayute--it also provided the chance to examine atmospheric effects of a power plant in a region that is new to such sources, possessing low background levels of the pollutants of primary interest. The Centralia study represents an intermediate situation between the relatively ideal controlled-release, zero-background study of Quillayute and a study of a large power plant--such as Keystone--in a heavily polluted area. In contrast with our Keystone experience, we were able to isolate the effects of the effluent plume with rain-concentration measurements and determine the effect of the plant on local levels of SO_2, $SO_4^=$, and H^+ in precipitation. The results of the measurements and model calculations provided a good test of the EPAEC model's effectiveness in a situation more real than that of Quillayute, but still having less uncertainty with regard to background levels and distinction of source.

The Centralia steam plant is located in Hanaford Valley, about five miles northeast of Centralia, Washington. The first of two generating units went into operation shortly before our field research began in February, 1972. Pertinent plant operation data with outputs at that time, are listed in Table 10. Precipitator testing was underway during the period of our experiments, and as a result the firing rate of the plant varied considerably, as is noted later in Table 13.

As indicated by the map in Figure 27, the plant is located in a wide valley. Surrounding hills rise to about 300 feet above the valley floor and thus to within about 200 feet of the top of the stacks.

Reproduced from
best available copy.

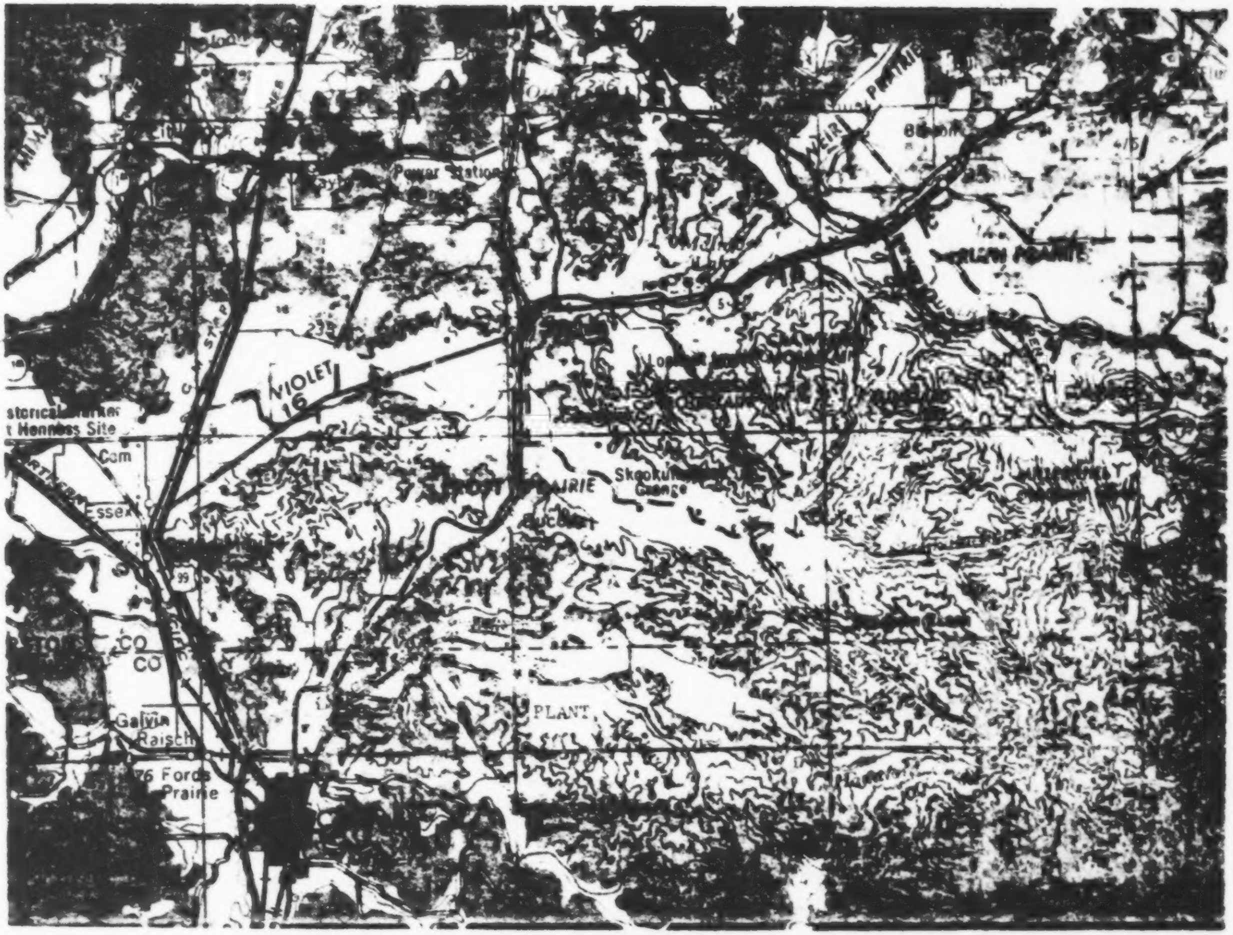
Power Station
VIOLET
16
Essex
Com
Historical Marker
Hennes Site
PRAIRIE
Skookumchuck
Grange
WEIR PRAIRIE
PLANT
Galvin
Raisch
Fords
Prairie
5
99

FIGURE 27. MAP OF CENTRALIA STEAM PLANT AREA.

TABLE 10. CENTRALIA STEAM-ELECTRIC PLANT STATISTICS
(February-March, 1972)

Generating Capacity	700 megawatts
Stack Height	470 feet
Coal Type	Subbituminous, 8100 BTU/lb
Sulfur Content (Average)	0.55%
Firing Rate (Average)	300 tons/hr
Cooling Towers	Forced-draft

EXPERIMENT DESIGN

Precipitation was collected on the sampling array shown in Figure 28. Line A (inset) was set up on power plant property, flanking the location of the experiment control center. Lines B-D were situated along existing state and county roads in mostly open valleys downwind of the plant. Line B is fragmentary because of impassability of a portion of one road in the area. Additional collection sites were located at a greater distance behind the resulting gap, providing more dense coverage in the expected downwind sector.

Each rain collector consisted of a 20 cm diameter funnel, supported by a steel rod and laboratory support. A 500 ml plastic bottle, capable of holding 1.5 cm of rainfall (enough for several hours of rainfall normally) was attached to each funnel. A collector containing TCM solution sampled rain-borne SO_2 at each active collection site, and a separate collector containing hydrogen peroxide sampled rain for subsequent sulfate analysis. Actually, the latter sampler indicated total sulfur, as it converted SO_2 to sulfate--the sulfate concentrations were derived later by subtraction of the SO_2 as measured from the TCM-doped collectors. At every third site an additional collector sampled untreated rainwater for pH and trace-metal measurement. Air concentrations of SO_2 were also measured at these sites using battery-driven bubbler boxes.

Supporting instrumentation was essentially the same as for the Quillayute studies, except that pilot balloons were flown to determine mean wind direction and speed prior to runs, and a portable rawinsonde unit was used to obtain wind, temperature and dew-point information during runs. The rawinsonde unit was located at the control center on Line A, as were raindrop sizing equipment (calibrated water sensitive paper), and the fast response rain gauge.

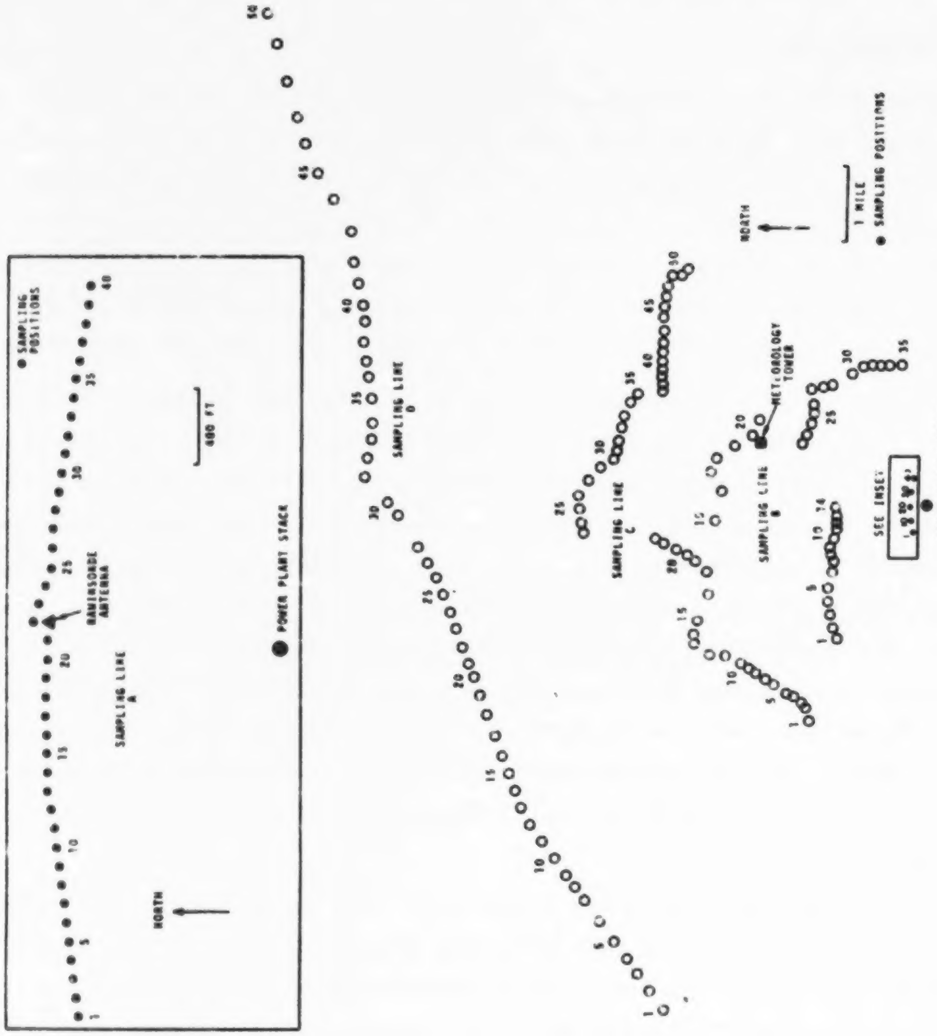
SAMPLING POSITIONS
RAWINSONDE ANTENNA
SAMPLING LINE A
400 FT
NORTH
POWER PLANT STACK
SAMPLING LINE D
SAMPLING LINE C
SAMPLING LINE B
METEOROLOGY TOWER
SEE INSET
POWER PLANT STACK
NORTH
1 MILE
SAMPLING POSITIONS

FIGURE 28. CENTRALIA SAMPLING NETWORK.

A Gill three-dimensional anemometer was operated atop a 30.5 m portable tower, which was erected on a hilltop approximately 3 km downwind from the plant site on Line B. The elevation of the Gill was about 140 feet below the level of the top of the active stack. Figures 29 and 30 are photographs of relevant installations.

Analyses of the samples (with the exception of trace metals) were performed on site at the Battelle portable air pollution laboratory. Technicon Autoanalyzers were used to determine sulfate and SO_2 concentrations; analyses were usually completed within 24 hours of sampling.

SO_2 analyses were conducted using the modified West and Gaeke method, which was employed for previous field studies under this program (HTW, DHW). Sulfate analyses were performed using the methylthymol blue methodology described by Lazrus, et al.[11] The accuracy of these methods can be stated approximately using the following expression for expected analytical error:

$$E \cong \pm(s + Bc_f) \quad . \tag{18}$$

Here, s is the sensitivity limit of the technique, B is an accuracy parameter, and c_f is the sample concentration. For the SO_2 analysis, B was about 0.05 and s was in the neighborhood of 0.1 micromoles/liter; for sulfate these values were about 0.1 and 0.2 milligrams per liter, respectively.

The field crew consisted of three sampling teams of two persons each, and a field director. When a suitable rainstorm was anticipated, these persons assembled at the control center, where initial pilot balloons were released to determine the suitability of the wind direction, and the appropriate sampling positions. The wind speed at plume level, thus estimated, aided in the decision as to which three of the four available sampling lines would be used (winds faster than about 10 miles per hour were deemed too fast for sampling on Line A because of plume undercutting). These matters settled (and in the event of continuing rain), collector setout was begun. When all samplers were in place, crew members monitored the wind system and operated other supporting instrumentation. Radio communication was maintained between the control center, the sampling lines, and the wind tower to

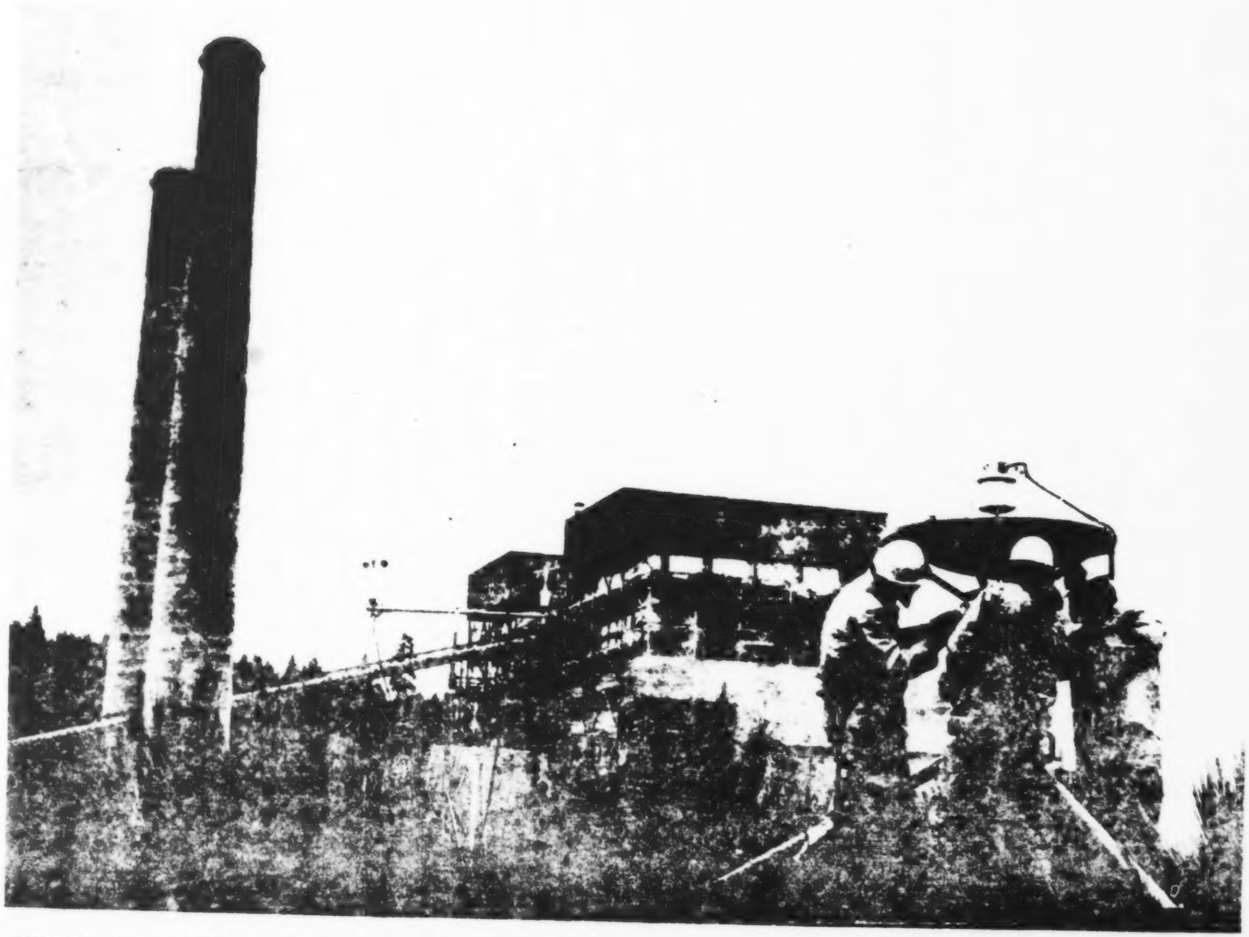

FIGURE 29. CENTRALIA STEAMPLANT WITH RAWINSONDE ANTENNA AT CONTROL CENTER IN FOREGROUND.

Reproduced from best available copy.

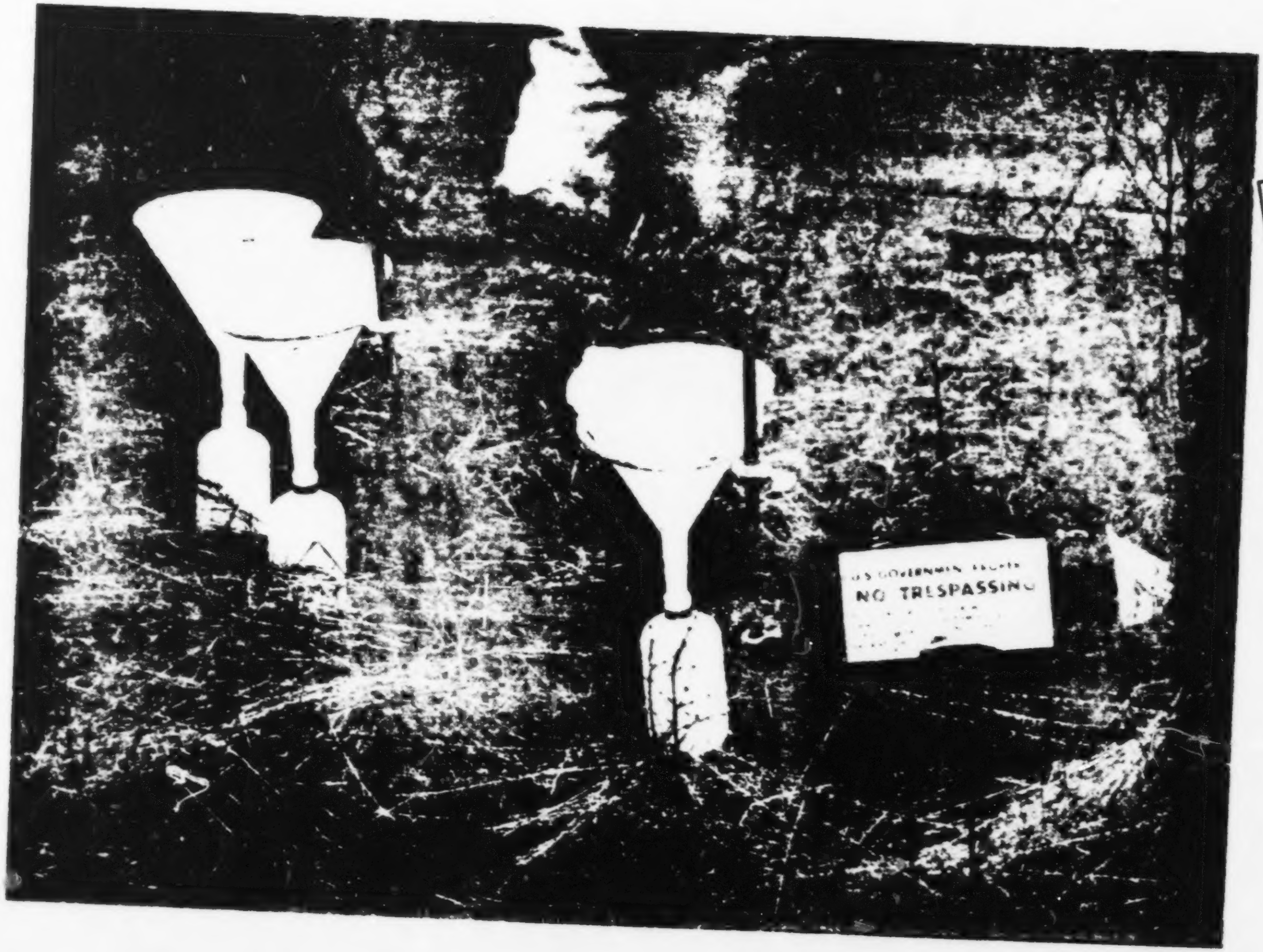
NO TRESPASSING

FIGURE 30. CENTRALIA SAMPLING LOCATION: $SO_4^=$ AND SO_2 SAMPLERS, LEFT; pH AND SO_2 BUBBLER BOX, RIGHT.

monitor rain conditions and wind direction. Since the setout usually took about 1 1/2 hours, several hours were generally allowed for sampling in order to collect sufficient rain for analysis and to smooth somewhat the effects of rain showers and short-term wind shifts.

EXPERIMENTAL RESULTS

Five experiments were performed during the February-March, 1972 field period. Four of these involved significant collections of precipitation; SO_2, sulfate and pH measurements of the samples were performed (owing to analytical difficulties Run C-3 did not include sulfate measurements). SO_2 air concentration measurements were made at selected sites during all runs.

Basic experimental data are provided in Tables 11 through 13; complete concentration data are given in Appendix A. In addition, the processed concentration and sounding data are shown graphically in Figures 31 through 52. These figures indicate concentration as a function of sampling location using radial lines extending outward from the sampling points. Points with no lines denote active sampling sites producing results too small to show on the figures. Rain concentrations shown in these plots have been corrected for background by subtraction of background concentration levels obtained from off-plume samples. Sulfate background levels ranged between 0.2 and 0.6 milligrams per liter, while free hydrogen-ion background levels (as determined from pH measurements) ranged from 0.7 to about 16 micromoles per liter. SO_2 did not appear in background rain samples in significant concentrations. Figures 31 through 52 are presented in the following paragraphs in the context of individual descriptions of meteorological conditions for each of the experiments.

Run C-1 (February 27)

An energetic storm dropped over one inch of rain on the area the night of February 26-27. Precipitation decreased in the morning and stopped completely shortly after sampler deployment. Strong winds continued throughout the sampling period. Although no significant rain was collected, air-concentrations of SO_2 were measured; these are shown as a function of sampling location in Figure 31.

TABLE 11. RUN DATA - CENTRALIA

Run & Date	Sampling Line	Mean Distance From Stack, km	Sampling Time PST	Rainfall Rate, mm/hr Rain Gauge[a]	Rainfall Rate, mm/hr Collectors[b]
2 2-28-72	A	0.41	1210-1528	3.5	3.0
	B	3.1	1224-1556	3.4	2.7
	D	11.5	1247-1528	3.5	2.3
3 3-1-72	A	0.39	1454-1706	0.88	0.82
	B	2.4	1518-1716	0.80	0.75
	D	10.9	1523-1656	0.78	1.2
4 3-5-72	B	3.4	0926-1213	2.4	2.5
	C	7.0	0922-1207	2.3	3.5
	D	11.2	0922-1122	1.7	5.6
5 3-9-72	A	0.39	1240-1537	1.4	1.2
	D	11.2	1315-1545	1.2	1.3

[a] Rain gauge located at Line A. Rate calculated for collection time of sampling line indicated.

[b] Average of all collectors on line.

TABLE 12. RAINDROP SIZE FREQUENCY[a] DISTRIBUTIONS - CENTRALIA.

	Diameter, cm									
Run	.024	.030	.038	.046	.060	.074	.094	.118	.148	.190
C-2	.02	.10	.19	.12	.08	.06	.11	.09	.16	.07
C-3	.07	.10	.35	.26	.11	.02	.08	.01		
C-4	.04	.26	.22	.12	.07	.06	.115	.085	.02	.01
C-5	.045	.285	.13	.11	.12	.11	.095	.06	.02	.025

[a] Raindrop size spectrometer located at sampling Line A (also, see footnote to Table 4).

TABLE 13. SUMMARY OF WASHOUT MEASUREMENTS - CENTRALIA.

Date	Run/ Line	Washout Rates M [gm-moles/(m hr)] × 10^3		pH		Firing Rate[a] Tons Coal/hr	Sulfur Emission[a] Rate, gm-moles/hr × 10^{-4}
		SO_2	$SO_4^=$	Peak	Bkg.		
2-28-72	C-2-A	9.48	10.7	4.45	5.7	219	3.35
	B	31.1	56.0	4.73			
	D	23.9	100.0	5.05			
3-1-72	C-3-A	0.052[b]	c	4.65	6.1	290	4.85
	B	11.8	c	4.31			
	D	30.0	c	4.50			
3-5-72	C-4-B	35.4[d]	97.1[d]	4.29	5.4	359	5.80
	C	49.1	71.3	4.51			
	D	83.8	85.6	4.58			
3-9-72	C-5-A	0.406	2.06	4.27	4.7	285	4.21
	D	7.39	16.5	4.45			

[a] Based on analyses provided by plant management.

[b] Only two non-zero concentrations on line.

[c] No data available.

[d] Approximate: Wide range of sampler separations and sampling times considered.

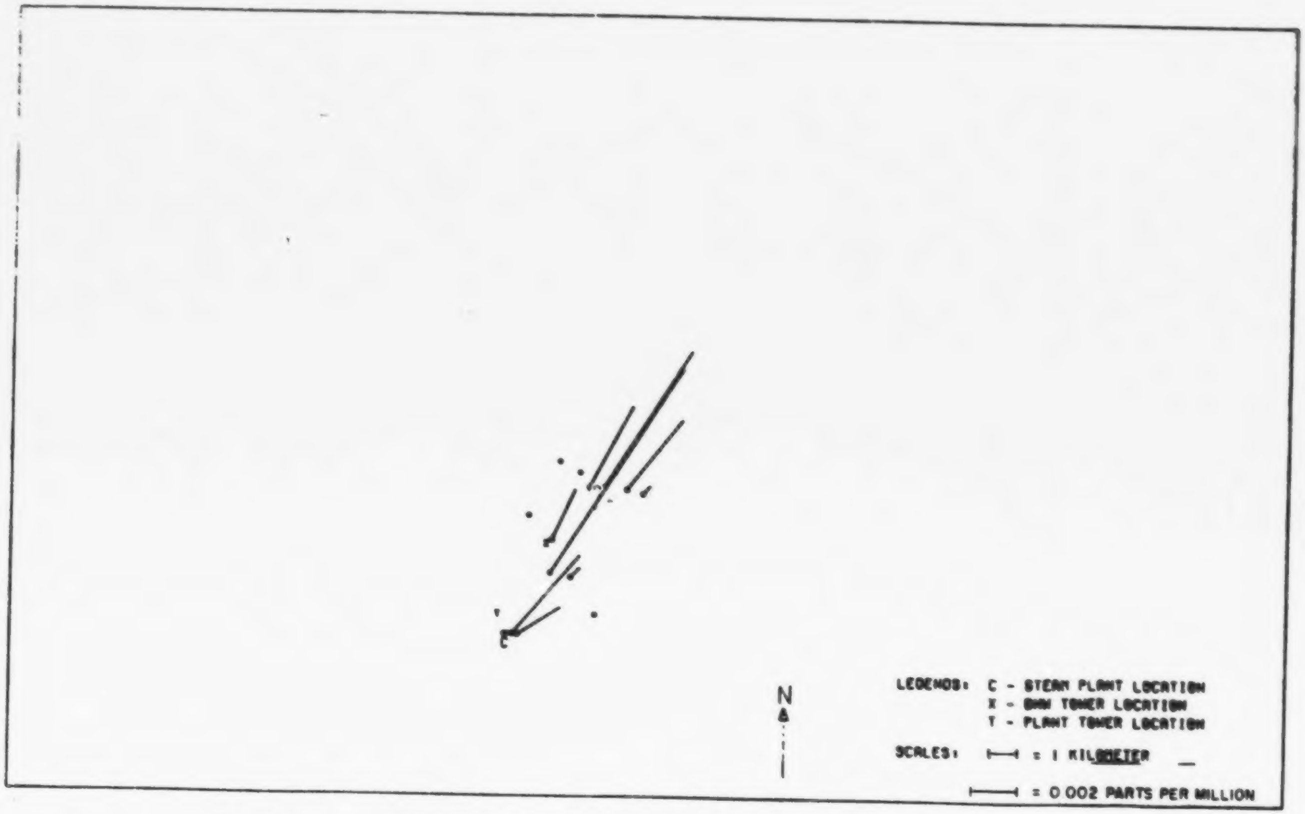

C
N
LEGENDS: C - STEAM PLANT LOCATION
X - BNW TOWER LOCATION
T - PLANT TOWER LOCATION
SCALES: = 1 KILOMETER
= 0.002 PARTS PER MILLION

FIGURE 31. MEASURED SO_2 CONCENTRATIONS IN AIR - RUN C-1.

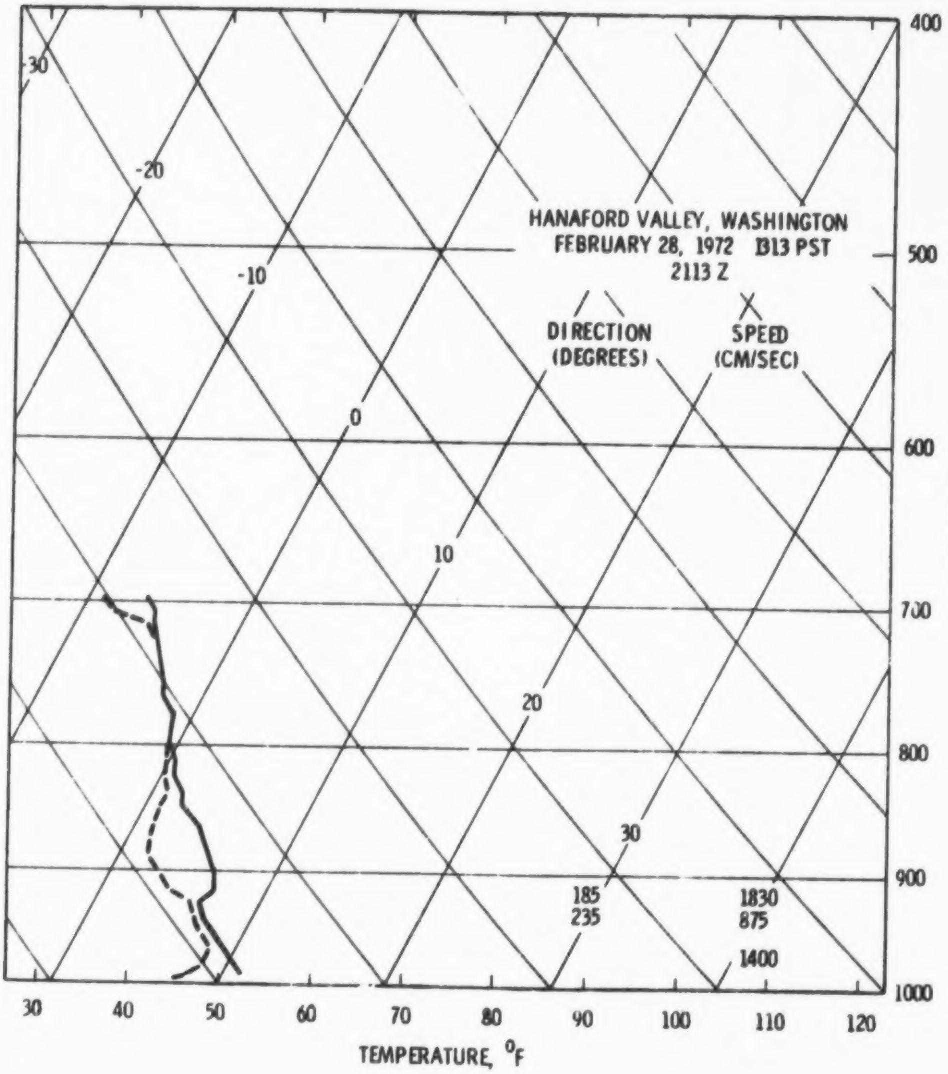

FIGURE 32. RAWINSONDE DATA - RUN C-2.

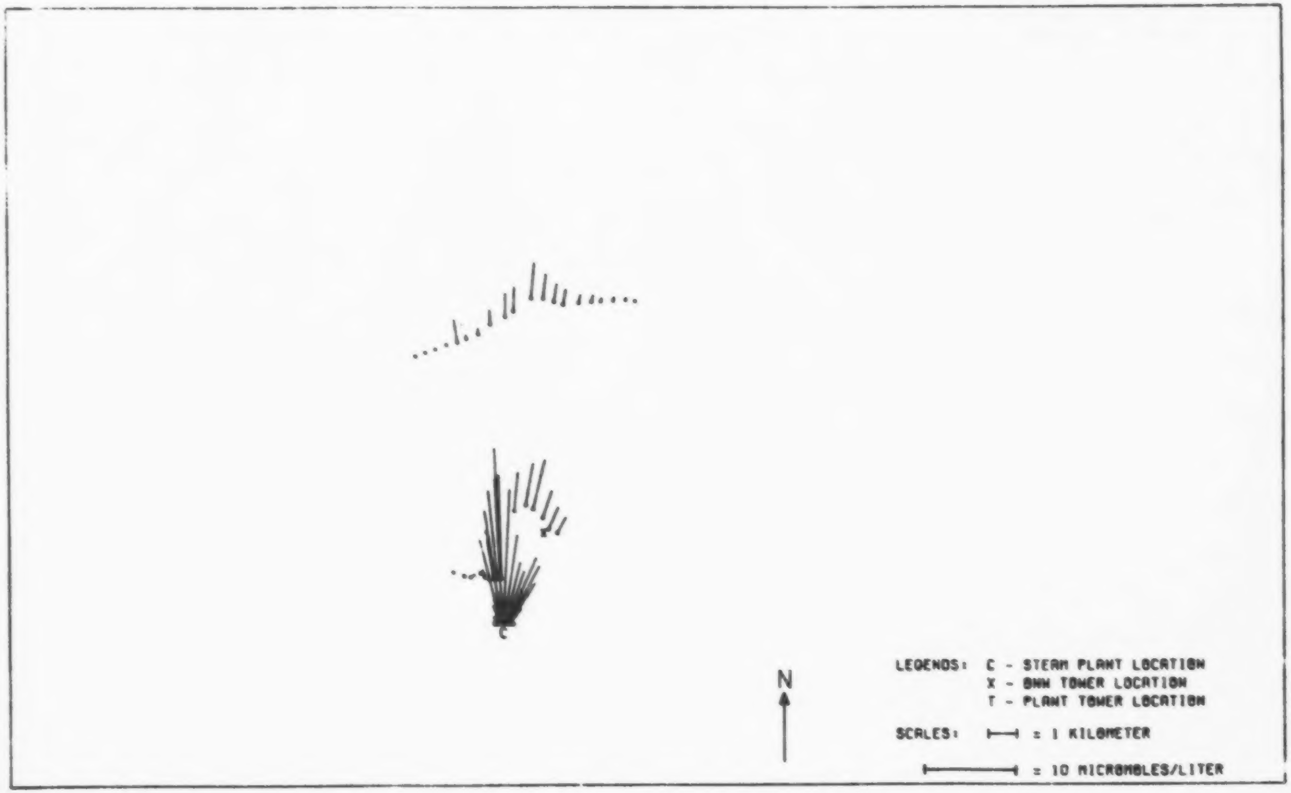
C
N
LEGENDS: C - STEAM PLANT LOCATION
X - BNW TOWER LOCATION
T - PLANT TOWER LOCATION
SCALES: = 1 KILOMETER
= 10 MICROMOLES/LITER

FIGURE 33. MEASURED SO_2 CONCENTRATIONS IN RAIN - RUN C-2.

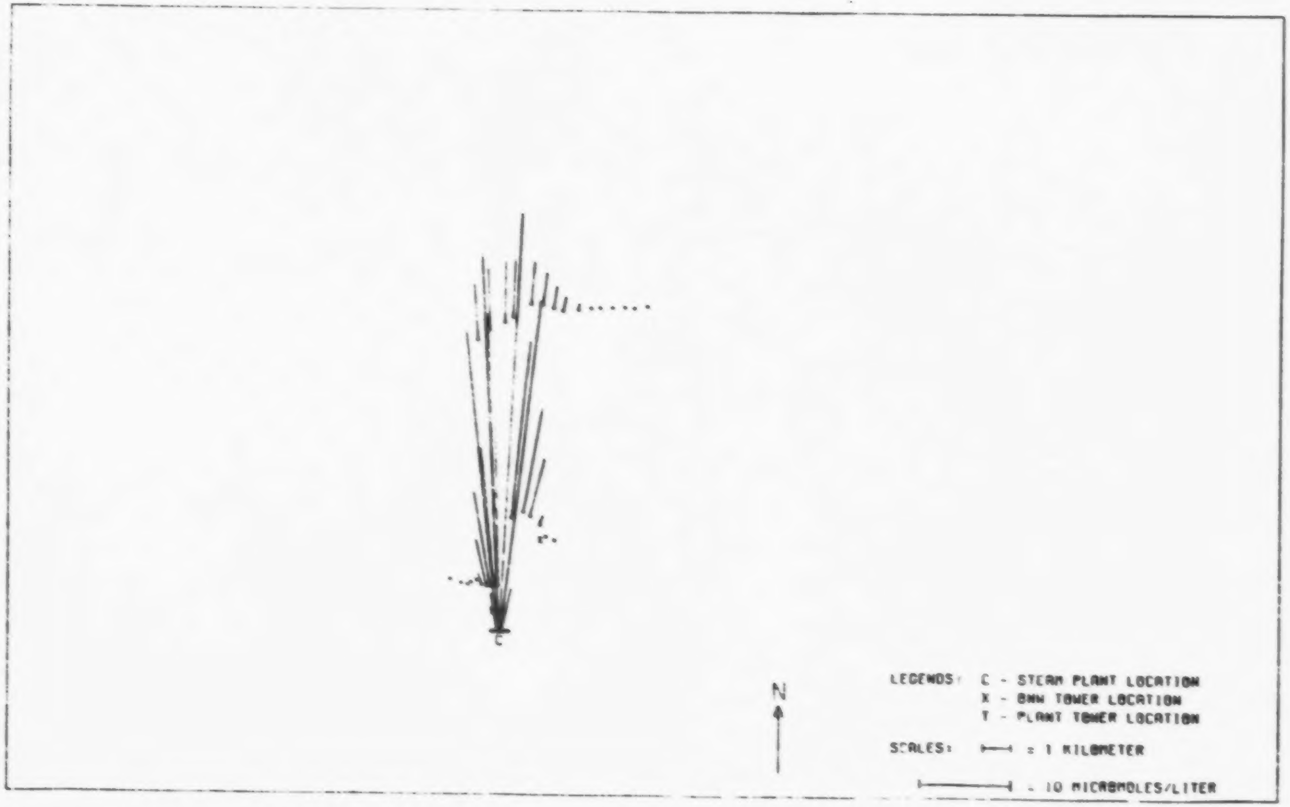

FIGURE 34. PREDICTED SO_2 CONCENTRATIONS IN RAIN - RUN C-2: EPAEC MODEL CALCULATIONS BASED ON GAS-PHASE LIMITED TRANSPORT AND AN SO_2 REACTION DECAY HALF-LIFE OF 15 MINUTES.

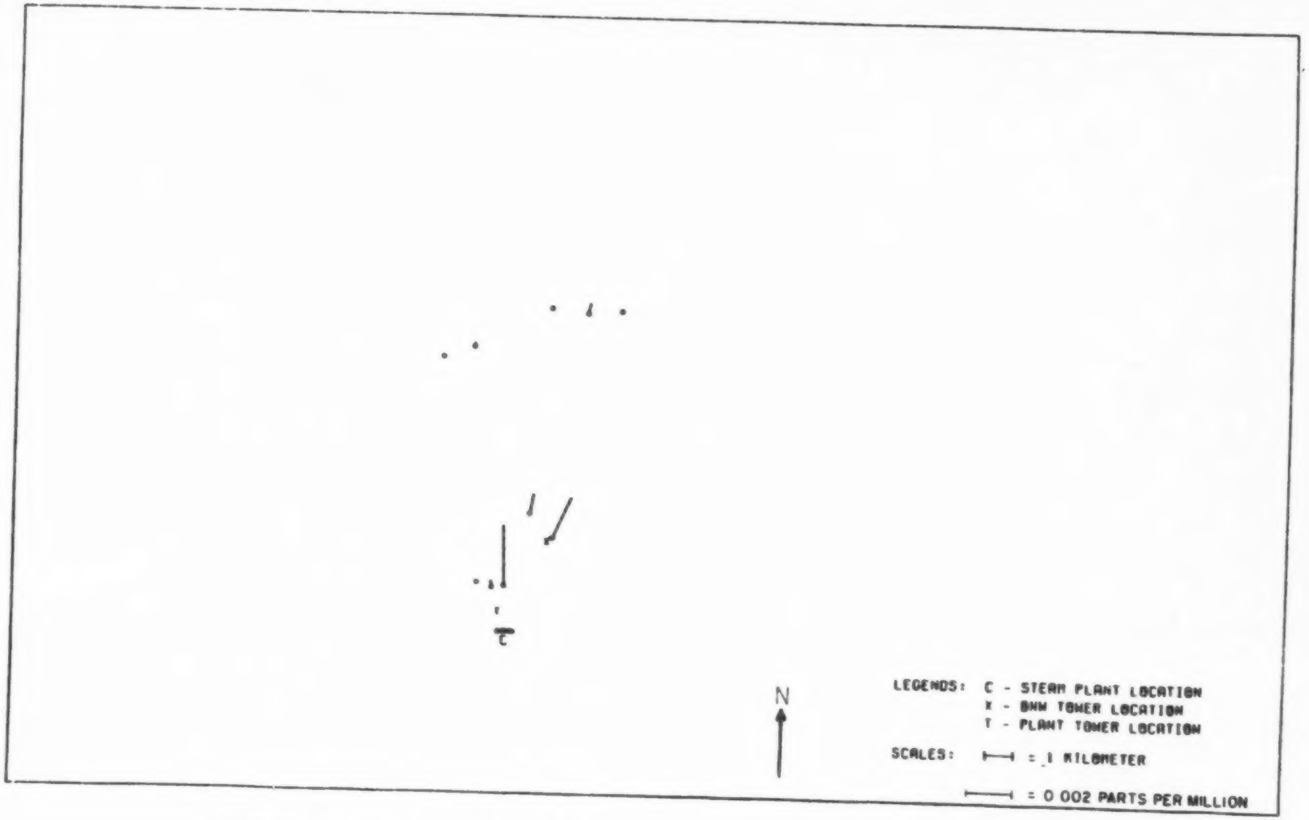
N
LEGENDS: C - STEAM PLANT LOCATION
X - BNW TOWER LOCATION
T - PLANT TOWER LOCATION
SCALES: = .1 KILOMETER
= 0.002 PARTS PER MILLION

FIGURE 35. MEASURED SO_2 CONCENTRATIONS IN AIR - RUN C-2.

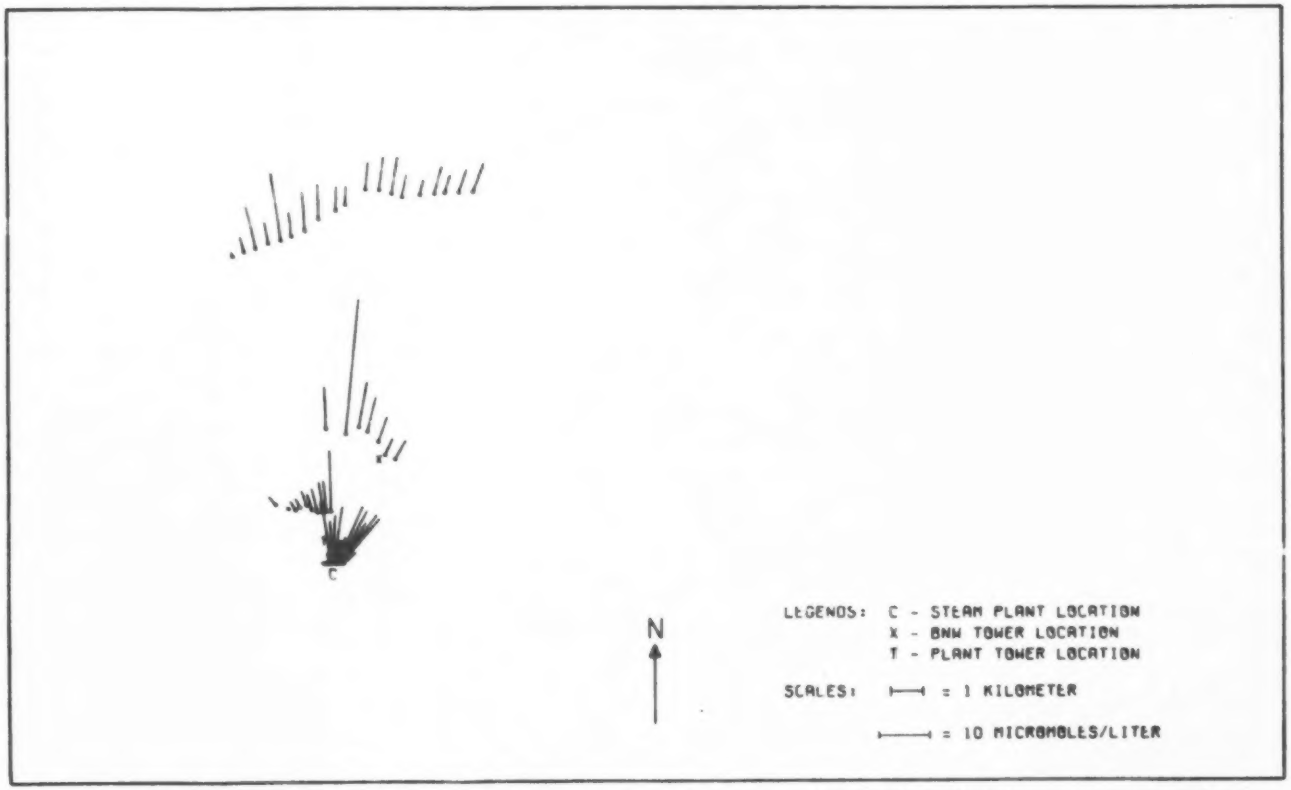
C
X
N
LEGENDS: C - STEAM PLANT LOCATION
X - BNW TOWER LOCATION
T - PLANT TOWER LOCATION
SCALES: = 1 KILOMETER
= 10 MICROMOLES/LITER

FIGURE 36. MEASURED SULFATE CONCENTRATIONS IN RAIN - RUN C-2 (BACKGROUND CORRECTED).

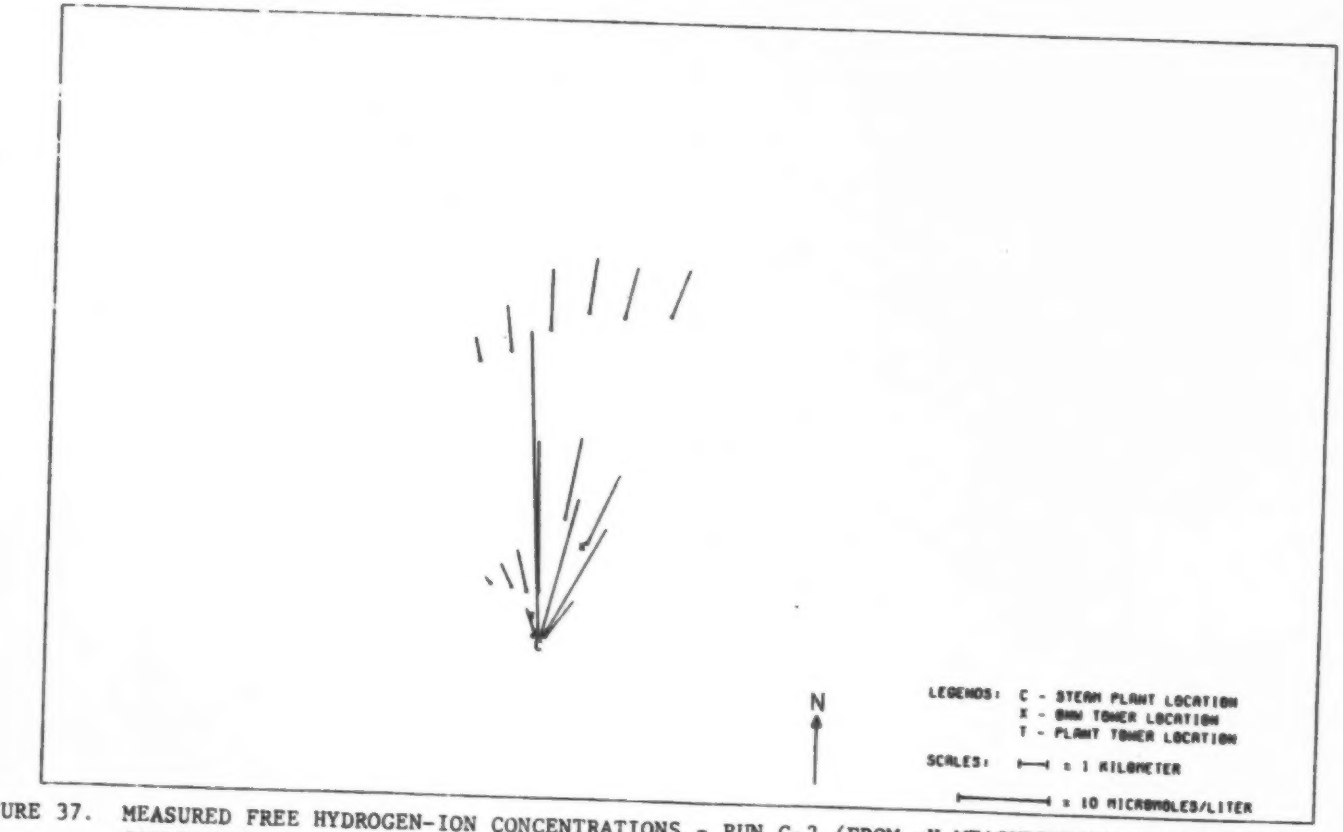
C
N
LEGENDS: C - STEAM PLANT LOCATION
X - BAW TOWER LOCATION
T - PLANT TOWER LOCATION
SCALES: = 1 KILOMETER
= 10 MICROMOLES/LITER

FIGURE 37. MEASURED FREE HYDROGEN-ION CONCENTRATIONS - RUN C-2 (FROM pH MEASUREMENTS, BACKGROUND CORRECTED).

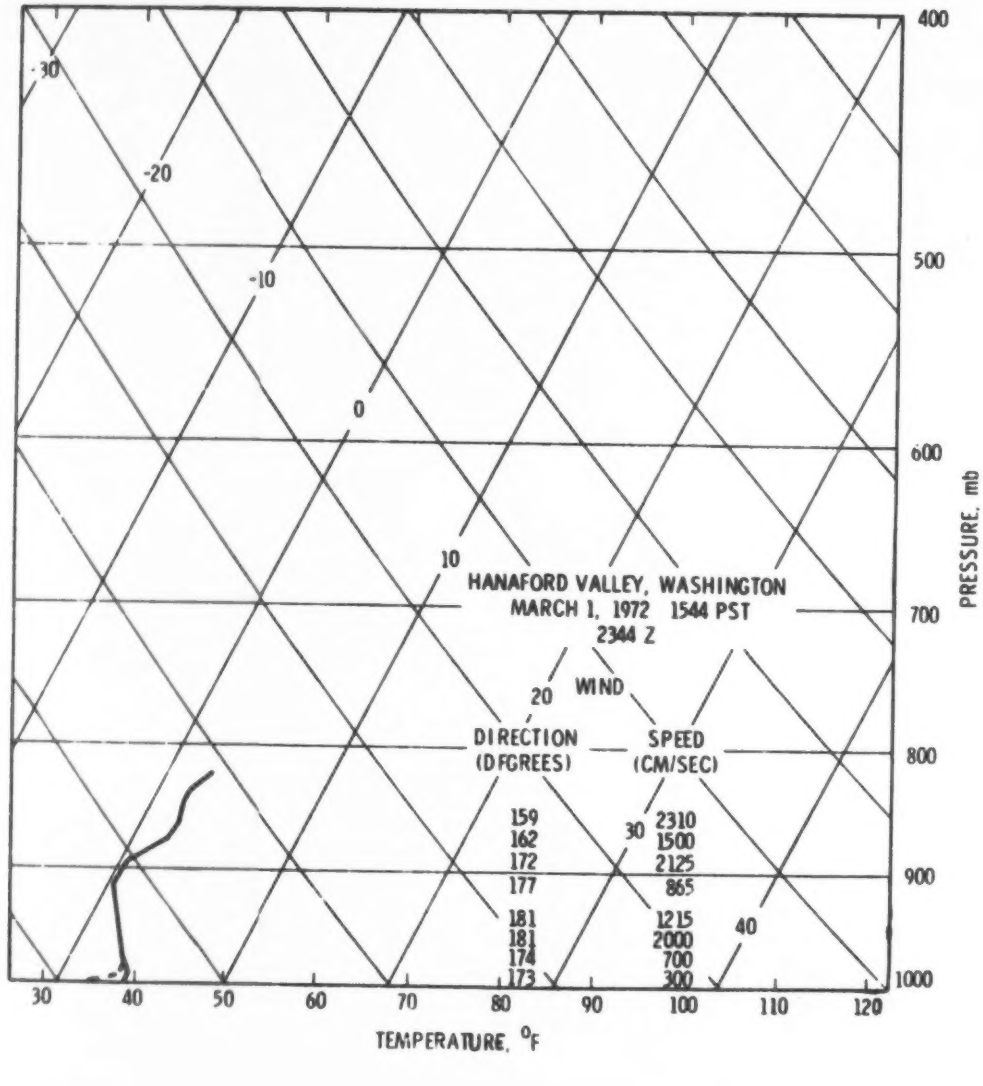

DIRECTION (DFGREES)	SPEED (CM/SEC)
159	2310
162	1500
172	2125
177	865
181	1215
181	2000
174	700
173	300

FIGURE 38. RAWINSONDE DATA - RUN C-3.

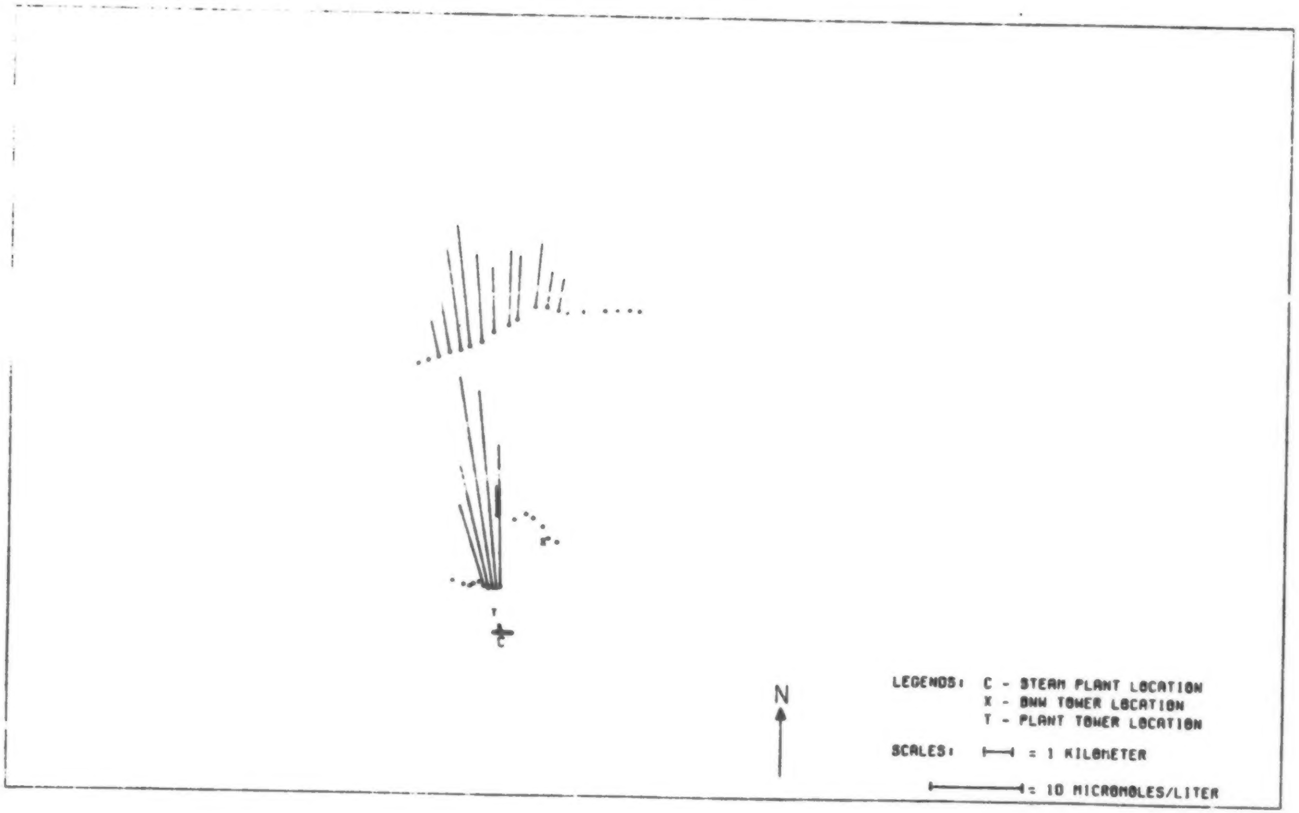
T
C
X
N
LEGENDS: C - STEAM PLANT LOCATION
X - BNW TOWER LOCATION
T - PLANT TOWER LOCATION
SCALES: = 1 KILOMETER
= 10 MICROMOLES/LITER

FIGURE 39. MEASURED SO_2 CONCENTRATIONS IN RAIN - RUN C-3.

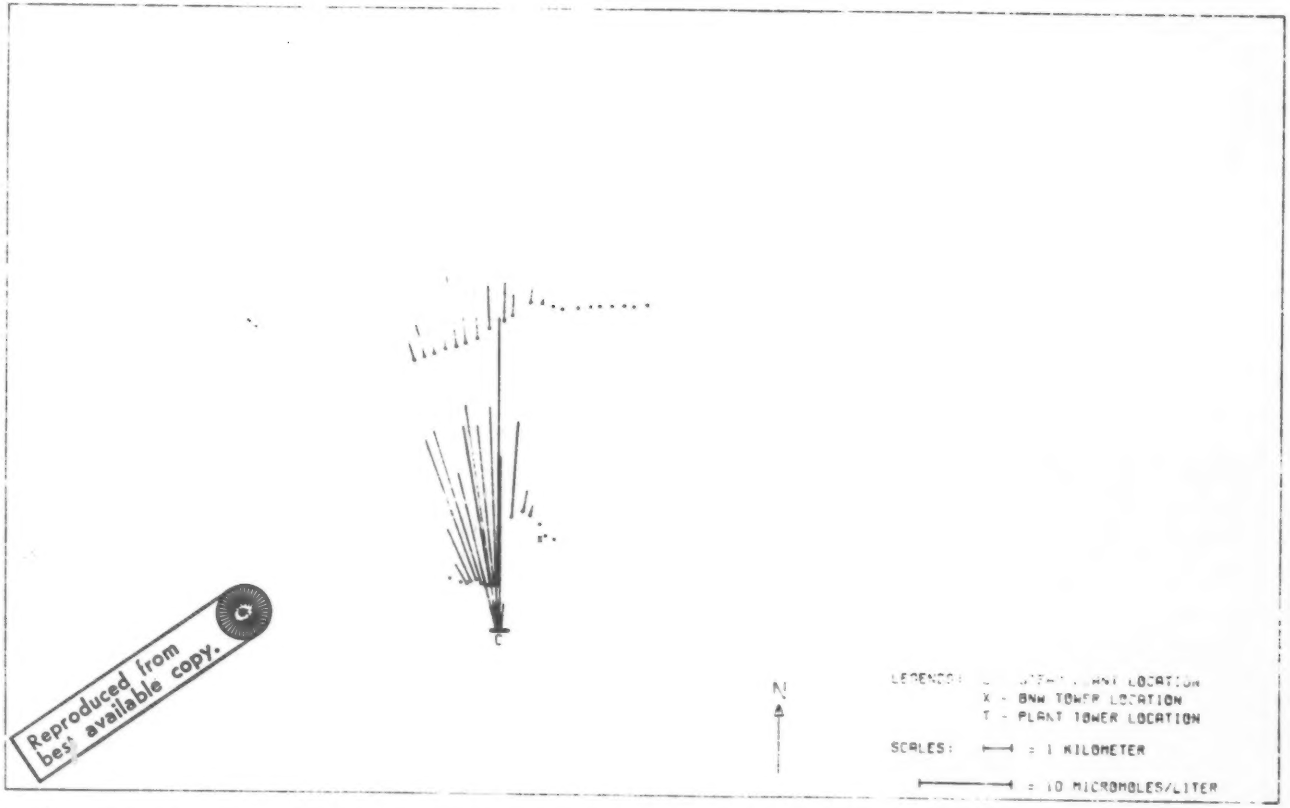

Reproduced from best available copy.

FIGURE 40. PREDICTED SO_2 CONCENTRATIONS IN RAIN - RUN C-3; EPAEC MODEL CALCULATIONS BASED ON GAS-PHASE LIMITED TRANSPORT AND AN SO_2 REACTION DECAY HALF-LIFE OF 15 MINUTES.

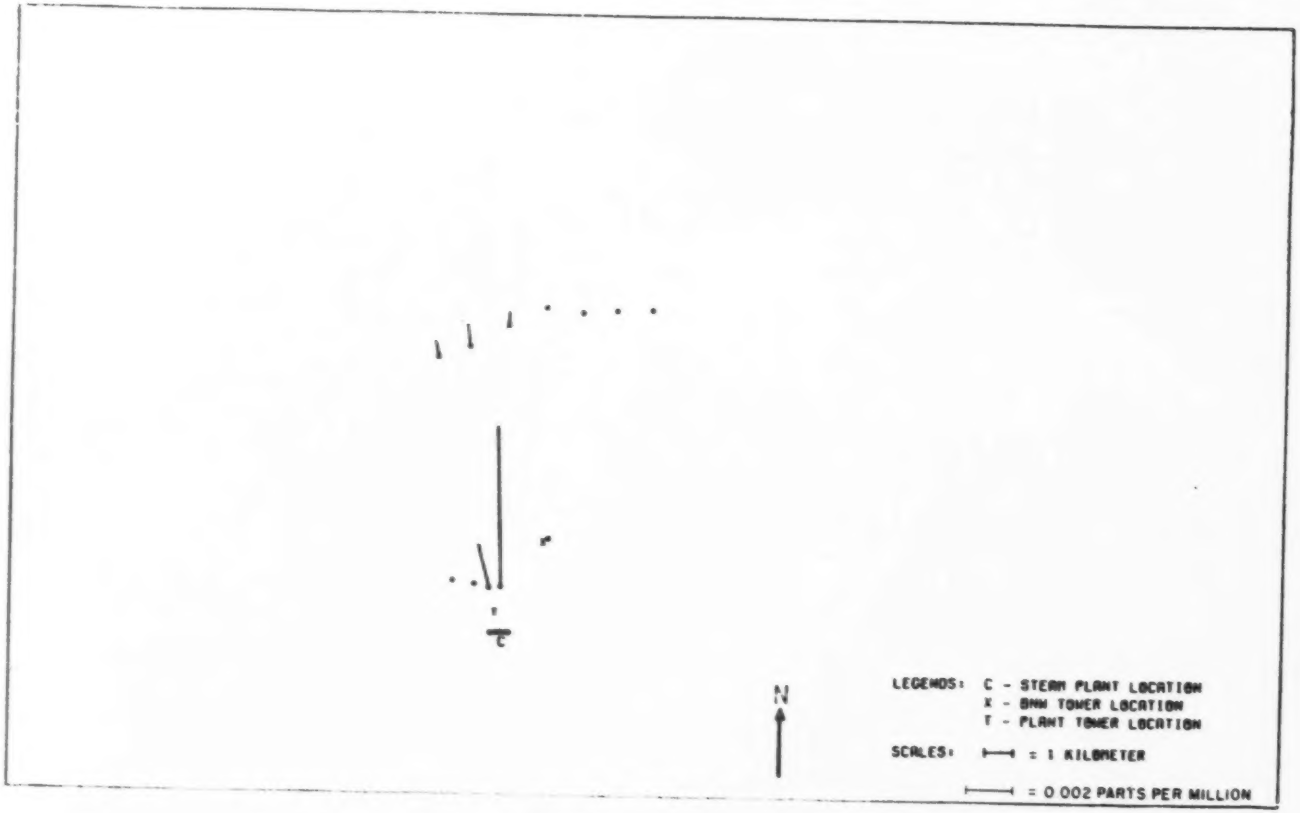
C
N
LEGENDS: C - STEAM PLANT LOCATION
X - BNW TOWER LOCATION
T - PLANT TOWER LOCATION
SCALES: = 1 KILOMETER
= 0 002 PARTS PER MILLION

FIGURE 41. MEASURED SO_2 CONCENTRATIONS IN AIR - RUN C-3.

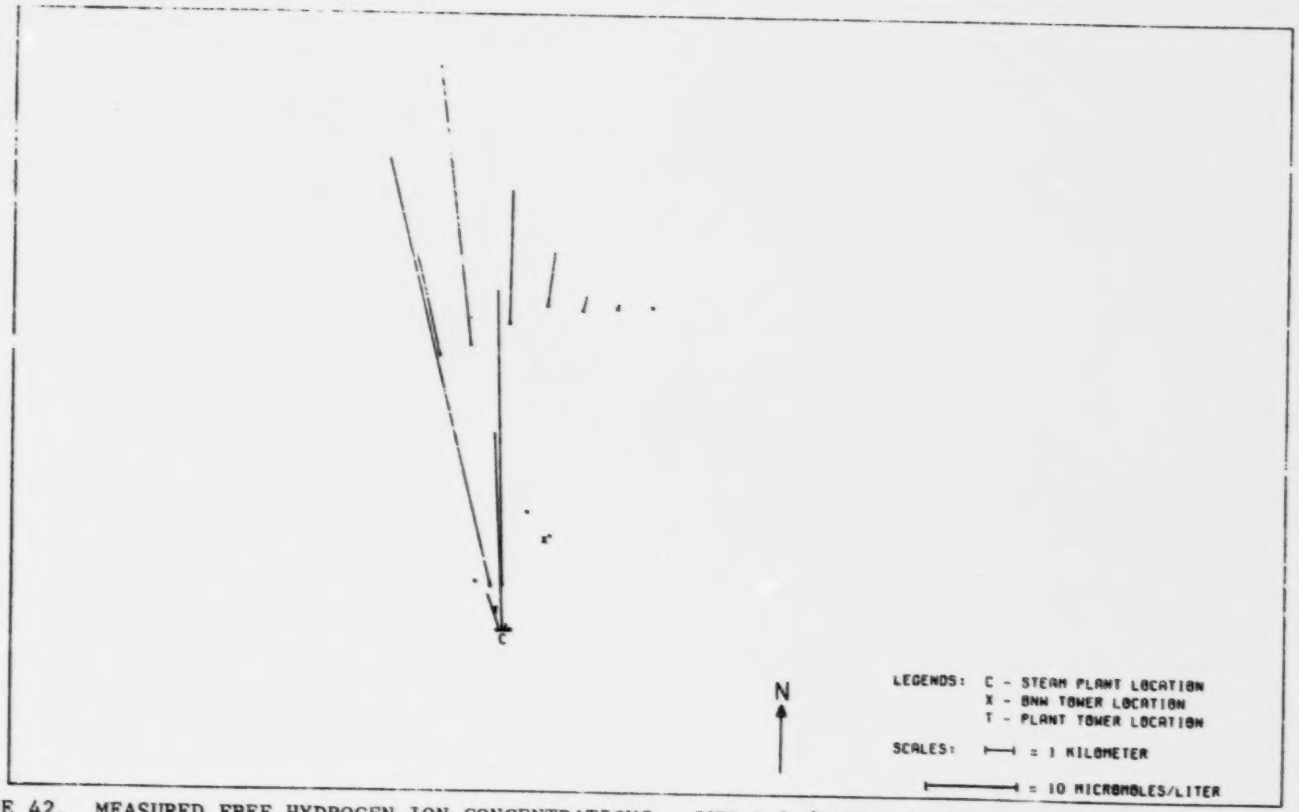
C
X
N
LEGENDS: C - STEAM PLANT LOCATION
X - BNW TOWER LOCATION
T - PLANT TOWER LOCATION
SCALES: = 1 KILOMETER
= 10 MICROMOLES/LITER

FIGURE 42. MEASURED FREE HYDROGEN-ION CONCENTRATIONS - RUN C-3 (FROM pH MEASUREMENTS, BACKGROUND CORRECTED).

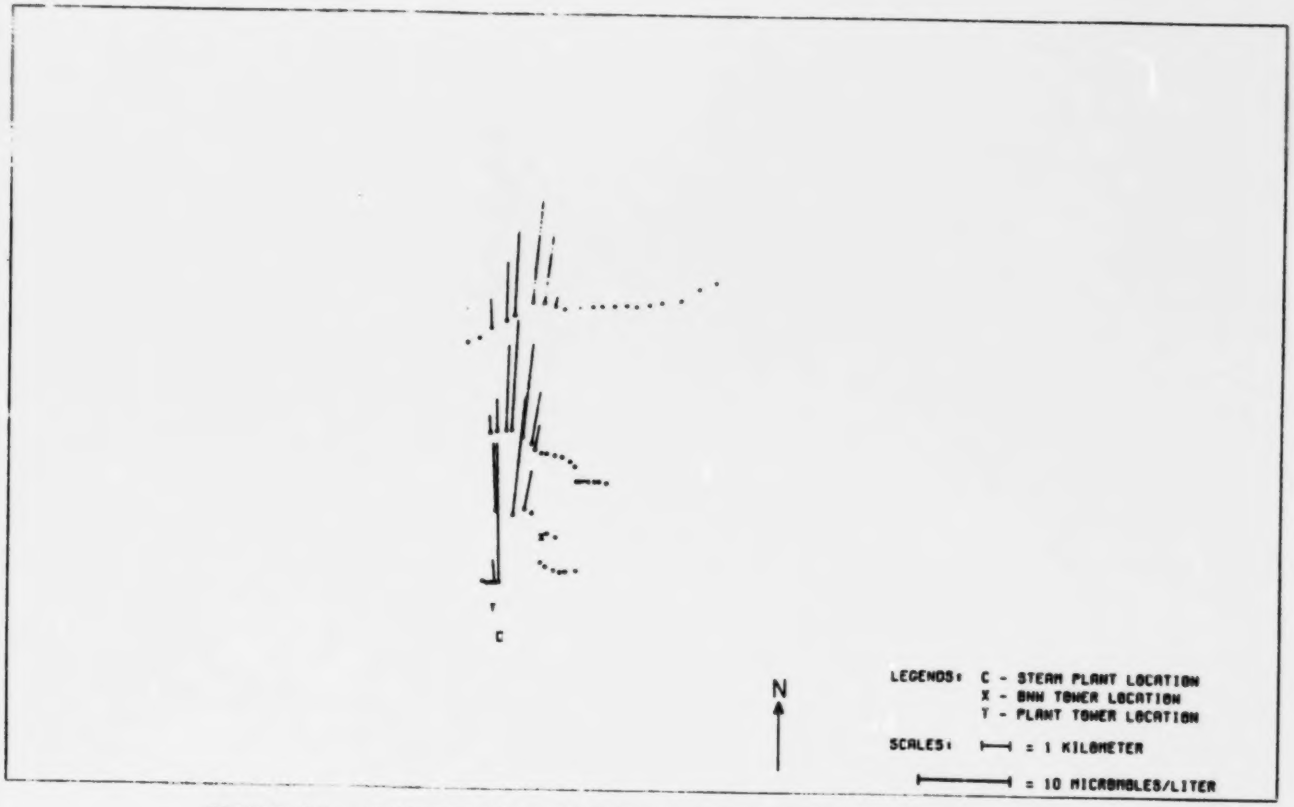
T
C
N
LEGENDS: C - STEAM PLANT LOCATION
X - BNW TOWER LOCATION
T - PLANT TOWER LOCATION
SCALES: = 1 KILOMETER
= 10 MICROMOLES/LITER

FIGURE 43. MEASURED SO_2 CONCENTRATIONS IN RAIN - RUN C-4.

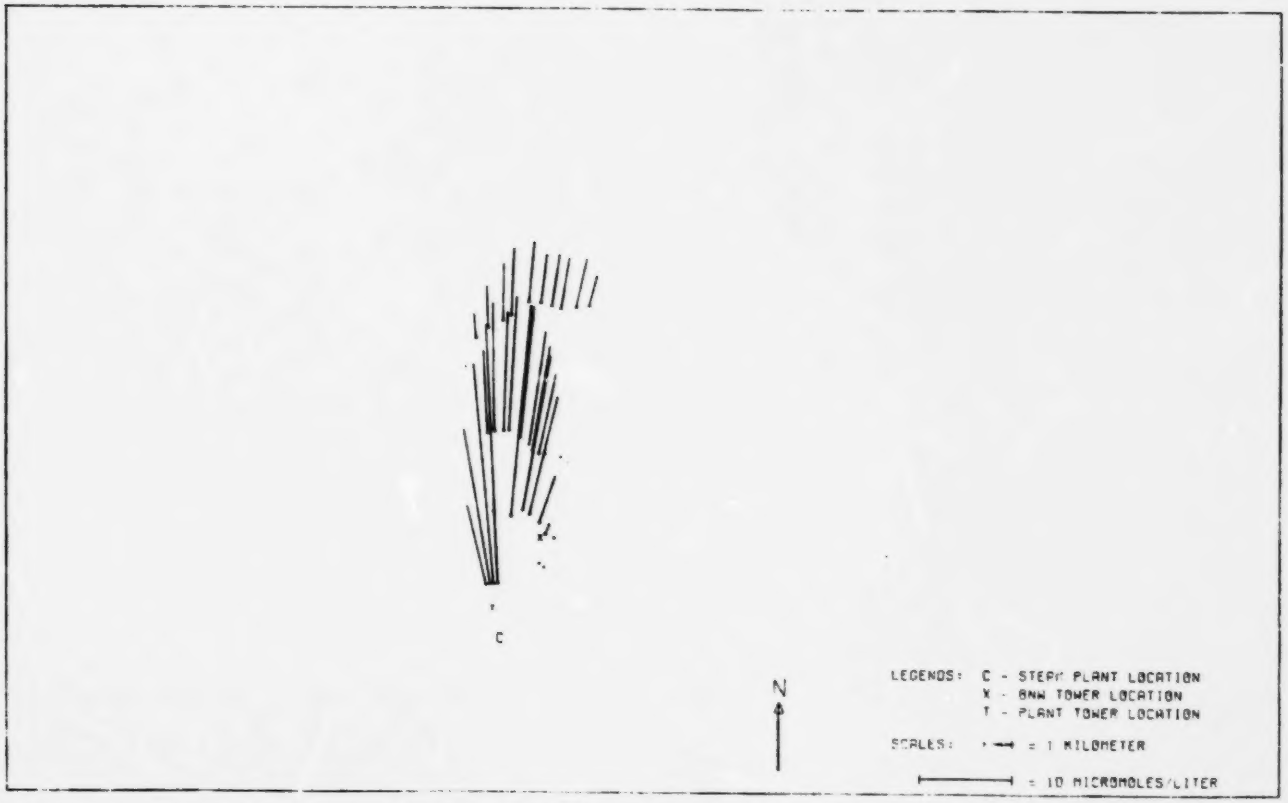
C
T
X
N
LEGENDS: C - STEAM PLANT LOCATION
X - BNW TOWER LOCATION
T - PLANT TOWER LOCATION
SCALES: = 1 KILOMETER
= 10 MICROMOLES/LITER

FIGURE 44. PREDICTED SO_2 CONCENTRATIONS IN RAIN - RUN C-4; EPAEC MODEL CALCULATIONS BASED ON GAS-PHASE LIMITED TRANSPORT AND AN SO_2 REACTION DECAY HALF-LIFE OF 15 MINUTES.

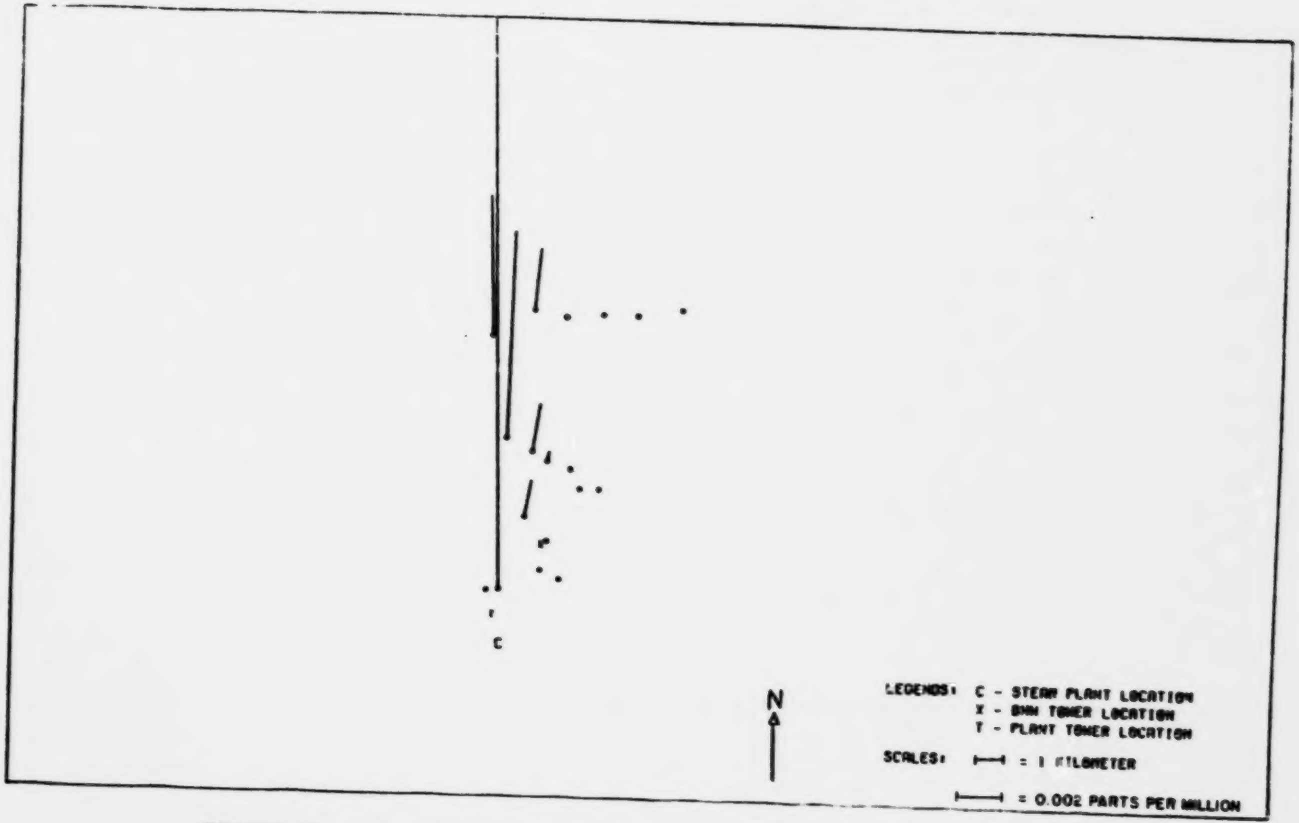

FIGURE 45. MEASURED SO_2 CONCENTRATIONS IN AIR - RUN C-4.

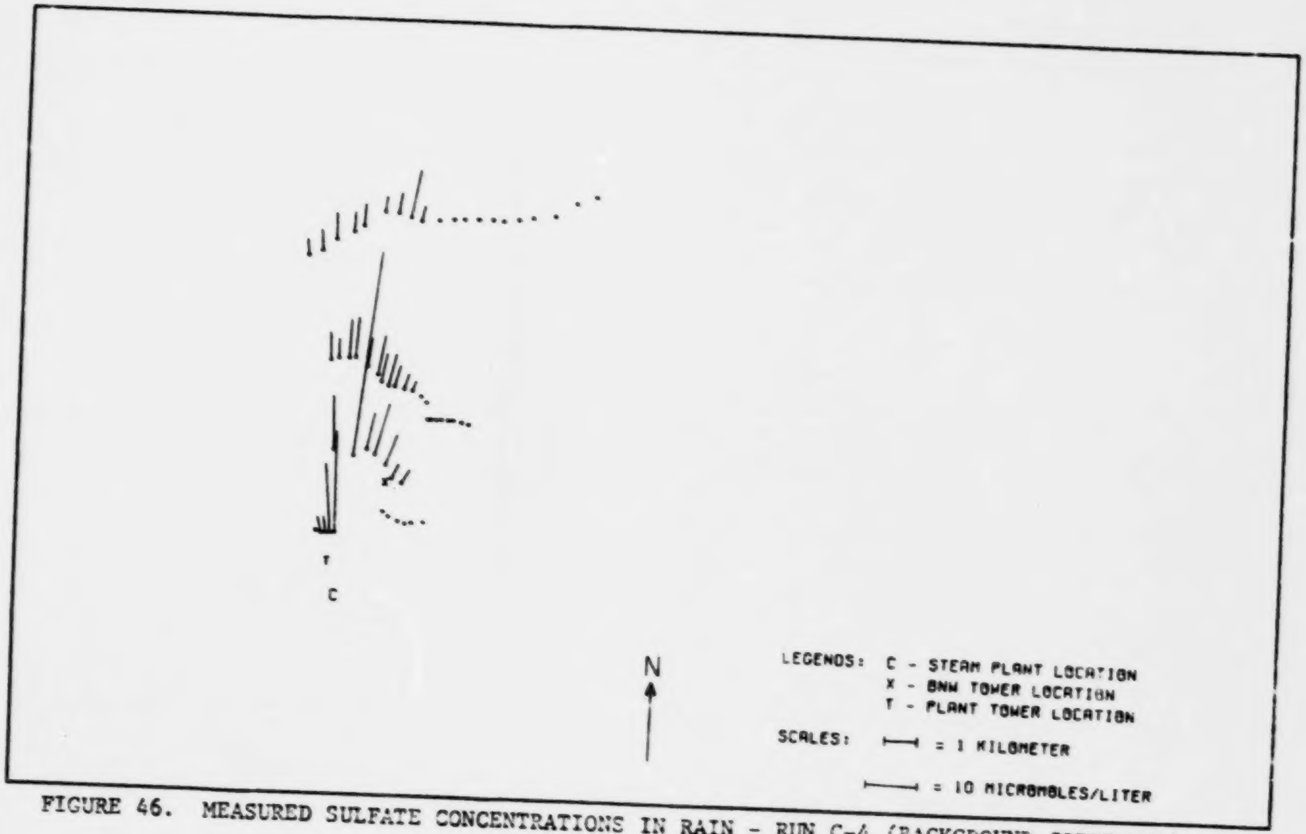
T
C
N
LEGENDS: C - STEAM PLANT LOCATION
X - BNW TOWER LOCATION
T - PLANT TOWER LOCATION
SCALES: = 1 KILOMETER
= 10 MICROMOLES/LITER

FIGURE 46. MEASURED SULFATE CONCENTRATIONS IN RAIN - RUN C-4 (BACKGROUND CORRECTED).

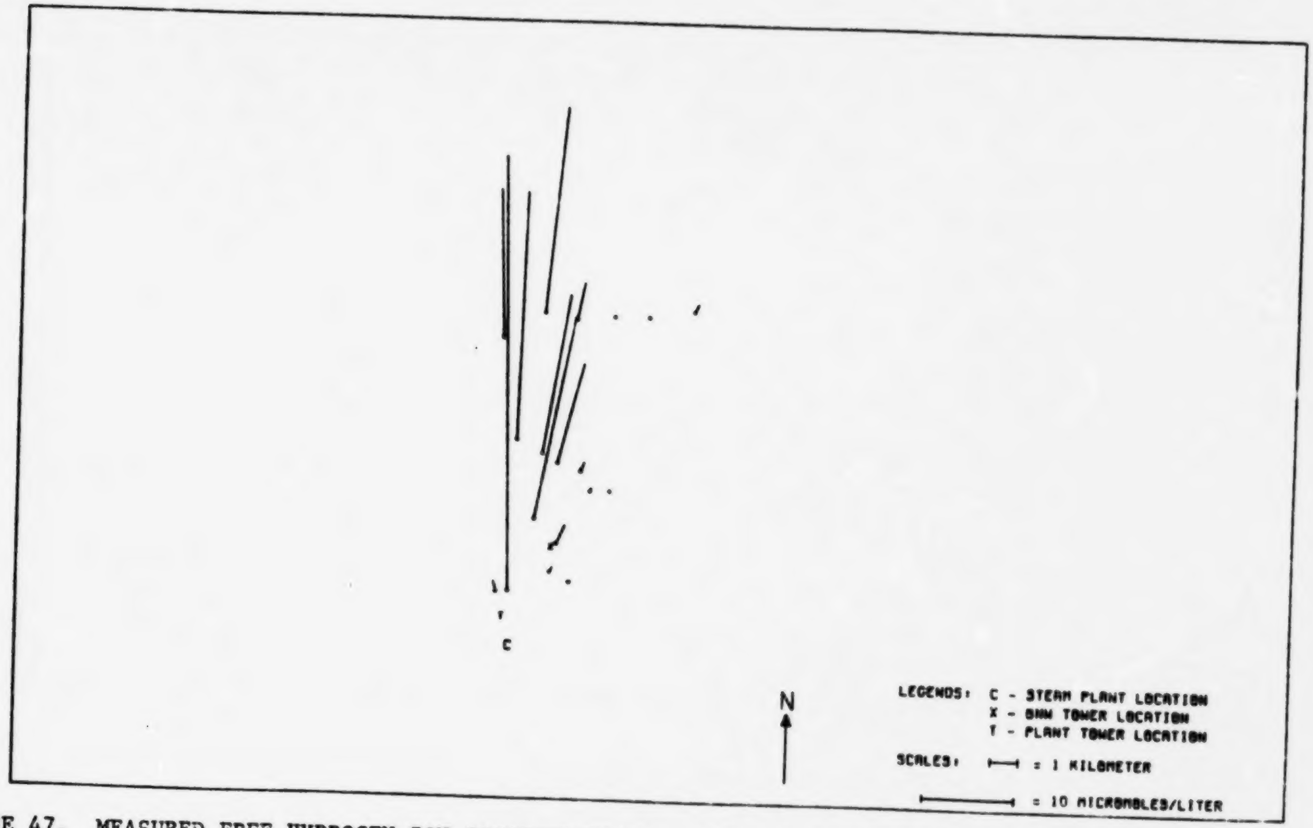
C
T
N
LEGENDS: C - STEAM PLANT LOCATION
X - BNW TOWER LOCATION
T - PLANT TOWER LOCATION
SCALES: = 1 KILOMETER
= 10 MICROMOLES/LITER

FIGURE 47. MEASURED FREE HYDROGEN-ION CONCENTRATIONS - RUN C-4 (FROM pH MEASUREMENTS, BACKGROUND CORRECTED).

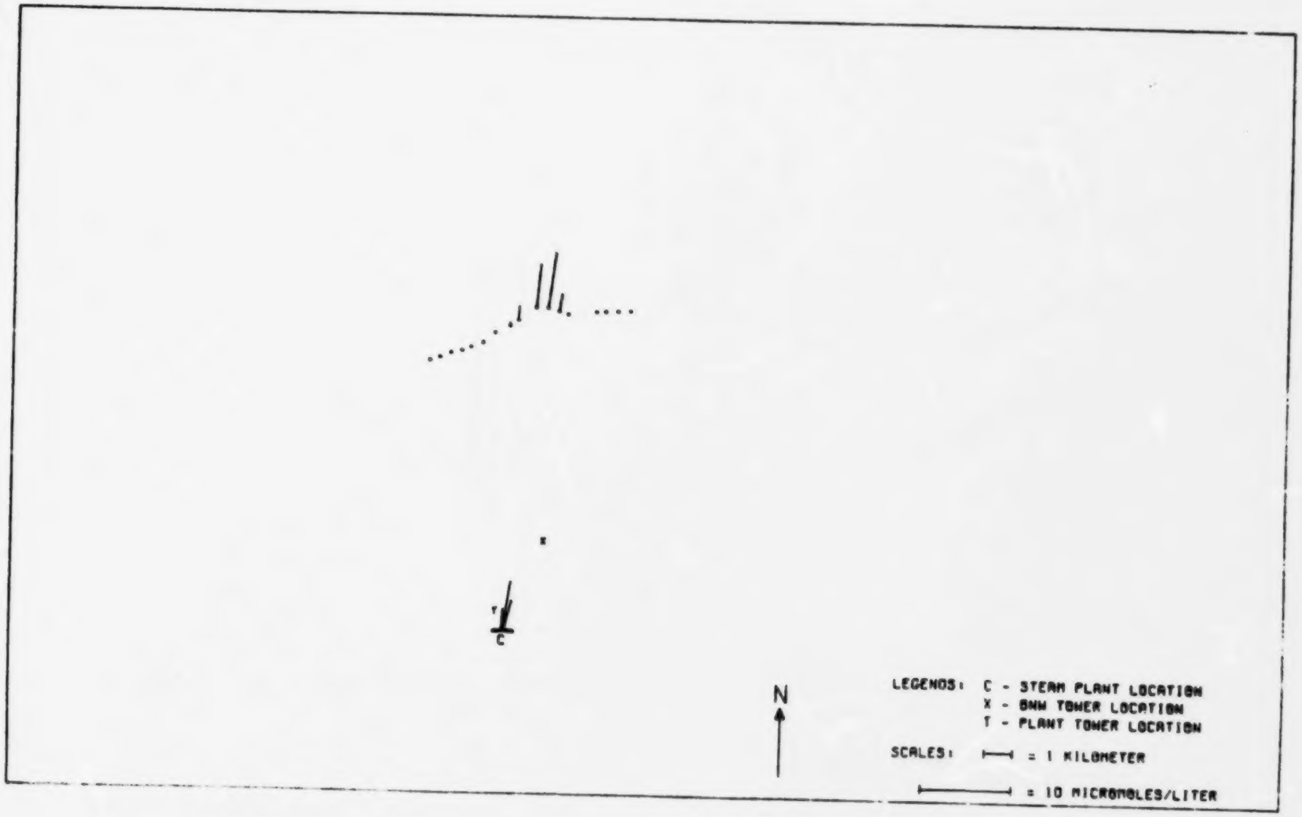
N
C
X
T
LEGENDS: C - STEAM PLANT LOCATION
X - BNW TOWER LOCATION
T - PLANT TOWER LOCATION
SCALES: = 1 KILOMETER
= 10 MICROMOLES/LITER

FIGURE 48. MEASURED SO_2 CONCENTRATIONS IN RAIN - RUN C-5.

Reproduced from best available copy.

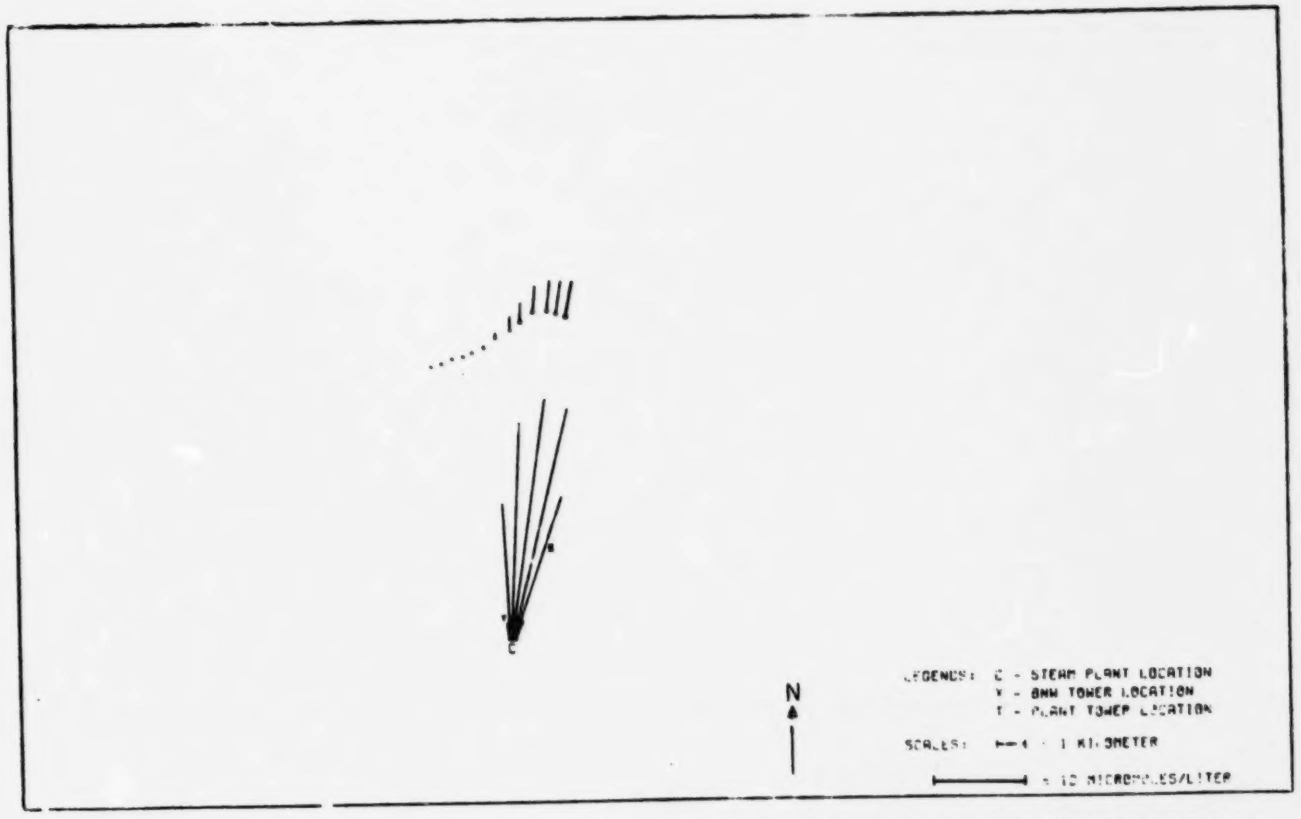

FIGURE 49. PREDICTED SO_2 CONCENTRATIONS IN RAIN - RUN C-5; EPAEC MODEL CALCULATIONS BASED ON GAS-PHASE LIMITED TRANSPORT AND AN SO_2 REACTION DECAY HALF-LIFE OF 15 MINUTES.

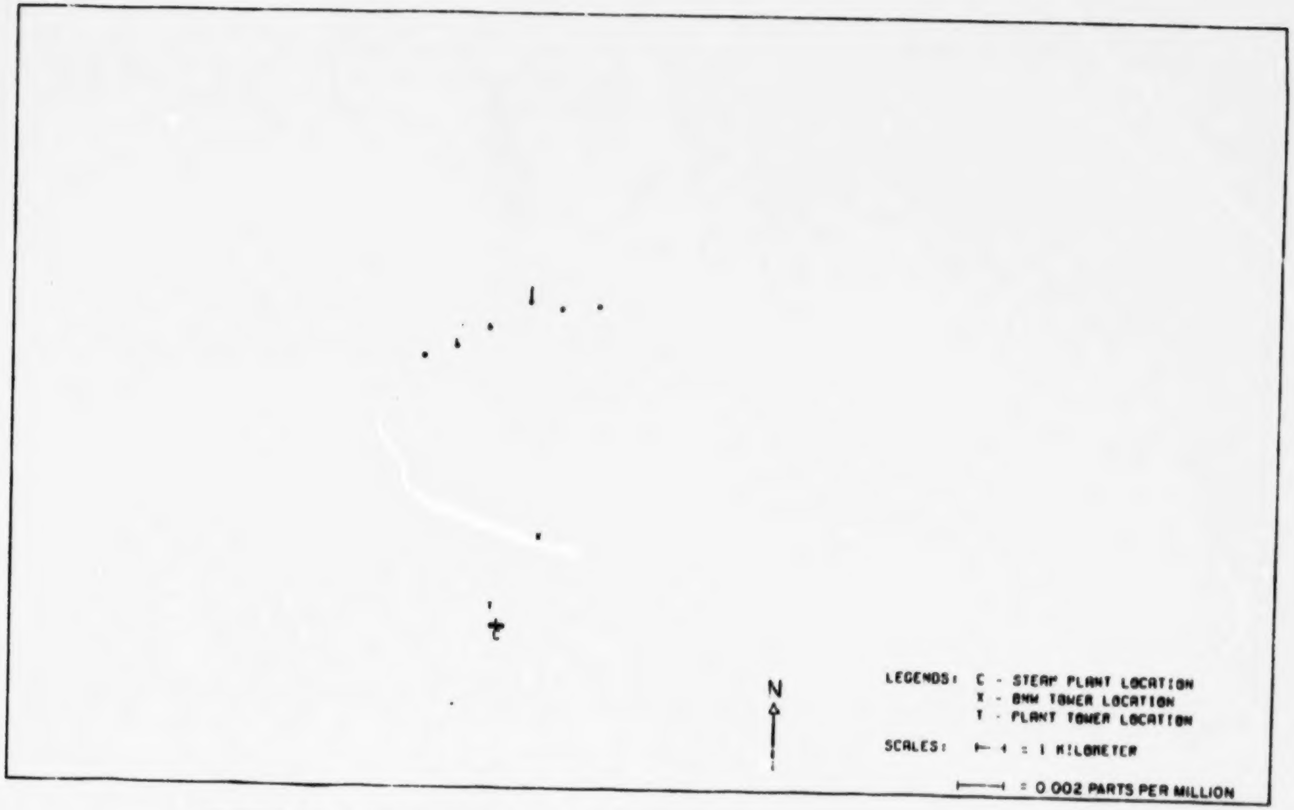

C
N
LEGENDS: C - STEAM PLANT LOCATION
X - BNW TOWER LOCATION
T - PLANT TOWER LOCATION
SCALES: ⊢ ⊣ = 1 KILOMETER
⊢—⊣ = 0 002 PARTS PER MILLION

FIGURE 50. MEASURED SO_2 CONCENTRATIONS IN AIR - RUN C-5.

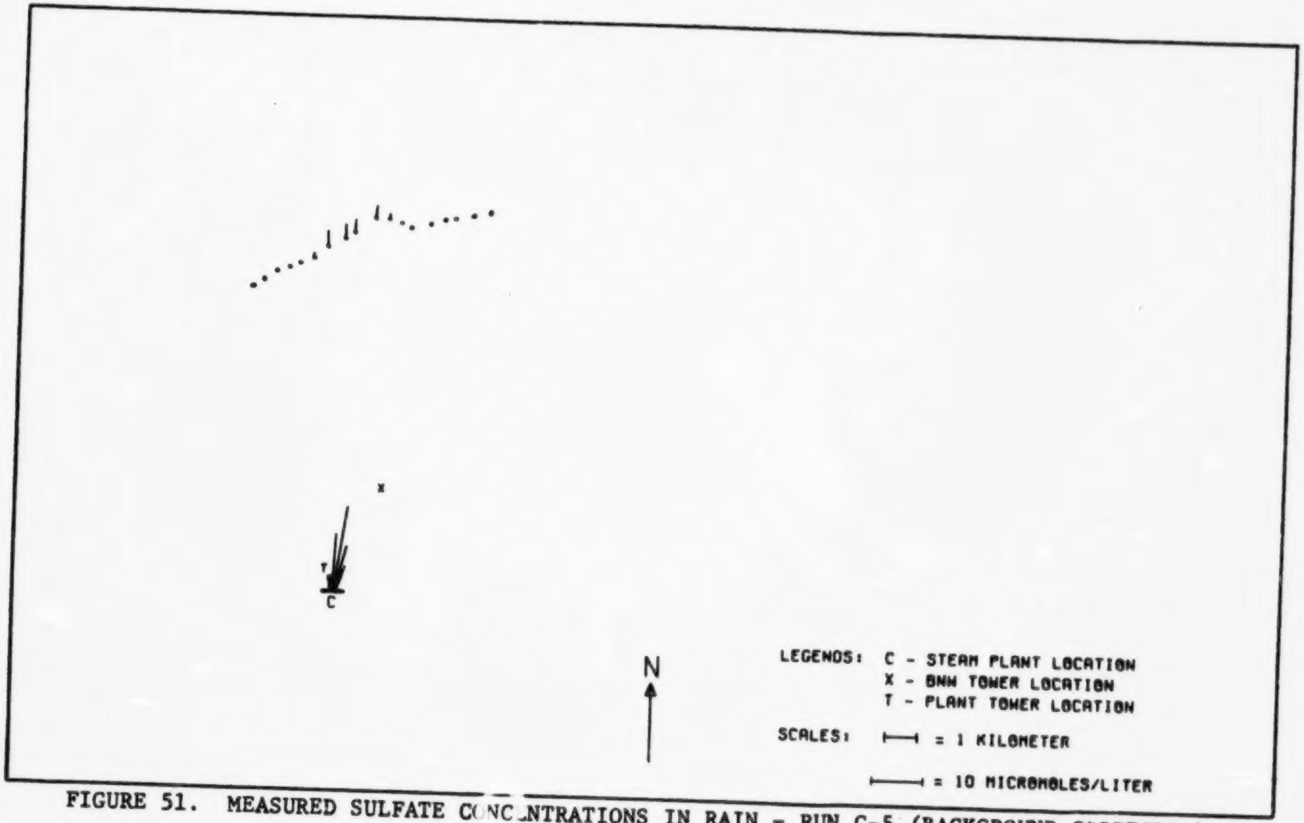
x
T
C
N
LEGENDS: C - STEAM PLANT LOCATION
X - BNW TOWER LOCATION
T - PLANT TOWER LOCATION
SCALES: = 1 KILOMETER
= 10 MICROMOLES/LITER

FIGURE 51. MEASURED SULFATE CONCENTRATIONS IN RAIN - RUN C-5 (BACKGROUND CORRECTED).

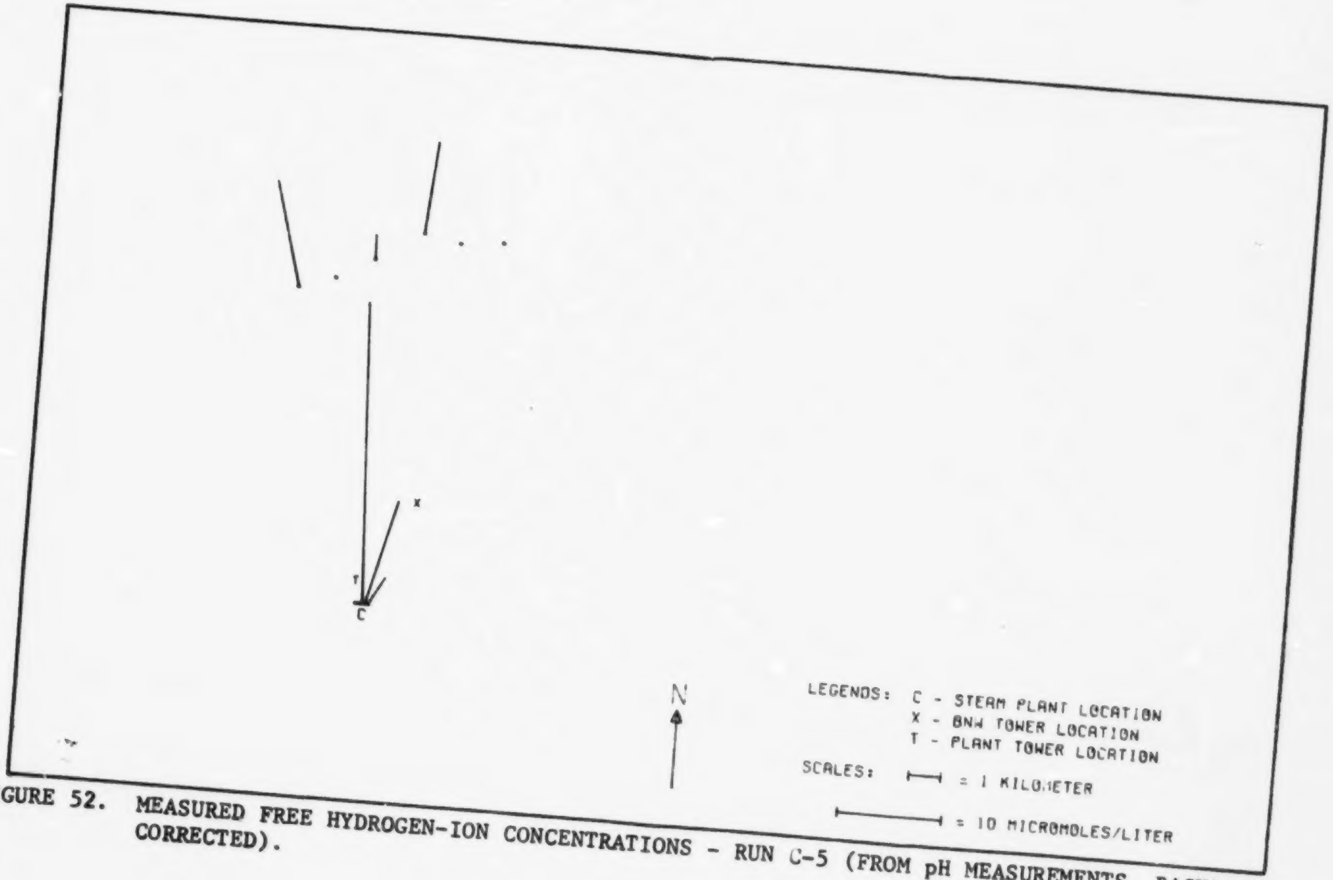
T
X
C
N
LEGENDS: C - STEAM PLANT LOCATION
X - BNW TOWER LOCATION
T - PLANT TOWER LOCATION
SCALES: = 1 KILOMETER
= 10 MICROMOLES/LITER

FIGURE 52. MEASURED FREE HYDROGEN-ION CONCENTRATIONS - RUN C-5 (FROM pH MEASUREMENTS, BACKGROUND CORRECTED).

Run C-2 (February 29)

A filling surface low off the Washington coast, moving northeast, created southwesterly flow of moist and unstable air over the area. Aloft, the jetstream was also southwest-to-northeast and very strong, bringing the liklihood of considerable precipitation. The freezing level was quite high (7500 feet) in the early morning and dropped to 4000 feet as the storm passed. Rainfall totalled 1.27 inches at Centralia; rainfall amounts collected by our samplers (averages for the sampling lines) are shown in Table 11. The lower-level temperature and dewpoint profiles, as well as winds recorded by the rawinsonde flight, are shown in Figure 32. Measured rain concentrations of SO_2 are shown in Figure 33, and for comparison, in Figure 34 is a plot of the concentrations calculated by the EPAEC model. This comparison and comparisons for the other runs will be discussed subsequently in the analysis section. Figures 35, 36, and 37, are plots of SO_2 air concentration, and $SO_4^=$ and H^+ rain concentration measurements, respectively.

Run C-3 (March 1)

This was a situation of a weakening storm; a warm front on the coast at 1300 PST was occluded by the time of its passage over the Centralia area at 2200. The surface flow of air was southerly, cold and moist, but aloft it was southwesterly below 10,000 feet and westerly above. The jetstream was weak overhead. The freezing level was near 3000 feet in the morning and dropped slightly by the next day. The precipitation in Centralia was only 0.37 inches during the day, commencing as snow. The snow changed to sleet near noon, and finally rain at the surface at about 1400. The wind direction at the plant throughout the morning was unsuitable for sampling (easterly), but changed to southerly near 1400, when setout began. Rawinsonde, SO_2, and H^+ concentration data are shown in Figures 38, 39, 41, and 42, with the corresponding EPAEC computations in Figure 40. The generally small volumes of rain collected created a problem for the sulfate analysis; the quantity of hydrogen peroxide pre-added to the sampler bottles proved to be too great in relation to the rain volume collected, resulting in the previously-noted obscuration of the sulfate levels. Despite later efforts to separate the sulfate by other methods, these data were not acquired for Run 3. (On later runs, a smaller amount of peroxide was pre-added, and no such problems were encountered.)

Run C-4 (March 5)

An occluded front passed the area near 0400 PST, and another front was near the coast at 1300. Southwesterly flow of warm, moist air continued throughout the sampling period. The freezing level was near 8000 feet in the morning, and dropped sharply after sampling was completed. Centralia recorded 1.76 inches of rain during the day, but the amounts varied considerably on our sampling network, as Table 11 indicates. The run was, in fact, terminated early because of heavy rain on the outer sampling lines.

The rain rate was variable at the plant, and totalled only a moderate amount. The winds were gusty, and an attempt to launch a radiosonde package--unfortunately during a heavy rain period--failed. The SO_2, $SO_4^=$, H^+ results are shown in Figures 43, 44, 45, 46, and 47.

Run C-5 (March 9)

An occluded front passed the area near 1800 PST. Warm and moist southwesterly flow occured over the area ahead of the front. The freezing level was high, near 10,000 feet in the morning. This run was unique among those conducted at Centralia, in that there had been no precipitation during the previous two days. Those days were calm and unusually warm, with a noticeable buildup of low-level visible smoke. This last run was conducted after the BNW tower had been removed, and was manned by a reduced crew of five persons; thus only two sampling lines were used. The rawinsonde flight failed. The rainfall, which totalled 0.21 inches at Centralia, was light and essentially occured entirely during the sampling period. SO_2, $SO_4^=$, and H^+ data are shown in Figures 48, 49, 50, 51, and 52.

As mentioned previously, some limited measurements of trace metals in the rainwater were performed. These were obtained by acidifying selected rain samples, freezing, and shipping back to the Battelle laboratories for analysis using an atomic absorption spectrophotometer. These results, shown in Table 14, appear to reflect the presence of the plume, although the high

TABLE 14. TRACE METALS ANALYSIS - CENTRALIA, RUN 4.

Sample	Concentration, (g/cm^3) × 10^9					SO$_2$, (moles/cm^3) × 10^9
	Fe	Mn	Ni	Cr	Cu	
BKG[a]	b	2.0	0.76	0.55	2.5	0.0
B10	94	2.3	0.39	0.32	1.8	0.0
B13	225	3.0	0.52	0.74	1.7	2.5
B16	380	25.5	0.87	0.72	2.8	13.0
B20	170	2.2	0.46	0.36	1.4	0.0
C23	130	2.2	0.26	0.32	2.1	1.9
C26	120	2.3	0.35	0.68	1.4	12.0
C28	260	5.5	0.46	0.37	1.0	5.9
C31	98	2.3	0.36	0.31	1.7	0.0
D28	96	1.8	0.57	0.24	1.1	3.2
D29	104	2.2	0.62	0.21	4.5	6.5
D35	240	5.8	0.57	0.50	1.1	0.0

[a] Background sample.

[b] No measurement.

values in the "background" sample, obtained just upwind from the power plant, introduce some definite questions in this respect. These measurements were performed in hopes of elucidating catalytic effects of trace metals in the SO$_2$ oxidation reaction; much more extensive measurement is needed, however, before any significant features can be evaluated in this manner.

The Gill anemometer data were recorded on magnetic tape, translated, and processed to provide short- and long-term average velocities, wind directions, and dispersion parameters using procedures similar to those employed for the Quillayute experiments. Table 15 gives the average velocities and directions for approximately half-hour intervals during Runs C-2 through C-4. The long-term averages for run C-5 appearing in the table were estimated from data from the plant-operated tower, since the BNW tower was removed before this run took place.

It was intended originally that the Gill anemometer results would be employed to calculate dispersion parameters for use with the washout modeling program. It was extremely difficult, however, to apply the resulting values to obtain reasonable or reliable estimates. The major problem in this regard arose because of the large range of times and distances involved. σ values

TABLE 15. AVERAGE WIND DATA FROM ANEMOMETERS - CENTRALIA

Run	Approximate Time Span (PST)	$\bar{u}$, cm/sec	$\bar{\theta}$, deg.[a]
2	1230-1311	747	170
	1315-1344	418	176
	1348-1417	509	182
	1421-1450	578	191
	1454-1523	475	191
	1527-1549	444	181
3	1510-1538	430	180
	1540-1610	531	184
	1612-1642	538	182
	1644-1705	754	186
4	0919-0959	741	173
	1004-1034	770	171
	1039-1109	911	177
5[b]	1230-1545	400	187

[a] Wind direction expressed in degrees from true north.

[b] These are averages of the 15 min. averages reported by wind instrumentation on the plant-operated tower.

calculated from anemometer data were in a reasonable range for receptors on sampling Lines A and B; they became troublesomely small, however, as the transit time (and thus the averaging time) became longer, thus filtering out most of the higher-frequency contributions of the turbulence. In addition, the corresponding sampling times became so long that they often exceeded the length of record of the anemometer data.

In view of the above difficulties we decided to apply one of the simpler, more realistic estimates of the dispersion coefficients. For this purpose we chose the expressions of Smith and Singer[12]

$$\sigma_y = 0.36\ x^{.86} \quad , \qquad (19)$$

$$\sigma_z = 0.33\ x^{.86} \quad , \qquad (20)$$

where x is the downwind distance in meters.

These are somewhat unsatisfying dimensionally, but they have been shown to represent true behavior reasonably well out to fairly large distances. In addition, these expressions represent Smith and Singer's findings for neutral atmospheres, which we have deemed most typical of frontal-type rainfall conditions at Centralia. The following section discusses application of these expressions in conjunction with the EPAEC model to provide SO_2 washout estimates.

ANALYSIS OF RESULTS: SO_2 WASHOUT

A striking feature of the Centralia SO_2 washout measurements is their regular appearance, reflecting the presence of the plume in a well-behaved, quasi-Gaussian manner. This is in sharp contrast to the Keystone results exemplified by Figures 3 through 5, where extremely complex behavior is indicated. Such features are a strong confirmation of earlier speculations, listed in Section III, with regard to the influence of reversibility and background effects. An additional noteworthy point is the difference between Runs C-2 and C-3 in Line A SO_2 concentration levels. Run C-3, characterized by rather small raindrop sizes (cf. Table 12), showed virtually zero SO_2 washout, while Run 2, characterized by abnormally large raindrop sizes and essentially the same wind speed as Run 3, indicated significant washout rates. This is totally in accord with the assumption of reversible washout behavior, and is considered to be strong evidence on its behalf.

The SO_2 washout measurements were examined by employing the EPAEC model in conjunction with input data from the previous section. The pH for each station was estimated from available data (cf. Appendix A) by linear interpolation. Calculations were performed for each experiment using the five different SO_2 reaction rate parameters shown in Table 16.

The values given in Table 16 pertain to the first-order reaction

$$\frac{dc_{SO_2}}{dt} = -kc_{SO_2} \quad . \qquad (21)$$

TABLE 16. FIRST-ORDER RATE CONSTANTS FOR SO_2 DECAY USED IN CENTRALIA MODEL CALCULATIONS.

Rate Constant k, $Hours^{-1}$	Corresponding SO_2 Half-Life, Hours
0	∞ (no reaction)
.35	2
.69	1
1.39	0.5
2.77	0.25

In the probable event that the actual reaction rate does not follow first-order kinetics, reaction (21) can be viewed as a linearization approximation to true behavior. The rate constants in Table 16 fall in the range of expected behavior from actual plumes, corresponding to observed SO_2 half-lives on the order of a few minutes up to the order of hours.

The Centralia results were computed using a special calling program in conjunction with the EPAEC model. This program memorized the topography and arrangement of the sampling stations and, in conjunction with the wind direction, calculated sampling station coordinates relative to the plume centerline. The EPAEC algorithm was then executed and resulting washout concentrations were printed in the usual manner.

Plume loft was calculated using the procedure recommended by Briggs.[13] For the purpose of modeling washout at the Line A stations, the plume was assumed to loft linearly with distance downwind from the stack exit. Calculations for other lines were performed, assuming that the plume had attained its ultimate loft height, by incorporation of an effective stack height with zero loft velocity. These provisions for plume loft can be interpreted visually by referring to Figur 53; effective stack heights and loft velocities employed for EPAEC calculations are given in Table 17.

EPAEC calculations based on gas phase limited behavior and an SO_2 reaction half-life of fifteen minutes are presented in the computer plots shown in Figures 34, 40, 44, and 49. These particular results were chosen for examples primarily because these conditions appeared to provide the best agreement with observation. Lowering the reaction rate in the washout model does not affect the Line A predictions significantly, but influences

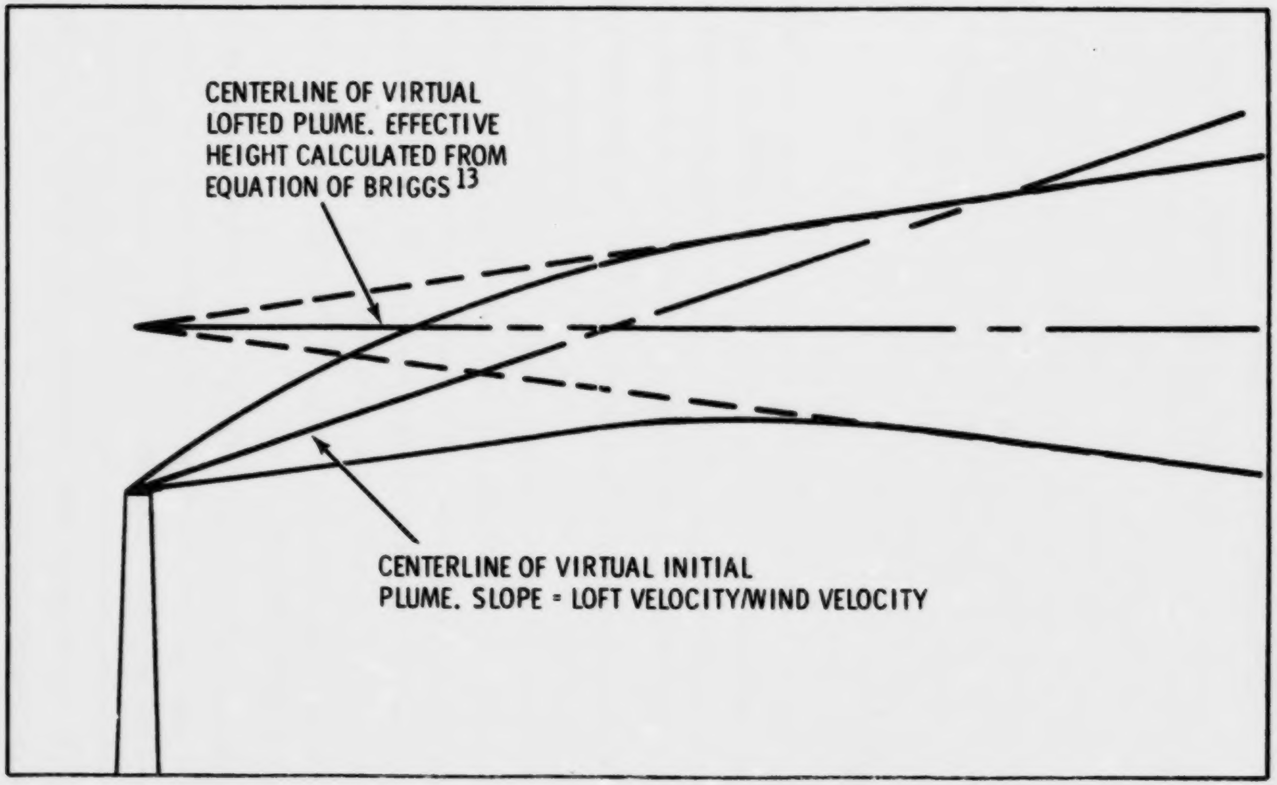
CENTERLINE OF VIRTUAL
LOFTED PLUME. EFFECTIVE
HEIGHT CALCULATED FROM
EQUATION OF BRIGGS 13
CENTERLINE OF VIRTUAL INITIAL
PLUME. SLOPE = LOFT VELOCITY/WIND VELOCITY

FIGURE 53. SCHEMATIC OF IDEALIZED PLUMES EMPLOYED BY EPAEC MODEL FOR CENTRALIA CALCULATIONS.

TABLE 17. EFFECTIVE STACK HEIGHTS AND LOFT VELOCITIES USED IN APPLYING THE EPAEC MODEL TO THE CENTRALIA RESULTS (After Briggs[13]).

Run/Arc	Loft Velocity (VERT), cm/sec	Effective Stack Height at Source, m
2/A	216	143
2/B	0	484
2/D	0	484
3/A	215	143
3/B	0	480
3/D	0	480
4/B	0	366
4/C	0	366
4/D	0	366
5/A	230	143
5/D	0	636

the outer line results increasingly with distance of the receptor from the source. Stagnant drop calculations tend to overestimate washout close to the source, and converge with gas-phase limited calculations as equilibrium washout conditions are approached (cf. criterion of Equation (1)).

An example of the effects of varying the mass-transfer coefficients and reaction rate constants is given by Table 18 which presents the total calculated results for Run 5. From these it is evident that--within the limits of comparison of calculated and observed values--varying the chemical reaction rate over the range shown does not affect the quality of the comparison strongly, except for the extreme cases on the outer sampling line. Here variation of the reaction half-life between fifteen minutes and infinity results in a corresponding change in SO_2 washout concentrations by approximately a factor of five.

Variation of mass-transfer behavior from gas-phase limited to stagnant-drop conditions, in addition to providing higher estimates, results in a more peaked concentration distribution in the crosswind direction. Although the concentrations themselves are less in agreement with measured values, the shape of the stagnant drop based distribution is more in conformity with observed behavior in this case.

TABLE 18. EPAEC CALCULATIONS OF SO_2 WASHOUT CONCENTRATIONS - CENTRALIA, RUN C-5

		Concentration, gm moles/cm^{-3} × 10^9					
Line	Position Number	k = 2.77 hr^{-1}	k = 1.35 hr^{-1}	k = .69 hr^{-1}	k = .35 hr^{-1}	k = 0	Observed
				Gas-Phase Controlled			
A	18	1.58	1.61	1.62	1.62	1.63	0
	19	14.6	14.7	14.8	14.8	14.8	0
	20	23.3	23.4	23.4	23.4	23.4	2.5
	21	26.1	26.1	26.2	26.2	26.2	5.5
	22	25.6	25.6	25.6	25.6	25.7	3.5
	23	16.2	16.3	16.3	16.4	16.4	0
	24	2.01	2.04	2.06	2.07	2.08	0
D	28	1.15	2.97	4.68	5.82	7.2	0
	29	1.99	5.18	8.09	10.0	12.3	0.4
	30	2.32	6.10	9.57	11.8	14.6	1.6
	31	2.74	7.46	11.8	14.7	18.2	4.8
	32	3.36	8.88	13.8	17.0	20.8	6.2
	33	3.75	9.61	14.7	17.9	21.8	2.0
	34	3.85	9.63	14.5	17.7	21.4	0
				Stagnant Drop			
A	18	.15	.15	.16	.16	.17	0
	19	4.36	4.42	4.46	4.47	4.48	0
	20	54.4	54.9	55.1	55.2	55.3	2.5
	21	142.	143.	144.	144.	145.	5.5
	22	40.6	41.0	41.2	41.4	41.5	3.5
	23	4.55	4.62	4.66	4.68	4.69	0
	24	.23	.23	.24	.24	.25	0
D	28	.51	1.35	2.18	2.70	3.37	0
	29	1.03	2.67	4.16	5.15	6.41	0.4
	30	1.26	3.30	5.12	6.37	7.93	1.6
	31	1.61	4.24	6.73	8.41	10.6	4.8
	32	2.05	5.18	8.14	10.1	12.5	6.2
	33	2.32	5.68	8.82	10.9	13.4	2.0
	34	2.37	5.68	8.76	10.8	13.2	0
				Irreversible			
A	18	2.95	3.00	3.02	3.03	3.05	0
	19	112.	115.	115.	116.	116.	0
	20	1852.	1875.	1887.	1892.	1899.	2.5
	21	9619.	9700.	9741.	9762.	9783.	5.5
	22	1050.	1065.	1072.	1076.	1080.	3.5
	23	76.8	78.0	78.7	79.1	79.4	0
	24	3.54	3.61	3.64	3.65	3.67	0
D	28	11.1	27.8	44.2	55.6	70.2	0
	29	28.4	71.6	114.	144.	182.	0.4
	30	40.6	103.	165.	209.	265.	1.6
	31	63.1	164.	266.	339.	434.	4.8
	32	73.7	191.	310.	393.	504.	6.2
	33	72.8	188.	304.	333.	493.	2.0
	34	62.5	162.	262.	70.2	426.	0

A comparison of observed and predicted SO_2 distributions for runs C-2 through C-5 shows that the EPAEC model tends to overpredict on the innermost sampling line. Because of the complexity of the situation involved, it is difficult to speculate meaningfully on the various reasons for this behavior. This sampling line, which was only 300 meters downwind from the source, experienced a considerable plume undercutting effect. Consequently, the EPAEC model encountered the same difficulties with near-miss of a point source by the raindrops as those which were mentioned previously in the context of the Quillayute analysis. The approximate treatment of the lofting plume undoubtedly introduced further inaccuracies in the treatment. Moreover, the longer experiment times at Centralia made it exceedingly difficult to designate representative spectra to characterize rain conditions. The extreme consequences of any non-representativeness in chosen raindrop spectra for Line A calculations is indicated in Figure 54, which is a plot of rain-borne SO_2 concentrations at ground level *versus* drop size. For outer-arc conditions (note the curve for Line D) this drop-size dependence is not nearly so pronounced, and here less refined estimates of drop spectra can be tolerated without severe consequences. In addition to the above factors, the Line A computations were found to be extremely sensitive to rain pH. Consequently, any errors in pH measurement caused large corresponding errors in predictions by the model.

Finally, the potential for rain sampling errors arising from SO_2 desorption from the funnel surfaces should be mentioned. If the values of $K_x a^*/c_x A$ determined from the Quillayute deposition experiments are applicable to the present situation, then for the rain rates experienced at Centralia, corresponding sampling errors could be as great as sixty percent (cf. Table 8 and Figure 26) in extreme cases. Moreover, this situation may have been worsened by an increase of the actual values of $K_x a^*/c_x A$ under Centralia conditions, which involved higher acidity levels in the rain. This effect can be explained in terms of the following relationship between the overall mass-transfer coefficient and the gas- and liquid-phase coefficients:[14]

$$K_x = \frac{1}{\frac{1}{k_x} + \frac{1}{Hk_y}} \quad . \tag{22}$$

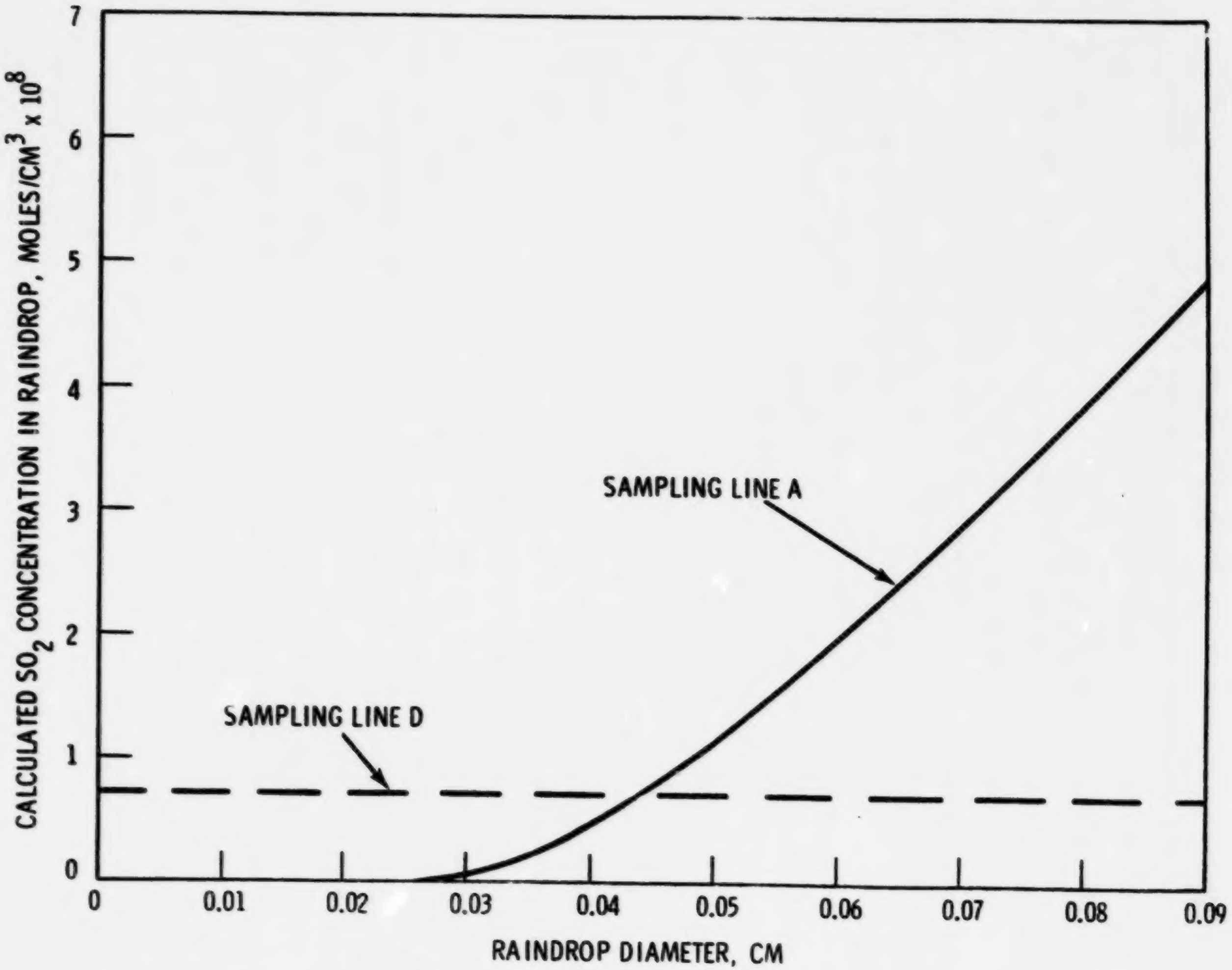

FIGURE 54. RAIN-BORNE SO_2 CONCENTRATIONS AT GROUND LEVEL AS FUNCTION OF RAINDROP SIZE.

The Quillayute experiments indicated that deposition on (or desorption from) the surface water of the samplers is influenced by both the gas- and liquid-phase stages of SO_2 transport; that is, k_x is of the same order of magnitude as Hk_y. Therefore, a decrease in solubility (increase in pH) will cause a corresponding increase in K_x.

Since owing to the higher acidity of the Centralia rain the solubility of SO_2 was indeed decreased, higher values of $K_x a^*/c_x A$ would be expected under these circumstances. It is impossible to give a quantitative estimate of this effect on the basis of available data. In view of these arguments, however, it appears reasonable to expect a large sampling error in the Line A measurements under low rain-rate conditions; it is entirely possible that the EPAEC model predicted values closer to reality than those indicated by the samplers under such circumstances.

Despite the relatively poor quantitative agreement between calculated and observed values for Line A, some of the more qualitative trends provide encouraging evidence in favor of EPAEC model assumptions. In particular, the previously mentioned difference in Line A values between Runs C-2 and C-3 is reflected strongly by the EPAEC estimates--this correspondence is further strong evidence on behalf of the basic EPAEC assumptions. Further dramatic evidence in this regard is given by the final portion of Table 18, which pertains to calculations based on irreversible theory. These values were obtained by altering the solubility function in the EPAEC model to predict total solubility ($d' = 0$) under all conditions. The corresponding results, orders of magnitude higher than both the experimental and reversible theory-predicted values, are considered to be conclusive evidence in favor of the existence of reversible behavior in the case of SO_2 washout.

From the general results, it is apparant that the Smith-Singer[12] equations for plume dispersion provide an adequate description for present purposes. This leads to their recommendation for use in conjunction with the washout model for applied impact analyses. This recommendation is tempered somewhat by the comparatively wide washout distributions observed in a number of the experiments. Much of this behavior, however, was caused by wind shifts during the experiments. These were especially prevalent in Run C-2 (note Table

15). Such behavior could have been modeled more accurately by sequential computations which accounted for the time-variation of plume position. Owing to the complications posed by the fact that each sampler was set out for a different (but overlapping) time period, however, such calculations were not attempted.

The reasonable agreement of the experimental and EPAEC-predicted results for SO_2 washout demonstrated by this study leads us to recommend the use of the EPAEC model, under the conditions indicated, to predict SO_2 washout from large as well as moderate and small plumes under clean-background conditions. Application of this model to contaminated-background conditions will be discussed in Section VII.

ANALYSIS OF RESULTS: SULFATE WASHOUT

The sulfate measurements obtained at Centralia, as shown by the preceeding figures and by the numerical data of Appendix A, distinctly indicate the presence of the power plant plume. As with the SO_2 measurements this behavior is in sharp contrast to that observed at Keystone, and is primarily a consequence of the relative background pollution levels at these two sites.

From the Centralia washout results it is apparent that an appreciable fraction of the plume-borne sulfur existed in the form of sulfate. It is also interesting to note that samples collected on sampling line A showed significant amounts of sulfate (and free hydrogen ions) being washed out--even under circumstances where extremely small quantities of rain-borne SO_2 were detected. From past considerations it is evident that this is a direct consequence of below-plume desorption of SO_2.

Assuming emission primarily as SO_2, the observation of substantial sulfate concentrations in Line A rain indicates a significant, rapid reaction to sulfate near the stack. An additional point of interest is the breadth of the sulfate washout patterns relative to those for SO_2. Several explanations for this effect, involving specific non-linearities in the chemical-reaction/washout process, are possible; none of these, however, has been investigated sufficiently to warrant any specific conclusions in this regard at the present time.

Past inventories[15] have indicated that sulfur leaving power plant stacks is released almost totally in the form of SO_2. The bulk of sulfate washed out of the Centralia plume must, therefore, have been formed by chemical conversion between the source and the receptors. Under conditions where the extent of conversion is small the fact that SO_2 is depleted rather than generated by chemical reaction within the plume permits its washout to be estimated using a rather casual approach to reaction kinetics. In the computer calculations of the previous section, for example, we varied the reaction rate between zero and rather large finite values; although the corresponding changes in predicted washout behavior were indeed noticeable, they were not excessively large compared with the deviations between the experimental and predicted results.

Owing to the fact that sulfate is generated rather than depleted within the plume, its washout should be expected to be much more critically dependent on chemical reaction behavior. Varying the reaction rate from zero to any positive value will, in contrast to similar treatment for SO_2, result in an infinite relative change in predicted sulfate washout. Any truly adequate theoretical assessment of sulfate washout, therefore, must attempt to treat reaction behavior in a more rigorous manner.

Determination of SO_2-sulfate reaction kinetics is not a goal of the present project; in a field study of this type, one cannot expect to describe explicitly the microphysics of the sulfate conversion and removal process. Because of the noted dependence on reaction behavior, however, the sulfate washout results of this study provide a number of important inferences with regard to SO_2 oxidation. The following subsections are addressed to the analysis of sulfate washout in this context.

Limiting Values of Washout and Reaction Parameters

There are a number of processes by which sulfate can be formed in, and subsequently removed from, industrial plumes. Formation can occur through liquid-phase reaction processes where SO_2 is converted to sulfate inside raindrops, or in the cloud-size ($\sim 10\mu$) water droplets which are likely to exist in such plumes in rainy weather. Gas-phase reaction processes may lead to free particles of sulfate whose sizes cover the range of the natural aerosols. Subsequent removal mechanisms, then, cover a corresponding range of possibilities including irreversible gas washout, aerosol washout, and cloud droplet nucleation processes.

In spite of these complexities, one can provide some insight into the properties of the overall process by expressing sulfate formation in terms of an equivalent first-order gas-phase reaction. By applying this approach in conjunction with the Centralia data, upper and lower limits for the reaction-rate constants and washout coefficients can be established. The fact that measurable sulfate was indeed washed out at Centralia precludes at the outset the choice of zero as a lower limit for either the pseudo first-order reaction constant or the washout coefficient. There is nothing initially obvious, however, that rules out the choice of infinity as the upper limit of one or the other of these parameters; the observed washout rates could be attributed, for instance, to a very fast (essentially infinite) reaction rate, with a finite washout rate being the rate-controlling step of the process.

Assuming that the upper-limit reaction rate is indeed infinitely fast, one can estimate a corresponding lower-limit washout coefficient. The well-known expression

$$\Lambda = \frac{M'\bar{u}}{Q'} \quad , \qquad (23)$$

can be modified for this purpose, upon making the conservative assumption of zero upwind removal of material in the plume, to obtain the following form for the lower-limit washout coefficient:

$$\Lambda_{k=\infty} = \frac{M'\bar{u}}{Q_o} \quad . \qquad (24)$$

In the above expressions M' is the molar rate of sulfate deposition (moles/cm sec) at a given downwind distance x_1, and Q' is the molar flow rate of sulfate across the plane defined by x_1. M' can be estimated from the Centralia measurements by crosswind integration of the amounts collected at the individual sampling positions. Figure 55 provides a schematic indication of the significance of the various entities employed in this discussion.

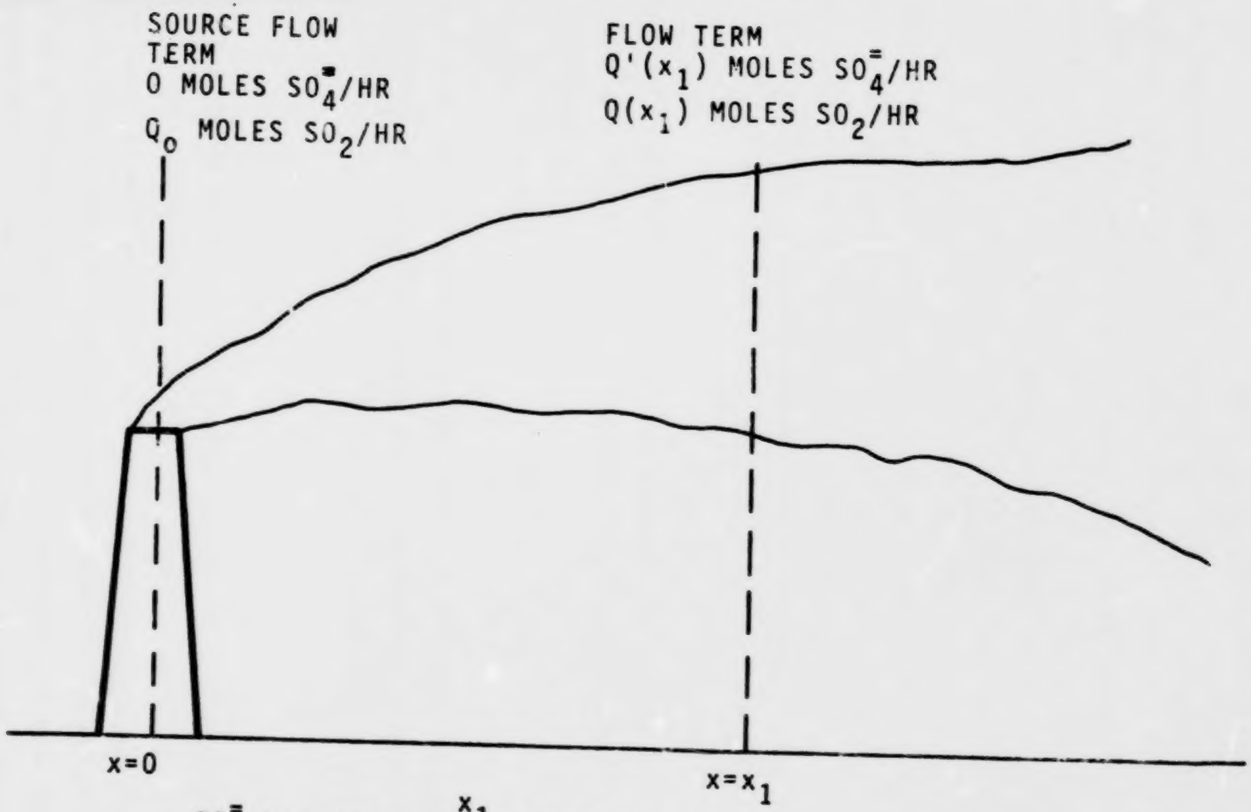
SOURCE FLOW
TERM
0 MOLES $SO_4^=$/HR
Q_o MOLES SO_2/HR
FLOW TERM
$Q'(x_1)$ MOLES $SO_4^=$/HR
$Q(x_1)$ MOLES SO_2/HR
x=0
$x=x_1$

$$SO_4^= \text{ WASHOUT} = \int_o^{x_1} M'(x)dx$$

FIGURE 55. SCHEMATIC OF FEATURES OF REACTION/WASHOUT PROCESS.

In a parallel sense, the lower-limit reaction-rate constant (corresponding to an infinite washout coefficient) can be obtained. Since in this event sulfate is assumed to be washed out the instant it is formed by reaction, the washout rate equals the reaction rate. Again assuming negligible depletion of SO_2 upwind from the receptors, a material balance on a volume of atmosphere defined by a vertical slice of thickness dx in the proximity of x_1 provides the following expression for the lower-limit, pseudo first-order reaction-rate constant:

$$k_{\Lambda=\infty} = \frac{M'\bar{u}}{Q_o} \quad . \tag{25}$$

The similarity of Equations (24) and (25) is not surprising in view of the fact that they both result from attempts to express washout in terms of first-order irreversible processes.

The extreme upper and lower limits of the rate constants and the washout coefficients obtained by applying the above analysis to the Centralia data are shown in Table 19. The actual ranges of washout coefficients, however, can be restricted further by replacing the infinite upper limit with more realistic limits obtained from washout theory. The semi-empirical analysis of Slinn[16] for example, can be used for this purpose. In his analysis Slinn presents the washout coefficient as a function of particle size, as shown in Figure 56; these curves are observed to approach upper limits as aerosol size is increased. The curve for a mean raindrop-radius of 0.2 mm represents a conservatively high estimate for the rains experienced at Centralia, and can be used in conjunction with the normal assumption of proportionality of Λ to the rainfall rate to obtain the revised upper limits of the washout coefficients shown in Table 20. For this estimation, a rainfall rate averaged for all sample lines is used to represent that of each run.

Corresponding lower limits of the washout coefficients could be obtained using the minima in Figure 56 in a similar manner. This proves to be impractical, however, since the resulting values are lower than those estimated using the Centralia results in conjunction with Equation (24), and therefore do not result in any further restriction in the ranges of the extrema.

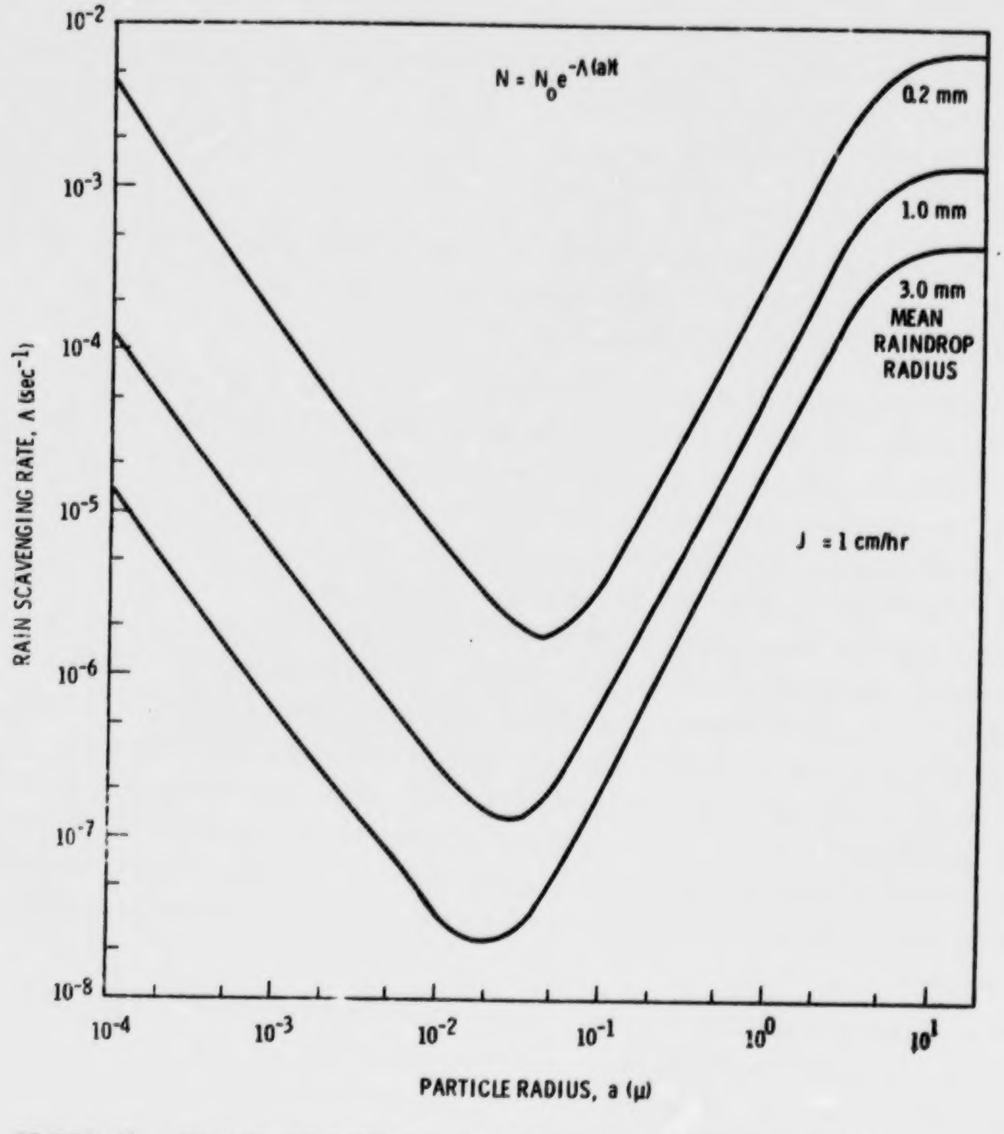

FIGURE 56. WASHOUT COEFFICIENT AS A FUNCTION OF PARTICLE SIZE.[16]

TABLE 19. EXTREME LIMITS OF SULFATE WASHOUT COEFFICIENTS AND REACTION RATE CONSTANTS[a]

Run/Sampling Line	Lower-Limit Parameters, hr^{-1} $\Lambda_{k=\infty}$ or $k_{\Lambda=\infty}$
C-2 A	.0062
B	.033
D	.058
C-4 B	.048
C	.035
D	.043
C-5 A	.00061
D	.0049

[a] Upper limit values for k and Λ are infinite.

The problem of estimating lower-limit rate constants based on these revised estimates of upper-limit washout behavior is not a trivial one. It can be approached in a somewhat superficial sense by formulating a simplified model of the washout process and calculating values of the rate constants from the corresponding equations. Thus, if one begins by assuming oxidation to be the primary mechanism for plume-borne SO_2 removal (dry deposition and washout of SO_2 negligible), then the molar flow rate of SO_2 in the plume at any downwind position x_1 is described in terms of the expression

$$\frac{dQ}{dt} = -kQ; \quad Q = Q_o \text{ at } x = 0 \quad , \tag{26}$$

where k is the reaction-rate constant. If sulfate is assumed to be produced only by reaction (26) and removed only by washout, the corresponding equations

$$\frac{dQ'}{dt} = -\Lambda Q' + kQ; \quad Q' = 0 \text{ at } x = 0 \quad , \tag{27}$$

are obtained.

Combination of the above expressions, integration, and substitution of Equation (23) results in the form

$$M' = \frac{\Lambda k Q_o}{\bar{u}(\Lambda - k)}[\exp(-kt) - \exp(-\Lambda t)] \quad , \tag{28}$$

which can be utilized in conjunction with the Table 20 values to obtain estimates of the limiting reaction-rate constants.

The rate constants thus calculated are shown in Table 20, which provides revised estimates of the extrema in k and Λ. Interpretation of these values, of course, must be weighted in view of the numerous linearizations and other simplifying assumptions used in their derivation.

TABLE 20. REVISED EXTREMA OF SULFATE WASHOUT COEFFICIENTS AND REACTION-RATE CONSTANTS.

Run/Sampling Line	Washout Coefficients, hr^{-1}		Reaction Rate Constants, hr^{-1}	
	$\Lambda_{k=\infty}$	$\Lambda^*_{u\ell}$	$k_{\Lambda=\Lambda_{u\ell}}$	$k_{u\ell}$
2 A	.00622	4.8	0.065	∞
B	.033	4.8	0.061	∞
D	.058	4.8	0.063	∞
4 B	.048	7.0	0.086	∞
C	.035	7.0	0.044	∞
D	.043	7.0	0.046	∞
5 A	.00061	2.2	0.006	∞
D	.0049	2.2	0.006	∞

*Based on analysis of Slinn[16] assuming Λ is proportional to average rainfall rate for all sample lines of run.

In spite of the restrictions of parameter ranges obtained here, the extrema shown in Table 20 are still too widely separated to be of quantitative use. Further extension of this simplified analysis, however, can be employed to provide some insight pertaining to absolute values within these extrema. Such an extension is described in the following subsection.

Non-Limiting Values of Washout and Reaction Parameters

Equation (28) expresses the washout rate M' as a function of the two parameters k and Λ. Since the Centralia experiments provided for measurement of more than one value of M' during each run (one value for each active sampling line), it is possible to express corresponding forms of Equation (28) as simultaneous equations, and solve for "absolute" values of k and Λ directly. Such a treatment presupposes that k and Λ are invariant with distance downwind from the source--an assumption that was used previously in the formulation of Equation (28).

Such calculations may be performed most conveniently by constructing plots of Λ versus k, as dictated by Equation (28), corresponding to the measured values of M'; points of intersection of any two curves then denote solutions for appropriate combinations of k and Λ. An example of such a determination is shown in Figure 57, which presents the solutions to Equation (28) for measured results from three sampling lines of Run C-2. This figure illustrates an unsettling aspect of this method: the fact that Equation (28) is symmetric with respect to k and Λ permits two possible solution pairs (Λ, k) for any two curves. Accordingly, solution pairs for all of the applicable Centralia runs, listed in Table 21, are presented in terms of the two possibilities with subscripts "high" and "low" indicating the alternative cases.

Examination of the numerical results in Table 21 yield the conclusion that the solutions corresponding to large Λ and small k (Λ_{high}, k_{low}) can be excluded on the basis of previous findings. The reaction rate constant, for example, is observed to fall in the vicinity of 0.05 hr^{-1} or less, which corresponds to SO_2 half-lives in the neighborhood of 15 hours or greater. Such lifetimes are more than an order of magnitude greater than those expected on the basis of numerous previous measurements of in-plume SO_2 oxidation behavior by other investigators.[17-21]

In addition, the high values of Λ, about 5 hr^{-1}, are unrealistic. Although washout coefficients of this magnitude are certainly not impossible on the basis of Figure 56, they do pertain to near-optimal conditions, involving washout of either extremely large or extremely small particles. Finally, the computed SO_2 washout results from the previous subsection provide some further (albeit weak) evidence in this regard. The observation of superior agreement between experimental and computed SO_2 washout rates using higher reaction-rate constants in the model appears to indicate that the low reaction rates predicted by the solution set (Λ_{high}, k_{low}) are inappropriate for present purposes.

The alternative solution pair (Λ_{low}, k_{high}), appears to conform with expected behavior in a more acceptable fashion. The washout coefficients, on the order of 0.05 hr^{-1}, correspond with those for particles in the neighborhoods of 10^{-3} and 1 micron (cf. Figure 56). The reaction-rate constants

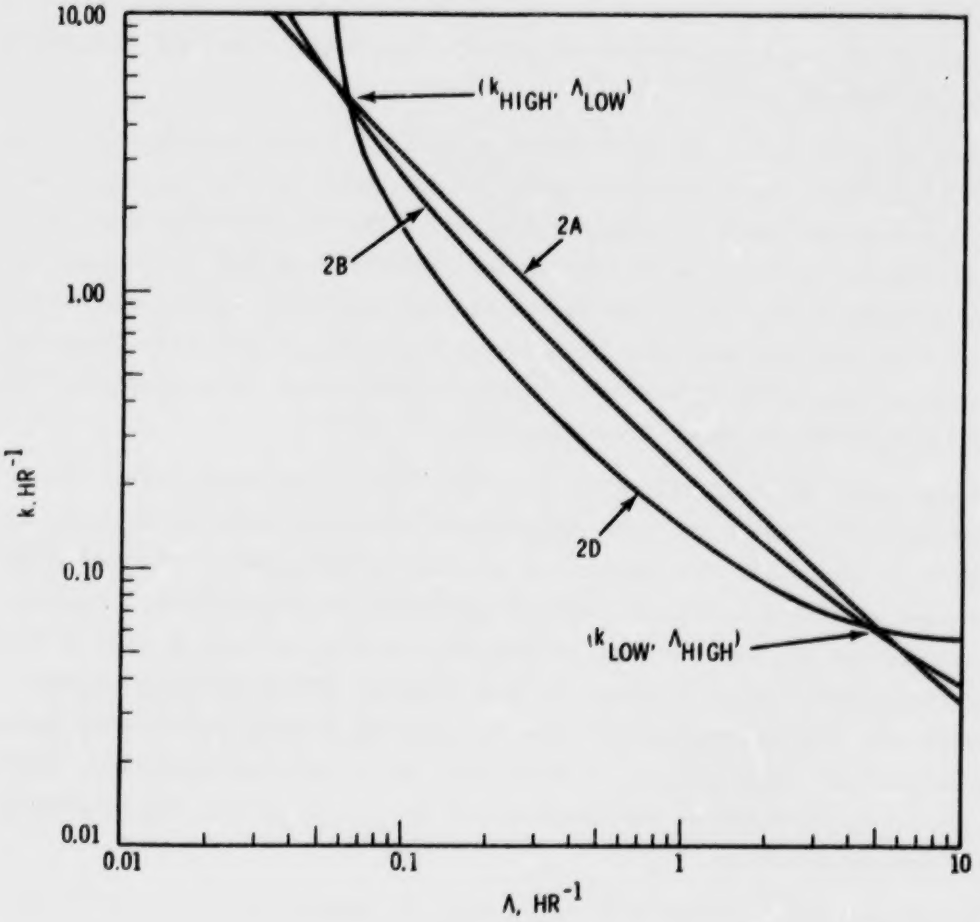

FIGURE 57. SOLUTIONS TO EQUATION (28) FOR RUN C-2.

Table 21. SOLUTIONS TO EQUATION (28) FOR APPLICABLE CENTRALIA SAMPLING LINE PAIRS

Run	Sampling Lines	Λ_{low}, hr^{-1}	k_{high}, hr^{-1}	Λ_{high}, hr^{-1}	k_{low}, hr^{-1}
2	A, B	0.056	5.7	5.7	0.056
2	A, D	0.063	5.1	5.1	0.063
2	B, D	0.064	4.7	4.7	0.064
4	C, D	0.048	5.7	5.7	0.048
5	A, D	0.005	4.1	4.1	0.005

from the pair (Λ_{low}, k_{high}), about 5 hr^{-1}, compare reasonably well with previous measurements[17-20] in view of the increases in reaction rate expected under high-humidity conditions.[22] Because of these considerations we shall proceed on the assumption that the most appropriate solution sets are (Λ_{low}, k_{high}), and shall focus all subsequent discussion on these values.

It is interesting to note that values of Λ and k are obtained which approximately satisfy all three sample lines for Run C-2, and these are close to those found for Run C-4, Lines C and D. (Run C-4, Line B deposition data were fragmented due to the gap in the sampling array; M' and t are very inaccurate for this line, and estimated values for them do not lead to a solution with either Line C or Line D.) This agreement, while somewhat encouraging, is probably rather fortuitous and cannot be cited as a strong argument on behalf of the precepts leading to formulation of Equation (28). In addition the Run C-5 results, while indicating a rate constant comparable to the previous runs, suggest that the washout coefficient should be an order of magnitude lower. Other than the observation that the pH of the background rain was significantly lower for Run C-5 than for the preceeding runs (4.7 *versus* about 5.5), there is little that is obvious to explain this reduction in washout rate.

A relationship between pH and sulfate washout rate could be used also as a plausible explanation for the observation of relatively wide crosswind distributions of this species in rain. Unfortunately there are insufficient data from this study to permit an adequate evaluation of the effect of background pH on sulfate washout rate. There is, however, ample evidence from laboratory investigations[22-28] to indicate that a lowering of M' with pH should indeed be expected. Beilke, et al.,[26] for example, shows that the sulfate-formation rate should be approximately proportional to the inverse square of the free hydrogen-ion concentration over the pH ranges encountered at Centralia. This is certainly in qualitative accordance with our Centralia findings, although on this basis one would expect the reduction in M' to be caused primarily by a reduction in k, rather than Λ as implied in Table 21. Further sulfate washout data with simultaneous pH measurements would do much to elucidate this behavior.

The predicted reaction-rate constants in Table 21, while in fair conformity with expectations from previous studies, are insufficient to explain total behavior observed at Centralia. Corresponding SO_2 half-lives are about ten minutes or less, and are probably too short to explain the airborne SO_2 levels actually observed on the outer sampling lines. In a retrospective analysis of the preceeding considerations it seems apparent that the in-plume SO_2 oxidation process proceeds very rapidly as the plume leaves the source and attenuates as distance downwind increases, leaving higher amounts of SO_2 at larger distances than would be predicted on the basis of linear kinetics in conjunction with the given rate constants.

In view of its simplistic interpretation of the sulfate washout process it is difficult to state just how far Equation (28) should be utilized in interpreting these field results. From previously mentioned studies in the laboratory and in the field it is strongly apparent that the assumption of first-order reaction kinetics is useful only as a first approximation. Moreover, it is evident that the effective washout coefficient used in Equation (28) is strongly cross-correlated with reaction phenomena, and the simple explicit behavior implied by this equation is not actually followed. Thus changes in reaction kinetics will be accompanied by corresponding changes in the apparent washout coefficient, and any microphysical interpretations using Equation (28) become of doubtful validity. In addition, inexact analysis of field behavior arising from plume undercutting, nonvertical rainfall, and approximate cross-plume integration of washout fluxes, present additional complications in this respect.

Additional direct measurements of in-plume SO_2 oxidation rates would obviously be of high interest in this regard. Also, a more refined analysis procedure which could calculate sulfate washout for a more realistic model of rain-plume conditions would be beneficial--both as a method of diagnosing suggested models of sulfate-formation microphysics and as a future tool for related applied impact analyses. The EPAEC model can, with a reasonably modest effort, be updated for this purpose; this modification is recommended as a topic of continued research.

Application of Sulfate Washout Results

In spite of the noted shortcomings of the approximate model of sulfate washout given in this subsection, it still may be applied for empirical estimations of sulfate washout behavior under relatively high background pH conditions ($pH \gtrsim 5.2$). For this purpose we recommend the application of Equation (28) using a reaction rate constant of $4.16\ hr^{-1}$ (SO_2 half-life = 10 minutes). This value is suggested because it is in approximate conformity with a majority of the experimentally observed behavior. Owing to the insensitivity of washout to the reaction constant in this range (cf. Figure 57), the deviations between this value and those in Table 21 do not result in any appreciable deviation in Λ. Insertion of this value in Equation (28) and solving for observed washout rates for Runs C-2 and C-4 yields the following expression for the sulfate washout coefficient:

$$\Lambda \simeq 0.026\ J \qquad (hr^{-1}) \quad , \qquad (29)$$

where the rainfall rate J is in units of $mm\ hr^{-1}$. The constant in this case represents an average of the values of Λ/J as derived from the Equation (28) curves for Runs C-2 and C-4.

Application of this set of values for Λ and k in conjunction with Equation (28) results in the washout rates given in Table 22. As seen from the comparison of measured and fitted values, this procedure provides a fairly consistent order of magnitude method for sulfate washout prediction and is recommended for impact analyses of sulfate washout in the vicinity of fossil-fueled power plants under "clean" background conditions. This recommendation is tempered by the noted deficiencies of the analysis, and by the realization that plant-to-plant variations in plume properties and meteorological situations are likely to result in considerable deviations--especially with regard to chemical reaction behavior. In view of the lack of more comprehensive results, however, the washout rates calculated using the above procedure are expected to constitute the most reliable estimates presently available under these circumstances.

Present results indicate that sulfate washout, under conditions where the background rain pH is of the order of 4.7, can be described in terms of Equation (28) using the same reaction rate constants and a washout coefficient of 0.005. The Run C-5 data providing this indication however are insufficient to warrant any recommendations for Equation (28)'s use under these conditions.

TABLE 22. COMPARISON OF SULFATE WASHOUT RATES: OBSERVED *VERSUS* THOSE CALCULATED USING EQUATIONS (28) AND (29) - CENTRALIA

Run/Sampling Line		Washout Rates, gm-moles/m hr	
		Observed	Calculated [Eq. (29)]
C-2	A	0.0107	0.011
	B	0.0560	0.058
	D	0.1000	0.092
C-3	A	[a]	0.004
	B	[a]	0.019
	D	[a]	0.052
C-4	B	0.0971[b]	0.050[b]
	C	0.0713	0.115
	D	0.0856	0.227
C-5	A	0.00206	0.012[b]
	D	0.0165	0.109[b]

[a] No measurement

[b] Uncertain, see text

SECTION VII.

FURTHER ANALYSES OF KEYSTONE RESULTS

The washout analyses described in this report have been applied in Sections V and VI to situations involving plumes in low-background environments. A more severe test of their predictive capability is in their application to the complex environment of the Keystone plant. This section presents comparisons of EPAEC-predicted and measured washout behavior under such conditions. Also presently considered is an application of the first-order washout and reaction rate analysis of Section VI, for comparison with Keystone sulfate measurements.

Because of the lack of comprehensive support data, particularly pH measurements, the comparisons of this section will be limited to one case. The case chosen for this purpose is Run 4 of the original Keystone series (cf. HTW), whose SO_2 washout distributions were presented in Figure 5 of this report. Additional information regarding this run is summarized in Table 23. Run 4 was chosen as a test example because it exhibits many of the apparent anomalies that were observed during the Keystone field series. In particular, the "negative washout" effect is highly apparent here, and it is of interest to determine the behavior of model predictions under these circumstances.

SO_2 WASHOUT

EPAEC model predictions for SO_2 washout corresponding to Run 4, Arc A, were obtained by executing computer runs using data given in Table 23. Computations were carried out for each station on the sampling line using pH values obtained by interpolating between the centerline and off-plume measurements. A first-order reaction-rate constant corresponding to a 15 minute SO_2 half-life ($k = 2.77\ hr^{-1}$) was employed for these computations. The results are shown in Figure 58, with the computed values depicted by the superimposed curve, and the measurements denoted by radial bars. The fact that the computed values do indeed conform with measurements in indicating a negative washout is considered to be rather dramatic evidence on behalf of the basic precepts employed by the EPAEC model.

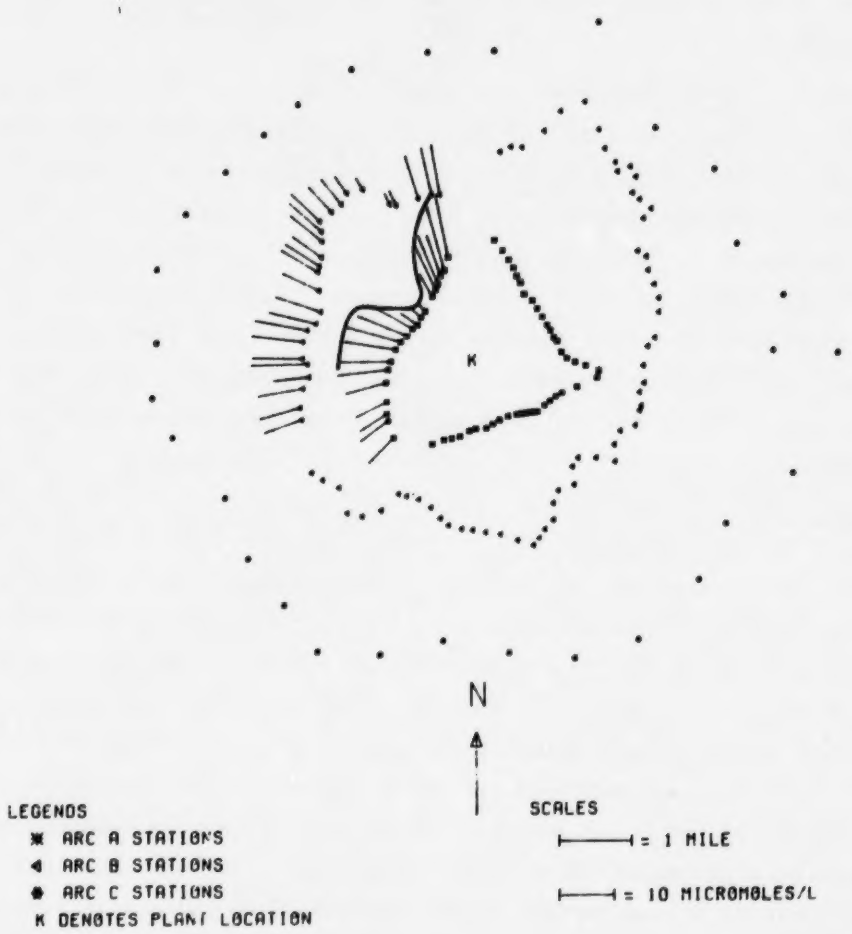
K
N
LEGENDS
✱ ARC A STATIONS
◄ ARC B STATIONS
● ARC C STATIONS
K DENOTES PLANT LOCATION
SCALES
= 1 MILE
= 10 MICROMOLES/L

FIGURE 58. EPAEC MODEL CALCULATION FOR KEYSTONE - RUN 4, ARC A, USING DATA OF TABLE 23.

This application of the model can be criticized on the basis of the fact that it employs some rather uncertain base data in its computations, particularly with regard to pH values and reaction rates. These are admittedly only best estimates used in lieu of more comprehensive measurements. The fact that these reasonable estimates of basic properties can be employed to predict the complex behavior exhibited in Figure 5, however, is still strong confirmation of the practical utility of the computational procedure. It leads to our recommendation for its use in applied washout analysis under high background conditions as well as for less complete atmospheric circumstances. The final section of this report describes a recommended procedure for application of the EPAEC model in this respect.

SULFATE WASHOUT

The semi-empirical sulfate washout equation of Section VI was applied to the Keystone Run 4 results to assess predictive capabilities in a manner similar to that used above to test the SO_2 washout model. This is a somewhat difficult comparison, since the high sulfate background levels and scattered data characteristic of the Keystone sulfate measurements permit only rough estimates of the corresponding washout rates. On the basis of previous considerations (HTW, pp. 101-103) this rate for Run 4, Arc A, at Keystone can be estimated to be roughly 0.01 gm-moles/m hr.

Predictions from Equation (28) for the conditions of Run 4 are shown with the measured washout rate value in Table 24. From this comparison it is apparent that the sulfate washout parameters corresponding to high pH Centralia conditions (Runs C-2 and C-4) substantially overpredict the washout observed at Keystone during Run 4. Washout parameters obtained from the low pH, Run C-5 results agree with the Keystone measurements in a more acceptable manner. Since the background pH's at Keystone were relatively low (5.1 or less) this is considered to be additional evidence of the negative effect of acidity on sulfate washout.

An additional factor to be considered is the higher sulfur-compound concentration existing in the Keystone plume. It seems likely that the resulting increases in acidity may have contributed rather substantially to the lowering of washout efficiency under these circumstances. In view of these complexities we cannot recommend the use of Equation (28) under low pH conditions at the present time, except as an order-of-magnitude approximation. As future washout data are acquired, however, limits on k and Λ should become more well established, and this equation could possibly become more valuable as a practical means of sulfate washout estimation. Additional field measurements taken under a wide variety of circumstances would be an important contribution in this regard.

CONCLUDING REMARKS

Although all quantitative aspects of this field of study are not presently defined in a totally satisfactory manner, the factors discussed in this and the previous sections lend to the significant qualitative conclusion that precipitation scavenging of both SO_2 and sulfate from power plant plumes becomes less efficient when concentration levels of these species are increased. In addition, since dry deposition processes share a number of mechanisms with those of precipitation scavenging, one can reasonably speculate that similar nonlinear behavior occurs for dry deposition as well.

These findings imply that (over meso- and larger scales of distance), ambient levels of SO_2 and sulfate originating from a power plant will not, generally, be linearly proportional to the strength of their source. Doubling the sulfur compound output from a power plant, for instance, would be expected to more than double its original ambient pollution contribution at some point located, say, ten miles downwind. Conversely, a given decrease in source strength can be expected to result in a more favorable resultant modification in ambient levels than would be expected on a strictly proportional basis.

Such behavior is of significance in the context of control policy considerations; it suggests that control policies such as the well-known "linear-rollback" approach may be rather lacking, at least when mesoscale and larger distances are involved. In view of these findings we suggest that evolving control policy plans, in order to achieve optimal benefit, should be designed to account for such nonlinearities in atmospheric response, and should be sufficiently flexible to incorporate additional aspects of atmospheric behavior as such features become known and validated through future studies.

TABLE 23. KEYSTONE RUN 4 BASE DATA

Wind speed at stack height					2.7 m/sec		
Nominal downwind distance, Arc A					1220 m		
Stack height plus estimated plume rise					428 m		
SO_2 release rate					46 gm-moles/sec		
Estimated dispersion parameters:							
σ_y					162 m		
σ_z					148 m		
Raindrop spectrum:							
Drop diameter, cm	.026	.042	.050	.070	.080	.090	.11
Frequency in size range	.011	.089	.1	.2	.2	.2	.2
Rainfall rate					0.13 cm/hr		
Rain pH:							
Centerline					3.9 (est.)		
Off-plume					5.1		
Background SO_2 concentration in air					0.02 ppm		

TABLE 24. RESULTS OF APPLICATION OF SULFATE WASHOUT MODEL TO KEYSTONE, RUN 4, ARC A DATA

Washout Parameters Λ, k (hr^{-1})	Basis for Parameters	Washout Rate M' gm-mole/m hr
0.033, 4.16	Centralia Runs C-2 and C-4	0.23
0.005, 4.16	Centralia Run C-5	0.035
—— Keystone Run 4 Measurement		0.01

SECTION VIII.

RECOMMENDED APPLICATIONS OF THE EPAEC MODEL FOR ENVIRONMENTAL IMPACT ANALYSIS

The purpose of this section is to outline a procedure for application of the EPAEC SO_2 washout model to general environmental impact analysis. The complete model is listed in Appendix C: we present here salient points regarding recommended input parameters and sub-models. In general, these recommendations derive from the experimental knowledge gained from this project; for example, the plume loft and diffusion parameters considered reflect continuous, frontal-type rainfall conditions (~ neutral stability). However, by example, we expect that it will be clear what modifications are required for other situations. The following may be considered a typical procedure; features of the approach which are variable, depending on the user's situation, are noted.

BASIC INPUT

The basic input to the model includes the following entities: plant operating characteristics and site factors; physical constants related to the pollutant gas, rain, and air; diffusion and other plume parameters: site meteorological parameters. The first two categories include various user-specified terms and known physical constants. These are summarized in Table 25. The latter two categories involve greater sophistication regarding choice of terms; our recommendations follow.

Plume Parameters

Briggs' revised formulae[13a] for power plant plume rise under neutral atmospheric conditions are given by

$$\Delta h = 1.6\, F^{\frac{1}{3}} x^{\frac{2}{3}}/\bar{u} \qquad (x < 3.5\, c_B\, F^{\frac{5}{8}}) \quad , \tag{30}$$

and

$$\Delta h = 1.6\, F^{\frac{1}{3}} (10\, h)^{\frac{2}{3}}/\bar{u} \qquad (x > 3.5\, c_B\, F^{\frac{5}{8}}) \quad , \tag{31}$$

where $F \cong 3.7 \times 10^{-5}\, Q_H$, m^4/sec^3

Q_H = rate of heat emission from the stack to the atmosphere, cal/sec

TABLE 25. SUMMARY OF REQUIRED INPUT DATA FOR THE EPAEC CODE, AND RECOMMENDED VALUES FOR INITIAL USE

Input Parameter	Computer Symbol	Value and/or Source
A. Plant and Site Characteristics		
Receptor location	XBUK,YBUK,ZBUK (cm)	Set XBUK as dictated by user; Set YBUK and ZBUK equal to zero (see text)
Grid-spacing parameters	DELTAY,DELTAZ (cm)	Set equal to zero
SO_2 release rate	Q moles/sec	Plant characteristics
Temperature	T	As dictated by user
B. Physical Constants		
Diffusivity of SO_2 in water	DAX cm^2/sec	9×10^{-6} cm^2/sec^2
Diffusivity of SO_2 in air	DAY cm^2/sec	0.136 cm^2/sec^2
Kinematic viscosity of air	XNU cm^2/sec	.0133 cm^2/sec^2
Atmospheric pressure	P atm	1 atm.
C. Plume Parameters		
Excess hydrogen-ion concentration	HEX molar	3.16×10^{-6} molar or as dictated by user
Effective release height	H	Equations (30) and (31)
SO_2 reaction-rate constant	RK sec^{-1}	0.00077 sec^{-1}
Plume-dispersion parameters	SIGPHI,SIGTHE cm	Equations (32) and (33)
SO_2 background	BKG mole fraction	Zero or as dictated by user
D. Meteorological (Climatological) Factors		
Raindrop spectrum parameters	N,D(I),F(I) number,cm,cm^{-1}	Representative values (see text)
Rain rate	XNT cm/sec	As dictated by user
Loft Velocity	VERT cm/sec	See Appendix C

h = stack height, m

x = distance of interest downwind, m

$\bar{u}$ = wind speed, m/sec

c_B = Briggs' constant: = 14 m for $F < 55$ m^4/sec^3, = 34 m for $F > 55$ m^4 sec^3

The separation into two equations reflects an approximate description of the bending over of the plume at distance; thus, the effective stack height $H = h + \Delta h$ is obtained through a choice of Equation (30) or (31) depending on the distance of interest to the user.

The Smith-Singer relationships,[12] as discussed in Sections VI and VII, provide a reasonably adequate estimate of diffusion parameters on a power plant siting study scale of distances. The parameters for neutral stability (which are not greatly different from those for unstable conditions), given in Equations (19) and (20), may be written in terms of the model's input requirements, as:

$$\sigma_\theta = 0.36\ x^{-.14} \quad , \tag{32}$$

$$\sigma_\varphi = 0.33\ x^{-.14} \quad . \tag{33}$$

On the basis of behavior observed from this study, a reaction-rate constant pertaining to a 15-minute SO_2 half-life ($k = 2.77\ hr^{-1}$) is recommended for use with power plant calculations. Insertion of SO_2 background levels and excess hydrogen-ion concentrations will depend on the information available to the user. If these levels are unknown, the use of a zero SO_2 background level and a hydrogen-ion concentration of 3.16×10^{-6} molar (corresponding to a pH of 5.5) will result in conservatively high washout predictions.

Meteorological Parameters

Certain meteorological parameters (or more properly, climatological, when dealing with year-round impact) are required, including wind speed and direction, rainfall rate, and raindrop size characteristics. The problem posed by variations in meteorological conditions and the corresponding difficulties in interpreting long-term washout behavior can be addressed by proceeding through the sequence of steps listed below:

1. Obtain wind and rain frequency records for the proposed plant location. Divide the wind speeds into three or more ranges, and note associated frequencies of occurence and directions.

2. From the rain records, divide the rain rates into three or more ranges and note associated frequencies of occurence.

3. Obtain representative drop-size spectra for each discreet rain intensity. These can be acquired from local measurements if available; if not, generalized spectra[29,30] can be employed.

4. Employ the EPAEC model under the conditions specified in this section to obtain cross-plume washout distributions for each chosen set of wind-velocity-rain conditions.

5. Combine the computed washout distributions according to the previously acquired synoptic records to obtain estimates of long-term washout behavior.

INTRODUCTION OF DATA

The physical data necessary for calculations involving the EPAEC code are summarized in Table 25. These are read using the general-purpose main program listed in Appendix C; an excerpt of this program showing the data-reading sequence is given below:

```
100   READ   (5,320)   N,J1,J2,J3,J4,JOPT,JP,JEND
      IF  (J1.EQ.1)  GO TO 110
      READ   (5,330)   (D(I),I=1, N)
      READ   (5,330)   (F(I),I=1, N)
110   IF  (J2.EQ.1)  GO TO 120
      READ   (5,340)   DAX,DAY,HEX,XNU,P,T,XNT,RK
120   IF  (J3.EQ.1)  GO TO 130
      READ   (5,350)   SIGTHE,SIGPHI,U,H,Q,VERT,BKG
130   IF  (J4.EQ.1)  GO TO 140
      READ   (5,360)   XBUK,YBUK,ZBUK,DELTAY,DELTAZ
```

The first READ statement reads the number of steps in the discrete raindrop-size spectrum (N) (cf. Table 12), in addition to a series of control variables. If these are set as follows:

J1-J4 = 0
JOPT = 1 for gas-phase limited conditions. JOPT = 0 for stagnant-drop conditions.*

JP = 1
JEND = 0 ,

then the program will proceed to calculate a distribution of washout concentrations about the plume's centerline, and integrate to provide a washout rate for the specified physical conditions of the problem.

Input formats for a typical application are shown in Table 26. For further details regarding formats, options, and extensions of the EPAEC model's capabilities, the reader is referred to the comprehensive description in Appendix C.

TABLE 26. EXAMPLE INPUT DATA FORMAT FOR EPAEC CODE

```
5     0     0     0     0     1     1
.01       .02       .03       .04      .05
.05       .10       .25       .45      .15
 9.E-6    1.36E-1   3.16E-6   1.33E-1  1.0E0   2.80E2   1.30E-4   1.16E-3
.062      .056      5.13E2    1.17E4   3.7E0
 3.0E5
```

---

*Gas-phase limited conditions recommended for impact analyses.

SECTION IX.

REFERENCES

1. Hales, J. M., J. M. Thorp, and M. A. Wolf. Field Investigation of Sulfur Dioxide Washout from the Plume of a Large Coal-Fired Power Plant by Natural Precipitation. Battelle, Pacific Northwest Laboratories. Richland, Washington. BNW-389. March 1971. 214 p.

2. Dana, M. T., J. M. Hales, and M. A. Wolf. Natural Precipitation Washout of Sulfur Dioxide. Battelle, Pacific Northwest Laboratories. Richland, Washington. BNW-389. February 1972. 148 p.

3. Hales, J. M. Fundamentals of the Theory of Gas Scavenging by Rain. *Atm. Environment* 6:635-659, 1972.

4. Hales, J. M. Scavenging of Gaseous Tritium Compounds by Rain. Battelle, Pacific Northwest Laboratories. Richland, Washington. BNWL-1659. April 1972. 35 p.

5. Hales, J. M., M. A. Wolf, and M. T. Dana. A Linear Model for Predicting the Washout of Pollutant Gases from Industrial Plumes. *A.I.Ch.E. J.* 19:242-247, March 1973.

6. Turner, D. B. Workbook of Dispersion Estimates. Environmental Protection Agency. U. S. Government Printing Office, Washington, D.C. Publication Number AP-26. 1971.

7. Churchill, R. V. Operational Mathematics. New York, McGraw-Hill, 1958. p. 229.

8. Carslaw, H. S. and J. C. Jaeger. Conduction of Heat in Solids. Oxford, Clarendon Press, 1959. p. 233.

9. Pasquill, F. Atmospheric Diffusion. London, Van Nostrand, 1962. 297 p.

10. Smith, F. B. and J. S. Hay. The Expansion of Clusters of Particles in the Atmosphere. *Quart. J. Roy. Meteorol. Soc.* 87:92-101, 1961.

11. Lazrus, A., E. Lorange, and J. P. Lodge. New Automated Microanalysis for Total Inorganic Fixed Nitrogen and for Sulfate Ion in Water. In: Trace Inorganics in Water. ACS Advances in Chemistry Series Number 73. Washington, D.C., American Chemical Society, 1968.

12. Smith, M. E. and I. A. Singer. An Improved Method of Estimating Concentrations and Related Phenomena from a Point Source Emission. *J. Appl. Meteorol.* 5:631-639, 1966.

13. Briggs, G. A. Plume Rise. AEC Critical Review Series. USAEC Division of Technical Information, Oak Ridge, Tennessee. 1969.

13a. Briggs, G.A. Some Recent Analyses of Plume Rise Observation. Proc. 2nd Int. Clean Air Congress. Washington, D.C. 1970.

14. Bird, R. B., W. E. Stewart, and E. N. Lightfoot. Transport Phenomena. New York, Wiley, 1960.

15. Smith, W. S. and C. W. Gruber. Atmospheric Emissions from Coal Combustion - An Inventory Guide. U.S. Public Health Service Publication Number 999-AP-24. 1966. 112 p.

16. W.G.N. Slinn. Numerical Explorations of Washout of Aerosol Particles. In: Pacific Northwest Laboratory Annual Report for 1970 to the USAEC Division of Biology and Medicine, BNWL-1551, Volume II, Part 1. Battelle, Pacific Northwest Laboratories, Richland, Washington. June 1971. p. 75-81.

17. Baldwin, R. D., L. Cohen, J. Forrest, B. Manswitz, L. Newman, M. E. Smith, M. Sternberg, and W. D. Tucker. The Atmospheric Diagnostics Program at Brookhaven National Laboratory. Second Status Report, BNL-50206. 1969. 42 p.

18. Arin, M. L., C. E. Billings, R. Dennis, J. Drescall, D. Lull, F. A. Record, P. Warneck, and J. E. Wilder. Study of Reactions of Sulfur in Stack Plumes. GCA Corporation, Bedford, Mass. Report No. GCA-TR-69-12-6. 85 p.

19. Foster, P. M. The Oxidation of Sulfur Dioxide in Power Plant Plumes. *Atmos. Environ.* 3:157-175, 1969.

20. Stephens, N. T. and R. O. McCaldin. Attenuation of Power Station Plumes as Determined by Instrumented Aircraft. *Environ. Sci. Tech.* 5:615-621, 1971.

21. Weber, E. Contribution to the Residence Time of Sulfur Dioxide in a Polluted Atmosphere. *J. Geophys. Res.* 75:2909-2914, 1970.

22. Cheng, R. T., J. O. Frohliger, and M. Corn. Aerosol Stabilization for Laboratory Studies of Aerosol-Gas Interactions. *J. Air Poll. Cont. Assoc.* 21:138-142, 1971.

23. Junge, C. E. and T. G. Ryan. Study of the SO_2 Oxidation in Solution and Its Rate in Atmospheric Chemistry. *Quart. J. Roy. Meteorol. Soc.* 84:46-55, 1958.

24. Miller, J. M. and R. G. DePena. The Rate of Sulfate Ion Formation in Water Droplets with Different Partial Pressures of SO_2. In: Proceedings, Second International Clean Air Congress. New York, New York, Academic Press, 1971. p. 375-380.

25. Van Den Heuvel, A. P. and B. J. Mason. The Formation of Ammonium Sulfate in Water Droplets Exposed to Gaseous Sulfur Dioxide and Ammonia. *Quart. J. Roy. Meteorol. Soc.* 89:271-275, 1963.

26. Beilke, S., D. Lamb, and J. M. Miller. Neure Untersuch ungen zur Oxidation von Schwefaldioxid in Gegenwant van Flüssigwasser. Bericht des Sonderforschungsberich 73 Deutchforschungnogemernshaft, 1973.

27. Johnstone, H. F. and D. R. Coughanour. Absorption of Sulfur Dioxide in Air, Oxidation in Drips Containing Dissolved Catalysts. *Ind. Eng. Chem.* 50:1169, 1958.

28. Matteson, M. J., W. Stober, and H. Luther. Kinetics of the Oxidations of SO_2 by Aerosols of Manganese Sulfate. *Ind. Eng. Chem. Fund.* 8:677-687, 1969.

29. Mason, B. J. The Physics of Clouds. London, Oxford University Press, 1957. p. 356.

30. Engelmann, R. J. The Calculation of Precipitation Scavenging. In: Meteorology and Atomic Energy, Slade, D. H. (ed.). Oak Ridge, USAEC Division of Technical Information Extension, July 1968. p. 208-221.

31. Johnstone, H. F. and P. W. Leppla. Solubility of SO_2 at Low Partial Pressures - Ionization Constant and Heat of Ionization of H_2SO_3. *J. Am. Chem. Soc.* 56:2233, 1934.

32. Gunn, R. and G. D. Kinzer. Terminal Velocity of Fall for Water Droplets in Stagnant Air. *J. Meteorol.* 6:246, 1949.

33. Carnahan, B., H. A. Luther, and J. O. Wilkes. Applied Numerical Methods. New York, Wiley Co., 1969. 604 p.

SECTION X.

NOMENCLATURE

Units: ℓ = length; t = time; none = dimensionless

a	Raindrop radius, ℓ
a^*	Area of precipitation collector covered by water, ℓ^2
A	Horizontal area of precipitation collector, ℓ^2
A^*	Total area of precipitation collector surface, ℓ^2
B	Accuracy parameter for chemical analysis
c_{avg}	Representative average concentration of SO_2 in water on precipitation collector surface, moles/ℓ^3
c_{eq}	Concentration in collected rainwater that would exist at ambient air concentration under equilibrium conditions, moles/ℓ^3
c_f	Concentration of SO_2 in the rainwater collected in the sampler bottle, moles/ℓ^3
c_r	Concentration of SO_2 in the rain impinging on the precipitation collector surface, moles/ℓ^3
c_{SO_2}	Air concentration of SO_2 used in rate expression, moles/ℓ^3
c_x	Total concentration of liquid phase, moles/ℓ^3
c_y	Total concentration of gas phase, moles/ℓ^3
C_R	Concentration of pollutant in rainwater collected during release (Quillayute) or sampling period (Centralia), moles/ℓ^3
D_{Ax}, D_{Ay}	Diffusivity of SO_2 in water, in air, ℓ^2/t
D_{Ex}, D_{Ey}	Effective diffusivities of SO_2 in liquid, gas phases, ℓ^2/t
D_x, D_y, D_z	Effective eddy diffusivities in x, y, z directions, ℓ^2/t
E	Error in chemical analysis
F	Plume depletion factor to account for upwind washout

F_d, F_r	Flux of SO_2 to precipitation collector by dry, wet processes, moles/ℓ^2t
F_t	Total flux of SO_2 to precipitation collector by dry and wet processes combined, moles/ℓ^2t
h	Stack height, ℓ; functional equilibrium relationship
H	Effective stack height due to plume, ℓ; Henry's-law constant, $H = (y_{Ab}/x_{Ab})_{equilibrium}$
H^o	"True" Henry's-law constant for undissociated SO_2 in water $H^o = ([SO_2]g/[SO_2]aq)_{equilibrium}$
H'	Modified Henry's-law constant $H' = H/c_x \quad , \quad \ell^3/\text{mole}$
H*	Modified Henry's-law constant, $H^* = H(c_y/c_x)$
i_θ, i_ϕ	Total intensity of turbulence in θ, ϕ directions, ℓ/t
J	Rainfall rate, ℓ/t
k	SO_2-sulfate reaction rate constant, t^{-1}
k_x, k_y	Mass-transfer coefficient in liquid, gas phase, moles/ℓ^2t
K_x, K_y	Overall mass-transfer coefficient: based on liquid phase driving force, based on gas phase driving force, moles/ℓ^2t
K_1	Dissociation constant for first ionization of SO_2 in water defined by Equation (40), moles/ℓ
M, M'	Washout rate of SO_2, sulfate, moles/ℓt
N	Number of discrete data portions in wind sample
N_{Ao}	Flux of pollutant A away from water drop at its interface, moles/ℓ^2t
Q	Molar flow rate of SO_2 across plane at downwind distance $x = \bar{u}t$, moles/t
Q_H	Rate of heat emission by stack to atmosphere, (energy)/t
Q_o	SO_2 source strength, moles/t
Q'	Molar flow rate of sulfate across plane at downwind distance $x = \bar{u}t$, moles/t
S	Sensitivity limit of chemical analysis technique
s	Laplace transform parameter

t	Time, t
T	Time of pollutant release, t
$\hat{t}$	Dimensionless time parameter
u	Wind velocity in x direction, ℓ/t
$\bar{u}$	Mean wind speed, ℓ/t
v	Wind velocity in y direction, ℓ/t
v_t	Terminal fall velocity, ℓ/t
w	Wind velocity in z direction, ℓ/t; washdown velocity, ℓ/t
w_d	Rate of transport of SO_2 to precipitation sampler by dry processes, moles/t
x	Downwind distance, ℓ
x_{Ab}	Interfacial mole fraction of pollutant A in liquid phase
x_{Ai}	Initial mole fraction of pollutant A in liquid phase
x_{Ao}	Interfacial mole fraction of pollutant A in liquid phase
y	Crossplume distance, ℓ
y_{Ab}	Mole fraction of pollutant A in gas phase
y_{Ae}	Gas phase mole fraction that would coexist in equilibrium with the mixed mean mole fraction in the liquid phase x_{Ab}
z	Vertical dimension, ℓ
α	Parameter defined in Equation (55) *et seq.*
α_n	Parameter defined in Equation (4) *et seq.*
β	Parameter defined in Equation (4) *et seq.*; Parameter defined in Equation (55) *et seq.*
δ	Diffusion film thickness, ℓ; also length parameter defined in Appendix D.

Δ_y	Distance between precipitation collectors, ℓ
ε	Radius of region on Bromwich contour
ζ	Fourier transform parameter
$\bar{\theta}$	Mean wind direction, degrees
Λ	Sulfate washout coefficient, t^{-1}
υ	Kinematic viscosity of air, ℓ^2/t
ξ	Fourier transform parameter
σ_w	Standard deviation of vertical wind velocity, ℓ/t
σ_y, σ_z	Plume dispersion parameter in y, z direction, ℓ
σ_θ, σ_ϕ	Plume dispersion parameter in azimuthal, elevational direction, radians
Σm_i	Total mass of SO_2 collected on sampling line, moles
τ	Time-integration variable, t
χ	Measured air concentration of SO_2, moles/ℓ^3

SUBSCRIPTS

aq	Aqueous
A	Pollutant A
b	Bulk
d	Dry deposition
e, eq	Equilibrium
ex	Excess
E	Effective
f	Final
g	Gaseous

i	Initial
o	Plume origin or surface condition
r	Rain
t	Total
w	Vertical component
x	Liquid phase in x direction
y	Gas phase in y direction
z	z direction
θ	Azimuthal direction
ϕ	Elevational direction

SECTION XI.

APPENDICES

Page

A. Tabulations of Measured Concentrations 140

B. A Synopsis of the Washout Modeling Procedure 170

C. Description of Computer Code for the EPAEC Nonlinear Nonfeedback Washout Model 176

D. Redistribution of a Gas Plume Caused by Reversible Washout 197

APPENDIX A.

TABULATIONS OF MEASURED SO_2 CONCENTRATIONS, QUILLAYUTE SECOND SERIES AND SO_2, $SO_4^=$, H^+ CONCENTRATIONS, CENTRALIA

In the following tables, the position numbers correspond with those of Figure 9 for Quillayute, and Figure 28 for Centralia.

Missing data indicate no measurement made or measurement lost.

The lower limit SO_2 air concentrations relate to the approximate minimum measurement capability.

The columns of data are aligned to indicate the approximate radial alignment of the sampling positions (cf. Figures 9 and 28).

C_R is the concentration of the material in rainwater collected during the release (Quillayute), or during the time of sampling (Centralia; cf. Table 11).

Note: SO_2 air concentration units are as follows:

Tables 11-35, 39-46: (gm-moles cm^{-3}) x 10^{12}
Tables 36-38: (gm-moles cm^{-3}) x 10^{15}

Erratum: Where "$<10^{-5}$" appears, it should be replaced by "$<10^{-2}$."

TABLE 27.

MEASURED SO_2 CONCENTRATIONS - RUN 11

(Units: gm-moles $cm^{-3} \times 10^9$)

In Rainwater							In Air	
	West Grid		East Grid					
	Arc	Arc	Arc C		Line D		(East)	Line D
Pos. #	C_R	C_R	Pos. #	C_R	Pos. #	C_R	Pos. #	χ
(No Release)			10-14	0	10	0	10	< 0.1
			15	0.384	11	3.14		
			16	3.20	12	7.57		
			17	8.21	13	10.0	13	< 0.1
			18	13.6	14	11.2		
			19	11.7	15	9.94		
			20	10.0	16	9.94	16	< 0.1
			21	7.04	17	9.54		
			22	4.44	18	11.3		
					19	11.6	19	< 0.1
					20	3.8		
					21	0.77		
					22	0	22	< 0.1
					23	0		
							25	< 0.1
							28,31,34,36	< 0.1

TABLE 28.

MEASURED SO_2 CONCENTRATIONS - RUN 12

(Units: gm-moles $cm^{-3} \times 10^9$)

In Rainwater							In Air	
	West Grid		East Grid					
	Arc B	Arc C	Arc C		Line D			
Pos. #	C_R	C_R	Pos. #	C_R	Pos. #	C_R	(East) Pos. #	Line D χ
10,13-14	0	0						
15	2.02	1.38	10	0	1	13.9[a]	1	0.74[a]
16	6.29	6.16	11	0	2	19.5[a]		
17	11.7	14.5	12	0	3	10.7[a]		
18	20.8	25.0	13	0	4	0.614[a]	4	0.318[a]
19	22.7	23.5	14	0	5			
20	18.4	27.6	10	0.342[a]	6			
21	14.7	18.3	11	0	7	0	7	<0.1
22	3.28	6.10	12	0	8			
23	0	0.369	13	0	9			
24-25	0	0	14	0	10	0	10	<0.1
28,31,33	0	0	15	0	11	0		
			16	0	12	0		
			17	0	13	0.764	13	<0.1
			18	5.77	14	4.53		
			19	3.90	15	7.21		
			20	0.463	16	6.00	16	0.508
			21-22	0	17	4.84	19,22,25	<0.1
			25,28,31,33	0	18	0.463		
					19,22	0		

[a] SO_2 from west source.

TABLE 29.

MEASURED SO_2 CONCENTRATIONS - RUN 14

(Units: gm-moles $cm^{-3} \times 10^9$)

In Rainwater							In Air	
	West Grid		East Grid					
	Arc B	Arc C	Arc C		Line D			
Pos. #	C_R	C_R	Pos. #	C_R	Pos. #	C_R	(East) Pos. #	Line D χ
10,13	0	0						
14	1.51	1.61			4	4.40[a]	4	< 0.1
15	13.1	10.3			5	0		
16	34.8	22.4	10	0	6	0		
17	37.6	43.1	11	0	7	0.390[a]	7	< 0.1
18	44.6	48.0	12	0	8	0		
19	44.0	53.1	13	0	9	0		
20	29.6	43.4	14	0	10	0.628	10	< 0.1
21	27.5	27.8	15	0	11	3.44		
22	16.1	16.6	16	2.90	12	5.19		
23	4.85	6.33	17	6.80	13	10.0	13	0.64
24	0	0	18	12.7	14	12.7		
25	0	0	19	12.2	15	12.4		
28,31,33	0	0	20	10.8	16	10.6	16	0.32
			21	6.97	17	9.67		
			22	4.88	18	6.28		
			23	0.958	19	4.60	19	< 0.1
			25,28,31	0	20	3.52		
					21	1.53		
					22	0.247	22	0.64
					25	0	25	< 0.1

[a] SO_2 from West source.

TABLE 30.

MEASURED SO_2 CONCENTRATIONS - RUN 15

(Units: gm-moles $cm^{-3} \times 10^9$)

In Rainwater							In Air	
	West Grid		East Grid					
	Arc A	Arc C	Arc C		Line D			
Pos. #	C_R	C_R	Pos. #	C_R	Pos. #	C_R	(East) Pos. #	Line D χ
10-12	0	0						
13	1.66	2.91			4	5.72[a]	(all < 0.1)	
14	3.02	7.05						
15	10.2	25.4	10	0				
16	19.4	32.0	11	0	7	0.338[a]		
17	22.2	55.0	12	0	8	0		
18	26.9	58.8	13	0	9	2.94		
19	33.8	48.5	14	0.438	10	11.0		
20	24.3	44.6	15	1.37	11	14.9		
21	10.9	27.6	16	7.80	12	16.5		
22	2.74	19.8	17	11.6	13	18.9		
23	0.525	6.49	18	15.8	14	17.2		
24	1.07	0	19	12.1	15	15.7		
25	0.443	0	20	8.74	16	14.6		
			21	3.09	17	11.8		
			22	0.564	18	6.70		
28	0.446	0	23	0	19	4.54		
			24	0	20	0		
			25	0	21	0		
31	0.716	0	28,31	0	22	0		
					25	0		

---

[a] SO_2 from West Source

TABLE 31.

MEASURED SO_2 CONCENTRATIONS - RUN 16

(Units: gm-moles $cm^{-3} \times 10^9$)

In Rainwater							In Air	
	West Grid		East Grid					
	Arc A	Arc C	Arc C		Line D		(East)	Line D
Pos. #	C_R	C_R	Pos. #	C_R	Pos. #	C_R	Pos. #	χ
10,13,16,19	0	0						
20	1.40	1.08			9	12.2[a]	(No Measurements)	
21	6.25	1.80	10	3.95[a]	10	20.2[a]		
22	12.8	12.8			11	13.2[a]		
23	21.6	26.1			12	14.9[a]		
24	25.7	43.2	13	5.40[a]	13	24.0[a]		
25	24.3	36.2	14	4.96[a]	14	11.2[a]		
26	28.2	35.2	15	3.77[a]	15	10.4[a]		
27	19.5	29.0	16	3.92[a]	16	8.55[a]		
28	16.2	23.0			17	8.16[a]		
29	15.8	15.8			18	5.25[a]		
30	8.93	3.03	19	0	19	5.09[a]		
31	0	0	20	0	20	6.41[a]		
			21	0	21	3.85		
			22	1.90	22	3.97		
			23	6.14	23	7.11		
			24	11.5	24	12.9		
			25	16.8	25	17.4		
			26	18.6	26	21.0		
			27	6.34	27	18.9		
			28	2.42	28	16.6		
			29	0	29	9.38		
					30	5.37		
			31	0	31	0.73		
					32	0		

[a] SO_2 from West source.

TABLE 32.

MEASURED SO_2 CONCENTRATIONS - RUN 17

(Units: gm-moles $cm^{-3} \times 10^9$)

	In Rainwater						In Air	
	West Grid		East Grid					
	Arc A	Arc C	Arc C		Line D			
Pos. #	C_R	C_R	Pos. #	C_R	Pos. #	C_R	(East) Pos. #	Line D χ
10-16	0	0						
17	0.462	10.9	(No Measurement)				(No Measurement)	
18	1.78	19.0						
19	6.44	38.6						
20	13.0	43.6						
21	12.5	52.4						
22	12.3	38.6						
23	5.15	31.1						
24	1.24	19.3						
25	0	0.44						
26-33	0	0						

TABLE 33.

MEASURED SO_2 CONCENTRATIONS - RUN 18

(Units: gm-moles $cm^{-3} \times 10^9$)

In Rainwater							In Air	
	West Grid		East Grid					
	Arc B	Arc C	Arc C		Line D			
Pos. #	C_R	C_R	Pos. #	C_R	Pos. #	C_R	(East) Pos. #	Line D X
14	1.47	0.765	(No Measurement)				(No Measurement)	
17	1.32	0.903						
20	1.10	0.903						
23	1.49	1.18						
24	2.16	1.08						
25	4.26	3.24						
26	9.90	19.3						
27	20.9	26.9						
28	46.2	42.0						
29	36.7	32.2						
30	30.0	25.3						
31	21.2	23.8						
32	16.8	23.4						
33	16.4	17.7						
34	11.3	12.3						
35	2.18	2.92						
36	1.20	1.57						
37	1.86	1.37						

TABLE 34.

MEASURED SO_2 CONCENTRATIONS - RUN 19

(Units: gm-moles $cm^{-3} \times 10^9$)

	In Rainwater						In Air	
	West Grid		East Grid					
	Arc B	Arc C	Arc C		Line D			Line D
Pos. #	C_R	C_R	Pos. #	C_R	Pos. #	C_R	Pos. #	χ
22-30	0	0						
31	1.73	8.04	(No Measurement)				(No Measurement)	
32	3.72	12.3						
33	10.9	23.8						
34	10.7	30.0						
35	14.5	26.8						
36	12.4	24.8						
37	10.8	9.36						

TABLE 35.

MEASURED SO_2 CONCENTRATIONS - RUN 20

(Units: gm-moles $cm^{-3} \times 10^9$)

	In Rainwater						In Air	
	West Grid		East Grid					
	Arc B	Arc C	Arc C		Line D			Line D
Pos. #	C_R	C_R	Pos. #	C_R	Pos. #	C_R	(East) Pos. #	χ
19,22,25,28	0	0						
30	2.44	8.03	(No Measurement)				(No Measurement)	
31	9.49	29.0						
32	24.2	38.9						
33	29.8	56.4						
34	20.2	26.4						
35	2.77	3.82						
36	0	2.68						
37	0	0						
40	0	0						

TABLE 36.

SO_2 CONCENTRATIONS - RUN C1, LINE A

(Units: gm-moles $cm^{-3} \times 10^9$)

Sample Position	In Rainwater Concentration	In Air Concentration
19	a	$< 10^{-5}$
22	a	2.4-3.9[b]
28	a	187
34	a	82-102[b]

[a] No rainfall.

[b] Uncertainty due to loss of bubbler fluid.

TABLE 37.

SO_2 CONCENTRATIONS - RUN C1, LINE B

(Units: gm-moles $cm^{-3} \times 10^9$)

Sample Position	In Rainwater Concentration	In Air Concentration
17	a	$< 10^{-5}$
20	a	102
23	a	300-600[b]
26	a	25.2
29	a	$< 10^{-5}$

[a] No rainfall.

[b] Uncertainty due to loss of bubbler fluid.

TABLE 38.

SO_2 CONCENTRATIONS - RUN C1, LINE C

(Units: gm-moles $cm^{-3} \times 10^9$)

Sample Position	In Rainwater Concentration	In Air Concentration
32	[a]	$< 10^{-5}$
35	[a]	$< 10^{-5}$
38	[a]	169
41	[a]	266-332[b]
44	[a]	111-222[b]
47	[a]	19.2

[a] No rainfall.

[b] Uncertainty due to loss of bubbler fluid.

TABLE 39.

SO_2 CONCENTRATIONS - RUN C2, LINE A

(Units: gm-moles $cm^{-3} \times 10^9$)

Sample Position	In Rainwater Concentration	In Air Concentration
11	0	
12	0.3	
13	0.4	$< 10^{-5}$
14	0.9	
15	0.7	
16	2.1	
17	9.4	
18	12.5	
19	15.8	0.004
20	14.7	
21	9.8	
22	6.9	
23	6.1	
24	7.9	
25	7.2	$< 10^{-5}$
26	5.3	
27	2.0	
28	0.3	0.0111
29	0.2	
30	0	

TABLE 40.

SO_2 CONCENTRATIONS - RUN C2, LINE B

(Units: gm-moles $cm^{-3} \times 10^9$)

Sample Position	In Rainwater Concentration	In Air Concentration
5-7	0	
8	0	0.0824
9	0	
10	0.9	
11	2.5	0.0159
12	5.3	
13	9.7	
14	11.3	0.113
15	6.4	
16	4.3	
17	4.7	0.0368
18	5.6	
19	3.2	
20	2.7	0.0834
21	2.0	

TABLE 41.

SO_2 CONCENTRATIONS - RUN C2, LINE D

(Units: gm-moles $cm^{-3} \times 10^9$)

Sample Position	In Rainwater Concentration	In Air Concentration
21-22	0	
23	0	$< 10^{-5}$
24	0	
25	2.6	
26	0.5	0.010
27	0.7	
28	1.6	
29	2.6	
30	2.7	
31	4.0	
32	2.8	$< 10^{-5}$
33	2.1	
34	1.8	
35	1.0	0.021
36	0.8	
37	0.5	
38	0.5	$< 10^{-5}$
39	0.4	
41	0	

TABLE 42.

SO_2 CONCENTRATIONS - RUN C3, LINE A

(Units: gm-moles $cm^{-3} \times 10^9$)

Sample Position	In Rainwater Concentration	In Air Concentration
11-17	0	(all < 10^{-5})
18	1.0	
19	0.9	
20-30	0	

TABLE 43.

SO_2 CONCENTRATIONS - RUN C3, LINE B

(Units: gm-moles $cm^{-3} \times 10^9$)

Sample Position	In Rainwater Concentration	In Air Concentration
5-9	0	
10	9.2	
11	13.9	0.088
12	23.2	
13	21.5	
14	15.5	0.031
15	4.8	
16	0	
17	0	
18	0	
19	0	
20	0	< 10^{-5}
21	0	

TABLE 44.

SO_2 CONCENTRATIONS - RUN C3, LINE D

(Units: gm-moles $cm^{-3} \times 10^9$)

Sample Position	In Rainwater Concentration	In Air Concentration
21	0	
22	0.2	
23	4.0	$< 10^{-5}$
24	6.6	
25	11.1	
26	13.3	0.030
27	9.6	
28	7.1	
29	8.1	0.043
30	7.0	
31	7.0	
32	4.0	0.026
33	3.6	
34	0.2	
35	0.3	$< 10^{-5}$
36	0	
37	0	
38	0	$< 10^{-5}$
39	0	
40	0	
41	0	$< 10^{-5}$

TABLE 45.

SO_2 CONCENTRATIONS - RUN C4, LINE B

(Units: gm-moles $cm^{-3} \times 10^9$)

Sample Position	In Rainwater Concentration	In Air Concentration
10-12	0	
13	2.5	
14	15.2	1.24
15	7.4	
16	13.0	
17	4.3	0.070
18	0.3	
19	-	
20	0.0	$< 10^{-5}$
21	0.1	
22	0	$< 10^{-5}$
23	0	
24	0	
25	0	$< 10^{-5}$
26	0	
27	0	

TABLE 46.

SO_2 CONCENTRATIONS - RUN C4, LINE C

(Units: gm-moles $cm^{-3} \times 10^9$)

Sample Position	In Rainwater Concentration	In Air Concentration
23	1.9	
24	3.5	
25	9.3	0.386
26	12.0	
27	10.2	
28	5.9	0.088
29	2.8	
30	0	
31	0	0.017
32	0	
33	0	
34	0	$< 10^{-5}$
35	0	
36	0	
37	0	
38	0	0.0064
39	0	
40	0	
41	0	0.0044
42	0	
43	0	

TABLE 47.

SO_2 CONCENTRATIONS - RUN C4, LINE D

(Units: gm-moles $cm^{-3} \times 10^9$)

Sample Position	In Rainwater Concentration	In Air Concentration
26	0	
27	0.1	
28	3.2	0.262
29	6.5	
30	9.3	
31	11.5	0.116
32	7.4	
33	1.1	
34	0	$< 10^{-5}$
35	0	
36	0	
37	0	$< 10^{-5}$
38	0	
39	0	
40	0	
41	0	$< 10^{-5}$
42	0	
43	0	$< 10^{-5}$
44	0	
45	0	

TABLE 48.

SO_2 CONCENTRATIONS - RUN C5, LINE A

(Units: gm-moles $cm^{-3} \times 10^9$)

Sample Position	In Rainwater Concentration	In Air Concentration
11	0	
12	0	
13	0	0.0011
14	0	
15	0	
16	0	0.0047
17	0	
18	0	
19	0	0.0138
20	2.5	
21	5.5	
22	3.5	$< 10^{-5}$
23	0	
24	0	
25	0	$< 10^{-5}$
26-30	0	

TABLE 49.

SO_2 CONCENTRATIONS - RUN C5, LINE D

(Units: gm-moles $cm^{-3} \times 10^9$)

Sample Position	In Rainwater Concentration	In Air Concentration
22	0	0.009
23	0	
24	0	
25	0	0.014
26	0	
27	0	
28	0	0.0010
29	0.4	
30	1.6	
31	4.8	0.0301
32	6.2	
33	2.0	
34	0	$< 10^{-5}$
35	0	
36	0	
37	0	$< 10^{-5}$
38	0	
39	0	

TABLE 50.

$SO_4^=$ and H^+ CONCENTRATIONS - RUN C2, LINE A IN RAINWATER (Units: gm-moles $cm^{-3} \times 10^9$)

Sample Position	Concentrations - Less Background	
	$SO_4^=$	H^+
11	0	
12	0	
13	0	0
14	0	
15	0	
16	2.1	3.2
17	11.5	
18	28.1	
19	24.0	33.3
20	24.0	
21	20.8	
22	11.5	15.6
23	11.5	
24	19.8	
25	18.8	13.6
26	14.6	
27	13.5	
28	11.5	5.0
29	1.0	
30	3.1	
Background	6.3	2.2

TABLE 51.

$SO_4^=$ AND H^+ CONCENTRATIONS - RUN C2, LINE B IN RAINWATER (Units: gm-moles $cm^{-3} \times 10^9$)

Sample Position	Concentrations - Less Background	
	$SO_4^=$	H^+
5	2.1	1.0
6	0	
7	2.1	
8	2.1	2.8
9	3.1	
10	4.2	
11	7.3	4.7
12	7.3	
13	15.6	
14	22.9	16.4
15	14.6	
16	30.2	
17	13.5	9.0
18	12.5	
19	8.3	
20	6.3	8.3
21	6.3	
Background	6.3	2.2

TABLE 52.

$SO_4^=$ AND H^+ CONCENTRATIONS - RUN C2, LINE D IN RAINWATER (Units: gm-moles $cm^{-3} \times 10^9$)

Sample Position	Concentrations - Less Background	
	$SO_4^=$	H^+
21	1.0	
22	3.1	
23	8.3	2.8
24	4.2	
25	15.6	
26	5.2	5.0
27	8.3	
28	8.3	
29	7.3	6.7
30	6.3	
31	9.4	
32	9.4	6.1
33	9.4	
34	6.3	
35	7.3	5.7
36	6.3	
37	4.2	
38	5.2	
39	6.3	4.9
40		
41	4.2	
Background	6.3	2.2

TABLE 53.

$SO_4^{=}$ AND H^+ CONCENTRATIONS - RUN C3, LINES A, B, D IN RAINWATER (Units: gm-moles $cm^{-3} \times 10^9$)

Sample Position	Concentrations - Less Background	
	$SO_4^{=}$	H^+
A 13	(1)	0
16		4.2
19		21.6
22		0.7
25		0
28		0.2
B 8		0
11		48.2
14		32.3
17		0
20		0
D 23		11.2
26		30.8
29		14.7
32		6.0
35		2.4
38		0.6
41		0.1
Background		0.8

(1) No measurement - Analytical difficulties arising from low sample volumes.

TABLE 54.

$SO_4^=$ AND H^+ CONCENTRATIONS - RUN C4, LINE B IN RAINWATER (Units: gm-moles $cm^{-3} \times 10^9$)

Sample Position	Concentrations - Less Background	
	$SO_4^=$	H^+
10	0	
11	3.1	1.8
12	3.1	
13	15.6	
14	34.4	48.1
15	17.7	
16	52.1	
17	11.5	23.1
18	10.4	
19	6.3	
20	3.1	2.8
21	3.1	
22	0	1.3
23	0	
24	0	
25	0	0.8
26	0	
27	0	
Background	2.1	3.2

TABLE 55.

$SO_4^=$ AND H^+ CONCENTRATIONS - RUN C4, LINE C IN RAINWATER (Units: gm-moles $cm^{-3} \times 10^9$)

Sample Position	Concentrations - Less Background	
	$SO_4^=$	H^+
23	7.3	
24	7.3	
25	16.7	27.7
26	19.8	
27	15.6	
28	13.5	18.2
29	8.3	
30	6.3	
31	4.2	11.9
32	3.1	
33	2.1	
34	0	1.7
35	0	
36	0	
37	0	1.0
38	0	
39	0	
40	0	
41	0	0.6
42	0	
43	0	
Background	2.1	3.2

TABLE 56.

$SO_4^=$ AND H^+ CONCENTRATIONS - RUN C4, LINE D
IN RAINWATER (Units: gm-moles $cm^{-3} \times 10^9$)

Sample Position	Concentrations - Less Background	
	$SO_4^=$	H^+
26	3.1	
27	4.2	
28	8.3	16.8
29	10.4	
30	13.5	
31	14.6	23.1
32	11.5	
33	10.4	
34	3.1	4.7
35	-	
36	0	
37	0	0
38	0	
39	0	
40	0	0
41	0	
42	0	
43	0	1.6
44	0	
45	0	
Background	2.1	3.2

TABLE 57.

$SO_4^=$ AND H^+ CONCENTRATIONS - RUN C5, LINE A IN RAINWATER (Units: gm-moles $cm^{-3} \times 10^9$)

Sample Position	Concentrations - Less Background	
	$SO_4^=$	H^+
11-12	0	
13	0	0
14	0	
15	0	
16	0	0
17	1.0	
18	5.2	
19	5.2	34.0
20	15.6	
21	24.0	
22	14.6	19.0
23	7.3	
24	2.1	
25	0	12.0
26	0	
27	0	
28	0	
29	0	
30	2.1	
Background	6.3	∿16.0

TABLE 58.

$SO_4^=$ AND H^+ CONCENTRATIONS - RUN C5, LINE D IN RAINWATER (Units: gm-moles $cm^{-3} \times 10^9$)

Sample Position	Concentrations - Less Background	
	$SO_4^=$	H^+
22	0	20.0
23	0	
24	0	
25	2.1	6.4
26	2.1	
27	3.1	
28	5.2	12.0
29	5.2	
30	6.3	
31	9.4	18.0
32	9.4	
33	4.2	
34	0	6.4
35	0	
36	0	
37	0	1.8
38	0	
39	0	
Background	6.3	∼16.0

APPENDIX B.

A SYNOPSIS OF THE WASHOUT MODELING PROCEDURE

The reversible gas washout calculations described in this report are based upon an approach that has been developed over the duration of Battelle's involvement in the EPA washout studies. This appendix provides a short description of the fundamentals of this approach, and should suffice to provide a basic understanding of the theory involved in this report. For a more detailed description the reader is referred to the previous reports and publications on this subject.[1-4]

The basis for all washout calculations utilized herein is the property that a gas will be absorbed or desorbed depending upon whether the concentration driving force is to or away from the falling raindrop. Mathematically, this may be expressed by the form

$$N_{Ao} = -K_y(y_{Ab} - y_{Ae}) \quad , \tag{34}$$

where, as shown in the Table of Nomenclature N_{Ao} is the flux of pollutant A away from the drop at its interface. The subscripts A and o denote "pollutant A" and "interface," respectively, in a manner consistent with terminology used throughout this text; the subscript b denotes "bulk," indicating that the entity being described is an average or "mixed-mean" value; y_{Ab} is the mole fraction of A in the local gas phase. y_{Ae} is the mole fraction of A in the liquid phase expressed in gas-phase terms to allow incorporation with y_{Ab} as a driving force; it is, more precisely, the gas phase mole fraction that would coexist in equilibrium with the mixed-mean mole fraction in the liquid phase x_{Ab}.

The above equilibrium relationship can be expressed by the functional form

$$y_{Ae} = h(x_{Ab}) \quad . \tag{35}$$

In the event that the gas-phase fraction is linearly dependent on the liquid-phase value, the above equation reduces to

$$y_{Ae} = Hx_{Ab} \quad , \tag{36}$$

where H is the Henry's-law constant. This may be expressed in terms of liquid-phase concentration by the essentially equivalent form

$$y_{Ae} = H'c_{Ab} \quad , \tag{37}$$

where $H' = H/c_x$ is a modified Henry's-law constant, c_x being the total liquid-phase concentration (nominally 1/18 moles/cm^3).* Nonlinear behavior in the equilibrium relationship is accounted for in the numerical model simply by applying the form (37) and varying H' as the computation progresses.

SO_2 solubility in water is known to depend upon concentration in a highly nonlinear fashion. Our previous laboratory measurements have shown this relationship to be given approximately by the form (cf. DHW, pg. 24),

$$\begin{aligned} c_{SO_2} &= [SO_2]_{aq} + [HSO_3^-] \\ &= \frac{[SO_2]_g}{H^o} + \frac{-[H_3O^+]_{ex} + \sqrt{[H_3O^+]_{ex}^2 + 4K_1[SO_2]_g/H^o}}{2} \quad , \end{aligned} \tag{38}$$

where the bracketted terms denote concentrations in moles/liter and $[H_3O^+]_{ex}$ is the concentration in solution of hydrogen ions donated by sources other than the SO_2 ionization reaction. H^o and K_1 are the ("true") Henry's-law and dissociation constants, respectively, for Reactions (39) and (40):

$$H^o = \frac{[SO_2]_g}{[SO_2]_{aq}} \quad , \tag{39}$$

$$K_1 = \frac{[HSO_3^-][H_3O^+]_{total}}{[SO_2]_{aq}} \quad . \tag{40}$$

Here it is important to note that $[SO_2]_{aq}$ denotes dissolved, undissociated SO_2, while the total dissolved SO_2 is denoted by c_{SO_2}.

---

*Owing to the variety of definitions of the Henry's-law constant that occur in the literature, one must take care to insure correct application.

The flux N_{Ao} in Equation (34) is defined as the moles of material leaving the drop per unit area per unit time; whether the process is one of absorption or desorption, therefore, depends on the sign of the term $(y_{Ab} - y_{Ae})$. Thus if a raindrop contains sufficient dissolved pollutant gas to render it supersaturated with respect to its surroundings $(y_{Ae} > y_{Ab})$, then the sign will be negative and desorption will occur. Conversely, if a relatively clean raindrop finds itself in an environment where y_{Ab} is large, then the driving-force sign will be positive, indicating an absorption process is taking place.

The overall mass-transfer coefficient K_y can be estimated by expressing it in terms of "film resistances" on the gaseous and liquid sides of the raindrop interface. For present purposes this relationship can be written as

$$\frac{1}{K_y} = \frac{H}{k_x} + \frac{1}{k_y} , \qquad (41)$$

where k_x and k_y respectively are the liquid- and gas-phase mole fractions defined as

$$N_{Ao} = -k_x(x_{Ao} - x_{Ab}) , \qquad (42)$$

and

$$N_{Ao} = -k_y(y_{Ab} - y_{Ao}) . \qquad (43)$$

Here x_{Ao} and y_{Ao} are the mole fractions of pollutant A existing precisely at the gas-liquid interface. The rationale for this procedure may be shown superficially, at least, in terms of the schematic of Figure 59. This drawing represents a close-up view of a raindrop interface; pollutant gas is being transferred to the drop (absorption) and the corresponding concentration gradients are established. By assigning film thicknesses and effective diffusivities to the gaseous and liquid regions, one can apply Fick's law of diffusion to formulate Equations (39) and (40), where

$$k_y = \frac{c_y D_{Ey}}{\delta_y} , \qquad (44)$$

and

$$k_x = \frac{c_x D_{Ex}}{\delta_x} . \qquad (45)$$

Reproduced from best available copy.

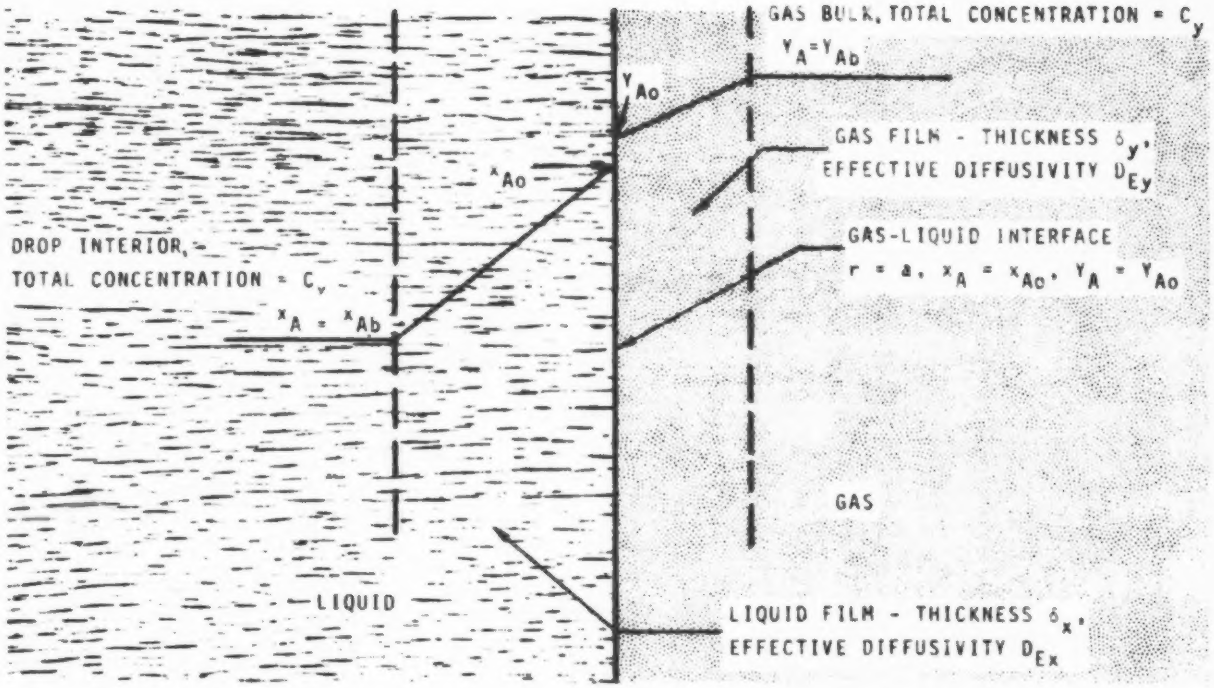
GAS BULK, TOTAL CONCENTRATION = C_y
$y_A = y_{Ab}$
y_{Ao}
x_{Ao}
GAS FILM - THICKNESS δ_y, EFFECTIVE DIFFUSIVITY D_{Ey}
DROP INTERIOR, TOTAL CONCENTRATION = C_x
GAS-LIQUID INTERFACE $r = a$, $x_A = x_{Ao}$, $y_A = y_{Ao}$
$x_A = x_{Ab}$
GAS
LIQUID
LIQUID FILM - THICKNESS δ_x, EFFECTIVE DIFFUSIVITY D_{Ex}

FIGURE 59. REPRESENTATION OF SIMPLIFIED FILM THEORY.

The situation depicted by the above analysis, obviously rather simplistic in nature, has found extended practical application. Continuing with this approach, one may employ the well-known Froessling equation to determine the gas-phase mass-transfer coefficient. This equation, given in dimensionless form as

$$\frac{2k_y a}{D_{Ay} c_y} = 2 + 0.6\left[\frac{-2av_z}{\upsilon}\right]^{\frac{1}{2}}\left[\frac{\upsilon}{D_{A_y}}\right]^{\frac{1}{3}} \quad , \tag{46}$$

has been validified for a wide range of conditions and is expected to provide an excellent estimate of k_y for falling raindrops.

The method of estimating the liquid-phase mass-transfer so efficiently is not so straight forward, and involves a number of inevitable assumptions. The approach utilized here is to assume that the lower limit of mass tranfer will occur if the raindrop is stagnant. In this event (if we treat this situation as one of pure "physical absorption" (cf. HTW, DHW)), one can solve the equation of continuity for diffusion into a sphere to determine corresponding mass-transfer rates (HTW, p. 40). Normally this results in variable mass-transfer coefficients; however, if one calculates for the special case of a linearly increasing gas concentration, the expression

$$k_x = \frac{5D_{Ax}c_x}{a} \quad , \tag{47}$$

is obtained. This equation can be used in conjunction with (39) to provide a linearized mass-transfer expression, if desired. Alternatively, one can employ the combined gas-liquid expression derived during this project and given in Section IV to provide a less direct but theoretically more satisfying means of estimation.

To calculate washout concentrations using the above approach one must rewrite (34) in terms of the liquid-phase concentration, c_{Ab}. The result is

$$\frac{dc_{Ab}}{dz} = \frac{3K_y}{v_t a}(y_{Ab} - H'c_{Ab}) \quad , \tag{48}$$

where v_t is the terminal fall velocity of the raindrop, and the gas-phase concentration field $y_{Ab}(x,y,z)$ must be furnished prior to calculation of numerical results. At the present time this procedure uses the Pasquill-Gifford bivariate-normal plume equation, modified to account for pseudo first-order chemical reaction and background, to fulfill this purpose. This is given as

$$y_{Ab} = \frac{Q}{2\pi\sigma_y\sigma_z\bar{u}} \exp[-\tfrac{1}{2}(\frac{y}{\sigma_y})^2]\{\exp[-\tfrac{1}{2}(\frac{z-h}{\sigma_z})^2] + \exp[-\tfrac{1}{2}(\frac{z+h}{\sigma_z})^2]\}$$

$$\exp(-\frac{kx}{\bar{u}}) + y_{Ab}|_{bkg} \quad . \qquad (49)$$

Execution of the EPAEC model consists simply of solving Equation (47) numerically in conjunction with Equation (48) for a number of selected drop sizes, and then distributing the results according to the raindrop spectrum to obtain average concentrations. The computer code described in Appendix C performs this function and allows for a number of sophistications including nonlinear solubility behavior, lofting plumes, and nonvertical rainfall. If these sophistications are not included, the above problem can be solved analytically, the result being given by

$$c_{Ab}(a,o) = -\frac{3QFk_y r}{2\sqrt{2\pi}\,\sigma_y\bar{u}v_t a} \exp(-\frac{y^2}{2\sigma_y^2} + \frac{\sigma_z^2\zeta^2}{2})$$

$$\{\exp(\zeta h)\,\mathrm{erfc}(\frac{-\sigma_z^2\zeta - h}{\sigma_z\sqrt{2}}) + \exp(-\zeta h)\,\mathrm{erfc}(\frac{-\sigma_z^2\zeta + h}{\sigma_z\sqrt{2}})\}$$

$$+ y_{Ab}|_{bkg}/H' \quad , \qquad (50)$$

where $r = \exp(-kx/\bar{u})$ and $\zeta = 3K_y H'/v_t a$.

APPENDIX C.

DESCRIPTION OF COMPUTER CODE FOR THE EPAEC NONLINEAR NONFEEDBACK WASHOUT MODEL

The computer code can be described, in a somewhat superficial sense, in terms of the flow chart shown in Figure 60. This figure demonstrates that washout calculations may be performed using the code simply by employing a main program that performs the following functions: 1) reading of appropriate input data; 2) execution of algorithm by the statement CALL MASTER; 3) printing of resulting computed values. MASTER is a master coordinating subroutine which employs all of the program functions to calculate washout as indicated in Figure 61.

The utility of the above arrangement is that it allows the code to be applied generally for a variety of specific purposes, one simply writes a main program designed to fulfill his particular requirements, and employs the statement CALL MASTER to execute the basic algorithms required. The Centralia computations described in Section VI, for example, were executed using a main program that memorized the topography of the surrounding area, computed relative distances based on the plume location, and then calculated corresponding washout concentrations by the statement CALL MASTER.

A generalized main program can be employed to perform the above functions, if desired. Use of such a program will provide results identical to those computed using customized main programs, the major disadvantages being probable increased inconvenience in data input and less control over output formats. An example of such a generalized program is shown on the pages immediately following Table 59 which defines the computer nomenclature. Named EPAEC, this program employs a common statement to facilitate exchange of information with the subroutine MASTER. The following EXTERNAL statement designates the function subroutines V, HPRIME, and YAB to be used internally; this statement is essential to the operation of any main program for this purpose.

Reading of input data proceeds, governed by the control variables J1-J4 which allow the bypass of designated READ statements if desired. Finally,

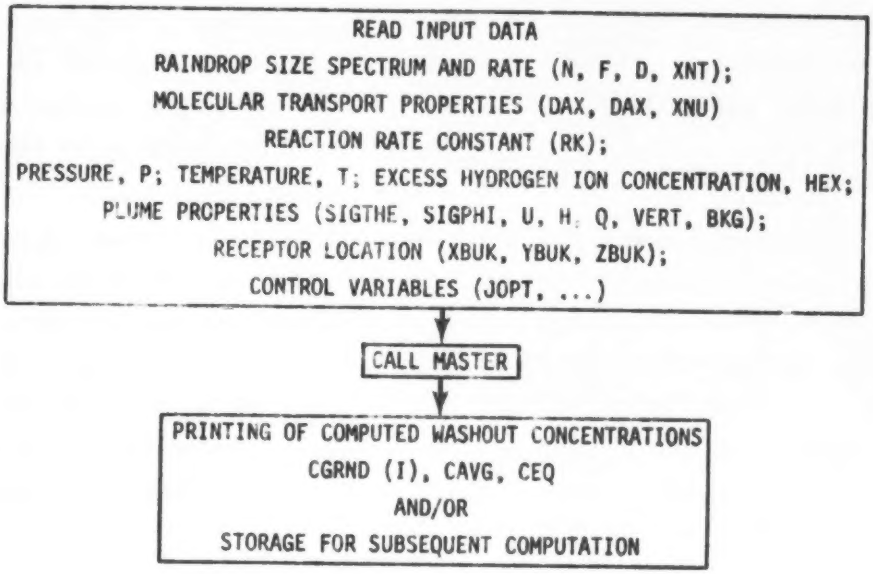
READ INPUT DATA
RAINDROP SIZE SPECTRUM AND RATE (N, F, D, XNT);
MOLECULAR TRANSPORT PROPERTIES (DAX, DAX, XNU)
REACTION RATE CONSTANT (RK);
PRESSURE, P; TEMPERATURE, T; EXCESS HYDROGEN ION CONCENTRATION, HEX;
PLUME PROPERTIES (SIGTHE, SIGPHI, U, H, Q, VERT, BKG);
RECEPTOR LOCATION (XBUK, YBUK, ZBUK);
CONTROL VARIABLES (JOPT, ...)
CALL MASTER
PRINTING OF COMPUTED WASHOUT CONCENTRATIONS
CGRND (I), CAVG, CEQ
AND/OR
STORAGE FOR SUBSEQUENT COMPUTATION

FIGURE 60. SUPERFICIAL FLOW DIAGRAM OF EPAEC MODEL.

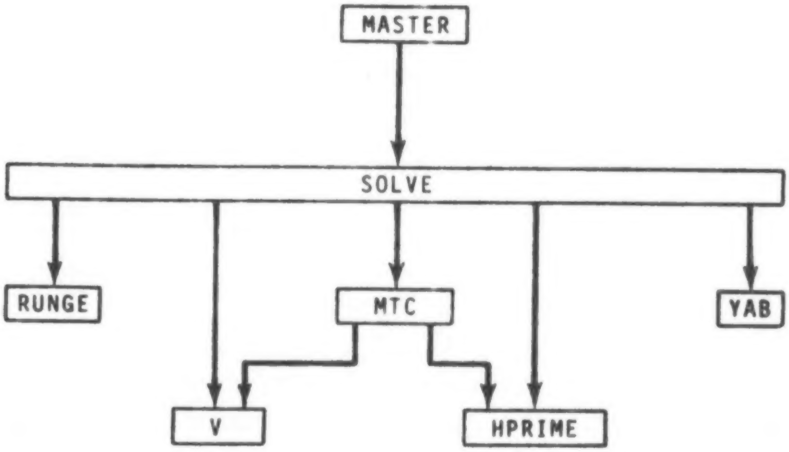
MASTER
SOLVE
RUNGE
MTC
YAB
V
HPRIME

FIGURE 61. SUBROUTINE HIERARCHY IN EPAEC MODEL.

an optional, internally-generated receptor spacing (DYDUM) is calculated. This provides for performance of subsequent calculations at 5-degree increasing cross-plume distances.

Upon printing the input data, MASTER is called. Execution of this subroutine pertains to a single receptor location. Upon completion of the calculations controlled by MASTER, appropriate printing is performed, including that of REF, which is the variable denoting height above the source passed by individual raindrops at $x = 0$.

At this point, depending upon the current value of the control variable JEND, the program has two options. It can either proceed to the adjoining cross-plume location, perform subsequent computations, and integrate to provide (ultimately) a downwind washout rate (WORATE) or it can read new input data and proceed to calculations for other conditions. In the event that cross-plume integrations are performed, the program terminates when relatively low concentrations are encountered on the edges of the plume, and the downwind washout rate is printed.

The program is terminated completely whenever no additional data cards are found, or when the control variable JEND is set equal to 1. An example data set for use with EPAEC has been given previously in Section VII.

DESCRIPTION OF BASIC COMPUTATIONAL ALGORITHM

Exclusive of the input-output functions governed by the main program, the basic computational algorithm can be described by the hierarchy of subroutines shown in Figure 61. The primary function of this algorithm is to solve the drop-response equation

$$\frac{dc_{Ab}}{dz} = \frac{3K_y}{v_t a}(y_{Ab} - H'c_{Ab}) \quad , \qquad (48)$$

which was given previously in Appendix B. The calculations performed by the computer listing given here envision a rain-plume situation as shown in Figure 62. In this visualization a single raindrop of radius R falls through the plume to a receptor over a linear trajectory determined by the wind speed U and the terminal fall velocity V. A computational grid is set up along the trajectory, and Equation (48) is solved numerically using

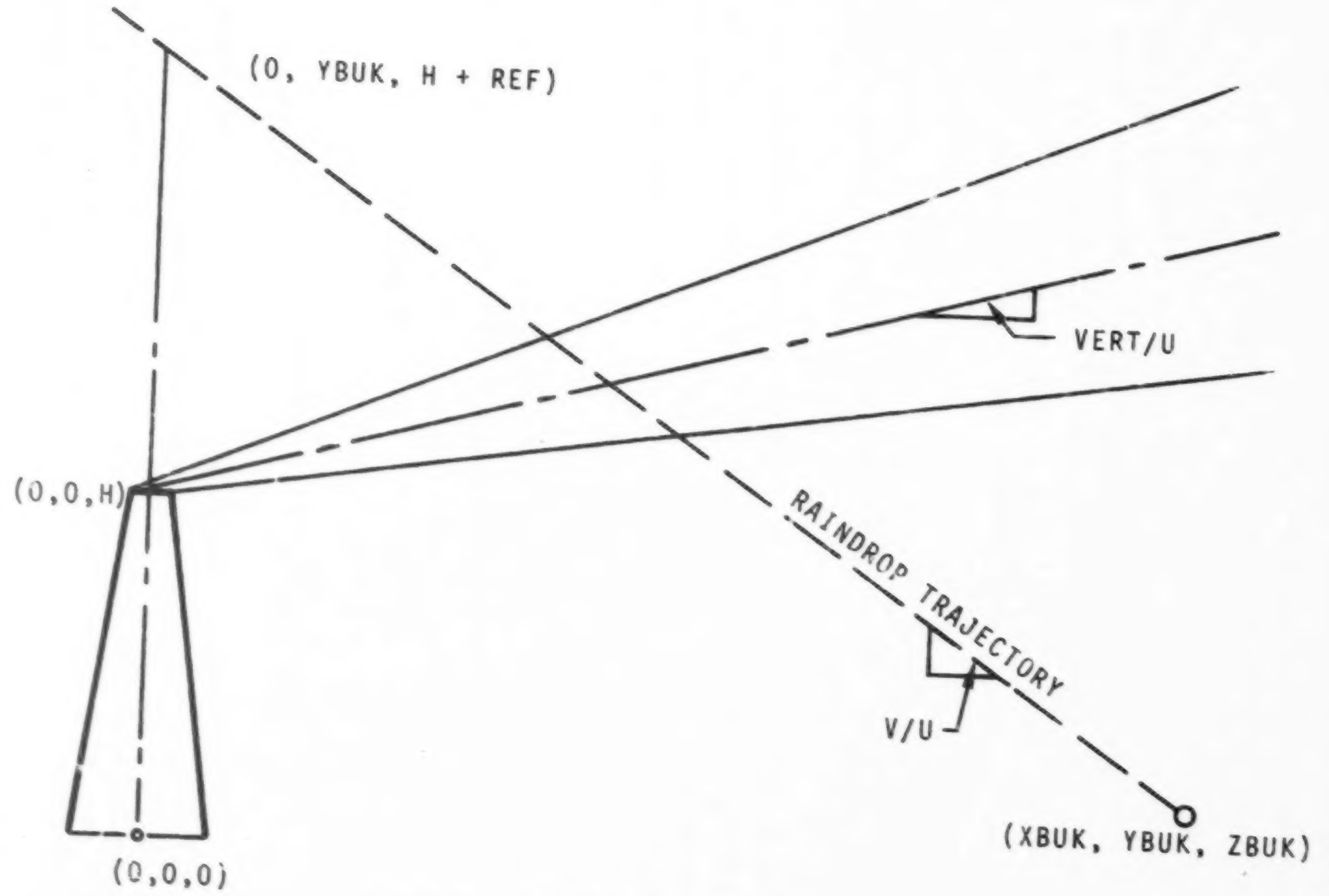
(0, YBUK, H + REF)
VERT/U
(0,0,H)
RAINDROP TRAJECTORY
V/U
(XBUK, YBUK, ZBUK)
(0,0,0)

FIGURE 62. PICTORIAL BASES FOR EPAEC MODEL.

a Runge-Kutta finite-difference approximation to obtain the value of c_{Ab} (CGRND in the computer code) at the receptor location. This procedure is repeated for all drop sizes in the discretized spectrum and the results are averaged to obtain a final mixed-mean concentration (CAVG) for that location.

y_{Ab} values along the trajectory are furnished by a plume model in the form of a subroutine (YAB). At present this subroutine is written to accomodate the Gifford-Pasquill Bivariate-Normal plume model,[6] modified to account for quasifirst-order chemical reaction, plume loft, and ambient background. Descriptions of the subroutines shown in Figure 61 are given individually in the following text. Listings of these subroutines are provided at the end of this appendix.

Subroutine V provides the terminal fall velocity dz/dt, as a function of raindrop radius R. This internal function is simply an empirical polynomial fit to measured terminal velocity data.[31]

Subroutine HPRIME utilizes Equation (38) or appropriate variations thereof, to determine values of the apparent Henry's-law constant appropriate to the current value of either c_{Ab} or y_{Ab}, depending on the value of the control variable LGOPT. If LGOPT is set equal to 1 in the calling sequence, calculation is based on the value of y_{Ab}; otherwise the current value of c_{Ab} is employed.

Upon being initiated, HPRIME first computes the dissociation constant (EQCON) and Henry's-law constant for undissociated SO_2 (HANK), as defined by

$$\mathrm{EQCON} = \frac{[\mathrm{HSO_3^-}][\mathrm{H_3O^+}]_{\mathrm{total}}}{[\mathrm{SO_2}]_{\mathrm{aq}}} \quad , \quad \text{(moles/liter)} \tag{51}$$

$$\mathrm{HANK} = \frac{y_{Ab}}{[\mathrm{SO_2}]_{\mathrm{aq}}} \quad , \quad \text{(liters/mole).} \tag{52}$$

This is done in accordance with Johnstone and Leppla's[32] measured values as interpreted in our previous analysis (DHW, p. 23 *et seq.*).

Upon computing EQCON and HANK the subroutine branches, depending on the value of LGOPT, to computations based on liquid or gas-phase concentrations. Each of these branches tests for low-concentration conditions and applies an

Reproduced from best available copy.

asymptotic approximation to the solubility expression if these conditions are satisfied. If low-concentration conditions do not exist, the complete solubility equations are employed for final assessment of the return value of the apparent Henry's-law constant,

$$\text{HPRIME} = \frac{y_{Ab}}{\text{total dissolved } SO_2} \quad , \quad (\text{cm}^3/\text{mole}). \qquad (53)$$

Conversion from units of liters to cm^3 is completed within the subroutine prior to returning to the calling routine.

Subroutine MTC computes the overall mass-transfer coefficient K_y. It begins by calculating the gas-phase coefficient using Equation (46). Then, if the control variable JOPT has been set equal to 1, (gas-phase limiting), the overall coefficient is returned as the gas-phase value. Otherwise, a liquid coefficient is calculated using Equation (47), and the gas and liquid coefficients are combined using Equation (41) to obtain the corresponding stagnant-drop values.

Subroutine RUNGE, in conjunction with subroutine SOLVE performs the numerical integration of Equation (48), SOLVE supplying RUNGE values of the derivative dc_{Ab}/dz (F in the computer code) and RUNGE returning values of c_{Ab}. RUNGE is a fourth-order Runge-Kutta algorithm which has been adapted from a previous work.[33] This algorithm is rather complex and will not be discussed in detail here, except to state that its expected errors are of the order of the fractional grid spacing to the fourth power. For a complete discussion of this method the reader is referred to the work of Carnahan, *et al.*[33]

Subroutine YAB, as mentioned previously, provides values of the gas-phase mole fraction of pollutant as a function of spatial location x, y, and z. Equation (49), which is the Gifford-Pasquill Bivariate-Normal equation, modified for quasifirst-order gas-phase chemical reaction, is employed for this purpose. The subroutine computes values of the dispersion parameters, and proceeds directly with a solution of Equation (49) to provide the return value YAB. H in this subroutine is a virtual value, and depends upon the value of emission height supplied by the calling program.

Subroutine SOLVE performs the function of establishing the computational grid and implementing RUNGE to obtain the solutions to Equation (47). The routine begins by initializing variables and then testing for the occurrence of equilibrium scavenging. This is accomplished by calculating a virtual emission height (HSTAR) and an appropriate dispersion parameter (SIGMAZ). This is followed by determination of an effective Henry's-law constant, which is employed in conjunction with the criterion of Equation (1) (GROUP > 15) to determine whether or not equilibrium scavenging occurs. If equilibrium conditions are indeed predicted, the scheme bypasses the solution of Equation (48) and simply returns the equilibrium washout concentration value.

In the event that equilibrium conditions are not predicted, the routine initializes the concentration of pollutant in the drop, C(1), to its appropriate above-plume value, and proceeds to establish a computation grid. In performing this function it first tests for plume undercut by the raindrop (REF < 0). In the event that undercutting occurs, the grid network is established by dividing the vertical distance between the sampler and the height at which the drop crosses $X = 0$ into thirty equally-spaced measurements.

If plume undercutting does not occur, a "normal" grid spacing is established. This is accomplished by finding an appropriate vertical spread parameter SIGMA) for early stages of the drop-plume encounter and (rather arbitrarily) beginning numerical computations at an elevation equal to the effective release heights plus three times the computed spread (HSTAR + 3 * SIGMA). Grid spacing is set at one-sixtieth of the vertical distance between the receptor and the point where calculations are initiated.

A final modification of the computation grid structure is performed if the raindrop encounters a plume having a low degree of spread ("compact plume"). This is done simply by testing for whether the current spacing is less than one-fourth the computed spread parameter SIGMA. If not, a top grid spacing (TDZ) is set equal to SIGMA/4 (SIGMA/8 if SIGPHI is greater than 0.5). If "compact" plumes are encountered, this finer grid spacing is employed for 25 increments, and the original grid spacing, DELTAZ, is employed thereafter.

The choices of grid spacings described above were arrived at after experimentation with various arrangements. This system provides for general stability and accuracy of the algorithm, with reasonable economy in execution time.

As described earlier, numerical solution of the object equation is accomplished using subroutine RUNGE. This subroutine is called repeatedly, and control is transferred between it and the calling subroutine SOLVE, which updates the downwind distance (x) and effective release height HSTAR. SOLVE also updates the derivative function F(1) and supplies this value to RUNGE, which in turn provides calculated values of the concentration C(1).

Calculations continue until the receptor location is encountered. Then the value of the ground-level rain concentration (COBJ) is calculated and returned with other pertinent variables in the calling sequence.

Subroutine MASTER coordinates calculations for the ensemble of drops in the descretized spectrum, and combines the resulting concentration values to obtain mixed-mean levels. MASTER simply calls subroutine SOLVE for each raindrop size in the spectrum, saves the individual concentrations in the array CGRND(I), and averages according to the equation

$$\mathrm{CAVG} = \frac{\sum_{1}^{N} F(I)D(I)^{3}\mathrm{CGND}(I)}{\sum_{1}^{N} F(I)D(I)^{3}} \quad . \qquad (54)$$

Control is then transferred to the main program for subsequent printing operations.

MODIFICATION OF THE COMPUTER CODE

The modular form of the general computer code enables it to be modified easily for use in other applications. Such modifications can be categorized into two types, depending on whether they are meant to improve the accuracy of the calculations or to adapt the algorithm for use with substances other than SO_2.

The first type of modification--an incorporation of an improved plume model for instance--can usually be accomplished by modular replacement of one or more subroutines in a straight-forward manner. The second type of modification usually can be accomplished easily, depending on the materials of interest. If this material is a nonreactive gas, one simply must replace the solubility function HPRIME with one appropriate to the gas in question. Other routines are generally applicable, and corresponding modifications are accomplished automatically by changes in the physical-properties input data. Scavenging of a totally soluble gas, for instance, can be calculated simply by modifying the function HPRIME to return a zero value whenever it is called.

Reproduced from best available copy.

TABLE 59.

COMPUTER NOMENCLATURE

Symbol	Units	Definition
AA	cm^2	Summing variable for calculation of average concentration
B	gm moles/liter	Dummy variable in subroutine HPRIME used for storage of sum of the equilibrium constant and the excess hydrogen ion concentration
BKG	dimensionless	Mixing ratio of pollutant in gas phase background (moles/mole)
C	gm moles/cm^3	Mixed-mean concentration of pollutant in a specific raindrop
CAVG	gm moles/cm^3	Mixed-mean concentration of pollutant in a collected rain sample
CAVGCL	gm moles/cm^3	Mixed-mean concentration of pollutant in rain sample collected beneath plume centerline
CCUM	gm moles/cm^3	Cumulative concentration used for integration across the plume to calculate washout rate
CDUM	gm moles/(liter)^2	Dummy variable used in HPRIME
CEQ	gm moles/cm^3	Concentration of pollutant in rain in equilibrium with ground-level gas-phase concentration
CGRND	gm moles/cm^3	Mixed-mean concentration of pollutant in a specific raindrop at receptor
CLAST	gm moles/cm^3	Dummy variable used for performing cross-plume integration
COBJ	gm moles/cm^3	Mixed-mean concentration of pollutant in a specific raindrop at receptor
CSET	gm moles/cm^3	Mixed-mean concentration of pollutant in a specific raindrop used for calculation of mass-transfer coefficient in subroutine TKY
CTEST	gm moles/cm^3	Dummy variable used to test for cross-plume integration termination conditions; also used to establish compact plume characteristics in SOLVE
D	cm	Raindrop diameter
DAX	cm^2/sec	Molecular diffusivity of pollutant in air
DAY	cm^2/sec	Molecular diffusivity of pollutant in water

TABLE 59 (Cont'd.)

Symbol	Units	Definition
DELTAY	cm	Cross-plume spacing of calculation points
DELTAZ	cm	Vertical grid spacing employed under non-compact plume conditions
DYDUM	cm	Cross-plume spacing of calculation points generated by computer if no value is entered as data
DZ	cm	Vertical grid spacing
DZTST	cm	Test variable for assessing compact plume conditions
EQCON	gm moles/liter	Equilibrium constant for first dissociation of SO_2 (cf. Equation (40))
F	cm^{-3}	Probability-density function for raindrops of size R in a distributed system; also denotes derivative used in subroutines SOLVE and RUNGE ($gm\text{-}moles/cm^4$)
GR	dimensionless	Dummy variable used in subroutine SOLVE
GROUP	dimensionless	Dimensionless group used to evaluate equilibrium scavenging conditions (cf. Equation (1))
H	cm	Effective emission release height
HANK	liters/gm mole	Henry's-law constant for undissociated SO_2 in water (cf. Equation (39))
HEX	gm moles/liter	Hydrogen ion in rain other than that contributed by dissolved SO_2
HPRIME	cm^3/gm mole	Effective Henry's-law constant for total dissolved SO_2 in water
HSTAR	cm	Plume height, or effective release height
HTEST	cm^3/gm mole	Effective Henry's-law constant used for evaluation of equilibrium scavenging conditions
I		Index integer
ICP		Internal control variable in subroutine SOLVE providing for grid spacing modifications in the case of a compact plume
IGRND		Internal control variable in subroutine SOLVE providing for termination of the algorithm as the raindrop encounters the receptor
IS		Internal control variable communicating status of solution between subroutines SOLVE and RUNGE

TABLE 59 (Cont'd.)

Symbol	Units	Definition
IY		Internal control variable providing a runaway trap on cross-plume integration sequence
J		Index integer
J1		Read control variable providing for optional reading of raindrop size distribution data
J2		Read control variable providing for optional reading of physical properties data
J3		Read control variable providing for optional reading of plume data
J4		Read control variable providing for optional reading of grid data
JEND		Program termination control variable
JOPT		Mass-transfer coefficient option control variable (JOPT = 1 gives gas-phase controlled coefficient: JOPT = 0 gives stagnant-drop contribution)
JP		Print control variable (JP set equal to 1 suppresses printing of individual raindrop data
LGOPT		Control variable for gas (= 1) or liquid (= 2) based solubility calculations
M		Internal/external control
N		Integer for RUNGE and SOLVE Number of discreet drop sizes in descretized spectrum; also number of simultaneous equations in RUNGE
P	atm	Ambient pressure
PHI		Internal computation variable in RUNGE
Q	gm moles/sec	Source strength of plume
R	cm	Raindrop radius
RE	dimensionless	Reynolds number for falling drop
REF	cm	Height above release point where raindrop passes $x = 0$
RK	sec^{-1}	First-order reaction constant for decay of pollutant in plume
S		(Integer) status variable used in subroutine RUNGE--counterpart of variable IS in subroutine SOLVE

TABLE 59 (Cont'd.)

Symbol	Units	Definition
SAVEY	dimensionless	Mixing ratio of pollutant in gas phase at receptor
SC	dimensionless	Schmidt number for falling drop
SIGMA	cm	Internal estimate of plume spread in z-direction--utilized when compact plumes are encountered
SIGMAY	cm	Plume spread in y-direction
SIGMAZ	cm	Plume spread in z-direction
SIGPHI	radians	Plume spread in φ-direction
SIGTHE	radians	Plume spread in θ-direction
SIGY	cm	Plume spread in y-direction at receptor
SIGZ	cm	Plume spread in z-direction at receptor
T	°K	Ambient temperature
TDZ	cm	Compact plume grid spacing
TEST1	liter/gm mole	Test variable for asymptotic dilution conditions
TKY	gm moles/cm^{2}sec	Overall mass-transfer coefficient (cf. Eq. (41)
TDZ	cm	Grid spacing for compact plume
U	cm/sec	Mean wind velocity
V	cm/sec	Terminal fall velocity of raindrop (fall in +z direction)
VERT	cm/sec	Plume loft velocity
WORATE	gm moles/cm	Downwind washout rate
X	cm	Downwind distance from source
XBUK	cm	Downwind distance of receptor from source
XCL	cm	X position where drop falls across release elevation
XK	gm moles/cm^{2}sec	Liquid-phase mass-transfer coefficient
XNT	cm/sec	Rainfall rate
Y	cm	Crosswind distance from source
YAB	dimensionless	Mixing ratio of pollutant in air (moles/mole)
YBUK	cm	Crosswind distance of receptor from source
YK	gm moles/cm^{2}sec	Gas-phase mass-transfer coefficient
Z	cm	Distance above stack base
ZBUK	cm	Distance of receptor above stack base

```
      PROGRAM EPAEC(INPUT,OUTPUT,TAPE5=INPUT,TAPE6=OUTPUT)
C     PROGRAM **EPAEC** TO SOLVE NONLINEAR-NONFEEDBACK MODEL FOR GAS
C     SCAVENGING.  PROGRAMMED IN FINAL FORM MARCH, 1973 BY
      J. M. HALES UNDER CONTRACT TO THE DIVISION OF METEOROLOGY,
C     ENVIRONMENTAL PROTECTION AGENCY.
C
C     PROGRAM READS IN THE NUMBER OF DISCRETE DROP SIZES IN THE RAIN
C     SPECTRUM AND THE VARIOUS DECISION VARIABLES. IT THEN READS THE
C     RAIN DISTRIBUTION DATA AND (OPTIONALLY) THE LIQUID-PHASE MASS-
C     TRANSFER COEFFICIENTS.  SUBSEQUENTLY IT READS IN THE PHYSICAL
C     PROPERTIES, THE WIND VELOCITY AND SOURCE STRENGTH, AND THE
C     LOCATION OF THE RECEPTOR.  CALCULATION THEN PROCEEDS AS DOCUMENTED
C     THROUGHOUT THE PROGRAM.  THIS CODE USES THE CGS SYSTEM OF UNITS,
C     EXCEPT FOR PRESSURE, WHICH IS IN ATMOSPHERES, AND FOR SOME
C     CONCENTRATIONS EMPLOYED IN THE SOLUBILITY CALCULATIONS,
C     WHICH ARE GIVEN IN MOLES PER LITER.  CONVENTIONAL CONCENTRATION
C     UNITS ARE MOLES PER CUBIC CENTIMETER.
      COMMON D(20),F(20),CGRND(20), SAVEY,N,J1,J2,J3,J4,JOPT,JP,JEND,
     1DAX,DAY,HEX,XNU,P,T,XNT,SIGTHE,SIGPHI,U,H,Q,XBUK,YBUK,ZBUK,
     2DELTAZ,SIGY,SIGZ,CEQ,CAVG,RK,BKG,VERT
      EXTERNAL V,HPRIME,YAB
100   READ (5,320) N,J1,J2,J3,J4,JOPT,JP,JEND
      IF (J1.EQ.1) GO TO 110
      READ (5,330) (D(I),I=1,10)
      READ (5,330) (F(I),I=1,10)
110   IF (J2.EQ.1) GO TO 120
      READ (5,340) DAX,DAY,HEX,XNU,P,T,XNT,RK
120   IF (J3.EQ.1) GO TO 130
      READ (5,350) SIGTHE,SIGPHI,U,H,Q,VERT,BKG
130   IF (J4.EQ.1) GO TO 140
      READ (5,360) XBUK,YBUK,ZBUK,DELTAY,DELTAZ
      DYDUM=.087266*XBUK
      IF (DELTAY.LT.1.) DELTAY=DYDUM
140   IF (J4.EQ.1) YBUK=0.
      WRITE (6,230)
      WRITE (6,240) DAX,DAY,XNU,HEX,P,T
      WRITE (6,250) SIGTHE,SIGPHI,U,H,Q
      WRITE (6,260) XBUK,YBUK,ZBUK
      CCUM=0.
      IY=0
150   CALL MASTER
C     TESTING FOR INITIAL COMPUTATION
      IF (IY.GT.0) GO TO 160
      WRITE (6,270)
C     PRINTING OF BULK RESULTS
160   WRITE (6,280) SIGY,SIGZ,CEQ,CAVG
      WRITE (6,310) SAVEY
      IF (JP.EQ.1) GO TO 180
      DO 170 I=1,N
      R=D(I)/2.
      REF=ZBUK-XBUK*V(R)/U-H
C     PRINTING OF INDIVIDUAL RESULTS
170   WRITE (6,290) D(I),CGRND(I),REF
      IF(JEND.EQ.3) GO TO 100
C     TESTING FOR WHETHER RECEPTOR IS ON CENTERLINE
```

```
180   IF (IY.EQ.0) GO TO 190
      IF (JEND.EQ.2) GO TO 200
C     TEST FOR OFF-PLUME CONDITIONS
      CTEST=1.-(CAVGCL-CAVG)/CAVGCL
      CCUM=CCUM+(CAVG+CLAST)
      IF (CTEST.LT..001) GO TO 210
      GO TO 200
190   CAVGCL=CAVG
200   YBUK=YBUK+DELTAY
      IY=IY+1
      IF (JEND.EQ.2) GO TO 100
      IF (IY.GT.35) GO TO 220
      CLAST=CAVG
C     CALCULATION AND PRINTING OF DOWNPLUME WASHOUT RATE (MOLES/CM SEC)
      WORATE=CCUM*DELTAY*XNT
      GO TO 150
210   WRITE (6,300) WORATE
      IF (JEND.NE.1) GO TO 100
220   CALL EXIT
C
230    FORMAT (1H1//,10X,"PRECIPITATION WASHOUT ESTIMATES",//,5X,
     1"VALUES GIVEN IN GM-MOLE - CM - SEC UNITS UNLESS SPECIFIED OTHERWI
     2SE",///,20X,"INPUT DATA")
240    FORMAT (1H ,"DAX = ",F12.9," DAY = ",F7.5," XNU = ",F7.5," HEX =
     1",F13.6," MOLAR P = ",F6.3," ATM T = ",F7.2," DEGREES K")
250    FORMAT (1H ,"SIGMA THETA = ",F6.4," SIGMA PHI = ",F6.4," U = ",
     1E13.6," H = ",E13.6," Q = ",E13.6)
260    FORMAT (1H ,10X,"XBUK = ",E13.6," YBUK = ",E13.6," ZBUK = ",E13.6)
270    FORMAT (1H ,//,20X,"COMPUTED VALUES")
280    FORMAT(1H ,///," SIGY = ",E13.6," SIGZ = ",E13.6," CEQ = ",E13.6,
     1" CAVG = ",E13.6)
290    FORMAT (1H ,"D = ",F7.4," CGND = ",E13.6," STACK INTERCEPT = ",
     1E13.6)
300    FORMAT (1H ,//,1H ,"CROSSWIND WASHOUT RATE = ",E14.7," MOLES/CM SE
     1C",//)
310    FORMAT (1H ,//,1H ,"GAS PHASE MOLE FRACTION AT GROUND LEVEL = ",
     1E14.7,//)
320    FORMAT (8I5)
330    FORMAT (10F7.4)
340    FORMAT (8E10.6)
350    FORMAT (2F10.6,5E10.6)
360    FORMAT (5E10.6)
       END
      SUBROUTINE MASTER
C     SUBROUTINE FOR CALCULATION OF WASHOUT CONCENTRATIONS IN RAIN
C     AT GROUND LEVEL USING GENERALIZED NONLINEAR MODEL.  IT ACCEPTS
C     INPUT DATA FROM MAIN PROGRAM THROUGH THE COMMON STATEMENT AND
C     THEN PROCEEDS TO CALCULATE RAINDROP CONCENTRATIONS BY CALLING THE
C     REQUIRED SUBROUTINES.  IT THEN CALCULATES THE AVERAGE
C     CONCENTRATION IN THE RAIN SAMPLE AND RETURNS CONTROL TO THE
C     CALLING PROGRAM
      COMMON D(20),F(20),CGRND(20), SAVEY,N,J1,J2,J3,J4,JOPT,JP,JEND,
     1DAX,DAY,HEX,XNU,P,T,XNT,SIGTHE,SIGPHI,U,H,Q,XBUK,YBUK,ZBUK,
     2DELTAZ,SIGY,SIGZ,CEQ,CAVG,RK,BKG,VERT
C     CALCULATION OF STANDARD DEVIATIONS
      SIGY=XBUK*SIGTHE
      SIGZ=XBUK*SIGPHI
      DO 100 I=1,N
      R=D(I)/2.
C     CALCULATION OF INDIVIDUAL CONCENTRATIONS FOR RADIUS R RAINDROPS
      CALL SOLVE (R,COBJ,JOPT,DAX,DAY,HEX,XNU,P,T,SIGTHE,SIGPHI,U,H,Q,XB
     1UK,YBUK,ZBUK,SAVEY,RK,BKG,VERT,CEQ)
      CGRND(I)=COBJ
100   CONTINUE
      CAVG=0.
      AA=0.
C     COMPUTATION OF AVERAGE CONCENTRATION BY DISTRIBUTION OVER DROP SIZES
      DO 110 I=1,N
110   AA=AA+F(I)*D(I)**3
      DO 120 I=1,N
120   CAVG=CAVG+F(I)*CGRND(I)*D(I)**3
      CAVG=CAVG/AA
      RETURN
      END
      SUBROUTINE SOLVE (R,COBJ,JUPT,DAX,DAY,HEX,XNU,P,T,SIGTHE,SIGPHI,U,
     1H,Q,XBUK,Y,ZBUK,SAVEY,RK,BKG,VERT,CEQ)
C     SUBROUTINE FOR CALCULATION OF INDIVIDUAL RAINDROP CONCENTRATIONS.
C     PROGRAM SETS UP APPROPRIATE COMPUTATION GRID FOR NUMERICAL
C     SOLUTION OF THE FIRST-ORDER, ORDINARY DIFFERENTIAL EQUATION
C     DESCRIBING DROP RESPONSE.  IT THEN CALLS THE RUNGE-KUTTA
C     ALGORITHM REPEATEDLY, PROGRESSING FROM THE TOP OF THE
C     COMPUTATION GRID TO GROUND LEVEL.
      DIMENSION C(1),F(1)
C     INITIALIZATION OF VARIABLES
      ICP=0
      H=0
      IGRND=0
      C(1)=0
      I=1
C     BYPASS TEST FOR EQUILIBRIUM SCAVENGING CONDITIONS
      HSTAR=H+VERT*XBUK/U
      SIGMAY=SIGTHE*XBUK
      SIGMAZ=SIGPHI*XBUK
      SAVEY=YAB(T,P,U,HSTAR,Q,XBUK,Y,ZBUK,SIGTHE,SIGPHI,RK,BKG)
      HTEST=HPRIME(SAVEY,HEX,T,P,1)
      IF(HTEST.LE.0.) GO TO 100
      CTEST=SAVEY/HTEST
      CALL MTC(R,DAX,DAY,XNU,T,P,JOPT,CTEST,HTEST,TKY)
      GR=18.9*TKY*HTEST*U*SIGMAY*SIGMAZ**2*EXP(.5*.5*Y*Y/SIGMAY**2)
      GR=-GR/(V(R)*R)
      GROUP=GR*SAVEY/(82.*Q*T/P)
      CORJ=CTEST
      CEQ=CTEST
      IF(GROUP.GT.15.) GO TO 190
C     CALCULATION OF INITIAL RAINDROP CONCENTRATION
      C(1)=BKG/HPRIME(BKG,HEX,T,P,1)
C     TEST FOR PLUME UNDERCUT
100   REF=-XBUK*V(R)/U+ZBUK-H
      Z=REF+H
      IF (REF.GT.0.) GO TO 120
C     SPACING FOR UNDERCUT GRID
      DELTAZ=-XBUK*V(R)/(U*30.)
      GO TO 130
C     SETTING OF NORMAL GRID SPACING
120   XCL=XBUK+U*(H-ZBUK)/V(R)
      SIGMA=SIGPHI*XCL
      HSTAR=H+VERT*XCL/U
      Z1=HSTAR+3.*SIGMA
      IF (Z1.LT.Z) Z=Z1
      DELTAZ=Z/60.
C     TEST FOR COMPACT PLUME
      DZTST=SIGMA/4.
      IF(SIGPHI.GT..5) DZTST=DZTST/2.
      IF(DZTST.GT.DELTAZ) GO TO 130
C     SETTING OF COMPACT GRID SPACING
      TDZ=DZTST
      ICP=1
C     START OF NUMERICAL INTEGRATION LOOP
130   IF (ICP.NE.1.OR.I.GT.25) GO TO 140
      DZ=-TDZ
      GO TO 150
140   DZ=-DELTAZ
C     INITIATION OF RUNGE-KUTTA ALGORITHM
150   CALL RUNGE (1,C,F,Z,DZ,IS,M)
      IF(C(1).LT.0.) C(1)=0.
      IF (IS.NE.1) GO TO 160
      X=XBUK+U*(Z-ZBUK)/V(R)
      HSTAR=H+VERT*X/U
C     CALCULATION OF MASS-TRANSFER COEFFICIENT
      CALL MTC (R,DAX,DAY,XNU,T,P,JOPT,C(1),HEX,TKY)
C     DETERMINATION OF FIRST DERIVATIVE FOR R-K ALGORITHM
      F(1)=(3.*TKY/(R*V(R)))*(YAM(T,P,U,HSTAR,Q,X,Y,Z,SIGTHE,SIGPHI,RK,M
     1KG)-HPRIME(C(1),HEX,T,P,2)*C(1))
      GO TO 150
C     TEST FOR APPROACH TO GROUND
160   ZTEST=Z+DZ-ZBUK
      IF(ZTEST.LT.100.) GO TO 170
      I=I+1
      GO TO 130
170   IF (IGRND.EQ.1) GO TO 180
      IGRND=1
      DZ=ZBUK-Z
      GO TO 150
180   CORJ=C(1)
190   RETURN
      END



      SUBROUTINE MTC (R,DAX,DAY,XNU,T,P,JOPT,CSET,HEX,TKY)
C     SUBROUTINE FOR MASS-TRANSFER COEFFICIENT CALCULATION.
C     GAS COEFFICIENT BASED ON FROESSLING EQUATION.  LIQUID
C     COEFFICIENT IS BASED ON CONTINUITY EQUATION SOLUTION FOR
C     RESPONSE TO RAMP CONCENTRATION FORCING FUNCTION.
C
C     CALCULATION OF GAS-PHASE COEFFICIENT
      RE=-2.*R*V(R)/XNU
      SC=XNU/DAY
      YK=(1.+.3*RE**.5*SC**.333)*DAY*P/(R*T*82.057)
      TKY=YK
      IF (JOPT.EQ.1) GO TO 100
C     CALCULATION OF LIQUID-PHASE  COEFFICIENT
      XK=.2778*DAX/R
      TKY=1/(HPRIME(CSET,HEX,T,P,2)/XK+1/YK)
100   RETURN
      END
      FUNCTION YAB(T,P,U,H,Q,X,Y,Z,SIGTHE,SIGPHI,RK,BKG)
C     SUBROUTINE FOR CALCULATING MOLE FRACTION OF POLLUTANT IN GAS PHASE
C     PASQUILL-GIFFORD BIVARIATE-NORMAL EQUATION IS MODIFIED TO ACCOUNT
C     FOR POSSIBLE BACKGROUND CONTRIBUTIONS AND FIRST-ORDER, GAS PHASE
C     REACTION.
      IF(X.LE.0.) YAB=BKG
      IF (X.LE.0.) GO TO 100
      SIGMAY=SIGTHE*X
      SIGMAZ=SIGPHI*X
      YAB=13.0598*Q*T*EXP(-Y**2/(2*SIGMAY**2))*(EXP(-(Z-H)**2/(2*SIGMAZ*
     1*2))+EXP(-(Z+H)**2/(2*SIGMAZ**2)))/(SIGMAY*SIGMAZ*U*P)
      YAB=YAB*EXP(-RK*X/U)+BKG
100   RETURN
      END
```

```
      FUNCTION V(R)
C     SUBROUTINE FOR CALCULATING VELOCITY OF FALLING DROP, USING POLYNOMIAL
C     FIT TO KINZER-GUNN DATA;
C     TO KINZER-GUNN DATA.
      V=8710.858*R-18029.72*R**2-32184.48*R**3
      V=-V
      RETURN
      END
      FUNCTION HPRIME(C,HEX,T,P,LGOPT)
C     SUBROUTINE FOR CALCULATING APPARANT HENRY"S-LAW CONSTANT USING
C     JOHNSTONE-LEPPLA PARAMETERS.

      HANK=EXP(9.94-3040./T)/P
      EQCON=EXP(-10.3+1780./T)
C     TRANSFER POINT FOR LIQUID- OR GAS-PHASE BASED CALCULATIONS
      IF(LGOPT.EQ.1) GO TO 100
      B=EQCON+HEX
      CDUM=EQCON*1000.*C
C     TEST FOR LOW-CONCENTRATION CONDITIONS
      TEST1=4.*CDUM/B**2
C     ASYMPTOTIC EXPRESSION FOR LOW-CONCENTRATION CONDITIONS
      HPRIME=1000.*(HANK-HANK*EQCON/B)
      IF(TEST1.LT..001) GO TO 110
C     SOLUTION OF TOTAL SOLUBILITY EQUATION
      HPRIME=HANK*(1.-(-B+SQRT(B**2+4.*CDUM))/(2000.*C))*1000.
      GO TO 110
C     TEST FOR LOW-CONCENTRATION CONDITIONS
100   DUMMY=HEX*HEX*HANK/(4*EQCON*C)
      IF(DUMMY.LT.1000.) GO TO 105
C     ASYMPTOTIC EXPRESSION FOR LOW-CONCENTRATION CONDITIONS
      HPRIME=1000.*HANK*HEX/(HEX+EQCON)
      GO TO 110
C     SOLUTION OF TOTAL SOLUBILITY EQUATION
105   CTEST=(C/HANK+(-HEX+SQRT(HEX**2+4*C*EQCON/HANK))/2)/1000.
      HPRIME=C/CTEST
C     RETURN VALUE OF HPRIME HAS UNITS OF CENTIMETERS CUBED PER MOLE
110   RETURN
      END
      SUBROUTINE RUNGE (N,Y,F,X,H,S,M)
C     SUBROUTINE TO SOLVE DIFFERENTIAL EQUATION DESCRIBING CONCENTRATION
C     RESPONSE OF A FALLING DROP.  RUNGE-KUTTA ALGORITHM IS ADAPTED FROM
C     GENERAL VERSION GIVEN BY CARNAHAN, LUTHER, AND WILKES.
      DIMENSION SAVEY(1),PHI(1),F(1),Y(1)
      INTEGER S
      M=M+1
      GO TO (100,110,130,150,170), M
100   S=1
      GO TO 190
110   DO 120 J=1,N
      SAVEY(J)=Y(J)
      PHI(J)=F(J)
120   Y(J)=SAVFY(J)+.5*H*F(J)
      X=X+.5*H
      S=1
      GO TO 190
130   DO 140 J=1,N
      PHI(J)=PHI(J)+2.*F(J)
140   Y(J)=SAVEY(J)+.5*H*F(J)
      S=1
      GO TO 190
150   DO 160 J=1,N
      PHI(J)=PHI(J)+2.*F(J)
160   Y(J)=SAVEY(J)+H*F(J)
      X=X+.5*H
      S=1
      GO TO 190
170   DO 180 J=1,N
180   Y(J)=SAVEY(J)+(PHI(J)+F(J))*H/6.
      M=0
      S=2
190   CONTINUE
      RETURN
      END
```

APPENDIX D.

REDISTRIBUTION OF A GAS PLUME CAUSED BY REVERSIBLE WASHOUT*

In Section IV we presented an expression (Equation (5)), for concentration in a plume modified by the sorption-desorption action of rain; this appendix presents a derivation of that equation. In proceeding with this derivation we start by assuming the rain to be composed of homogeneous, vertically-falling drops. As discussed elsewhere,[5] this assumption can be used to approximate actual conditions reasonably well under most practical circumstances.

Having made this assumption, one can focus attention on any single drop of rain falling through a gaseous plume. As the raindrop traverses the plume, sorption will occur and the drop's concentration will approach a saturation value with respect to the concentration in the plume. It then can emerge from the plume with a concentration, supersaturated with respect to that of its surroundings, and desorption of the gas may occur. This can result in an effective lowering of the plume with an increased dosage to low-level receptors as well as a modified washout pattern.

We proceed with the further assumption that mass-transfer and solubility behavior can be linearized (invariant mass-transfer coefficient and Henry's-law constant). In addition, we utilize a majority of the assumptions necessary for derivation for the Pasquill-Gifford plume equation, i.e., neglect of longitudinal diffusion, constant effective eddy diffusivities in the vertical and crosswind directions, negligible wind shear, and a point-source release.

With the above assumptions the coupled equations of conservation for pollutant in the gas (air) and liquid (rain) phases set forth in previous publications reduce to mathematically tractable forms. In presenting these equations here it is convenient to drop some of the subscripts used in previous nomenclature, since the following derivations are rather cumbersome, and since there is no danger of ambiguity at present. Thus we will denote the mixed-mean gas- and liquid-phase concentrations of pollutant A, c_{Ay} and c_{Ax}, simply by the symbols χ and c, respectively.

---

*The work of this section was sponsored in part by Battelle Institute, Physical Sciences Program.

With the above assumptions, the conservation equations become

$$u \frac{\partial \chi}{\partial x} = D_y \frac{\partial^2 \chi}{\partial y^2} + D_z \frac{\partial^2 \chi}{\partial z^2} + \beta c \quad , \tag{55}$$

and

$$-J \frac{\partial c}{\partial z} = \alpha \chi - \beta c \quad , \tag{56}$$

where $\alpha = - 3JK_y/ac_x v_t$ and $\beta = - 3JK_y/aH^*c_x v_t$. Here the nomenclature is consistent with our previous usage; H^* is a modified, apparent Henry's-law constant defined by the relationship

$$\chi = H^*c \text{ at equilibrium} \quad . \tag{57}$$

CASE 1: IGNORING DIFFUSION

We look first at the simpler case for which diffusion of the plume can be ignored. In this case, if we let $t = x/\bar{u}$, then Equations (55) and (56) simplify to

$$\frac{\partial \chi}{\partial t} = \beta c - \alpha \chi \quad , \tag{58}$$

and

$$-J \frac{\partial c}{\partial z} = \alpha \chi - \beta c \quad . \tag{59}$$

If c is eliminated between Equations (58) and (59) we obtain an equation describing only the plume:

$$\frac{\partial \chi}{\partial t} = \frac{\alpha J}{\beta} \frac{\partial \chi}{\partial z} + \frac{J}{\beta} \frac{\partial^2 \chi}{\partial z \partial t} \quad . \tag{60}$$

To solve Equation (60), a Laplace transform (parameter s) is taken in time. Solving the resulting ordinary differential equation in z, subject to the single boundary condition $\hat{\chi}(z \to \infty, s) = 0$, gives

$$\hat{\chi}(z,s) = \frac{\chi_o(z,o)}{s + \alpha} + \frac{\alpha\beta}{J} \frac{e^{Az}}{(s + \alpha)^2} \int_z^\infty \chi_o e^{-A\zeta} d\zeta \quad , \tag{61}$$

where $A = (\beta/J)(s/(\alpha + s))$. Inverting the first term on the right hand side of Equation (61) is trivial. It leads to an exponential decay of the initial plume profile: $\chi_o(z,o)\exp\{-\alpha t\}$.

The second term is a little more difficult. The integral to be evaluated is the integral on the Bromwich contour:

$$I = \frac{1}{2\pi i}\int_{B.C.} \frac{e^{A(z - \zeta)}e^{st}}{(s + \alpha)^2}\,ds \quad . \tag{62}$$

Point $-\alpha$ in the complex s plane is an essential singularity because of the s dependence of A. If near $s = -\alpha$ we take $s = \varepsilon - \alpha$, then the expansion of the integrand for small ε leads to

$$\frac{e^{A(z - \zeta) + st}}{(s + \alpha)^2} = \frac{1}{\varepsilon^2}\exp\{\frac{-\beta}{J}\eta - \alpha t\}[1 + \varepsilon t + \frac{(\varepsilon t)^2}{2!} + \ldots]$$

$$\cdot\ [1 + \frac{\eta\alpha\beta}{J\varepsilon} + \frac{1}{2!}(\frac{\eta\alpha\beta}{J\varepsilon})^2 + \ldots] \quad , \tag{63}$$

where $\eta = \zeta - z$. By collecting all terms of the coefficient of ε^{-1}, and identifying the resulting series as that for a first order modified Bessel function, we obtain the residue

$$\frac{2t}{q}\exp\{\frac{-\alpha\beta}{J}\eta - \alpha t\}I_1(q) \quad , \tag{64}$$

where $q^2 = 4\alpha t\,\frac{\beta}{J}(\zeta - z)$. The solution is then obtained from Equation (61) to be

$$\chi(z,t) = \chi_o(z)e^{-\alpha t} + \tfrac{1}{2}\,e^{-\alpha t}\int_z^\infty d\zeta\,\chi_o\,\frac{e^{-\frac{\alpha}{\beta}(\zeta - z)}}{(\zeta - z)}\,qI_1(q) \quad . \tag{65}$$

Into Equation (65) can be substituted any initial plume concentration, including, for example, a plume which has diffused to any realistic provile downwind of the stack.

A particular case for Equation (65) is quite informative. If initially the plume is a delta function at the height h, then subsequently, $\chi = 0$ for $z > h$, and for $z \leq h$,

$$\chi(z,t) = \delta(z - h)e^{-\alpha t} + \tfrac{1}{2}\exp\{-\alpha t - \frac{\beta}{J}(h - z)\}\,\frac{qI_1\,(q)}{(h - z)} \quad , \tag{66}$$

with $q^2 = 4\alpha t \frac{\beta}{J}(h - z)$. A plot of this solution is given in Section IV. The large q behavior of Equation (66) can be found using the known asymptotic expansion of $I_1(q)$ and leads to

$$\chi(z,t) \sim \frac{1}{(h-z)}\left(\frac{q}{8\pi}\right)^{\frac{1}{2}} \exp\{-[(\alpha t)^{\frac{1}{2}} - \sqrt{\frac{\beta}{J}}\,(h-z)^{\frac{1}{2}}]^2\}\{1 - \frac{3}{8q} + \ldots\} \quad . \qquad (67)$$

To obtain the concentration in the rain, we return to the original equation, Equation (59), and obtain

$$c(z,t) = \frac{\alpha}{J}\, e^{\frac{\beta}{J} z} \int_z^{\infty} \chi(\zeta,t)\, e^{-\frac{\beta}{J}\zeta}\, d\zeta \quad . \qquad (68)$$

In particular, if the Green's function (66) is substituted into Equation (68), and if known integrals of Bessel functions are utilized, then for $z \leq h$,

$$c(z,t) = \frac{\alpha}{J}\, I_o(q)\, \exp\{-\alpha t - \frac{\beta}{J}(h - z)\} \quad . \qquad (69)$$

THE "WASHDOWN" VELOCITY

It is of interest to obtain an estimate of the rate at which the plume is "washed down" by precipitation. One way to evaluate this is to determine the centroid of the plume as a function of time. If the centroid is taken about the top of the stack, then for the case of a delta function initial plume Equation (66) yields

$$<z> = -\frac{e^{-\alpha t}}{2}\int_o^{\infty} d\xi\; e^{-\frac{\beta}{J}\xi}\, qI(q) = -\frac{\alpha J}{\beta}\, t \quad . \qquad (70)$$

The "washdown" velocity of the plume is then

$$w \equiv \frac{d<z>}{dt} = -\frac{\alpha J}{\beta} \quad . \qquad (71)$$

GENERAL CASE: INCLUDING DIFFUSION

We now return to the general case given by Equations (55) and (56). In this case, when the effects of diffusion are included, some approximations will be made. These will be justified using the results of the previous section. If the liquid phase concentration is eliminated between Equations (55) and (56), there results the single equation for the gas-phase concentration

$$\frac{\partial \chi}{\partial t} = w \frac{\partial \chi}{\partial z} + \delta \frac{\partial^2 \chi}{\partial t \partial z} + D_y \frac{\partial^2 \chi}{\partial y^2} + D_z \frac{\partial^2 \chi}{\partial z^2} - \delta D_y \frac{\partial^2 \chi}{\partial z \partial y^2} - \delta D_z \frac{\partial^3 \chi}{\partial z^3} \quad , \qquad (72)$$

where $w = \alpha J/\beta$ is the washdown velocity and $\delta = J/\beta$ is a characteristic length which for the example shown in Figure 8 is about 5.5 m. Equation (72) is to be solved subject to the boundary and initial conditions: $\chi(t \to o,y,z) = \chi_o \delta(y)\delta(z - h)$; $\chi(t,y \to \pm\infty,z) = 0$; and $\chi(t,y,z \to \pm\infty) = 0$. These conditions correspond to the case downwind $(t = x/\bar{u})$ of a stack of height h and source strength χ_o, for those situations when the influence of the ground can be ignored.

To solve Equation (72), the method of multiple transforms will be used. Taking first a Laplace transform in time (parameter s), then infinite Fourier transforms in y (parameter η) and z (parameter ζ), leads to the algebraic equation which contains the boundary conditions:

$$\tilde{\tilde{\chi}}(s,\eta,\zeta) = \frac{\chi_o e^{-i\zeta h}(1 - i\delta\zeta)}{[s(1 - i\delta\zeta) + \eta^2 D_y + \zeta^2 D_z - i\zeta(w + \delta D_y \eta^2 + \delta D_z \zeta^2)]} \quad . \qquad (73)$$

Inverting the Laplace transform is trivial since there is only one simple-pole in the complex s-plane. Next, the simple η-Fourier transform is inverted. Finally, the ostensible inversion of the ζ-transform leads to

$$\chi(t,y,z) = \frac{1}{2\pi} \frac{\chi_o}{(4\pi t D_y)^{\frac{1}{2}}} \exp\{- \frac{y^2}{4tD_y}\}$$

$$\cdot \int_{-\infty}^{+\infty} \exp\{-tD_{Az}\zeta^2 - ih\zeta + iz\zeta - \frac{wt}{\delta} \frac{\zeta}{(\zeta + i/\delta)}\} d\zeta \quad . \qquad (74)$$

The integral in Equation (74) is rather difficult to evaluate. It converges only in the region $|Im\zeta| < |Re\zeta|$; there is an essential singularity at $\zeta = -i/\delta$; in order to find paths of steepest descent it is necessary to find the roots of the obvious cubic in ζ. Rather than pursue the interesting mathematics involved in evaluating Equation (74), we attempt to simplify the last term in the exponential for the cases of practical interest. From the previous section we notice that for the washdown of SO_2, $\delta \simeq 5.5$ m. On the other hand, the largest ζ value that will contribute significantly to the integral is seen from the first term in the exponential to be $\simeq (tD_z)^{-\frac{1}{2}}$. Thus ζ is small compared with δ^{-1} provided $t >> \delta^2/D_z$. This condition is satisfied, for the case with D_z as small as 1 $m^2 sec^{-1}$ and for the SO_2 plume considered in the previous section, provided only that $t >> 1$ minute. This is not at all a serious restriction. Then expanding the last term in the exponential according to

$$-\frac{wt}{\delta}\frac{\zeta}{(\zeta + i/\delta)} \simeq iwt\zeta - wt\delta\zeta^2 \quad , \qquad (75)$$

and performing the simple integral, we obtain

$$\chi(t,y,z) = \chi_o \frac{\exp\{\frac{-y^2}{4tD_y}\}}{(4\pi tD_y)^{\frac{1}{2}}} \frac{\exp\{\frac{-[z - (h - wt)]^2}{4t(D_z + w\delta)}\}}{[4\pi t(D_z + w\delta)]^{\frac{1}{2}}} \quad , \qquad (76)$$

which was presented earlier (in the form of mixing ratios) in Section IV. Thus in the general case (for the approximations stated), the influence of the reversible scavenging by rain is that the plume diffuses about the effective plume height $(h - wt)$, where $w = JH^*$ is the washdown velocity, and the diffusivity is slightly enhanced by the factor $w\delta$.